POLITECNICO DI MILANO

School of Industrial and Information Engineering

Department of Energy

BESS Energy Management Strategies for Multiple Ancillary Services Provision

Supervisor: Prof. Marco Merlo

Co-supervisor: Eng. Giuliano Rancilio

Master Graduation Thesis by:

Martino Alborghetti ID 878382

Claudio Di Profio ID 878103

Academic Year 2017/2018

Acknowledgements

EXTENDED ABSTRACT

1. INTRODUCTION

The global demand of electricity is continuously increasing [1]. In recent years, the power generation mix has evolved due to the spread of Renewable Energy Sources (RESs). RESs are fundamental towards decarbonisation and reduction of Greenhouse Gases emissions as stated in many international agreements [119]-[120]. Unlike traditional fossil fuel plants, most of RESs are non-programmable. At high levels of penetration of non-programmable RES, electricity production fluctuations may affect the reliability of the system. This is because, in the electric power system, generation and demand must be always balanced. System operators measure this balance by monitoring system frequency. In Europe, the nominal frequency is 50 Hz, while in the USA it is 60 Hz. Failure to operate the system at its required frequency can disrupt the operation of equipment and lead to large-scale blackouts.

Battery Energy Storage Systems (BESS) are an important option to provide grid services, also known as Ancillary Services (AS). In particular, they are suitable to mitigate frequency deviations. Two are the main services for regulating frequency: Primary Control Reserve (PCR) and Secondary Control Reserve (SCR) provision. The former is adopted to block the frequency variation and to bring it to a generic stable value. The latter is used to restore the nominal value of frequency. There is also a third control action, known as Tertiary Control Reserve (TCR) provision, which is activated in order to restore the reserves that have been used in the other control actions.

ASs, including frequency regulation services, are traded on the Ancillary Services Market (ASM). The ASM represents the instrument through which the Transmission System Operator (TSO) acquires all the resources necessary to manage and control the system. Nowadays, the regulatory frameworks of the majority of ASM are tailor made on traditional generators. They are not open to BESS yet since batteries are different from conventional generators and more studies and feasibility analysis are needed. For this reason, several pilot projects involving BESSs have been deployed in the last years [10]-[124].

The objective of this work is to verify the ability of a BESS in providing frequency services to the electrical network from both technical and economical point of view. In particular, two cases are analysed:

- Single service provision of PCR.
- Multi-service provision of PCR and asymmetric SCR.

Two ASM models are considered for PCR remuneration: the Italian and the German paradigms. SCR market structure and remuneration mainly follows Italian ASM regulation. The only difference is the possibility to bid asymmetric bands, as happens in Germany. This variation is necessary in order to use SCR as SoC restoration strategy for PCR and leads to a hybrid framework useful to promote the integration of BESS in this kind of market.

In case of multi-service provision, it is very important to forecast the SoC of the BESS at the end of the following market session. Therefore, various forecasting techniques are implemented in order to optimally allocate SCR regulating bands.

This kind of analysis requires a BESS model able to estimate with good accuracy SoC and energy losses, since they may play an important role in revenues, and at the same time it must allow to simulate long periods, up to several months, in order to avoid the effect of peculiarities of single days or weeks and provide more generalizable results.

This extended abstract is organized as follows. *Section 2* presents a literature review on BESSs. The ASM is described in *Section 3*. *Section 4* is dedicated to an introduction to predictive analytics. In *Section 5,* the methodology, the models and performance evaluation indices are detailed. *Section 6* shows the results of PCR provision.

Section 7 is dedicated to the results of multi-service provision. *Section 8* summarizes the main outcomes.

2. BATTERY ENERGY STORAGE SYSTEMS

BESS are complex systems that can be explored at many levels. At first, there is the cell level, which is the core. Cells are electrochemical systems composed of two parts: (i) anode, in which oxidation reactions occur; (ii) cathode, in which reduction reactions occur. Both anode and cathode are composed by an electrode, an electrolyte and are separated by a semi-permeable membrane whose role is allowing positive ions created by oxidation to migrate from one electrode to another. In electrochemical systems flux of charges (i.e. currents) are generated by redox reactions on electrode-electrolyte interface, triggered by reactant concentration and voltage difference between electrodes [60]-[61].

Batteries are closed systems, meaning that the mass of reactants and products stored inside is constant. The State of Charge (SoC) measures the energetic content of a cell. It ranges from 0% (battery fully discharged) to 100% (battery fully charged). Current is usually taken into account in terms of C-rate, which is the ratio between current and nominal capacity.

Regarding the technological level, different types of battery are available in commerce [67]-[68]. The most promising in terms of specific energy and power, range of applications and efficiency is the Li-ion technology. The main issues about Li-ion are two: the high investment cost and lifetime. Lifetime is defined as the period after which a certain decay in performances is achieved (it is usually considered a capacity decay of 20%). Hence, a battery operational strategy should be able to exploit battery potential without stressing it too much, decreasing lifetime. Main stress factors associated to cycle ageing are average C-rates, operational temperature and voltages [5]-[66]-[69]-[70]. Instead, the quantities that most affect calendar ageing are storage temperature and SoC level [76]-[79]. However, most of ageing processes cannot be studied independently and occur at similar timescales, complicating the investigation. Safe and correct operation of battery requires auxiliaries. A BESS is made by several components:

- Cell modules and packs
- Air conditioning system
- Sensors and control system
- Inverter
- Battery Management System (BMS)

The role of the BMS is to prevent excessive operating voltages in order to reduce oxidative stress.

A BESS is characterized by a nominal capacity, nominal voltage and a nominal current. The product of the former two is the nominal energy. The product of the latter two is the nominal power. The ratio between nominal energy and power is called EPR (Energy-to-Power Ratio).

The last level concerns battery modelling. Different types of models are present in literature [80]:

- Electrochemical (or physical) models: technical parameters derive from the solution of differential equations, capturing the actual physical processes during cell operation.
- Electrical models: the battery is treated as an electrical RC circuit with variable number of parallel and series RC branches.
- Empirical models: the battery operation is approximated by simple equations derived experimentally.

The electrochemical model is the more accurate and, in principle, it is able to evaluate, every quantity and phenomenon happening inside the cell, from chemical reactions to mass transport. On the other hand, it is time consuming. The empirical model shows opposite characteristics: high computational speed, but poor description of cell operation. An example of this family is the variable efficiency model, in which efficiency is a function of power in per unit. A tradeoff between the previous two is the electrical model: still, it does not consider the physics of the cell but it is still able to deliver useful quantities like operating

voltage and currents. Other types of models are also present, such as Stochastic ones.

3. ANCILLARY SERVICES MARKET

The Ancillary Services Market (ASM) is a particular phase of the electricity market in which the TSO acquires all the resources necessary to guarantee a high level of reliability and security of the network. For what concerns frequency regulation, three reserves are traded on the ASM: Primary, Secondary and Tertiary control reserves. In this Section, PCR and SCR provision are detailed.

The goal of PCR is to contain the frequency variation occurring soon after a perturbation and stabilize it at a generic constant value within admissible limits. The activation of this reserve is automatic and very fast. The control action of PCR is named Droop Control Law and its representation is given in *Fig. I*.

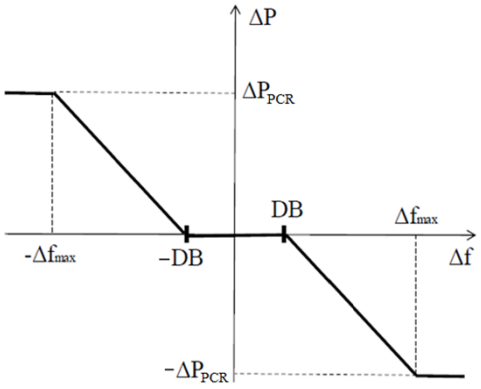

Fig. I – Droop control curve.

The main parameter is the droop: it represents the ratio between the frequency variation in per unit and the real power variation in per unit. The equation for droop calculation is the following:

$$droop = -\frac{\frac{\Delta f}{f_{nom}}}{\frac{\Delta P}{\Delta P_{PCR}}} \cdot 100 \quad [\%] \qquad (I)$$

Where f_{nom} is the nominal frequency and ΔP_{PCR} is the regulating band offered for this service. Another parameter is the Dead Band (DB): it is a small band around the nominal frequency where no power needs to be provided. The working principle of PCR is the following: in case of under frequency ($\Delta f < 0$), generators are asked to increase their power production $\Delta P > 0$ (the positive reserve is exploited); in case of over frequency ($\Delta f > 0$), generators are asked to decrease their power production $\Delta P < 0$ (the negative reserve is used). In Italy, Terna defines the service specifications in [24]. In particular, PCR provision is mandatory for all the production units with nominal power greater than 10 MVA (Relevant Production Units). All the relevant units must guarantee at least 1.5% of nominal power as PCR. Other technical prescriptions are: intentional DB not greater than 10-20 mHz and fixed droop between 2-5% depending on the type of generating unit. Nowadays, BESSs are not allowed to provide PCR in Italy. Unlikely traditional generators, BESSs do not have a scheduled production and they can be fully dedicated to this service. Hence, the droop could be rescaled according to the following expression:

$$droop_{BESS} = \frac{1.5}{100} \cdot \frac{droop}{\dot{\Delta P}_{PCR}} \quad [\%] \qquad (II)$$

Where $\dot{\Delta P}_{PCR}$ is the regulating band of the BESS offered for PCR in per unit. For instance, the range 2-5% for droop is translated in the range 0.03-0.075% for BESSs that adopt 100% of their nominal power as regulating band for PCR.

The scope of SCR is to bring the frequency back to its nominal value. SCR operates on a longer time scale with respect to PCR and can be activated either automatically or manually [18]. SCR provision is centrally directed by the TSO. In Italy, SCR provision is a symmetric service and the TSO defines each minute a signal, called Area Control Error - ACE (Livello Regolazione Secondaria is the Italian name), which represents the percentage of SCR (ΔP_{SCR}) required to each production unit [24]. The ACE is a signal between 0 and 100, whose meaning is:

$$\begin{cases} \Delta P = \Delta P_{SCR} & if\ ACE = 100 \\ \Delta P = 0 & if\ ACE = 50 \\ \Delta P = -\Delta P_{SCR} & if\ ACE = 0 \end{cases} \qquad (III)$$

The regulating power ΔP varies linearly for intermediate values of ACE. Asymmetric

SCR bands can be an innovative solution for BESSs: positive and negative bands are decoupled and they can be used separately to control the SoC of the battery.
The most challenging requirement for a BESS is service continuity. If the battery reaches its capacity limits, service provision is interrupted and penalties must be paid. In this study, an indicator of technical performance to evaluate service continuity is introduced: Loss of Regulation (LoR).

$$LoR = \frac{E_{np,service}}{E_{req,service}} \cdot 100 \quad [\%] \qquad (IV)$$

Where $E_{np,service}$ is the energy not provided and $E_{req,service}$ is the total energy required by the service in the evaluated period.

4. PREDICTIVE ANALYTICS

As previously introduced, in case of multi-service provision, a forecasting tool is needed to optimally allocate SCR bands. Therefore, the main concepts are introduced in this Section. Predictive analytics is a broad term describing a variety of advanced statistical and analytical techniques used to develop models that predict future events or behaviors [40]. It involves a large amount of data. Hence, data management represents one of the main issues in this field. All the available data are typically separated in two sets: (i) a training set, used to build forecasting model; (ii) a test set, used to evaluate its accuracy.
The forecast error is defined as the difference between an actual value y_t and its forecast $\hat{y}_t$. Starting from the forecast error, forecast accuracy can be measured through different metrics. Two of the most commonly used metrics are:

- Mean Absolute Error (MAE)

$$MAE = \frac{1}{T} \cdot \sum_{t=1}^{T} |y_t - \hat{y}_t| \qquad (V)$$

- Root Mean Square Error (RMSE)

$$RMSE = \sqrt{\frac{1}{T} \cdot \sum_{t=1}^{T} (y_t - \hat{y}_t)^2} \qquad (VI)$$

Where T is the number of predicted time steps (i.e. the number of predictions). A selection criterion for the choice of the prediction method could be to compare the RMSE with the standard deviation, which represents the spread of actual data around the mean. If the RMSE is higher than the standard deviation, the prediction method is worse than predicting with the mean and vice versa.
In this work, the focus is on time-series prediction. Many predictive models for time-series may be found in literature [46]-[50]-[51]. In particular, two Artificial Intelligence (AI) methods are highlighted in this study: Random Forest (RF) and Non-linear Autoregressive Exogenous (NARX) Neural Network.
A RF is an ensemble of simple Decision Trees. The Random Forest generates several subsets of data from the original training sample through random sampling with replacement. Each subset is used to train a decision tree (see *Fig. II*).

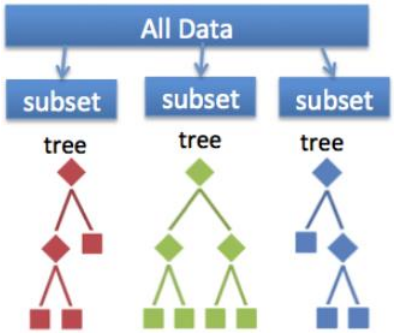

Fig. II – Structure of a Random Forest.

In each tree, the RF takes a random selection rather than all features when splitting data: splitting is based on the most significant feature in the random subset until a stopping criterion is met. Once the RF is created, several forecasts are generated starting from the same inputs. The final prediction is obtained by averaging all the predictions of the decision trees.
A NARX Neural Network is a type of Artificial Neural Network (ANN) suitable for predicting time-series [57]-[58]. In general, an ANN is a black-box modelling tool, which models complex non-linear relationships

between inputs and outputs. It is inspired on the biological nervous systems [55]. The architecture of an ANN consists of: (i) input layer, which collects information from the external environment; (ii) hidden layer, which performs computations and does not have any direct connection with the outside world; (iii) output layer, which transfers information coming from the network to the outside world.

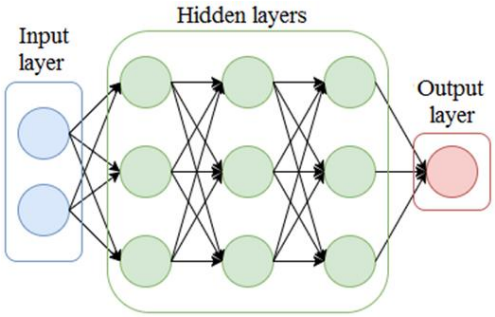

Fig. III – Architecture of an ANN.

The NARX neural network uses a time-delayed architecture with a feedback connection from the output to the input layer [59]: this memory ability allows the use of the past values of predicted or true time series and it may improve the overall performance. Two are the possible architectures of a NARX neural network: (i) open loop, where the forecast is made by using the present and past values of the inputs and the true past value of the time-series; (ii) closed loop, in which the prediction is made starting from the present and past values of the inputs and the past predicted values of the time-series.

5. PROPOSED METHODOLOGY

This Section is dedicated to the models adopted in the simulations of single and multi-service provision. All the models are developed in a MATLAB®-Simulink™ environment. Moreover, the main indices for performance evaluation are explained.

BESS model

The cell model adopted in this study is a simple passive electrical model in the time-domain, shown in *Fig. IV*.

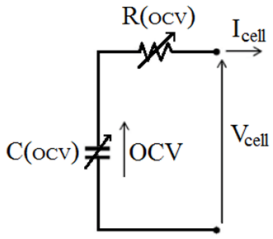

Fig. IV – Electrical model of the cell.

The resistance and the capacitance have been identified experimentally through EIS and OCV tests performed on a particular Li-ion cell: the Boston Power Swing 5300 [5]. The cell is characterized by a simple Battery Management System (BMS), which limits the current output of the cell if the voltage reaches its lower or upper limits.

In this model, a full charge-discharge cycle is defined when the throughput Ah are equal to twice its nominal capacity of the cell (C_{nom}).

$$cycles_{tot} = \int_{t_{start}}^{t_{end}} \frac{|I_{cell}(t)| \cdot dt}{2 \cdot C_{nom}} \quad [\,] \qquad \text{(VII)}$$

Regarding BESS lifetime, calendar ageing is given (12 years), while cycle ageing is modelled through a simple empirical model: capacity decay per cycle is a function of the average C-rate, according to the experimental curve in *Fig. V* [5].

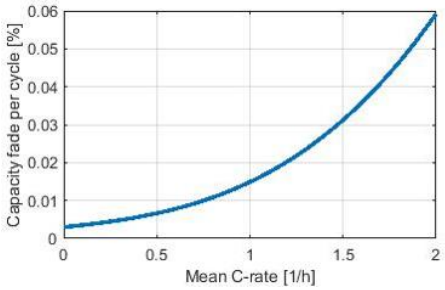

Fig. V – Capacity fade estimation [5].

The maximum number of cycles is calculated by taking into account that the End of Life (EoL) of a battery is when the capacity becomes the 80% of the initial value. Finally, the BESS lifetime in years is calculated dividing the maximum number of cycles by the equivalent number of cycles in one year.

The inverter is modelled through a simple low-pass filter, with an efficiency (as function of the power in per unit) and a time constant.

The energy efficiency of the cell $\eta_{E,cell}$ and the system $\eta_{E,sys}$ are computed as the ratio between the energy cycled during the discharging phase and the energy cycled during the charging process when the final SoC variation is equal to zero:

$$\eta_{E,cell} = \frac{\int_{disch} V_{cell} \cdot I_{cell}\, dt}{\int_{ch} V_{cell} \cdot I_{cell}\, dt} \quad \text{(VIII)}$$

$$\eta_{E,sys} = \frac{\int_{disch} P_{out,sys}\, dt}{\int_{ch} P_{out,sys}\, dt} \quad \text{(IX)}$$

Where V_{cell} is the cell voltage, I_{cell} is the current flowing in the cell and $P_{out,sys}$ is the real power exchanged by the BESS with the electrical grid.

Model for single service provision: PCR

The standard fixed Droop Control Law is considered as base case. Moreover, different SoC restoration strategies are implemented:

A. Variable droop strategy: the droop is not fixed, but it can vary in a defined interval depending on the SoC of the BESS; no power set point is imposed, but the droop characteristics is modified.
B. Dead Band strategy: when the frequency variation is inside the DB, the controller defines a power set point to bring the SoC back to the reference value.
C. SoC restoration with service interruption: when this strategy is activated, PCR provision is interrupted and a high power set point is defined to restore the SoC and limit the duration of the interruption.
D. SoC restoration without service interruption: the power set point to restore the SoC is superimposed to the power required for PCR provision.

Two types of PCR remuneration schemes are adopted: the Italian and the Central Western Europe (CWE) one. In Italy, PCR is not subject to a market and its remuneration is energy-based. In particular, the hourly prices are defined in [25]. In CWE (e.g. in Germany), PCR is traded through a weekly auction and its remuneration is based on capacity (power) according to a pay-as-bid mechanism [28].

In case of SoC control strategy, also the revenues/costs for the energy traded for SoC restoration must be taken into account. In this study, a hypothesis is made: this energy is traded always considering the average remunerations for positive and negative PCR over the period of simulation.

Model for multi-service provision: PCR and asymmetric SCR

In this case, PCR and asymmetric SCR provision are implemented. The SCR market model is mainly inspired on the framework of the Italian ASM. In particular, two constraints are considered: there are 6 market sessions of 4 hours each (i.e. the regulating bands offered on the market are constant for 4 hours) and offers must be placed on the market at least one and a half hours before the beginning of the market session [15]. The only difference is represented by the possibility to have asymmetric SCR bands, as already happens in Germany: in this case, SCR band allocation can be used as a SoC restoration strategy. The SCR controller includes a MATLAB® function, which receives many inputs, including the forecasts of the regulating energies associated to both PCR and SCR in the successive five and a half hours, and calculates the asymmetric SCR bands for the following market session ($\Delta\dot{P}_{SCR,+}$ and $\Delta\dot{P}_{SCR,-}$ in per unit of nominal power of the BESS). Finally, the actual power set points required to the BESS are determined by the ACE, which represents the percentage of SCR band required by the TSO:

$$\begin{cases} \Delta P_{SCR} = \Delta\dot{P}_{SCR,+} \cdot P_{nom}, & ACE = 100 \\ \Delta P_{SCR} = 0, & ACE = 50 \\ \Delta P_{SCR} = -\Delta\dot{P}_{SCR,-} \cdot P_{nom}, & ACE = 0 \end{cases} \quad \text{(X)}$$

The regulating power ΔP_{SCR} varies linearly for intermediate values of ACE.

Regarding the remuneration models, for what concerns PCR, both the Italian and the CWE mechanisms described in the previous Section are considered.

The only SCR remuneration scheme adopted is inspired to the Italian one. In this study, a simplifying assumption is made: the SCR bands are always accepted on the market at

the average hourly prices in €/MWh bid for both positive and negative SCR.

Performance evaluation

Performance evaluation of both single and multi-service provision is mainly based on the following quantities: (i) LoR, as the main indicator of technical performance; (ii) Net Present Value (NPV) and Profitability Index (PI), as indices of economic performance.

The NPV [€] is defined as follows:

$$NPV = -C_{inv} + \sum_{y=1}^{N} \frac{NCF(y)}{(1+r)^y} + \frac{RV(N)}{(1+r)^N} \quad \text{(XI)}$$

Where C_{inv} is the initial investment, N is the investment period (20 years), $RV(N)$ is the residual value of the BESS, r is the actualization rate (6%) and $NCF(y)$ is the yearly Net Cash Flow. $NCF(y)$ includes the revenues for single or multi-service provision, the penalties for service interruptions, the revenues for energy transactions (in case of SoC restoration strategy) and the eventual replacement cost of the battery. If $NPV > 0$ the investment is convenient.

The PI is used for comparing investments of different sizes (i.e. sensitivity analysis on the EPR) and it can be calculated as follows:

$$PI = 1 + \frac{NPV}{C_{inv} + \sum_{y=y_{replacement}} \frac{C_{rep}(y)}{(1+r)^y}} \quad \text{(XII)}$$

Where $C_{rep}(y)$ is the replacement cost in year y. If $PI > 1$ the investment is attractive.

6. SIMULATION & RESULTS: SINGLE SERVICE PROVISION (PCR)

Setup of simulations

All the simulations of PCR provision are performed on 30 days considering a real frequency profile measured in the IoT-Storage Lab in Politecnico di Milano in the period 15 Februray-16 March 2017.

The technical and the economical parameters adopted in the simulations are collected in *Tab. I*. The data necessary for the Italian PCR remuneration, according to the mechanism described in [25], are given by GME [115] and Terna [116].

Comparison of SoC restoration strategies

The simulation of standard PCR provision (i.e. fixed droop) is considered as base case. A high LoR of 17.5% is obtained and this is not positive from the technical point of view. For what concerns the NPV, the Italian remuneration scheme is absolutely not convenient ($NPV_{ITA} = -497.3\ k€$), while the German one generates a positive NPV after 20 years ($NPV_{GER} = 726.0\ k€$). For this reason, in the following analysis, only the NPV calculated with the German remuneration mechanism is considered.

For each SoC control strategy, a sensitivity analysis is performed in order to identify the optimal configuration to be compared with the other methods:

A. Variable droop: the optimal droop range is identified in 0.075±0.045%.

Parameters	Symbol	Value
Nominal power	P_{nom}	1 MW
Nominal energy	E_{nom}	1 MWh
Initial SoC	SoC_{start}	50%
Minimum/maximum SoC	SoC_{min}/SoC_{max}	0%/100%
Droop	-	0.075% (equivalent to 5%)
Dead band	DB	20 mHz
PCR regulating band	$\Delta\dot{P}_{PCR}$	100%
Reference SoC	SoC_{ref}	55%
Specific BESS cost	c_{BESS}	400 €/MWh
Replacement factor	k_{rep}	0.5
German PCR remuneration	p_{GER}	2500 €/MW per week
LoR valorization	p_{LoR}	150 €/MWh
Price of restoration energy injected	$p_{rest,+}$	95 €/MWh
Price of restoration energy absorbed	$p_{rest,-}$	30 €/MWh

Tab. I – Technical and economic parameters adopted in single service simulations.

B. Dead Band: a restoration power equal to 10% the nominal power is taken as optimal value.
C. SoC restoration with service interruption: a 200% restoration power set point is considered.
D. SoC restoration without service interruption: 10-90% SoC activation thresholds and a restoration power equal to 50% the nominal power are used.

The main results of the comparison among the different SoC control strategies are shown in *Tab. II*. Any SoC control strategy improves the service provision (i.e. LoR decreases), but BESS lifetime is reduced due to a higher utilization of the battery in terms of average C-rate and cycles. From the economic perspective, all the strategies improve the NPV with respect to the base case. The highest NPV belongs to the DB strategy, followed by SoC restoration without service interruption. In particular, SoC restoration without service interruption shows a high NPV and a LoR close to zero: it does not suffer a possible increase of LoR valorization (p_{LoR}). Conversely, the NPV of all the other strategies decreases a lot if the price for the energy not provided increases, as shown in *Fig. VIII*. For this reason, SoC restoration without service interruption is identified as the best strategy and an optimization of its main parameters is performed.

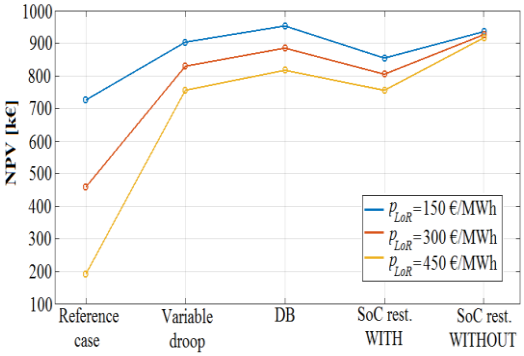

Fig. VI - Impact of p_{LoR} on the NPV of the different strategies.

Optimization of the best strategy

Firstly, SoC activation thresholds and restoration power set point are investigated: (i) 5-95%, 10-90% and 15-85% SoC thresholds; (ii) 25%, 50% and 75% of the nominal power as restoration power set points. SoC thresholds equal to 5% and 95% show the worst performances (i.e. highest LoR and lowest NPV) in all the cases. The optimal configuration is identified in 15-85% SoC thresholds with 50% of nominal power as restoration power set point: its NPV is the highest among all the configurations (954.8 k€) and LoR is zero.

Afterwards, a sensitivity analysis is performed on the reference SoC (SoC_{ref}) at which the restoration strategy stops. Four values are considered: 50%, 55%, 60% and 65%. LoR is null for all SoC_{ref} values. For what concerns the NPV, the lowest value is

STRATEGIES	BASE CASE	VARIABLE DROOP	DB	SoC REST. WITH	SoC REST. WITHOUT
Tot. energy [MWh/month]	64.8	69.8	119.9	85.9	84.0
Cycles [#/month]	32.0	34.5	59.2	42.4	41.2
Average C-rate [1/h]	0.252	0.279	0.164	0.341	0.315
LoR	17.5%	4.9%	4.4%	3.2%	0.6%
BESS lifetime [years]	15.1	10.3	7.2	7.6	8.2
NPV_{GER} [k€]	726.0	903.4	953.1	854.5	935.6

Tab. II – Results of the different SoC restoration strategies.

EPR	0.5	0.75	1	1.25	1.5	1.75
Tot. energy [MWh/month]	89.7	86.5	85.0	85.7	83.5	83.6
Cycles [#/month]	88.9	57.0	41.7	33.5	27.3	23.4
Average C-rate [1/h]	0.650	0.427	0.316	0.254	0.210	0.179
LoR	2.8%	0.3%	0.0%	0.0%	0.0%	0.0%
BESS lifetime [years]	2.2	4.9	8.1	11.1	14.6	17.8
PI	2.22	2.58	2.61	2.44	2.05	1.77

Tab. III – Results of the sensitivity analysis on the EPR (single service).

obtained for a reference SoC equal to 50% ($NPV = 939.7\ k€$), while the other NPVs are similar. Therefore, in order not to have an excessive unbalance between the reference SoC and SoC thresholds (15-85%), SoC_{ref} equal to 55% is chosen as the optimal value ($NPV = 954.8\ k€$).

Finally, a sensitivity analysis is made on the EPR, assuming a constant nominal power (1 MW) and varying the nominal energy of the BESS. Six values of EPR are considered: 0.5, 0.75, 1, 1.25, 1.5 and 1.75.

The results in *Tab. III* show that by increasing the EPR, the number of cycles and the average C-rate decrease. In particular, when the EPR is equal to 0.5 and 0.75, the average C-rate is very high: the battery is particularly stressed and this causes a very low lifetime. Moreover, since the BESS is smaller for those values of EPR, a non-zero LoR is observed. In all the other cases ($EPR \geq 1$) LoR is null. In this case, the PI is considered for comparing investments of different sizes. All the configurations are characterized by $PI > 1$, which means that the investment is always attractive. The lowest values for the PI are registered for EPR equal to 1.5 and 1.75: this is because the initial investment costs are very high due to the big dimensions of the BESS (i.e. high nominal energy). EPR equal to 0.5 is not the best solution because the lifetime of the BESS is too short and replacement costs decrease the overall PI. A maximum for the PI may be identified for EPR values between 0.75 and 1.25. In particular, an EPR equal to 1 is identified as the best value because it is characterized by the highest PI and a LoR equal to zero.

7. SIMULATION & RESULTS: MULTI-SERVICE PROVISION (PCR AND ASYMMETRIC SCR)

In this case, asymmetric SCR band allocation works as SoC restoration strategy. As stated in *Section 5*, the SCR controller needs to be fed with predictions of regulating energy associated to PCR and SCR covering the next five hours and a half. These quantities fully depend on regulating signals that are European grid frequency for PCR [114] and ACE for SCR [118].

A preliminary statistical study has been performed in order to understand the main characteristics of these signals, which are useful for the implementation of prediction methods. Even if they may appear stochastic, daily patterns related to market structure, together with seasonal features, have been spotted. After this assessment, an optimization of the prediction methods has been performed, considering label-type predictors (month, time of the day, type of day) and endogenous-type predictors (i.e. predictors built starting from past values of regulating signals and regulating energy). The methods considered in this study are:

- Statistical method
- Random Forest
- NARX neural network
- Floating NARX (the net is trained not considering the whole training set but only few days before prediction)
- Hybrid Approach (two or more methods are matched together)

Tab. IV shows the comparison among the different methods considering the RMSE on test set, regulating bands of 1 MW for both services and droop equal to 0.075%. Y_{1P} and Y_{2P} refer to PCR, respectively considering the hour and half after prediction instant and the following four-hour market session. Y_{1S} and Y_{2S} refer to SCR regulating energy for the same periods.

	Stat	RF	NARX	Fl. NARX	Hybrid
Y_{1P}	0.106	0.096	0.094	0.108	0.090
Y_{2P}	0.208	0.191	0.188	0.239	0.177
Y_{1S}	0.630	0.600	0.589	0.595	0.545
Y_{2S}	11.856	11.425	11.508	11.536	10.807

Tab. IV – Comparison of RMSE (in MWh) for different prediction methods.

Setup of simulations

All simulations are performed on 294 days (13/03/2017-31/12/2017) and results are scaled on a monthly basis. The technical setup is given in *Tab. V*. The economic parameters are the same of Tab. I. PCR

Parameters	Symbol	Value
Nominal power	P_{nom}	1 MW
Nominal energy	E_{nom}	1 MWh
Initial SoC	SoC_{start}	50%
Minimum/maximum SoC	SoC_{min}/SoC_{max}	0%/100%
Droop	-	0.15% (equivalent to 5%)
Dead band	DB	20 mHz
PCR regulating band	$\Delta\dot{P}_{PCR}$	50%
SCR regulating band	$\Delta\dot{P}_{PCR}$	Variable – Max 80%

Tab. V – Technical parameters adopted in multi-service simulation.

remuneration is computed using the German ASM paradigm, while SCR remuneration, as stated in Section 5, is inspired by the Italian regulation. The rational behind this hybrid market structure is the following: Italian PCR, being mandatory, does not have a dedicated market, hence it is not profitable by itself. Conversely, German SCR is traded on weekly auctions, making it ineligible for a SoC restoration strategy.

Forecasting methods comparison

Results of forecasting methods comparison are shown in *Tab. VI*. Single PCR provision ($\Delta\dot{P}_{PCR}$ =100%) is used as base case. Its results are similar to previous base case (*Tab. II*) since the only aspect for which they are different is the simulation period. All methods show similar results. In particular, frequency regulation is enhanced (+30% energy fluxed by the battery) with a positive impact on LoR. Moreover, a lower C-rate means that the battery is working more continuously, reducing time in which it is idle. In all the cases, the NPV is lower with respect to the base case because PCR remuneration still plays a major role: considering the Hybrid Approach, in each month, 5536 € come from PCR provision (equal for all the multi-service cases since the PCR band is the same), 2760 € come from SCR provision and 358 € are the LoR penalties. In the base case, monthly net revenues are 8871 €, consisting of 11072 €, coming from PCR, minus 2201 € that represents LoR penalties (much higher than the previous case). Subsequent analysis evaluates the impact of EPR on the operation using the Hybrid approach, which is the best in terms of NPV and LoR.

Sensitivity analysis on EPR

Results are shown in *Tab. VII*. The main difference varying EPR values regards energy fluxes, which are determined by energy required by SCR. This happens because the BESS has a higher capacity and larger SCR bands are defined, as shown in *Fig. VII*. This helps to understand the working principle of the controller: when SoC is close to 100%, a big discharging band and a small charging band are allocated and the opposite when the SoC is close to 0%. The increase in fluxes is coupled with a decrease in LoR, enhancing service provision: the larger the SCR bands, the higher the SoC restoration potential. At high EPR, both cycles and C-rate decrease, leading to lower stress for the battery.

PREDICTION METHOD	BASE CASE	STATISTICAL	NARX	HYBRID APPROACH
Tot. energy [MWh/month]	59.4	89.8	95.9	95.2
PCR required [MWh/month]	70.1	35.0	35.0	35.0
SCR required [MWh/month]	-	66.8	73.4	72.1
Cycles [#/month]	30.1	43.7	46.7	46.3
Average C-rate [1/h]	0.241	0.124	0.133	0.132
LoR	20.9	3.3	2.8	2.2
BESS lifetime [years]	12.8	10.6	9.8	9.9
NPV [k€]	719.3	517.0	551.0	558.9

Tab. VI – Results of multi-service with different prediction methods.

EPR	0.5	0.75	1	1.25	1.5	1.75	2
Tot. energy [MWh/month]	55.4	76.7	95.2	113.3	131.3	148.9	166.1
PCR required [MWh/month]	35.0	35.0	35.0	35.0	35.0	35.0	35.0
SCR required [MWh/month]	26.7	51.3	72.1	92.1	111.6	130.6	149.0
Cycles [#/month]	53.8	49.7	46.3	44.2	42.7	41.6	40.7
Average C-rate [1/h]	0.176	0.143	0.132	0.125	0.120	0.117	0.114
LoR	5.0	2.8	2.2	1.9	1.7	1.6	1.5
BESS lifetime [years]	7.9	9.1	9.9	10.5	10.9	11.3	11.6
NPV [k€]	509.1	550.5	558.9	566.1	563.2	568.4	561.2
PI	2.69	2.27	1.97	1.90	1.74	1.65	1.56

Tab. VII - Results of the sensitivity analysis on the EPR (multi-service).

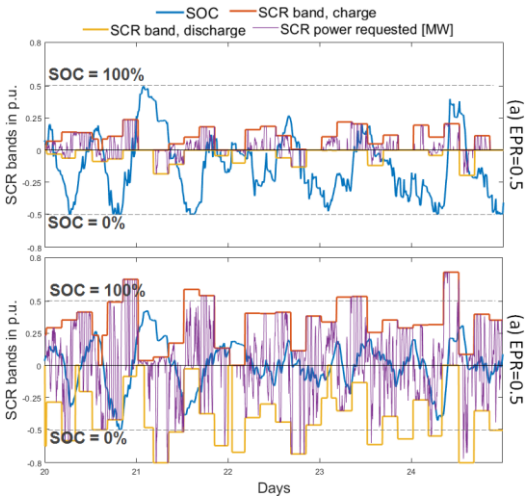

Fig. VII - SoC and SCR band management at: (a) EPR=0.5; (b) EPR=2.

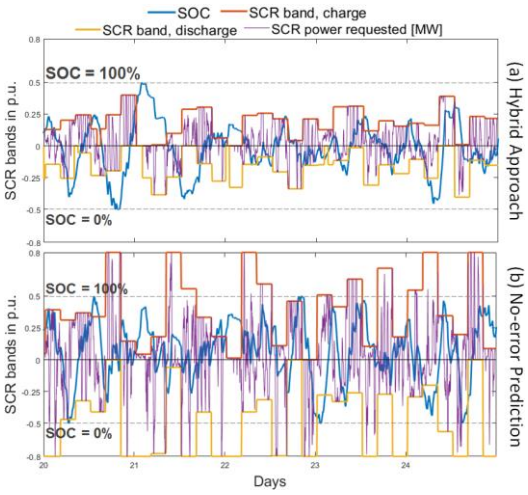

Fig. VIII - SoC and SCR band management in case of: (a) Hybrid Approach; (b) No-error Prediction.

The NPV presents a maximum at EPR=1.25, while the PI decreases with the increment of EPR because of higher investment cost.

No-error Prediction

Lastly, an ideal case is investigated: No-error Prediction, which consists in feeding the SCR controller with actual values of regulating energy. The aim of this Section is to provide an upper limit of prediction accuracy in order to evaluate the response of the system. The net effect is the doubling of SCR regulating energy, together with the revenues from this service. SCR bands often saturate, since there is no uncertainty to manage (*Fig. VIII)*. Despite these increased fluxes, LoR remains at 2.6% and NPV is the highest obtained in Multi-service simulations (717.4 k€). This outcome opens fruitful possibilities for further researches aimed to improve the prediction tools proposed in this study and investigate new ones.

8. CONCLUSION

In this work, the ability of a Battery Energy Storage System (BESS) in providing frequency services to the electrical network has been investigated. Two cases have been analysed: Single Service (PCR) and multi-service (PCR and Asymmetric SCR). PCR and SCR remuneration have been modelled following respectively German and Italian regulation.

Concerning single service provision, a SoC management strategy is necessary. Four strategies have been compared: all of them are able to improve the quality of service, decreasing the LoR and improving the economic return of BESS operation.

Regarding multi-service, SCR bands allocation is used for SoC restoration. A prediction tool is necessary since, in Italy, SCR bands must be placed on the market one hour and a half before the market session

begins. Five methods have been compared (Statistical, Radom Forest, NARX, Floating NARX, Hybrid Approach) and the best among them have been used to feed the SCR controller, which is an innovation introduced in this work. Results show how SCR can be effectively used for this purpose, leading to enhanced energy fluxes and acceptable levels of LoR. The value of EPR has a remarkable impact on the operation, especially in terms of LoR and PI.

Computational time must be taken into account when dealing with BESS models and the use of advanced modelling approaches, such as electrochemical, should be carefully evaluated if a large number of simulations is required or a large timeframe is considered.

Tab. VIII collects computational times for the analysis performed in the context of this study, considering an Intel® Core™ i7 4790-16GB RAM.

Main limitations of this work are the absence of a model for BESS auxiliaries and the fact that SCR bands are always accepted on the market.

Possible directions for future researches regard the inclusion of the effect of the auxiliaries, the implementation of a price allocation strategy for SCR, the improvement of forecasting techniques and the coupling of BESS providing grid services with other applications, such as renewables plant.

Simulation	Days	Computational effort	Number of scenarios simulated
Single service	30	1.15-1.30 h	32
Multi-service	294	12 h	12

Prediction Method	Training Period	Computational effort	Number of trainings performed
RF	2 years	2 h	30
NARX	2 years	1 h	120
Floating NARX	7 days	Seconds	25

Tab. VIII - Computational cost of the analysis performed in this work.

Contents

ABSTRACT

The scope of this work is to verify the ability of a Battery Energy Storage System (BESS) in providing Ancillary Services to the electrical grid. In particular, two services are investigated: Primary Control Reserve (PCR) and Secondary Control Reserve (SCR) provision. Firstly, only PCR provision is analysed considering both the Italian and German market models. Various State of Charge (SoC) restoration strategies are compared and the best one is optimized by varying its main parameters. Afterwards, multi-service provision is considered: PCR and asymmetric SCR. Either the Italian or the German market models are considered for PCR, while the SCR remuneration mechanism is inspired on the Italian scheme. The allocation of asymmetric SCR bands acts as a SoC control strategy. In case of multi-service, it is fundamental to forecast the SoC at the end of the following market session in order to optimally allocate SCR bands: different forecasting techniques are implemented and their performances on multi-service provision are evaluated.

The first three chapters provide a literature review of: (i) BESS, with particular focus on the Li-ion technology adopted in this work; (ii) Ancillary Services Market, with particular attention to the Italian and German paradigms; (iii) predictive analytics, useful for multi-service implementation. In *Chapter 4*, the methodology is explained and the models of the BESS, PCR controller and SCR controller are presented. All the models are developed in a MATLAB®-Simulink™ environment. The last two chapters show the results of the simulations.

Performance evaluation of both single and multi-service provision is mainly based on: (i) Loss of Regulation (LoR), as main indicator of technical performance; it is the percentage of power not provided with respect to the required quantity; (ii) Net Present Value (NPV) and Profitability Index (PI), as economic performance indices.

The main outcomes show that: (i) in case of single service provision, all the SoC management techniques improve both technical and economic performances and SoC restoration without service interruption is the best strategy; (ii) in case of multi-service provision, asymmetric SCR band allocation based on forecasting tools works as a passive SoC restoration strategy, leading to enhanced energy fluxes, low values of LoR and positive economic return.

Keywords: battery energy storage system; ancillary services; primary control reserve; secondary control reserve; multi-service; predictive analytics.

SOMMARIO

L'obiettivo di questo lavoro è verificare l'abilità dei sistemi d'accumulo a batteria (BESS) nel fornire servizi ancillari alle rete elettrica. In particolare, si analizzano due servizi: fornitura di riserva di controllo primaria (PCR) e secondaria (SCR). Inizialmente, si analizza esclusivamente la fornitura di PCR considerando sia il modello di mercato italiano che quello tedesco. Si confrontano varie strategie di controllo dello stato di carica (SoC) e si ottimizza la migliore. In seguito, si considera la fornitura di molteplici servizi: PCR e SCR asimmetrica. Per la PCR, si considerano i modelli di mercato italiano e tedesco, mentre la remunerazione della SCR si ispira allo schema italiano. L'allocazione di bande asimmetriche di SCR agisce come strategia di controllo del SoC. Nel caso di multi-servizio, è fondamentale prevedere lo stato di carica al termine della successiva sessione di mercato per allocare le bande di SCR in maniera ottimale: si implementano vari metodi di previsione e si valutano le loro prestazioni nella fornitura di multi-servizio.

I primi tre capitoli forniscono una revisione letteraria su: (i) BESS, in particolar modo sulla tecnologia a ioni di litio adottata in questo studio; (ii) mercato dei servizi ancillari, con particolare attenzione al modello italiano e tedesco; (iii) analisi predittiva, utile all'implementazione del multi-servizio. Nel *Capitolo 4*, si presentano la metodologia e i modelli del BESS, del controllore PCR e del controllore SCR. Tali modelli sono sviluppati in ambiente MATLAB®-Simulink™. Gli ultimi due capitoli mostrano i risultati delle simulazioni.

La valutazione delle prestazioni della fornitura di singolo o molteplici servizi si basa principalmente su: (i) perdita di regolazione (LoR), come principale indice tecnico; esso rappresenta la percentuale di potenza non fornita rispetto a quella richiesta; (ii) valore attuale netto (NPV) e indice di profittabilità (PI), come indici di valutazione delle prestazioni economiche.

I risultati principali mostrano che: (i) nel caso di singolo servizio, tutta le strategie di gestione del SoC migliorano sia le prestazioni tecniche che economiche e il ripristino del SoC senza interruzione del servizio è la strategia migliore; (ii) nel caso di multi-servizio, l'allocazione di bande asimmetriche di SCR tramite l'utilizzo di metodi di previsione funge da strategia di ripristino del SoC, determinando maggiori flussi energetici, diminuendo la LoR e generando un ritorno economico positivo.

Parole chiave: sistema d'accumulo a batteria; servizi ancillari; riserva di controllo primaria; riserva di controllo secondaria; multi-servizio; analisi predittiva.

INTRODUCTION

The global demand of electricity is continuously increasing. Developing economies, such as China and India, according to New Policies Scenario (NPS) defined by the International Energy Agency (IEA) [1], will account for the largest share of new demand, driven by rapid economic and population growth, the need for more goods and services and increasing policy push towards electrification. In particular, motor systems used in Chinese industry alone will account for almost a fifth of the increase in global electricity demand to 2040. Accelerating uptake of electric vehicles, air conditioners and electric water heaters in developing economies could increase demand growth even more rapidly. Meanwhile, in advanced economies, such as USA, European Union (EU) and Japan, continued efficiency improvements result in electricity demand staying relatively flat. The spread of electro-mobility and heaters for homes, offices and factories in the next years will cause a slight increase in electricity demand in these regions, but the higher efficiency of electric cars and heat pumps will reduce the additional amount of electricity needed for transportation and for heating purposes [1].

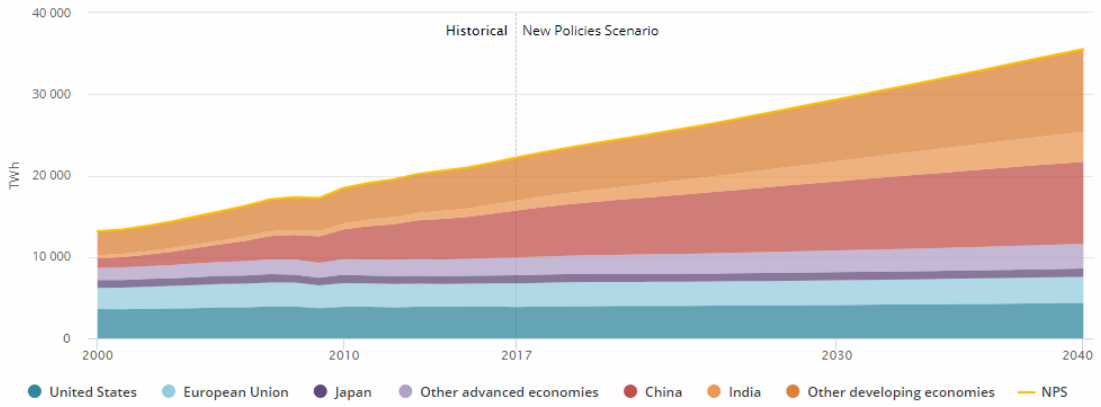

Figure 0.1 - Global electricity demand by region in the New Policies Scenario (NPS) [1].

Decarbonisation of electric energy production is one of the main outcome to achieve in order to mitigate climate change. International cooperation and paradigm shifts are necessary. Several steps have been made to design a roadmap for this achievement: Kyoto protocol was the first international agreement with this purpose, whose application started in 2007 [119]. Goal 7 and 13 of Sustainable Development Goals (SDGs), present in the 2030 Agenda for Sustainable Development (signed by

all UN Member States in 2015) also highlight the pivotal importance of this issue [120]. In recent years, the power generation mix has evolved due to the spread of Renewable Energy Sources (RES). RES are fundamental towards decarbonisation and reduction of Greenhouse Gases emissions. In the period 2011-2017, solar photovoltaic (PV) and wind energy experienced an annual capacity growth rate worldwide of 77% and 23% respectively [2]. Thanks to falling costs of technologies and favorable government policies, their power generation capacity is set to surge. In particular, solar PV will account for the largest growth, overtaking wind and hydropower generation capacity by 2025 and coal in the mid-2030s and becoming the second largest installed capacity globally, after gas.

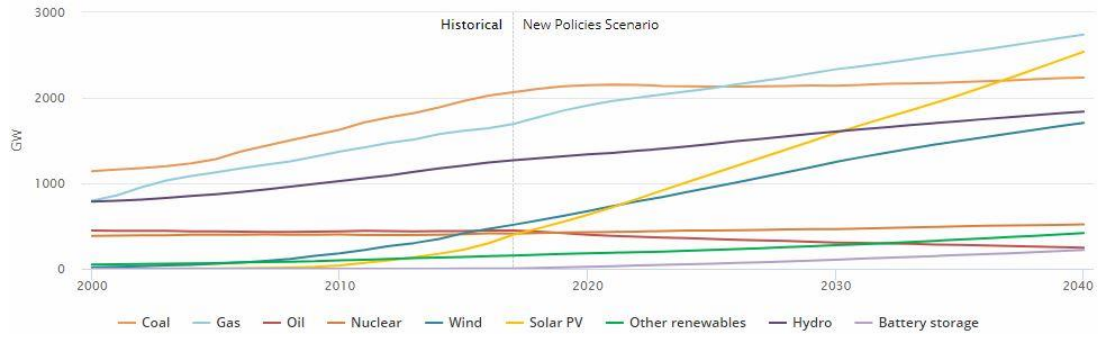

Figure 0.2 – Installed power capacity in the New Policies Scenario (NPS) [1].

Nevertheless, coal will remain the largest source of electricity generation, even though its share will stay relatively flat over time, and gas will nearly close the gap. Hydro will remain the largest source of low carbon electricity, followed by wind power and solar PV.

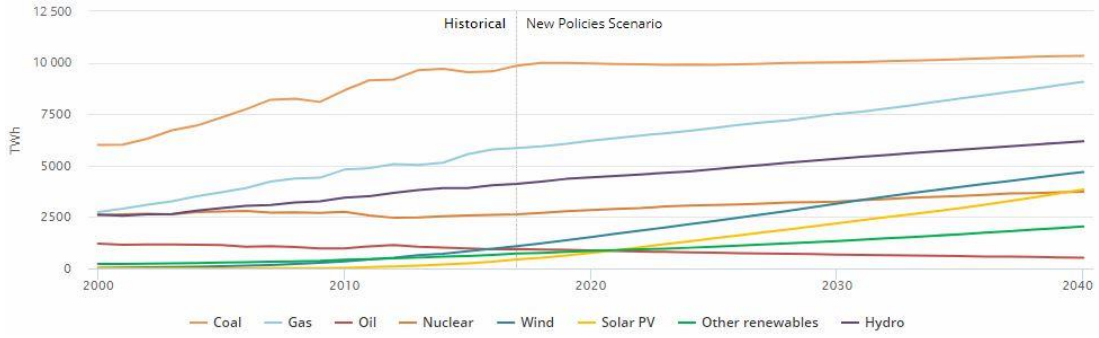

Figure 0.3 – Electricity generation in the New Policies Scenario (NPS) [1].

Unlike traditional fossil fuel plants and some forms of renewable electricity production (i.e. pumped hydropower, biomass and geothermal), solar PV and wind are non-programmable: they provide power only when the renewable resource is

available. This makes them less predictable and introduces variability in electricity supply. Furthermore, solar PV and wind generators are inverter-based systems and their diffusion causes a loss in the global inertia of the network, which is proportional to the overall mass of spinning turbines directly connected to the grid through transformers. At high levels of penetration of non-programmable RES, increased electricity production fluctuations may affect the reliability of the system. This is because, in the electric power system, electricity generation and demand must be always balanced. System operators measure this balance by monitoring system frequency. In Europe the system target is a grid-level frequency of 50 Hz, while in the USA it is 60 Hz. Failure to operate the system at its required frequency can disrupt the operation of equipment, disconnect power plants to prevent damage and lead to large-scale blackouts. For instance, on January 10, 2019, at 9 p.m., the frequency of the Continental Europe synchronous area decreased in few minutes down to a critical value of 49.8 (see *Figure 0.4*), putting in danger the whole power system. Blackout was avoided only thanks to the fast reduction of interruptible loads all around Europe. One of the causes of this disservice is recognized to be the political situation between Serbia and Kosovo [121].

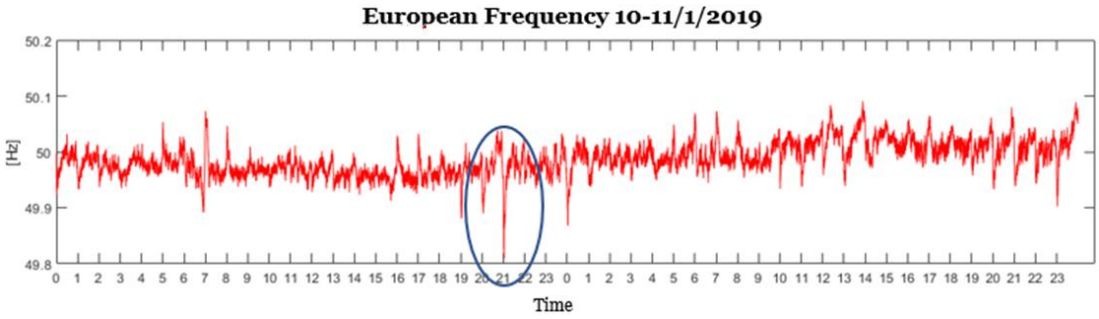

Figure 0.4 - Remarkable variation of Continental Europe frequency on 10/01/2019 [122].

Therefore, grid flexibility is necessary to ensure electricity supply reliability. Currently, traditional fossil fuel plants mainly provide flexibility by increasing or decreasing their electricity production. Nevertheless, the continuous growth of RES in the coming years may require other alternatives to maintain the system frequency. Dispatchable plants, demand side measures and energy storage systems represent a range of facilities for providing flexibility.

Energy storage is an important option to mitigate frequency deviations. Moreover, it can make variable renewables more dispatchable by storing excess electricity

production on site. According to literature [3], the large family of Electrical Energy Storage (EES) technologies includes:

- Mechanical Energy Storage (MES), such as pumped hydropower (PHS), flywheels (FES) and compressed air systems (CAES);
- Chemical Energy Storage (CES), which includes batteries (BESS), Hydrogen-based systems (HESS), such as fuel cells, and Flow-batteries (FB);
- Electro-Magnetic Energy Storage (EMES), such as capacitors, supercapacitors (SCES), superconducting magnetic coils (SMES);
- Thermal Energy Storage (TES), which includes high temperature (HTES) and cryogenic (CrES) energy storages.

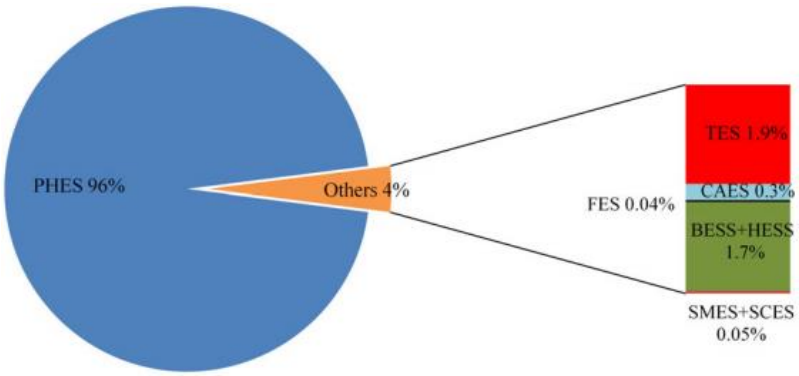

Figure 0.5 – Share of global installed EES capacity in 2018 [4].

The most mature energy storage technology, among the aforementioned ones, is pumped hydropower. It is economically and technically proven throughout the world. Presently, the 96% of the world's total installed EES comes from PHS alone and the remaining 4% capacity comes from all the other technologies (*Figure 0.5*).

By contrast, BESS represents a relatively new technology. In the last years, the installation of such a storage technology all over the world exponentially increased, as shown in *Figure 0.6 - (a)*. Batteries have found application in many industrial sectors, like automotive, energy, telecommunication, electronics, medical, etc. This huge increase in BESS demand can be explained by the fact that some of the aforementioned industrial sectors are the market response to some of the most important challenges of our today's society, such as the rise of electric vehicles (EV), the energy transition towards a renewable-based energy system and the rural electrification of developing countries [5]. Another key factor, which has encouraged the spread of BESS all over the world, is the continuous reduction of BESS cost over time. Among the leading BESS technologies available on the market, a special focus is

dedicated to Li-ion batteries in this work. In recent years, Li-ion cells have experienced a strong reduction of their cost (*see Figure 0.6 - (b)*), passing from about 800 €/kWh in 2010 to 250-300 €/kWh in 2018. Projections estimate a further cost reduction in the following years, reaching 100 €/kWh before 2030 [6].

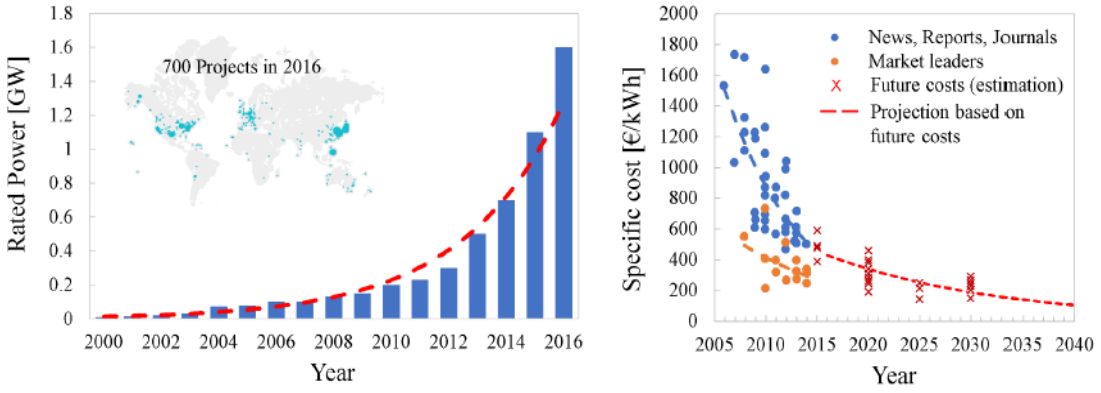

Figure 0.6 – (a) BESS stationary project installations over time [7]; (b) Cost of Li-ion battery packs [6].

BESS and other Energy Storage Systems, in general, are suitable for many stationary applications in the electricity sector, both off-grid and grid-tied applications. Off-grid BESS are typically coupled with renewables to provide electricity to remote areas of the world in the form of small stand-alone systems up to micro-grids. On the other hand, grid-tied BESS may be used to provide grid services on utility scale or for consumer use on domestic scale. In this study, the focus is on grid-tied BESS for the provision of grid services, better known as Ancillary Services (AS). Nowadays, AS are mainly provided by conventional generators, which are programmable and reliable. The unpredictable nature of RES, such as wind and solar PV, makes this kind of sources not suitable for ancillary services provision. In this context, either BESS can support non-programmable RES or they can be used as individual units in order to provide AS. Among the many grid-tied stationary applications of batteries, those related to frequency regulation are analysed since frequency balance represents an important issue in the power system, as previously introduced. In the specific case of batteries, when frequency is above the rated value, BESS are required to absorb power. Conversely, when frequency is below the nominal value, BESS are asked to release power. Two types of actions can be taken in order to control frequency: Primary Frequency Regulation (PFR) and Secondary Frequency Regulation (SFR). The goal of PFR is to block the frequency variation and to bring it to a generic stable value. This control action is referred as Droop Control Law and it is autonomous for

each resource in charge of providing this service. Primary frequency regulation starts automatically as soon as a frequency perturbation occurs (i.e. within seconds) in order to prevent the interruption of electric service. A Primary Control Reserve (PCR) is dedicated to this service. On the other side, the objective of SFR is to restore the nominal value of frequency. Its control action is not autonomous, but centrally directed. In Italy, the Transmission System Operator (TSO) defines each minute a signal, the Area Control Error (ACE), which defines the fraction of the regulating band to be used by each unit selected for SFR provision. This specific regulating band is known as Secondary Control Reserve (SCR). Secondary frequency control is slower than PFR (i.e. from tens of seconds to some minutes) and it is typically initiated automatically, but it can be also activated in response to manual dispatch commands. Moreover, there is a third control action, which operates on a longer time scale than PFR and SFR (i.e. from some minutes to tens of minutes), known as Tertiary Frequency Regulation (TFR). The Tertiary Control Reserve (TCR) is activated in order to restore the secondary control reserve. This service is centrally coordinated and its activation can be either manual or automatic. The deployment of TFR represents the final stage of the recovery period indicated on *Figure 0.7*. *Table 0.1* summarizes the main characteristics of the three services just described.

Table 0.1 - Main features of Primary, Secondary and Tertiary frequency regulation.

Service	Description
Primary Frequency Regulation (PFR)	To block the frequency variation and to bring it to a generic stable value. It starts automatically as soon as a frequency perturbation occurs.
Secondary Frequency Regulation (SFR)	To restore the nominal value of frequency. It is centrally directed and it is typically activated automatically.
Tertiary Frequency Regulation (TFR)	To restore the Secondary Control Reserves. It is centrally coordinated and it can be activated either automatically or manually.

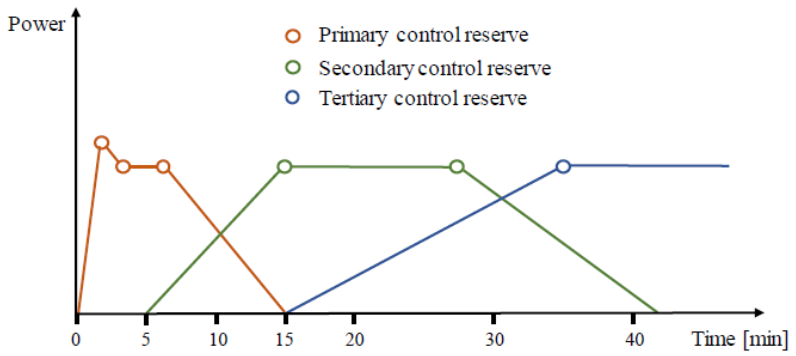

Figure 0.7 – Sequential actions of Primary, Secondary and Tertiary frequency control.

Ancillary Services, including frequency regulation services, are traded on the Ancillary Services Market (ASM). It is a phase of the electricity market, which typically takes place after the main market session, known as Day-Ahead Market (DAM). Most of energy is traded in the DAM, but this market session neglects the possibility of faults and errors by generators selected to provide their energy. The ASM represents the instrument through which the TSO acquires all the resources necessary to manage and control the system (creation of reserves, resolution of congestions between market zones, real-time balancing …). In order to guarantee the security of network, the TSO must find some reserves of power (capacity). Usually, these reserves are offered in subsequent ASM sessions by those generators, which still have capacity available after the DAM. Nowadays, the regulatory frameworks of the majority of ASM are tailor made on traditional generators. Most of ASM, including the Italian one (Mercato dei Servizi di Dispacciamento-MSD), are not open to BESS yet since batteries are different from conventional generators and more studies and feasibility analysis are needed. For this reason, several pilot projects involving BESS have been deployed all over the world in the last years. In Italy, the Transmission System Operator (Terna) has put in place many pilot projects in some critical areas of the Country, especially in Southern Italy, in order to analyse if BESSs can be used to reduce congestions and increase the security of the network [10]. Moreover, after the resolution 300/2017/R/eel by the Italian Authority [123], Terna has developed the pilot project UPI (Unità di Produzione Integrate), in which traditional plants delegate primary frequency regulation to a BESS [124].

Problem formulation

The scope of this work is to verify the ability of BESS in providing frequency grid services to the electrical network from both technical and economical point of view. This topic involves many complex fields and requires a comprehensive analysis. In particular, two services are deeply described and developed in the following chapters: Primary and Secondary frequency regulation. Initially, only PFR is analysed. Different State of Charge (SoC) management techniques are investigated, both in the Italian and Central Western Europe - CWE (e.g. Germany) ASM, in order to identify the best strategy and underline the main differences between the two market structures. Afterwards, the technical and economic feasibility of multi-service provision by using BESS in the Italian ASM perspective is analysed. It has been already investigated in some works [9]-[11]-[12]. In previous studies, statistical methods have been used to

allocate the Secondary Control Reserve. Instead, in this work, a step forward is made by using advanced forecasting techniques and a novel energy management control system.

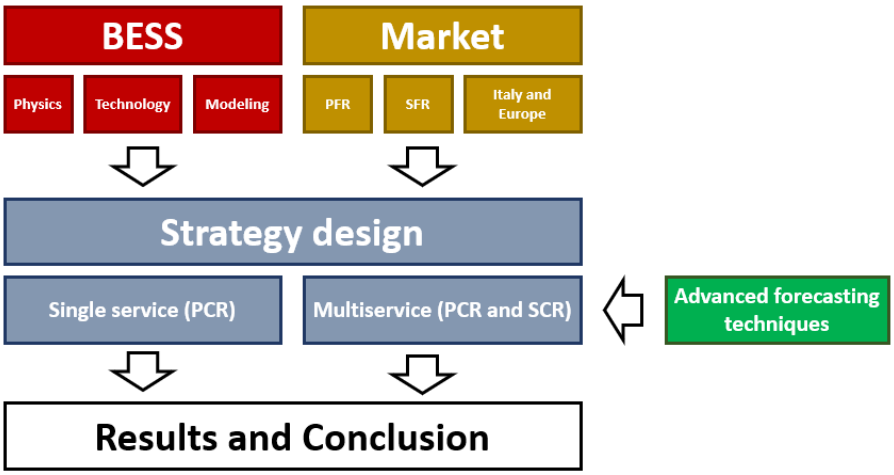

Figure 0.8 - General framework of problem assessment.

In case of multi-service provision, it is very important to forecast the SoC of the BESS at the end of the following market session in order to optimally allocate bands for the Secondary Frequency Regulation. This is because SFR is the most remunerative service in Italy and a good forecast may increase the overall revenues. In particular, different forecasting techniques are compared. At first, a statistical method is investigated. Then, two different Machine Learning algorithms are adopted: Random Forest (RF) and Artificial Neural Network (ANN). Moreover, a Hybrid Approach is proposed, which consist in mixing different techniques in order to improve the accuracy of the prediction. Finally, the best forecasting approaches is adopted in the simulation of multi-service provision and the overall economic performances are compared with the one obtained with the "standard" statistical method.

Thesis layout

The structure of the thesis is outlined in the following lines and summarized in *Figure 0.9*.

Chapter 1 provides a physical and technical background about Battery Energy Storage Systems, by linking different levels of approach and highlighting which constraints these levels impose to a safe, correct and profitable operation. In particular, three

levels are investigated. At first, the cell level is analysed: the focus is on the working principles and physics of electrochemical devices, together with the parameters that characterize battery operation. Then, the technological level is explored: it concerns the different types of batteries available in commerce, with a special focus on the Li-ion technology, and the different components of a BESS. Finally, the computational level is touched by listing the possible approaches to battery numerical modelling that are present in Literature.

Chapter 2 focuses on the Ancillary Services Market. Initially, a brief description of the general structure of the electricity market is given. Then, an overview of the main ancillary services is provided, with particular attention to Frequency Regulation. Moreover, two ASM paradigms for frequency services are analysed (the Italian and the German models) and possible future scenarios are presented. The last part of the Chapter talks about the role that BESSs can have in this type of market due to the suitability of the technology to this kind of services: single PFR service provision is introduced and multi-service provision is described.

Chapter 3 introduces the theme of predictive analytics. Initially, the forecasting process is described and the main metrics for evaluating forecast accuracy are explained. Then, an overview of predictive models for time-series is given, with particular attention on two algorithms: Random Forest and NARX Neural Network. The last part of the Chapter presents some case studies about forecasting techniques applied to BESS.

Chapter 4 is about the methodology and the models adopted in this study. At first, the BESS model adopted and the MATLAB®-Simulink™ tools implementing it are presented, together with a detailed explanation of the assumptions and the equations used to evaluate parameters. Secondly, the PCR controller is explained, with a focus on different SoC management strategies. Lastly, the multiservice controller is described: a novel energy management strategy is introduced, together with the description on how energy fluxes are accounted and remunerated and how LoR is allocated between services. This energy management strategy is one of the innovations of this work, it is enhanced by the utilization of advanced forecasting techniques and it can be generalized and utilized with other kind of services.

Chapter 5 presents the results of the simulations of BESS called to only PFR provision, with a comparison among the different SoC management strategies from both

technical and economical point of view. Moreover, a sensitivity analysis is performed on the main parameters of the best strategy to optimize the performance. Economic remuneration considers both the Italian and the CWE models.

Chapter 6 presents the results of multiservice provision: asymmetric SCR band management works as SoC restoration strategy. At first, the results of the optimization of the forecasting techniques are shown. Then, these forecasts are used to feed the multiservice controller described in *Chapter 4* and the results of these simulations are presented, with an additional sensitivity analysis on the main parameters involved in the simulation. Again, both the Italian and the German models are considered for PCR remuneration, while the SCR remuneration mechanism adopted is inspired on the Italian one. The reason of this lies in the fact that market sessions of German SFR last an entire week, while Italian ones last 4 hours, allowing to manage the bands in order to restore SoC.

The *Conclusion* summarizes the original contributions and the main outcomes of this work and proposes directions for further researches.

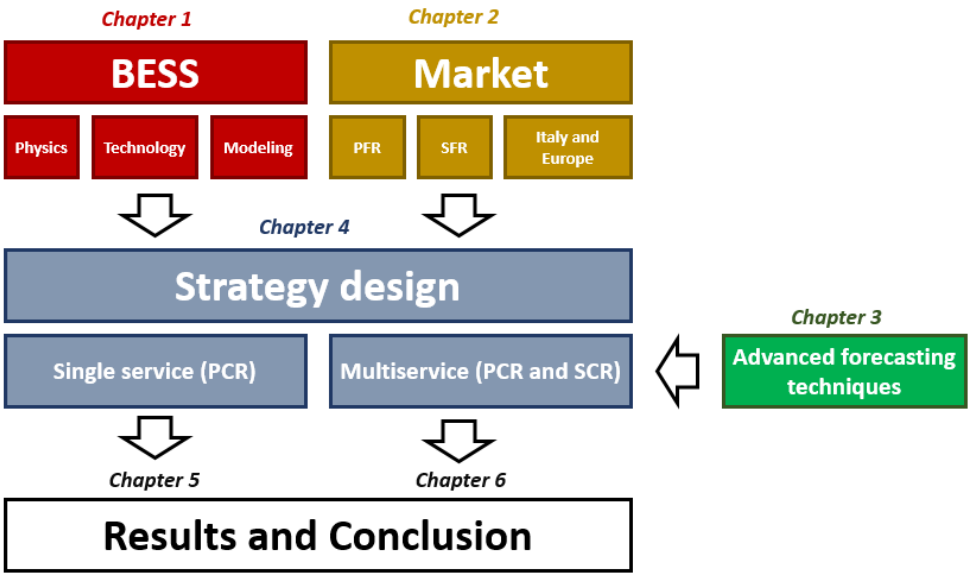

Figure 0.9 - Thesis outline representation.

1. BATTERY ENERGY STORAGE SYSTEMS

Battery Energy Storage Systems (BESSs) can be described at many levels. They involve thermodynamics, electrochemistry and material science together with control systems, technology and economy. The identification of a strategy that exploits at best the characteristics of these systems requires an understanding on how these levels are interrelated and what limits they impose to operation. The aim of this Chapter is to give an overview of these topics in order to assess a theoretical and technical background useful to understand the problems and the constrains that could be faced in practical applications.

In the *Introduction*, a brief overview on nowadays installations and costs has been given. In *Chapter 2*, the suitability of these systems for providing grid services are highlighted. The main topics of this Chapter are the physics behind electrochemical reactions (*Section 1.1*), the Li-ion technology (*Section 1.2*) and the approaches to modelling BESS (*Section 1.3)*.

1.1 Working principle: cell level

The cell is the core of any electrochemical device. As shown in *Figure 1.1*, a cell can be divided in two parts:

- The Anode, where oxidation reactions occur.
- The Cathode, where reduction reactions occur.

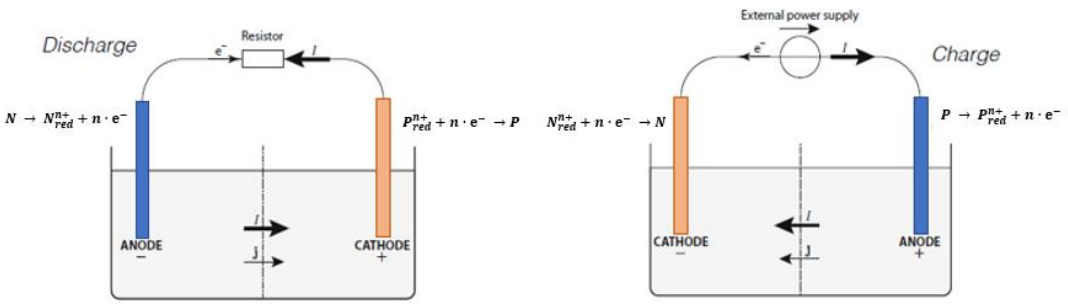

Figure 1.1 - General scheme of an electrochemical cell [60].

The sum of the two reactions is electrically neutral: the n electrons produced during oxidation are used in the reduction reaction. If anode and cathode are connected by a conductive material, electrons flow from one part to the other and an electric current is generated.

Both anode and cathode are the sum of three components:

- An electrode: the part in which the reaction occurs.
- The electrolyte: the liquid substance in which electrodes are immerged.
- An active species (*N* or *P*) with its reduced counterpart (N_{red}^{n+} or P_{red}^{n+}).

The functions of the electrodes are: (i) catalyse the reaction, (ii) canalize the electrons to the current collector. Function of the electrolyte is allowing positive ions to pass from one electrode (anode) to the other (cathode). The two parts are separated by a membrane, which is permeable to positive ions and impermeable to other species. The flow of positive charges ("*j*" in *Figure 1.1*) must balance the flow of electrons in order to close the electric circuit and sustain both reactions.

1.1.1 Open circuit voltage and State of Charge

The two electrodes inside a cell are called negative electrode and positive electrode. Depending on the operation, the negative electrode could work as anode (discharge) or as cathode (charge). The reason of these names (positive and negative) depends on the voltage difference that is created between electrode and electrolyte when they are put in contact. Taking as example the negative electrode, the reaction increases both the number of electrons in the metal and the number of positive ions in electrolyte (i.e. it creates a voltage difference between these two parts), as shown in *Figure 1.2*. Having more negative charges than before, the voltage of negative electrode decreases; due to the increase of concentration of N_{red}^{n+}, the voltage of the electrolyte increases. The more molecules of *N* react, the higher the voltage difference between the electrolyte and the electrode. The reaction rate depends on the concentration of reactants: hence, reaction (and voltage difference increase) stops when the concentration of *N* decreases below a certain threshold (which depends on materials, temperature, pressure, species involved in the reaction) and electrochemical equilibrium is met.

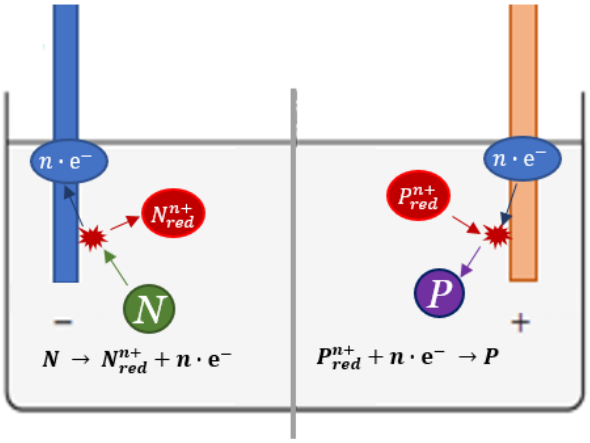

Figure 1.2 - Reactions occurring after the electrode is put in contact with the electrolyte.

The opposite occurs at the positive side; in this case, the voltage of the positive electrode increases due to the loss of electrons. The relation between equilibrium voltage and concentration of products and reactants is now introduced in the equation:

$$\begin{cases} \Delta V^- = V^- - V_{el}^- = V_0^- + \frac{RT}{nF} ln \frac{a_{N^{n+}_{\text{red}}}}{a_N} < 0 \ [V] \\ \Delta V^+ = V^+ - V_{el}^+ = V_0^+ - \frac{RT}{nF} ln \frac{a_P}{a_{P^{n+}_{\text{red}}}} > 0 \ [V] \end{cases} \tag{1.1}$$

Where V^- and V^+ are the voltages of positive and negative electrodes, V_{el}^- and V_{el}^+ are the voltages of electrolyte on the negative and positive side, V_0^- and V_0^+ are equilibrium voltages when activity of species involved is equal to 0 (these latter voltages can be found experimentally), a_i is the chemical activity of species i (the higher the concentration, the higher the chemical activity), R is the universal constant of gas, T is the temperature of the system, n is the number of electrons involved in the redox reaction. Since membrane allows passage of positive ions, the concentration of positive ions is constant throughout the electrolyte (i.e. the electrical potential of the electrolyte is the same on the two sides):

$$V_{el}^- = V_{el}^+ = V_{el} \ \rightarrow \ E_{ocv} = V^+ - V^- = \ \Delta V^+ - \Delta V^- > 0 \ [V] \tag{1.2}$$

Where E_{ocv} is the Open Circuit Voltage (OCV) between positive and negative electrodes. Combining (1.1) and (1.2) and defining $E_{ocv}^0 = V_0^+ - V_0^- \ [V]$, it is possible to relate E_{ocv} and chemical activities in an electrochemical equation called Nernst law:

$$E_{ocv} = E^0_{ocv} + \frac{RT}{nF} \cdot ln \frac{a_N a_{P^{n+}_{red}}}{a_P a_{N^{n+}_{red}}} \; [V] \tag{1.3}$$

The whole voltage gradient is concentrated in a small layer that covers the surface of the electrode: this interface is called electric double layer. An intuitive explanation of the phenomenon (according to Helmoltz theory) is presented in *Figure 1.3*: the negative charged electrode attracts positive ions that are present in the electrolyte; water (orange circles), being a polar molecule, interposes between the two charges. Charged particles and water act as capacitance and the effect is the separation of two iso-potential regions. The order of magnitude of the thickness of this layer is nanometres, that is molecular scale [61].

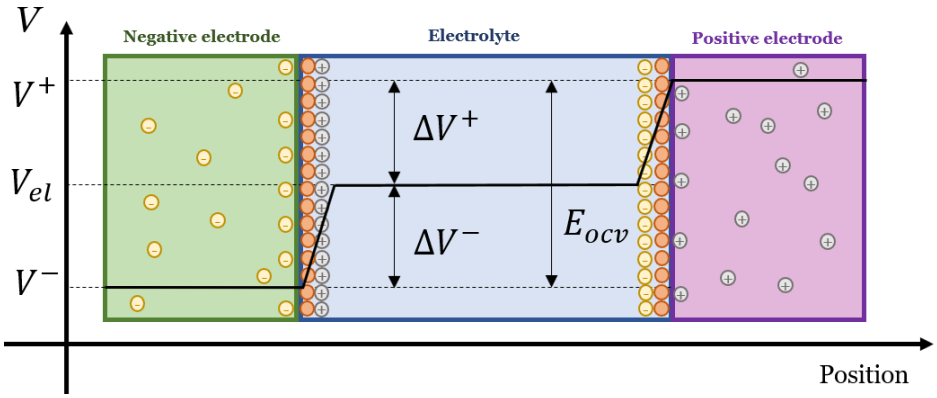

Figure 1.3 – Open circuit voltage of an electrochemical cell at equilibrium.

According to Nernst Law, the higher the concentration of N and P^{n+}_{red}, the higher the voltage and the higher the number of molecules that can react and create current. Battery is a closed system, meaning that the mass of material stored inside is constant during the life of the device. Nominal capacity C_{nom} $[Ah]$ is defined as the maximum amount of electric charges that can be created by a redox reaction and so that can be exploited as electric current. State of charge (SoC) is defined as the ratio between actual capacity (C) and nominal capacity:

$$SoC = \frac{C}{C_{nom}} \; [\%] \tag{1.4}$$

The SoC captures the energetic content of a cell with respect to the nominal one. It goes from 0% (fully discharged) to 100% (fully charged). It depends on the concentration of reactants and products and can be related to E_{ocv} through the nonlinear relation (1.3).

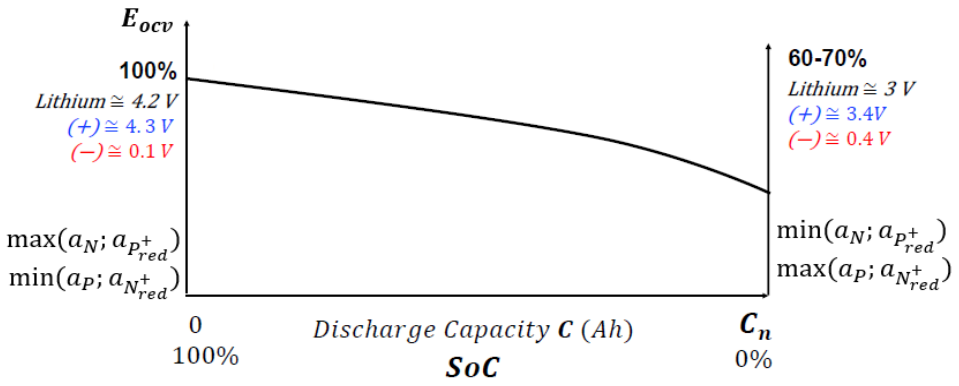

Figure 1.4 - OCV-SoC relationship for Li-ion batteries.

When battery is discharged (*SoC* close to 0%), the open circuit voltage decays with respect to fully charged case due to the decrease of reactants activity, that have been consumed. *Figure 1.4* also shows the typical voltage value that is possible to find using a Li-ion technology. This aspect is further detailed in *Section 1.2*.

1.1.2 Charge and discharge process

The voltage difference between positive and negative electrode can be exploited by connecting them through an external circuit, as shown in *Figure 1.5*. Connecting electrodes with a resistor decreases the voltage drop across electrodes and makes battery consume reactants, creating a current that goes from positive to negative electrode. The power is absorbed by the load and consumed by the battery. On the other hand, if a higher potential with respect to E_{ocv} is imposed by a voltage generator, current flows from lower to higher potential and the energy flow is from the generator to the battery. This behaviour is described by Butler Volmer equation and its logarithmic simplification, the Tafel equation, which involve electrochemical disequilibrium and kinetics [60]-[61].

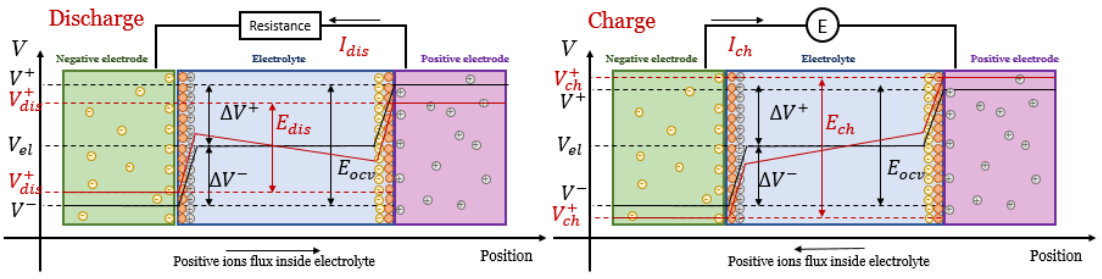

Figure 1.5 - Voltage profile inside the battery during charge and discharge processes.

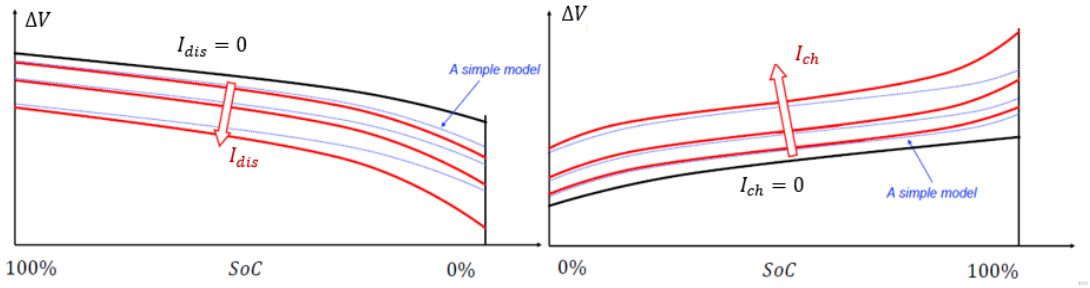

Figure 1.6 - Relation among voltage, current and SoC during charge and discharge processes [60].

Current is usually taken into account in terms of $C - rate$ $[1/h]$, which represents the number of times in which battery can be fully charged or discharged in an hour:

$$C - rate = \frac{I}{C_{nom}} \quad \left[\frac{1}{h}\right] \tag{1.5}$$

Voltage gradient inside the electrolyte is due to the movement of positive ions, whose migration induces an ohmic voltage drop (i.e. proportional to current) [75].

The upward Section highlights how the driving force of battery operation is voltage: calling η the difference between $E_{ocv}(SoC)$ and actual voltage between electrodes during operation (also called *overpotential*):

$$\eta = (V^{+}_{dis/ch} - V^{-}_{dis/ch}) - E_{ocv} \quad [V] \tag{1.6}$$

Figure 1.5 (and Butler Volmer equation) shows that if a positive overpotential is imposed (by a voltage generator that increases voltage difference between electrodes), battery is charged; if a negative overpotential is imposed (by connecting electrodes with a resistor), battery is discharged.

A simple relation among current, voltage and SoC can be written, assuming Tafel simplification is valid and constant material and kinetic parameters [60]:

$$E = E_{ocv} - b \cdot \ln\frac{I}{I_{max}} - R_{mem} \cdot I - \eta_{MT} \quad [V] \tag{1.7}$$

Where:

- E_{ocv} is equilibrium open circuit voltage depending on the SoC of the cell.

- $b \cdot ln\frac{I}{I_{max}}$ is equal to $-\eta$, the overpotential defined in (1.6), which accounts for kinetic activation of reactions (I is considered positive if discharges battery; b is the Tafel slope, I_{max} is the maximum current that can be produced by the surface reaction and depends on surface characteristics).
- $R_{mem} \cdot I$ considers ohmic losses of positive charge migration through the separation.
- η_{MT} accounts for mass transfer issues that arise at high currents. This relation better explains *Figure 1.6*; difference between blue and black line is η_{MT}.

1.1.3 Cycle and efficiency

There are different ways to define a battery cycle. A possible definition describes a cycle as a process that takes a battery from an initial SoC value to an equal final SoC value [9]. Other possibilities consider energy fluxes and nominal capacity (*see Paragraph 4.1.2*) rather than SoC levels.

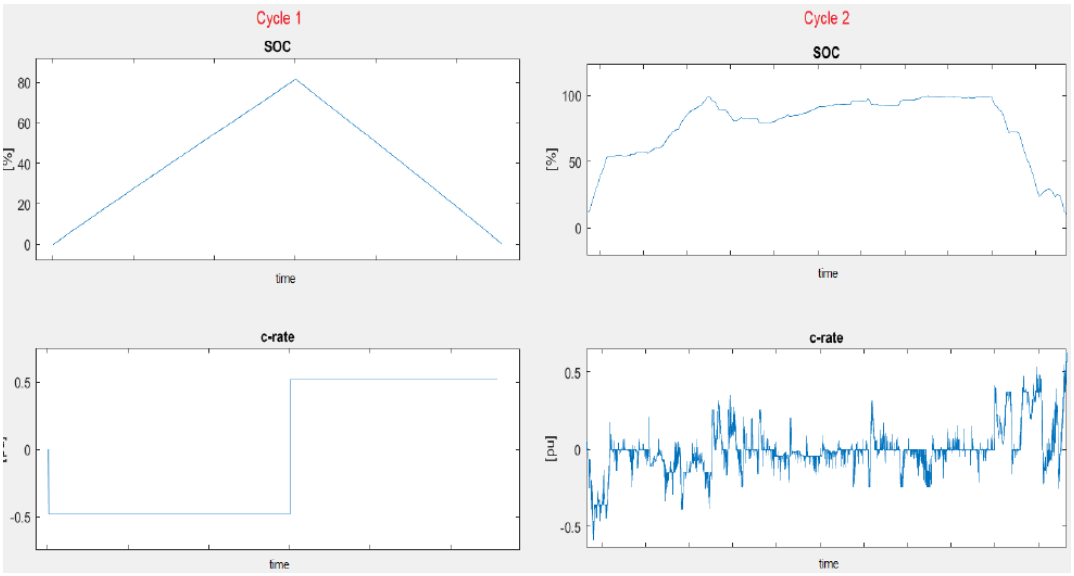

Figure 1.7 - Examples of battery cycles [9].

Efficiency of a cycle can be computed with respect to charges or energy:

$$\eta_C = \frac{\int_{dis} dC}{\int_{ch} dC} \tag{1.8}$$

$$\eta_E = \frac{\int_{dis} VdC}{\int_{ch} VdC} \tag{1.9}$$

The first expression is the coulombic efficiency and takes into account the loss of charges during the cycle: it can be different from 100% if: (i) battery is not perfectly sealed and species leak out from the system, (ii) parasite reactions change internal composition.

The second expression is the energy efficiency, which can be rewritten as:

$$\eta_E = \frac{\int_{dis} VdC}{\int_{ch} VdC} = \frac{\overline{V}_{dis} \cdot \Delta C}{\overline{V}_{ch} \cdot \Delta C} = \frac{\overline{V}_{dis}}{\overline{V}_{ch}} \tag{1.10}$$

In order to have a meaningful number, efficiency must be computed between two instants that have the same SoC. Energy efficiency is also known as roundtrip efficiency. Average charge and discharge voltages depend on several characteristics of the cycle:

- Depth of Discharge (DoD): the maximum ΔSoC during a charge or discharge process.
- Average $C - rate$.
- Type of cycle: operation at extreme SoC has a bad impact on efficiency.

1.1.4 Lifetime and State of Health

The lifetime of a battery is defined as the time elapsed before performance decay meets a certain threshold. Performance decay can be evaluated in terms of capacity, power or efficiency. Two are the mechanism for which a battery experiences a decay in performance:

- Capacity fade: it involves the decrease in capability of electrodes to store the reactants or the consumptions of reactants due to parasite reactions.
- Power fade: it involves the increase in internal resistance of the cell and impacts on the efficiency.

These fades, in principle, can depend on charge and discharge cycles (*cycle ageing*) or on detrimental effect of time (*calendar ageing*). The sum of the two defines the decay rate. If a battery is kept "on the shelf", calendar ageing will be the only one involved in performance decay. More details about what parameters affects these fades and the reasons behind them for Li-ion technology are given in *Paragraph 1.2.3*.

SoH is a value in percentage, measuring 100% at Beginning of Life (BoL) and then decreasing, which captures the decay in performances due to ageing. It can be related to capacity, efficiency, power and it has the same formulation for every one of them. E.g. for capacity:

$$SoH(t) = \frac{C_{SoC=100\%}(t)}{C_{nom}} \tag{1.11}$$

1.2 Li-ion batteries: technological level

In the previous Section, the relation between voltage, current, SoC and cycles efficiency has been explained considering the physics of the cell, which is the starting point in order to understand battery operation. In this Section, an overview on chemistries and technologies available in commerce is presented, with a focus on the Li-ion technology. The other aspects that are important to highlight with respect to technology concerns the degradation mechanisms and safe operations, which covers the second part of this Section.

1.2.1 Overview on battery chemistries

Battery Energy Storage Systems are part of a wider family of Electric Energy Storage (EES) (*see Introduction*). The peculiarity of BESSs is the form in which electric energy is stored, that is electrochemical. Different chemistries are present in commerce: *Figure 1.8* represents the most representative for grid purposes [63]. *Table 1.1* compares the same technologies including typical voltage ranges and efficiencies.

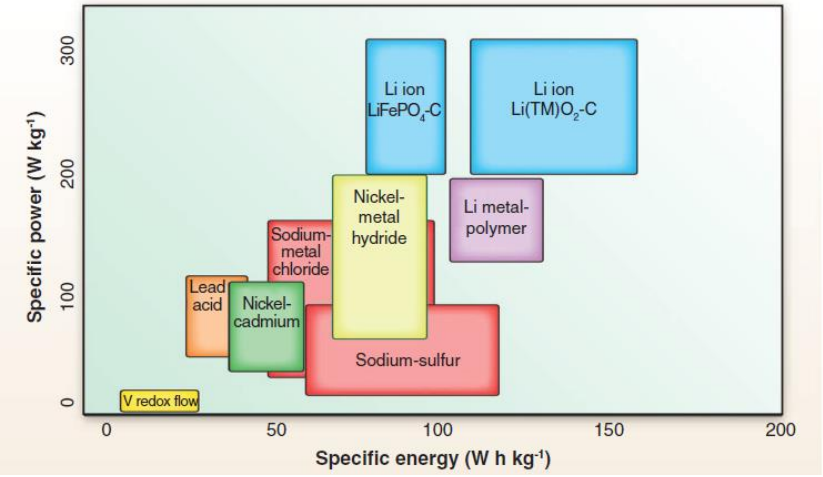

Figure 1.8 – Power and energy density for different battery technologies [63].

Table 1.1 - Comparison among different battery technologies [60]-[62]-[63].

Battery type	Voltage range [V]	Specific Energy [Wh/kg]	Specific power [Wh/kg]	Typical efficiency
Lead Acid	2.1- 1.8	30 - 40	60 - 110	80 - 85% [64]
Nickel-Cadmium	1.3 - 0.8	40 - 60	40 - 100	40-80%
Nickel-Metal Hydride	1.3 - 0.9	70 - 100	70 - 200	
Li-ion - Li(TM)O_2-C	4.2 – 2.5	120 - 160	200 – 300	>95%
Li-Ion - $LiFePO_4$-C	3.5 – 2.5	80 – 90	200 - 300	
Lithium Metal-Polymer	4.0 – 2.4	100 - 110	130 – 170	
Sodium-Sulphur	2.1 – 1.8	60 - 120	15 – 70	75 – 85% [67]
Sodium-Metal Chloride	2.6	50 - 100	30 – 150	
Vanadium Redox Flow	1.6 – 1.1	10 - 20	1 - 4	70-85%

The main characteristics of these technologies are the following:

- Lead-acid: it is the oldest battery technology, discovered by Plante in 1860. The main components are: cathode made of PbO_2, anode made of Pb, electrolyte that is sulphuric acid. Manufacturing costs are not so high and manufacturing process is relatively simple. However, it is very detrimental to keep them at low SoC and their energy and power density are not so high. Common fields of application are automotive for vented type (VLA) and portable electronics and Uninterruptable Power Supply for sealed type (VRLA) [64]-[65].
- Nickel-based: these batteries are composed by the association of nickel with different materials, leading to the production of a variety of technologies [5]. Nickel-Cadmium batteries uses nickel hydroxide and metallic cadmium as the two electrodes and an aqueous alkaline solution as electrolyte such as potassium hydroxide (KOH) or sodium hydroxide (NaOH). It presents two main issues: “memory effect”, that is the decrease in capacity when battery is charged without being fully discharged and toxicity of materials [5]. Nickel-Metal Hydride instead, use hydride metal instead of cadmium as negative electrode: this implies a reduction in “memory effect” and a lower toxicity due to the absence of cadmium.
- Li-ion: negative electrode is a carbon structure able to store inside Lithium ions, while positive electrode is usually a transition metal oxide (e.g. NiO_2, CoO_2, MnO_2). The electrolyte consists of a solution of a lithium salt (e.g. $LiPF_6$) in a mixed organic solvent [66]. This technology outstands the others present in *Table 1.1* in terms of energy and power density: this is due to low molecular weight of

Lithium, which enhances diffusion, and very low redox potential ($E^0_{ocv} = 3 - 4\,V$, *see Paragraph 1.1.1*) [63]. This latter aspect leads to remarkable energy and power densities, if compared to other technologies in *Table 1.1*. Together with high efficiencies, these characteristics make this technology appealing for a wide range of applications, from portable electronics to stationary application related to renewable energy generation [68].

- Sodium-based: these batteries are also called "molten-salt batteries" because of the physical state of electrodes at operating temperature (270 up to 350 °C for NaS). Additional important features of NaS batteries are no self-discharge, low maintenance and their 99% recyclability [67]. Because of the high investment cost, the need of good insulation and thermal management, these are usually large-scale systems.
- Flow batteries: peculiarity of this family is the fact that reactants, together with electrolyte, are stored in tanks and are pumped inside the cells in order to react. In this case, unlike closed batteries, power and energy are not necessarily related: an increase of nominal energy can be achieved by using a larger tank, keeping the same cell. This can lead to very long time of charge and discharge, making them suitable for energy-intensive applications. Most common chemistries are based on Vanadium or Zinc. Main drawback regards their low energy and power densities.

This comparison highlights potential of Li-ion batteries and explains the rising interest of industry and research to solve the main problems that affect this technology, which are safety of operation, lifetime and investment cost. Moreover, manufacturing processes and specific materials are under strict intellectual properties, being this technology relatively new (1990). The following Section focuses on Li-ion cell and its components.

1.2.2 Li-ion cell chemistries

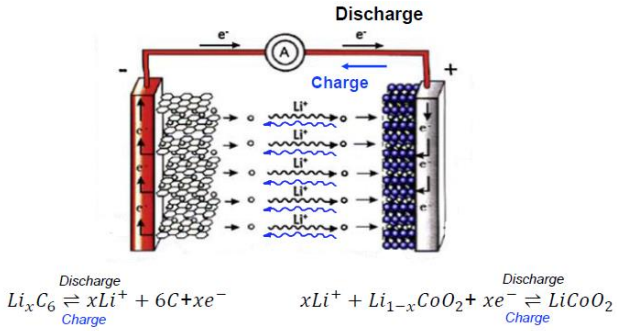

Figure 1.9 - Li-ion cell.

Figure 1.9 shows a typical Li-ion cell: carbon based negative electrode, transition metal oxide at positive electrode. During the charge cycle, Li^+ flows from the positive electrode, made of $LiCoO_2$, to the graphene sheets of the negative electrode. The discharge cycle consists of the reverse process [67]. When the battery is fully charged, all Lithium is trapped inside the carbon grid. Depending on anode, cathode and electrolyte composition, several chemistries can be found on the market:

- LCO ($LiCoO_2$-Graphite). High energy density makes this group suitable for portable electronics. Typical voltage is 3.7 V. Main issue is related to thermal stability, short lifespan and low specific power.
- LMO ($LiMn_2O_4$-Graphite). The Manganese oxide cathode enhances ion flow in the electrode (leading to lower internal resistance and improved current handling) and presents the highest nominal voltage (3.8 V). Combination of these aspects brings to a good power density. Moreover, it presents a good thermal stability and operation safety. On the other hand, energy density is 20% lower with respect to LCO, and cycle and calendar life are limited.
- NMC ($LiNiMnCoO_2$-Graphite). This type of battery is mostly used for power tools, e-bikes and other electric powertrains. The cathode combination is typically one-third nickel, one-third manganese and one-third cobalt, also known as 1-1-1. Typical voltage is 3.6 V.
- NCA ($LiNiCoAlO_2$-Graphite). The lithium nickel cobalt aluminium oxide-based battery has a nominal voltage of 3.6 V and a better safety characteristic if compared with LCO-based battery, but worst with respect to NMC. They share a Nickel based positive electrode, hence energy and power density are still good, but NCA presents higher costs.

- LFP ($LiFePo_4$-Graphite). $LiFePo_4$ is an olivine cathode, which presents several advantages as: (i) a cost which in principle is lower than that of $LiCoO_2$; (ii) a high intrinsic safety (the strength of the P–O covalent bond rule out any risk of oxygen release) [66]; (iii) high current rating; (iv) good resilience at high voltages. These characteristics make this chemistry one of the most promising for both stationary and automotive application, even if nominal voltage has the lower value among the competitors in this list (3.3 V).
- LTO ($Li_4Ti_5O_{12}$-various). Main difference between this technology and the other present in this list is the negative electrode, that is a Lithium-Titanate nanocrystals instead of graphite. Positive electrode can be NMC or NCA. Main advantages are: (i) absence of SEI formation (*see Section 1.2.3*); (ii) higher cycling performance; (iii) capability to operate at low temperatures. On the other hand, there are problems about costs (still high) and low voltages (2.4 V), leading to poor energy densities.

1.2.3 Ageing mechanisms and safe operation

Despite the remarkable gravimetric parameters and high efficiencies, which are making Li-ion technology the most promising type of electrochemical storage, these systems present some issues that limit operation and profitability, mainly related to security of operation and lifetime. Concerning lifetime, (as introduced in *Paragraph 1.1.4*), these issues can imply a decay in capacity (if related to reactant's consumption or to a decrease in storage capability of electrodes) or a decay in power (if related to an increase of internal resistance). Moreover, they can depend on charge and discharge cycles (cycle ageing) or be independent from it (calendar ageing). The focus of this Paragraph is on the stress factors and ageing mechanisms of Li-ion batteries and how they can be kept under control in order to ensure a safe and correct operation.

Operating voltage range

Electrochemical reactions are triggered by concentration of reactants and voltage (*see Section 1.1*). Hence, in an electrochemical system, voltage must be kept under control in order not to promote any parasite reaction, which can create irreversibly unsolicited species starting from reactants stored inside. *Figure 1.10*, taken from [66], shows the effect of this phenomenon for an LCO cell: green lines represent current generated by electrodes (negative carbon electrode on the right and positive Cobalt-based electrode on the left); the blue line represents the current generated by the

oxidation (right) and reduction (left) of electrolyte. Outside the range 1,5–3,5 V vs Li+/Li, the electrolyte starts reacting, leading to two main effects: gas evolution (that causes pressure increases and cracking of solid parts of the cell) [66] and Solid Electrolyte Interface (SEI) formation at the surface of negative electrode [69]-[70].

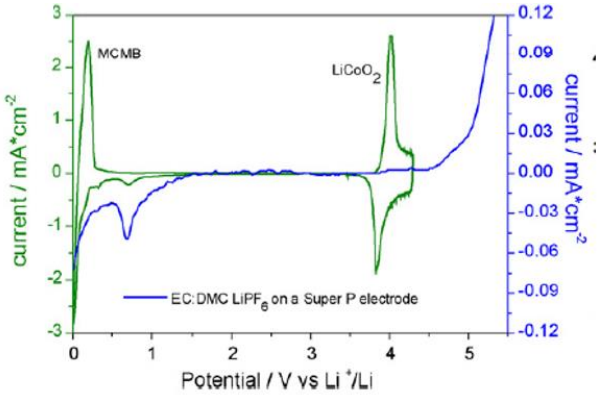

Figure 1.10 - Cyclic voltammetry profiles (potential vs. Li/Li+) of Li-ion battery components [66].

Hence, there is the need of a system which grants that voltage stays inside these allowed range (specified in datasheet). In BESSs, this component is called Battery Management System (BMS) its effect is explained in *Figure 1.11*.

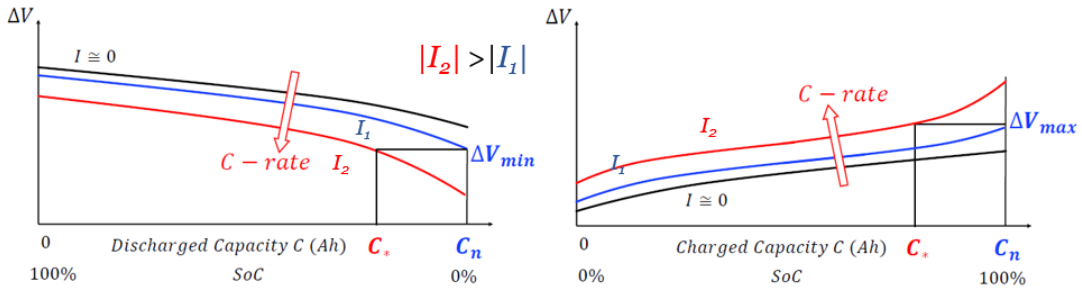

Figure 1.11 - Capacity reduction due to voltage limits and high C-rates [60].

An important effect is the reduction of battery capacity at high C-rates: when charging or discharging at $|I_2|$, a high current, SoC range that battery can explore is decurted by the difference between C_* and C_n, hence energy per cycle decreases. This aspect is is an intrinsic characteristic of Li-ion technology and it is independent from all ageing mechanisms that are discussed in the next Paragraph.

Solid Electrolyte Interface (SEI) formation

Solid Electrolyte Interface is formed spontaneously after the first cycle of the life of the battery on the surface of carbon electrode [66].

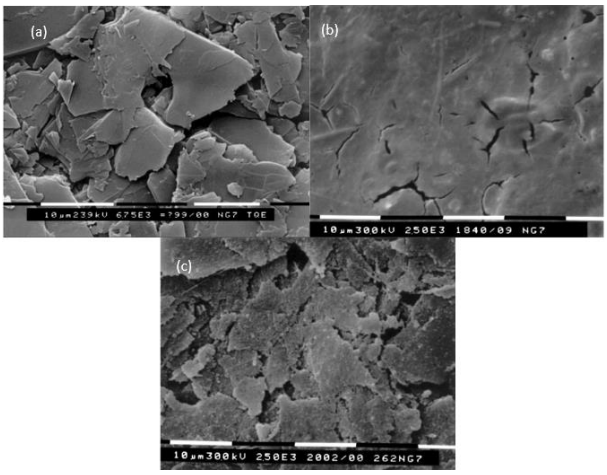

Figure 1.12 – SEM micrograph of a surface SEI film on a graphite electrode in $LiBF_4$ EC/PC 3/1 solution (a) before any electrochemical treatment; (b) after first discharge; (c) after prolonged cycling [71].

[71] investigates the effect of the electrolyte in the formation of SEI and highlights the impact of this layer on performance. On one hand, it consumes Lithium and creates a further ohmic resistance to Li+ passage, impacting both on power and capacity fade. Being SEI permeable to ions, its presence is not irreconcilable with operation, but its thickening over time remains a cause of efficiency decay. On the other hand, it creates a solid division between electrolyte and electrode, decreasing the velocity of formation of the layer itself, which is catalyzed by the direct solid-liquid contact [69]. Last important issue concerns negative electrode exfoliation: solvent can still interact with graphene after diffusing through SEI, filtering inside the carbon grid and solidifying. This causes mechanical stress and exfoliation and leads to an addictive internal resistance increase, in addition to the loss of sites able to store Lithium [73]. Again, both capacity and power are weakened.

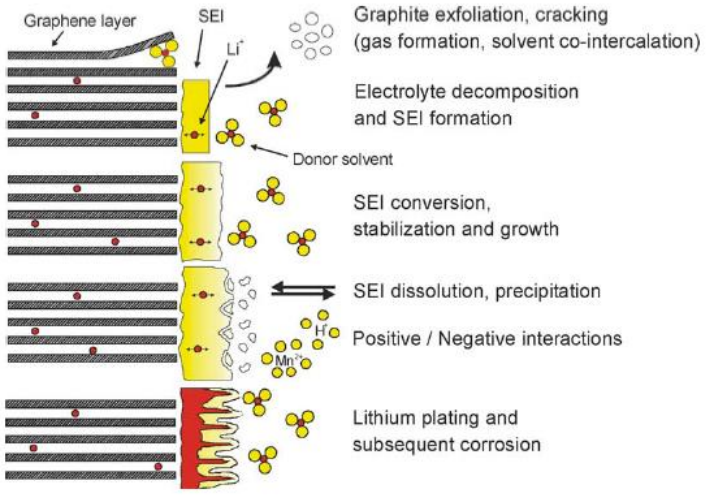

Figure 1.13 – SEI evolution in electrode-electrolyte interface [74].

Another aspect that plays a crucial role in the impact that SEI has on the operation is temperature: at high temperature SEI may dissolve and create Lithium salts less permeable to Lithium ions; low temperatures instead decrease the diffusion of Lithium within the SEI and graphite, which can overlay the electrode with Lithium plating [60]-[69]-[74]. *Figure 1.14* captures the importance of temperature with respect to charge and discharge curves: low temperatures have a more relevant detrimental effect since they affect more the ions diffusivity inside the cell [60]-[72].

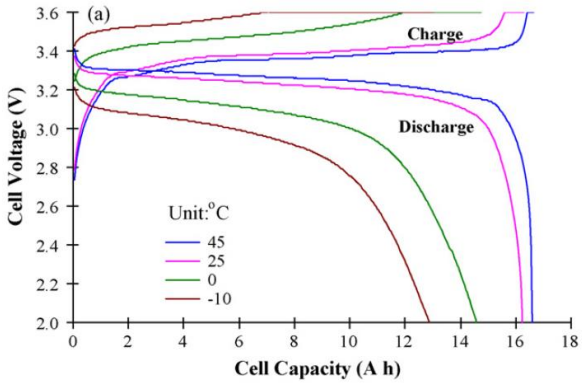

Figure 1.14 - Charge and discharge curve at C-rate=1 for a fresh cell [72].

C-rate and mechanical fatigue

C-rate impacts on degradation at two levels: first, it pushes voltages through limits of electrochemical stability of compounds; second, it is related to the velocity at which Lithium passes from one electrode to another. When battery is fully charged, all Lithium is stored inside the carbon structure of negative electrode. Then, when an

overpotential is applied, Lithium oxidizes and migrates to positive electrode, in which takes part in the reduction reaction and remains there. Thus, the mass of electrodes changes over time. The higher the C-rate, the higher the velocity of this process, the greater the mechanical stress that arises inside the electrodes. C-rate is recognized as one of the key parameters that impacts on ageing mechanisms [5]. For instance, in [70], Authors perform tests on a LMO Sanyo battery ($C_{nom} = 1.5\ Ah$), evaluating capacity fade as function of C-rate and temperature.

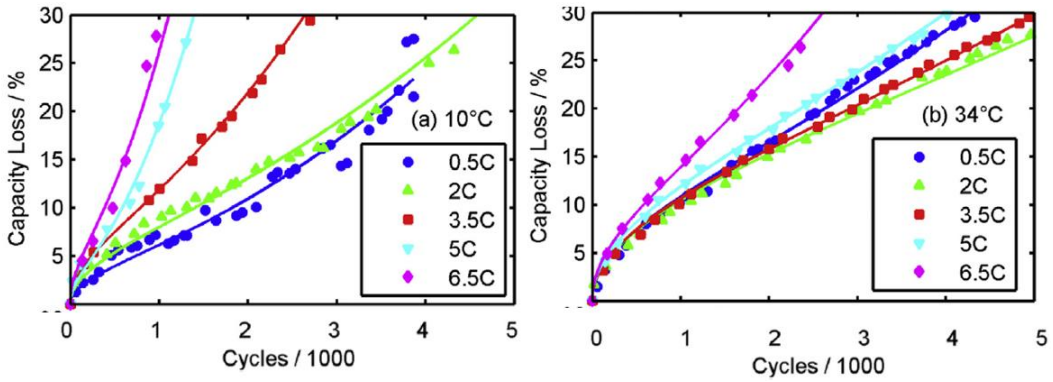

Figure 1.15 - Capacity fade for two different temperatures as function of number of cycles and C-rate [70].

The other parameter that influences this mechanism is the DoD of the cycle: the higher it is, the more relevant is the increase and decrease of electrodes volume.

Calendar ageing: temperature and SoC level

In literature, the main stress factors associated with calendar ageing are temperature and SoC level [76]-[77]-[78]-[79]. The reason behind this is that parasite reactions that decrease the cycling Lithium depend, as already stated, on the temperature and on the concentration of reactants. The latter implies a voltage difference between the electrode and the electrolyte that further enhances these reactions [69]. When the temperature is high, secondary reactions, such as carbon corrosion, are facilitated and the Lithium loss and electrodes degradation are more important than in moderate temperature conditions. However, while an operating strategy could tackle the issues of cycle ageing, calendar ageing is an inevitable side effect, which can be mitigated by restoring SoC to intermediate levels after the operation is terminated and putting the battery in a temperature-controlled room.

SoC evaluation

Last issue regards SoC level evaluation. Measuring SoC means measuring how many Lithium atoms are present in the negative electrode network. This measure is difficult to gain and can be derived only indirectly in two ways: measuring E_{ocv} and relating this quantity to reactant concentration ($SoC = f(E_{ocv})$) or measuring the current during all operation, relating its integral over time to capacity variations. The latter method is called Coulomb counting and SoC variation between two instants is computed as:

$$SoC(t) = SoC(t_0) + \frac{1}{C_{nom}} \int_{t_0}^{t} I \cdot dt \tag{1.12}$$

Where I is current in Ampere, positive if charging. There are two problems: (i) in this relation many parameters are subject to changes during life because all of the aforementioned ageing mechanisms; (ii) accuracy of instruments is not perfect. Thus, SoC evaluation can be less and less accurate over time if a recalibration of these parameters is not considered.

Final remarks

The aim of upward sections is to highlight how capacity decay and power fading do not originate from one single cause, but from a number of various processes and their interactions. Moreover, most of these processes cannot be studied independently and occur at similar timescales, complicating the investigation of ageing mechanisms. Literature is rich and presents many more secondary mechanisms and a detailed explanation of every one of them goes beyond the scope of this Chapter.

A good operational strategy should include all the critical issues treated in this Section:

- A BMS, whose function is to prevent excessive operating voltages in order to reduce oxidative stress in the interface electrolyte-electrode, is necessary.
- Operational and storage temperature must be kept inside certain thresholds.
- C-rate management is a crucial issue as long as energy fluxes are remunerated. End of Life due to cycle ageing is preferable, since it means that battery potential has been fully exploited.

- When the battery is not used, a SoC restoration would prevent excessive decay of performances.
- Cycles have a primary importance in ageing: high C-rates and long periods at extreme SoC should be avoided in order to increase lifetime. Some studies use DoD as parameters for performance decay [112], others instead declass it to secondary-importance parameter [5].

1.2.4 From cell to BESS

As already stated, the cell is the core of a BESS. It is characterized by a nominal voltage, a nominal current and a nominal power, which is the product of the two. Previous sections described how these measures are far from capturing every possible working condition. Indeed, actual voltage depends on temperature, SoC, C-rate, number and type of cycles performed since BoL, storing conditions, age of the cell. Depending on the application, a wide range of nominal voltages and currents can be achieved by stacking different number of cells in parallel or series. An ensemble of cells packed and organized in this way is called module. Modules can further be stacked in packs.

For many applications, modules and packs are not enough. Other devices are necessary:

- An inverter, for the connection with the AC grid.
- Sensors, which monitor currents, voltages, temperatures.
- BMS, which eventually cuts voltage in order to prevent excessive oxidative stress to the cells.
- Control system, which defines power set points and governs BESS operation.
- Air conditioning unit, which grants operating temperature into optimal intervals.

Eventually, a transformer can be put in series with the inverter. While inverter cost is usually in charge of BESS owner, in case of grid connected applications, transformers are already put in place by the Transmission System Operator. The presence of these components does not have a secondary importance while approaching BESS modelling: inverter has its own dynamic and efficiency, limitation of voltages (or powers) due to BMS must be taken into account and auxiliaries' consumption can be fed directly by the energy stored in the BESS, causing an additional discharge bias.

Reliable models that want to capture real behaviors cannot neglect these issues, neither by a technical nor by an economical point of view.

A BESS is characterized by a nominal capacity, nominal voltage and a nominal current. The product of the former two is nominal energy. The product of the latter two is nominal power. The ratio between nominal energy and power is called EPR (Energy-to-Power Ratio). While the nominal energy is a realistic approximation of the energetic content of the battery, the nominal power is a technical parameter decided by the manufacturer, which suggests the maximum current that battery can cycle so that, if this limit is respected, operation is safe and a certain lifetime is granted. The higher the EPR, the lower C-rates that a battery can cycle, the more conservative the operation.

1.3 Approaches to modelling: computational level

When dealing with BESSs, investment cost is an important aspect and it must be paid back exploiting at best the potential of batteries. BESS are complex systems involving, as seen in previous sections, different scales and phenomena. Technical parameters are correlated by non-trivial relations and depend on battery utilization patterns. Models can take into account these aspects with different degrees of accuracy, gaining extra information and reliable results at the expense of additional computational time. On one hand, requiring a high level of detail can limit the number of tests performed, on the other hand unreliable models can deliver results far from reality. The choice of the model for testing a strategy should consider this trade-off. The following Section addresses this issue. At first, a review of different approaches present in Literature is given. Secondly, a comparison among three popular approaches (electrochemical, electrical and empirical) is performed, focusing on advantages and disadvantages related to the aforementioned accuracy-computational time trade-off.

1.3.1 Literature review: different types of models

A first distinction can be made concerning the technological level, i.e. the number of components of the BESS considered by the model [5]:

- Material level, in which materials of cell (electrodes, electrolytes, separators, current collectors) are investigated.
- Cell level, which captures behaviour at the cell's terminals.

- Module level, in which a stack of cells together with the BMS is taken into account.
- BESS level, which implies the modelling of auxiliaries (see *Paragraph 1.2.4*) as well as the modules, separately or joint.

Depending on application, from R&D to grid-tied power intensive operations, different levels can be chosen.

A second type of categorization, which deals with the level of simplification of the working principle, is the following (from the most accurate to the least) [80]:

- Electrochemical (or physical) models: technical parameters derive from the solution of differential equations capturing the actual physical process during cell operation.
- Electrical models: battery is treated as an electrical circuit with variable number of parallel and series RC branches.
- Empirical models: battery operation is approximated by simple equations derived experimentally.

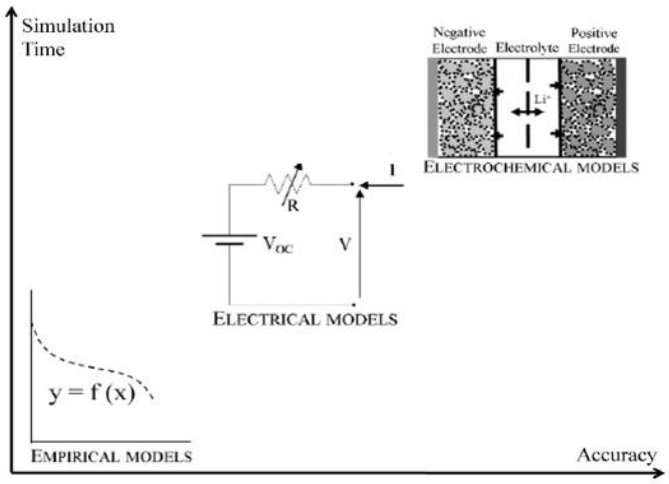

Figure 1.16 - Main approaches to battery modeling.

Other minor approaches are present in literature, such as stochastic models (battery is treated as a stochastic system) and analytical models (which describe operation using equations that are not necessarily related to physics, like Peukert or Sheperd model [5]).

The three approaches present in *Figure 1.16* are further detailed in the following paragraphs. An additional taxonomy is based on which quantities they should evaluate [9]:

- Operating conditions: their aim is approximating the cell operation. The most important quantities to estimate are power exchanged and SoC level.
- Ageing: they are concerned in defining evolution of BESS characteristics along time, evaluating their lifetime starting from on usage patterns. The main quantity estimated is SoH.

Some models take into account both SoC and SoH simultaneously, but most of models have focused on one of the two quantities, depending on their application.

1.3.2 Electrochemical models

This is the most accurate and time-consuming type of model, since it tries to capture all the physical phenomena that happen inside the cell solving differential equation. Equations involved deal with [75]:

- Electrochemical reactions: Nernst law for equilibrium voltage with respect to reactants and products concentration, Butler Volmer equation or Tafel for reaction kinetics and activation overpotential.
- Mass diffusion: positive ions flux inside the electrolyte, through the membrane and inside the electrode in order to reach the active site. Reactants and products move inside the domain following concentration gradient. These equations require the specific parameters of materials, like diffusivity and porosity, and consider concentration's distribution inside the cell.
- Charge migration: voltage gradient inside the electrode enhances or discourage positive ions flux. Both migration and mass diffusion are involved when positive charges pass from anode to cathode and are related by Nernst-Planck relation.
- Mechanical stress due to mass variation of electrodes.
- Thermodynamic equation dealing with Gibbs free energy: real electrochemical reactions are usually exothermic [60], hence temperature increases during operation.

In general, these models require a high number of physical parameters and high computational effort. Moreover, scientific literature provides different equations that model the same phenomena, hence a further degree of freedom is introduced. They

allow to monitor all physical quantities inside the cell during operation and are very popular in R&D application. However, such a degree in complexity could not be necessary when dealing with power intensive application. [5]-[80] provide more details about these models.

SoC and SoH evaluation depends mainly on the choices previously described. SoC can be evaluated integrating currents or reaction rates or it can be derived by open circuit voltages. Instead, SoH requires additional relations that capture performance decays or internal parameters' variation due to ageing mechanisms [69].

1.3.3 Electrical models

Electrical models treat the cell like an electric circuit. There is a wide range of circuital models: the simplest ones, with few constant circuital elements, are far from describing the real physics of the battery and they could be compared with the empirical models. The most advanced models have all the necessary elements that directly reflect the electrochemical characteristics of the cell. The latter are usually composed by two parts, capturing separately the static behavior related to energetic content of the cell (i.e. open circuit voltage) and the dynamic one (i.e. overpotential, mass transport and capacity effects) [37].

Electric models are successfully used in a large variety of research and commercial applications, showing high level of accuracy: a typical field in which these models are used is automotive [81]-[82], since their enhanced speed with respect to electrochemical models can be used in real time control systems [83].

Depending on the representation of the open-circuit voltage [85], two types of electric models can be identified:

- Active models: the open circuit voltage is modelled through an ideal source that is typically a voltage generator, with voltage varying according to the SoC level. In this case the battery is seen as DC electric generators driven by chemical reactions.
- Passive models: the open circuit voltage is modelled as the voltage drop across a capacitor of big-variable capacitance. Such a passive element represents the charge stored in the cell in chemical way rather than electric way. Capacitance and voltage drop across the capacitor vary with the SoC.

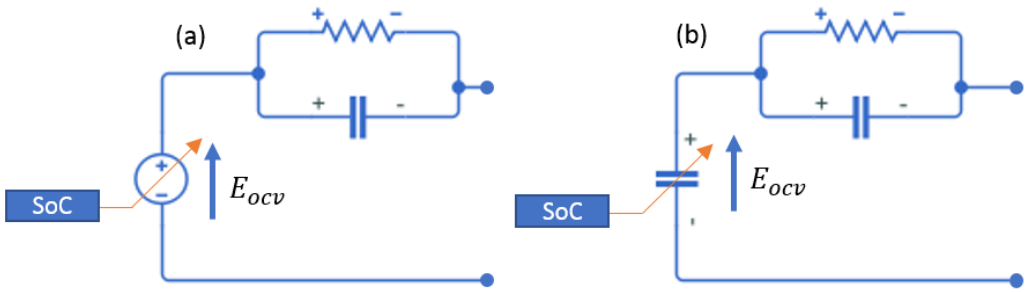

Figure 1.17 - (a) Active and (b) passive electrical model.

An advantage of these kind of models is related to experimental practices: one of the most popular way of evaluating internal impedances of a cell and how they evolve over time is the Electrochemical Impedance Spectroscopy (EIS), in which battery's voltage and current are cycled at different frequencies [86]. Usually frequency spans from 0 to 65 kHz [88]: each frequency is typical to stimulate a peculiar phenomenon in cells, hence behaviour changes at different frequencies can provide information on which mechanism is involved in that change. These measures, which are useful to better investigate ageing mechanisms, can be directly used for characterizing the circuit. The class of electrical models that accounts for this aspect, whose domain is hence frequency, are called "impedance-based model". Models that instead approach resistances in time domain, considering ohmic behaviour, are called "Thevenin-based models" [83]. In this case, the values of circuital elements are usually found by fitting discharge curves in different conditions [89].

Literature presents different levels of complexity for these circuits [5]-[84]: the more the RC branches, the more physical phenomena the model is able to capture separately. A representative setting for this class is Double Polarization model (DP), consisting of a resistance in series with two RC parallel branches (see *Figure 1.18*).

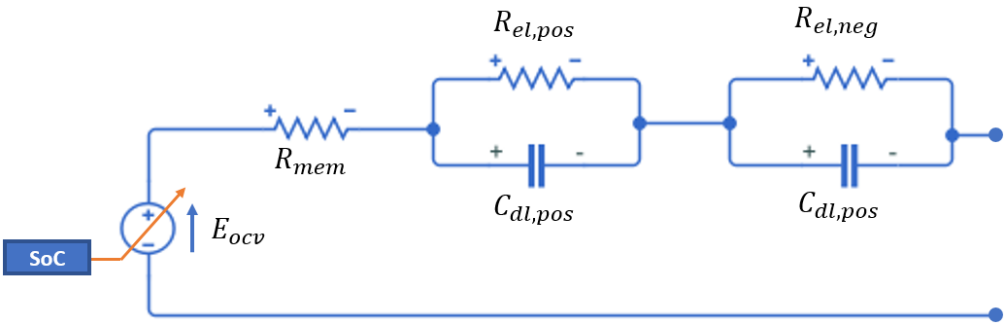

Figure 1.18 – Double Polarization model.

R_{mem} is the ohmic resistance of the membrane, $R_{el,pos}$ and $R_{el,neg}$ are resistances due to ion diffusivity inside the electrodes and in the interface electrode/electrolye, $C_{dl,pos}$ and $C_{dl,neg}$ are the capacitances of the double layer. [87] compares different electrical models' architectures and finds out that DP best fits to experimental data.

Electrical models, considering currents and voltages, are still able to deliver those quantities that are important to be known during operation: voltage can be directly interfaced with a BMS model, current can be counted and SoC variations can be better evaluated. Moreover, canonical laboratory practices are directly usable in the implementation of these equivalent circuits, so SoH can be easily included if a consistent model is found in an experimental campaign. Cell efficiency is intrinsic in the model; hence its calculation comes straight out from the formula, that is the ratio between all the energy that has been charged and discharged between two moments at equal SoC. If the temperature of operation is not the same of the testing temperature, an additional model is needed in order to capture this effect. By this point of view, there is no problem for BESSs that work in temperature-controlled rooms.

1.3.4 Empirical models

Empiricical models use few mathematical equations to describe the system. The electrochemical processes are not considered but they are empirically fitted. Because of the absence of physics, these types of model cannot be used for research. Their computational lightness makes them suitable for sizing a battery or other commercial application, for which a low level of accuracy is necessary [9].

A typical relation experimentally inferable is the link between BESS power in per unit and its efficiency:

$$\eta = f(\dot{P}) \tag{1.13}$$

Function can be a constant, polynomial, exponential or even more complex. However, whichever the function, computational effort is much lower with other approaches in this list.

Usually voltage and current are not taken into account, hence SoC computation cannot rely on Coulomb counting. State of Charge is approximated with State of Energy (SoE) and it is accounted using this formula:

$$SoE(t) = SoE(t_0) + \int_{t_0}^{t} \dot{P} \cdot dt \tag{1.14}$$

This approximation can lead to errors if cycles are performed at average State of Charges close to saturation limits. In this case, another issue arises: analytical models cannot represent some typical behaviors of a battery close to saturation. In particular, it does not consider that the BMS always works for keeping cell voltage within a safe window. As a result, the model can lead to some unrealistic behaviors.

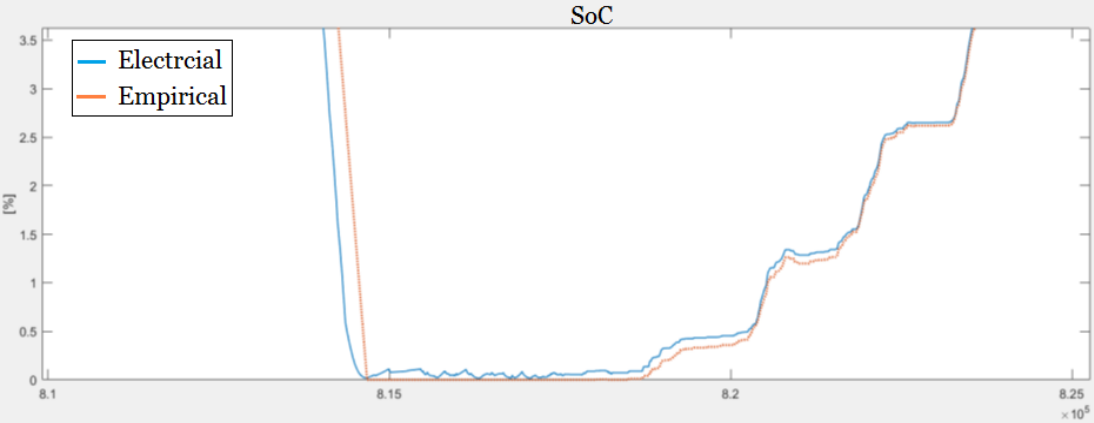

Figure 1.19 - SoC behavior of electric and empirical model at saturation [9].

However, even if extreme behaviors can hardly be captured, empirical models can offer an acceptable of accuracy level with respect to electric ones, as shown in *Figure 1.19*. Empirical models can represent a cell, a module or a whole BESS. Only difference is where sensors are put when gaining data. Instead, electrochemical and electrical models aim to capture the cell's behavior; auxiliaries are modeled separately. Hence, they are better generalizable. On one hand, this aspect makes testing procedure more complex. On the other hand, once the cell model is done, scaling it to a BESS or testing it with different assets is easier: the same cell with a different BMS requires a brand new empirical model; instead, if an electric or electrochemical model is adopted, updating with the new BMS model is enough. Moreover, the separate evaluation of the effects of electrochemistry and auxiliaries in BESS operation can be useful in order to spot critical issues that would be hidden if dealing with empirical models.

2. ANCILLARY SERVICES MARKET

In *Chapter 1*, a detailed description of BESS has been provided, with special focus on the Li-ion technology. In particular, electrochemical phenomena occurring inside a cell, BESS structure and models have been described. In this Chapter, the focus is on a particular application of BESS: the provision of grid services, which are known as Ancillary Services (AS). Ancillary Services are traded on the Ancillary Services Market (ASM), which represents a particular phase of the electricity market. Therefore, a description of the overall structure of the electricity market is necessary.

2.1 Electricity market structure

In order to foster the economic competition among market players, in recent years, many liberalized electricity markets have been activated worldwide. Nowadays, the most common structure of the electricity market is made up of three main elements. The Day-Ahead Market (DAM) represents the main market session, in which energy is traded for satisfying the final consumption. The Intra-Day Market (IDM) allows market participants to change the schedules determined in the DAM. The Ancillary Services Market (ASM) typically takes place after the DAM and represents the instrument through which the Transmission System Operator acquires all the resources necessary to manage and control the power system: in this market session, the traded resource is capacity (power).

The Day-Ahead Market, as its name suggests, is a market for electricity that operates one day in advance with respect to the actual delivery time. It allows the market to be both “financial” and “physical”. A financial market allows participants to buy or sell energy on the market, with no actual delivery obligation. A financial transfer will meet any energy that is not delivered. In contrast, a physical market requires any trading to correspond to an actual transfer of power. The DAM allows both financial and physical participation [13]. The DAM is an auction market and it is not a continuous trading market. It hosts most of the transactions of purchase and sale of electricity. Producers (sellers) and consumers (buyers) place their offer in an Electricity Pool, which is managed by a central entity called Power Exchange (in Italy, Gestore dei Mercati Energetici - GME). The Power Exchange (PX) represents the only counterparty for the market players, by acting as the only buyer for producers and the only seller for

consumers [15]. Note that when buyers and sellers communicate with the PX, they do not know whom they are dealing with. The Day-Ahead Market is typically based on a clearing procedure, whose process is described in the following steps [14]:

1. Every producer, for each contracted period, offers a certain amount of energy (MWh) at a minimum price (€/MWh). Usually, the period is an hour or half an hour.
2. Similarly, every consumer, for each contracted period, requests a quantity (MWh) at a maximum price (€/MWh).
3. The PX receives all the bids and builds two cumulative curves. All the producers' offers are sorted from the lowest to highest price, forming a cumulative supply curve. On the other side, all the consumers' bids are listed from highest to lowest price, forming a cumulative demand curve.
4. The equilibrium point, which represents the solution of the market for each contracted period, is given by the intersection between the two cumulative curves (as shown in *Figure 2.1* –). The Clearing Quantity (CQ) represents the total energy traded and the Marginal Clearing Price (MCP) is the price at which each unit of energy is traded.

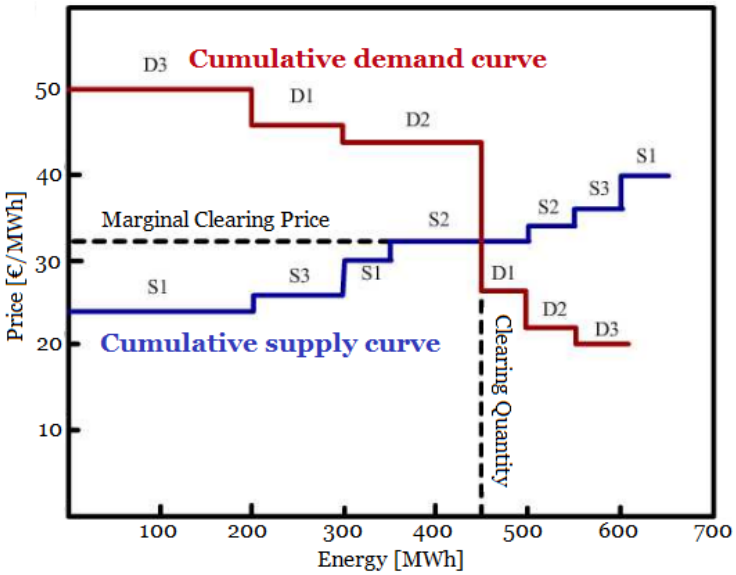

Figure 2.1 – Calculation of the equilibrium point for each contracted period in the Day-Ahead Market [14].

The Intra-Day Market (IDM) allows market participants to change the injection and withdrawal schedules defined in the DAM through additional supply and demand

offers [15]. The IDM consists of different sessions and each one of them is based on the same clearing procedure previously described for the DAM. Market players submit their bids to the power exchange by taking into account the updated information regarding the status of their own power plants (in case of producers) and the requirements for consuming units (in case of consumers). An example for generating units is presented in the following lines [16]. Since in the DAM each hour is solved independently from the previous and the next one, the resulting commitment for a generating unit could be not feasible from the technical point of view. In the Intra-Day Market, it is possible to handle this situation, as shown in *Figure 2.2*.

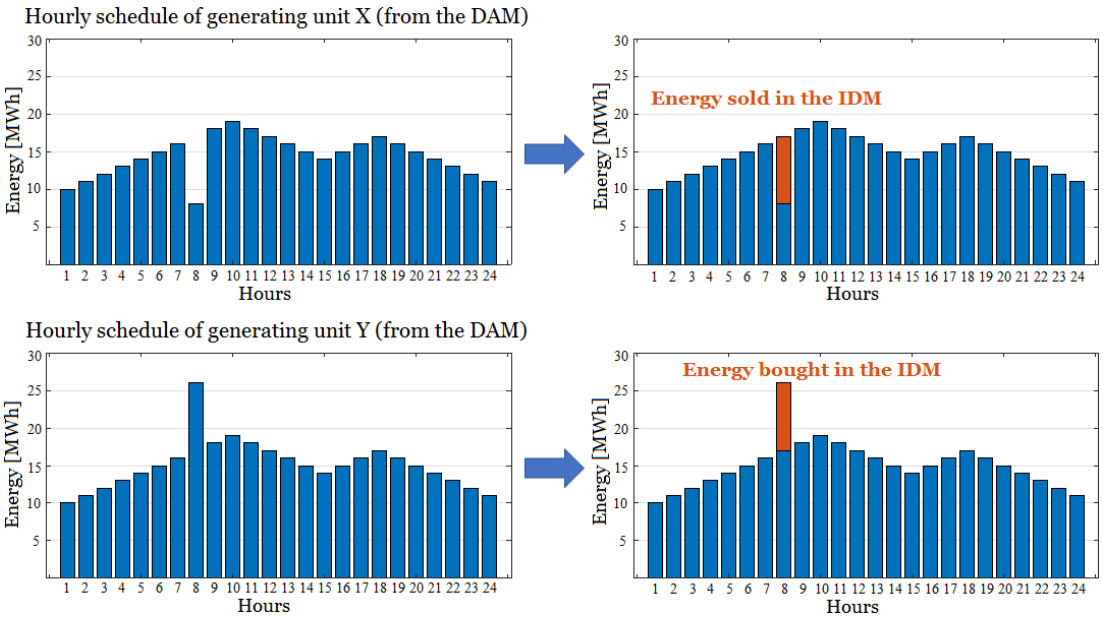

Figure 2.2 – Example regarding generating units on the Intra-Day Market.

Either the DAM or the IDM do not take into account network constraints and the possibility of faults and errors by generators selected to provide their energy. In these two phases of the electricity market, producers and consumers submit their offers to the Power Exchange based on the forecasts of what they are expected to produce or consume. Nevertheless, some market players are not able to predict with high precision their production or consumption. For instance, the actual electricity generation from non-programmable RES could be much different from the forecasted production [17]. On the other side, even precise generators can undergo a fault. Therefore, fluctuations of production and demand result in a divergence between forecasts and reality. Due to network constraints and fluctuations, the schedules defined in the DAM and in the IDM are hardly ever respected and an Ancillary

Services Market (ASM) is necessary in order to allow the TSO to define the reserves of power to optimally manage and control the power system. Before going into the detail of the mechanism and structure of the ASM, a description of the main grid services and their respective reserves is provided, with special focus on those related to frequency regulation.

2.2 Ancillary Services

Ancillary Services (AS) are defined as all those activities on the interconnected grid that are necessary to support the transmission of power while maintaining reliable operation and ensuring the required degree of quality and safety. The identification and definition of a particular ancillary service is system dependent. Therefore, there is no global definition of a particular AS that is applicable in all systems. Moreover, there is not a uniform and standardized categorization of AS. Looking at the different classifications of ancillary services found in literature, three main categories of services appear in all lists [18]:

- **Frequency control**: It is related to the short-term balance of the frequency of the power system. It includes Primary, Secondary and Tertiary frequency regulation. This is the main service provided by generators and it can be provided also by other facilities such as flexible loads, aggregators and energy storage systems.
- **Voltage control**: It is required for maintaining the power system voltage within the prescribed limits through reactive power injection or absorption. It can be provided by both dynamic sources (i.e. generators, synchronous compensators) and static sources (i.e. capacitor banks, FACTS devices, tap-changing transformers…).
- **System restoration**: It includes all the services required to return the electrical power system to its normal operation after a complete blackout (Black-start capability). The restoration of the system consists of a very complex sequence of coordinated actions whose framework is studied and, as far as possible, prepared in advance. This process has several stages: re-energization from blackout, frequency management and re-synchronization.

Among the aforementioned services, frequency regulation is deeply analysed since frequency represents the main marker for assessing the power quality in AC networks.

2.3 Frequency regulation

In the electric power system, it is of fundamental importance to guarantee the balance between total electricity generation and demand at all times. Frequency is the main indicator for assessing the status and "health" of the electrical network. In particular, when generation and demand are balanced, frequency remains constant. The nominal value of frequency in Europe is 50 Hz, while in the USA it is 60 Hz. A very large power system with the same frequency target, such as EU and USA, is subdivided into synchronous areas in order to better manage the system from both technical and economical point of view [19]. In *Figure 2.3*, the five European Regional Groups (RG) are shown. All the TSO operating within these five regions are members of the European Union of Transmission System Operators for Electricity (ENTSO-E).

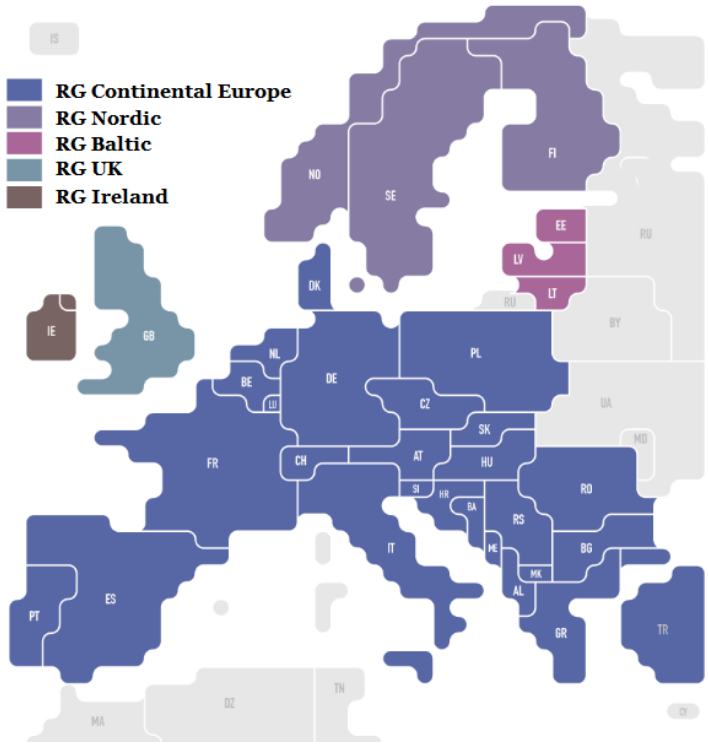

Figure 2.3 – Map of the five European synchronous areas [20].

Any disturbance within each synchronous area is registered across the entire zone and it can disrupt the operation of equipment, disconnect power plants to prevent damage and lead to large-scale blackouts. For instance, in mid-January 2018, the Continental Europe synchronous area experienced a reduction of frequency average up to 49.996 Hz: one of the reasons is related to the fact that Kosovo deliberately decreased its output as a tactic in pursuit of ENTSO-E membership status on the same footing as

Serbia. This particular event affected also those electric clocks that are steered by the frequency of the power system, leading to a delay close to six minutes ([21]-[22]): this phenomenon is called grid time deviation.

In general, the frequency behavior is the following:

- If generation is equal to the demand, frequency is stable at its rated value.
- If generation is greater than demand, frequency increases.
- If generation is lower than demand, frequency decreases.

Therefore, in case of a perturbation on the electrical network, frequency regulation is needed. It is characterized by several time scales of operation that differ in their response times: Primary, Secondary and Tertiary frequency control. Power Reserves are associated to each phase of frequency regulation. Three are the main objectives of these power reserves:

1. Block the frequency variation and bring it to a constant value, soon after a disturbance, in order to re-establish the balance between generation and loads.
2. Drive the frequency back to its nominal value by causing a temporary unbalance in the opposite direction.
3. Restore the reserves previously used in order to be ready for a successive perturbation.

Here below, a description of each service and of its respective power reserve is provided.

2.3.1 Primary Frequency Regulation: Primary Control Reserve (PCR)

The goal of Primary Frequency Regulation (PFR) is to contain the frequency variation occurring soon after a perturbation and stabilize it at a generic constant value within admissible limits. A Primary Control Reserve (PCR), also known as Frequency Containment Reserve, is associated to this control action. Once the frequency reaches a new constant value, PFR ends and the balance between generation and demand is restored. The activation of this reserve is very fast: its action starts automatically as soon as a frequency event occurs and fully activated in typically 30 seconds and it must be maintained for at least 15 minutes [18]. In 2016, the UK introduced the so called Enhanced Frequency Response (EFR), whose full activation time is much lower

than the one adopted in other European Countries: EFR providers must be capable of responding within one second to frequency deviations [23].

The control action of PFR is based on the Droop Control Law. It is decentralized and autonomous for each resource in charge of providing this service (i.e. conventional generators). This control law, describes the relationship between the frequency variation from its nominal value Δf and the variation of regulating power required to generators ΔP. The main parameter is the droop: it represents the ratio between the frequency variation in per unit and the real power variation in per unit. The change in frequency is expressed as a ratio with respect to nominal frequency and the change in active power is expressed as a ratio with respect to the maximum power offered as PCR by the unit. Therefore, a single value of droop chosen by TSO allows every unit to know their power output in each moment of regulation. The equation for droop is the following:

$$droop = -\frac{\frac{\Delta f}{f_{nom}}}{\frac{\Delta P}{\Delta P_{PCR}}} \cdot 100 \quad [\%] \tag{2.1}$$

Where f_{nom} is the nominal frequency and ΔP_{PCR} is the regulating band offered for this service.

The droop control curve is represented in *Figure 2.4*:

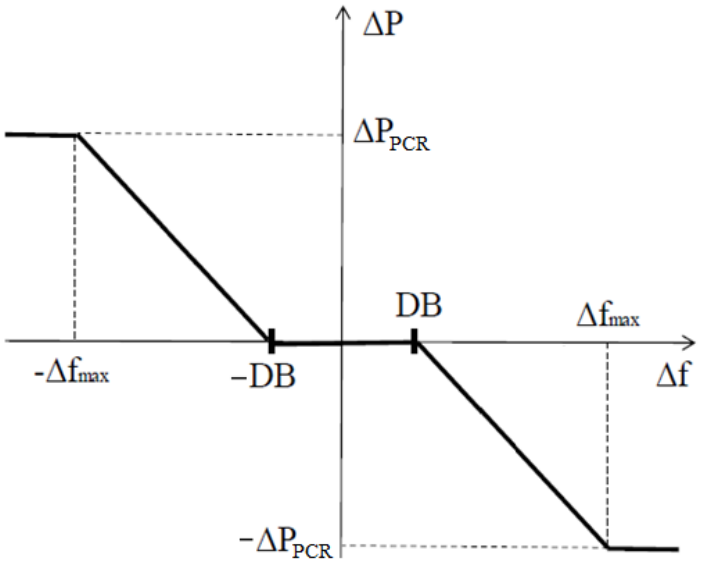

Figure 2.4 – Droop Control Curve.

The droop control curve allows to describe the working principle of PFR:

- In case of under frequency ($\Delta f < 0$), generators are asked to increase their power production $\Delta P > 0$ (the positive reserve is exploited).
- In case of over frequency ($\Delta f > 0$), generators are asked to decrease their power production $\Delta P < 0$ (the negative reserve is exploited).

Moreover, three flat parts can be identified in *Figure 2.4*:

- The flat part in the centre of the graph is called Dead Band (DB). It means that no regulating power is required for PFR when the frequency variation is too small ($|\Delta f| < DB$). A typical value for dead band is 20 mHz.
- An upper flat part and a lower flat part, in which the power output is constant respectively at the maximum and at the minimum regulating power since frequency is very far from its rated value.

All the rules regarding PFR are specified by TSOs in the National Grid Codes. In Italy, Terna defines the service specifications in [24]. In particular, PFR is mandatory for all the production units with nominal power greater than 10 MVA, except for non-programmable RES. These units are named Relevant Production Units (RPU). All the RPU must guarantee at least 1.5% of nominal power as primary control reserve. Therefore, their working range is slightly reduced, as shown in *Figure 2.5*.

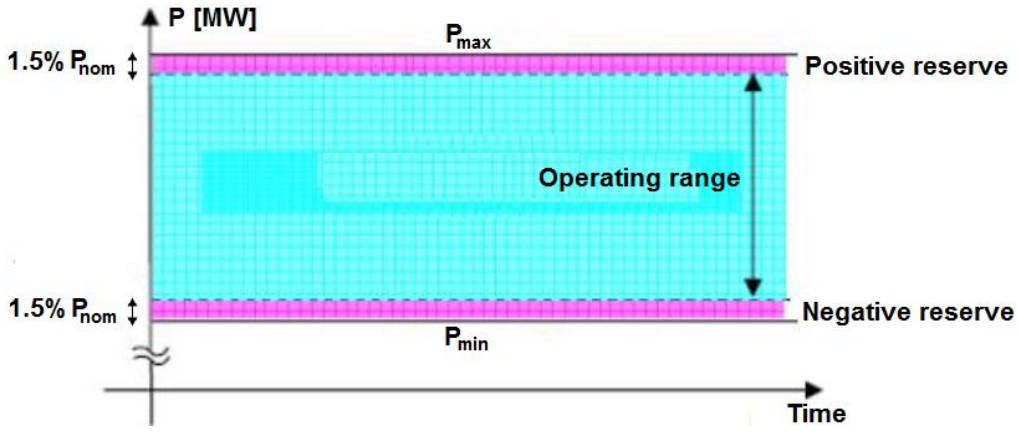

Figure 2.5 – Operating range and regulating bands for relevant production units [24].

The PFR contribution is subject to some time constraints: at least half of the power required must be provided within 15 seconds and all the power set point within 30

seconds. Other technical prescriptions are: intentional dead band not greater than 10 mHz-20 mHz and fixed droop equal to 2-5% depending on the type of generating unit.

2.3.2 Secondary Frequency Regulation: Secondary Control Reserve (SCR)

PFR blocks the frequency variation occurring after a sudden event, but it does not restore the rated value of frequency. The goal of Secondary Frequency Regulation is to bring the frequency back to its nominal value. A Secondary Control Reserve (SCR), also known as Frequency Restoration Reserve, is associated to this control action. The SCR operates starting from few seconds up to 15 minutes after a frequency perturbation [18]. It can be activated either automatically or in response to manual dispatch commands. While PFR is characterized by a decentralized operation, SFR is centrally directed by the Transmission System Operator. This service is not mandatory and there is a lower number of service providers: this means that larger power set points are required to each player. Consequently, topology constraints may arise. The TSO, given the total available quantity of PCR, calculates the total power required to restore the nominal value of frequency and shares it among all the generators.

In Italy, the TSO defines each minute a signal, called Area Control Error – ACE (Livello Regolazione Secondaria is the Italian name), which is valid simultaneously for all generators. It represents the percentage of power reserve required to each production unit selected in the market [24]. Note that, since SFR is not mandatory, the Secondary Control Reserve is traded and remunerated on the Ancillary Services Market. Each generating unit willing to participate to the ASM must offer the same power band for positive and negative reserve: SFR is a symmetric service. All the units that are selected on the market follow the power set points defined by the ACE for the whole period in which they are accepted. The ACE is a signal between 0 and 100 [118], whose meaning is:

$$\begin{cases} \Delta P = \Delta P_{SCR} & if\ ACE = 100 \\ \Delta P = 0 & if\ ACE = 50 \\ \Delta P = -\Delta P_{SCR} & if\ ACE = 0 \end{cases} \tag{2.2}$$

The regulating power ΔP varies linearly for intermediate values of ACE. Another requirement for SFR involves the activation time: the maximum delay for fully SCR activation is 15 minutes.

2.3.3 Tertiary Frequency Regulation: Tertiary Control Reserve (TCR)

At the end of SFR, frequency is equal to its nominal value. Nevertheless, the SCR may have been used completely or partially and it would be useful to restore them in order to be ready for new frequency events. This is the goal of Tertiary Frequency Regulation (TFR). In this case, a Tertiary Control Reserve (TCR), also known as Replacement Reserve, is defined. This control action can be manually activated after the SFR. For instance, if the positive reserve of a plant providing SFR has been completely exploited, the TCR provides positive power to grid in order to allow the plant enrolled in the SFR to reduce its power output and get back to the power set point it was following before SFR. In this way, that power plant can be ready to provide again positive reserve. TFR operates on a longer time scale with respect to the other control services: its activation time can go from 15 minutes to hours [18].

In Italy, the Replacement Reserve is a service traded on Ancillary Services Market. This service is centrally coordinated by Terna and activated manually in case of observed or expected sustained activation of SCR and in the absence of a market response. It requires slower but longer action (as shown in *Figure 0.7*): therefore, slow ramp and large energy output.

2.4 Two ASM paradigms for PCR and SCR: Italy and Germany

As previously introduced, power reserves related to frequency control are generally traded on the ASM in order face unbalances between generation and demand within the electrical network. In particular, PFR and SFR are two of the most widespread services and they have been characterized by the highest and more constant remunerations along the years. In this Paragraph, the focus is on two ASM models for Primary and Secondary control reserves' remuneration: the Italian and the German ASM.

In Italy, PFR is not subject to a market, but it is mandatory for all the Relevant Units, which are generating units with nominal power greater than 10 MVA, except non-programmable RES. They are obligated to reserve a certain amount of capacity (1.5% of their nominal power) in order to meet TSO requirements and this service is poorly

remunerated. All the relevant units willing to be remunerated for this service must follow a enabling procedure and install a monitoring system, called UVRP (Unità per la Verifica della Regolazione Primaria), whose correct operation must be verified by Terna. PCR remuneration depends on the zonal price, defined in the DAM clearing procedure, and it is energy-based. In particular, the prices applied for PCR remuneration are defined in the Grid Code as follows [25]:

- The remuneration paid for positive PCR is equal to zonal price plus a half of a particular constant considering the difference between the average price for positive SCR and the average price on the DAM of the previous year.
- The payment requested for negative PCR is equal to the zonal price minus a constant considering the difference between the average price for negative SCR and the average price on the DAM in the previous year.

On the other side, in Germany there is no obligation for a grid user to provide Frequency Containment Reserve, as shown in *Figure 2.6*.

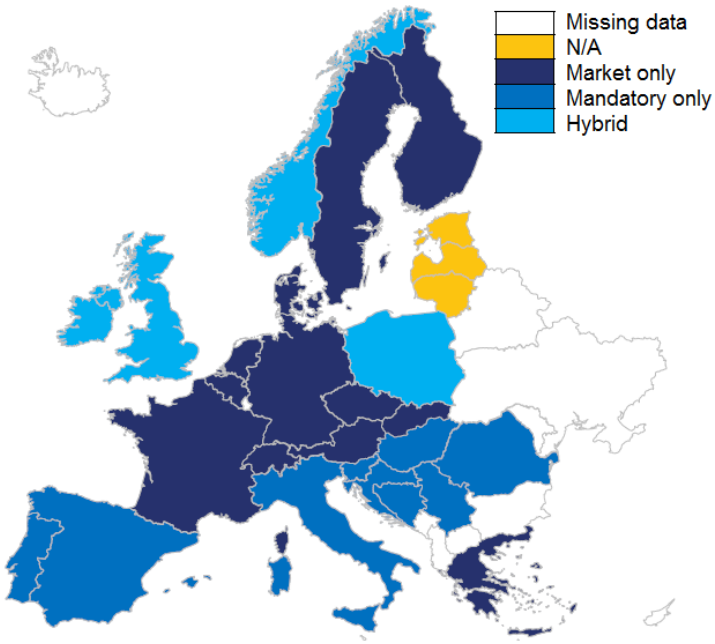

Figure 2.6 – Procurement scheme of Primary Control Reserve in European Countries [26].

In Germany, generating units with nominal power ≥ 100 MW must be capable of providing PCR, as specified in the German Grid Code. Moreover, generating units with a nominal capacity < 100 MW may also be employed for PCR provision after an agreement with the TSO [27]. All the generating units willing to provide this service

must follow a prequalification procedure, managed by the TSO, in which they must prove that they fulfil all the requirements specified by the Grid Code. This phase concludes with a framework agreement, which represents a precondition for taking part in a joint tender for PCR. In the last years, an international PCR cooperation among some European Countries has been born: Germany, France, Austria, Belgium, Netherlands and Switzerland belong to this common market (Central Western Europe-CWE). Nevertheless, for technical and/or regulatory reasons, it might be necessary to decouple the common market. In this case, the coupled markets are split up into two sub-markets: Switzerland and Germany-Austria-Belgium-Netherlands-France. PCR is traded through a weekly auction, which takes place on each Tuesday for the next week. Contrarily to what happens in Italy, PCR remuneration is based on capacity (power): the power offered on the market must be at least 1 MW for both positive and negative reserve [28]. The capacity is remunerated based on a pay-as-bid mechanism. *Table 2.1* summarizes the main features of PCR in Italy and Germany.

Table 2.1 – Main features of PCR in Italy and Germany.

Primary Control Reserve (PCR)	Italy	Germany
Procurement scheme	Mandatory	Market based
Nominal power of service providers	≥ 10 MVA	≥ 100 MW <100 MW (after agreement with TSO)
Minimum capacity reserve	± 1.5 % of nominal power	± 1 MW
Type of reserve	Symmetric	Symmetric
Auction type	-	Weekly
Bid remuneration	Energy (fixed price)	Capacity (pay-as-bid)

For what concerns Secondary Frequency Regulation, both in Italy and in Germany the SCR is a service traded on the ASM. In Italy, all the generating units willing to provide this service submit their offers in terms of capacity generally one hour and a half before the beginning of the market session [15]. The SCR must be symmetric and each reserve must be greater than 15% of nominal power (hydroelectric) or greater than the higher value between 10 MW and 6% of nominal power (thermoelectric) [24]. This phase of the Italian ASM is named Mercato di Bilanciamento (MB) and it is divided in 6 sessions occurring every 4 hours [15]. The remuneration is instead energy based (€/MWh) and a pay-as-bid mechanism is adopted. Each generating unit offers, for each hour of the day, two prices:

- A price in €/MWh associated to positive reserve, which represents how much money it asks for injecting extra power in to the grid.
- A price in €/MWh for negative Reserve, which represents how much money it is willing to pay for reducing its power injection.

Hourly offers are selected every 4 hours for the following 4-hours period. The acceptance criterion depends on the difference between the prices associated to positive and negative reserves: the lower the difference, the higher the probability to be accepted. Since SCR bands are symmetric, a production unit is accepted or rejected for both reserves.

On the German ASM, there are weekly auctions for different time-periods during the day, defined as peak and off-peak hours. The minimum capacity that must be guaranteed by service providers for SCR is 5 MW [29]. More than one price exists for SCR (€/MW/week). Unlike the Italian case, secondary reserves are asymmetric and tendered in four products:

- Incremental peak and off-peak (positive reserve).
- Decremental peak and off-peak (negative reserve).

Furthermore, the auctions include also an energy price for the energy delivered (€/MWh). Therefore, SCR remuneration is both in terms of capacity offered and in terms of energy actually exchanged and the pricing rule is pay-as-bid. A table is provided also for SCR.

Table 2.2 – Main features of SCR in Italy and Germany.

Secondary Control Reserve (SCR)	Italy	Germany
Procurement scheme	Market based	Market based
Minimum capacity reserve	± 15 % of nominal power (hydro) ± 10 MW or ± 15 % of nominal power (thermal)	± 5 MW
Type of reserve	Symmetric	Asymmetric Peak/off-peak
Auction type	4-hours	Weekly
Bid remuneration	Energy (pay-as-bid)	Capacity + Energy (pay-as-bid)

2.5 Future scenarios for the ASM

In recent years, the large penetration of non-programmable RES and Distributed Generation (DG) has introduced a large variability in the power production, affecting the overall reliability of the power system. It is clear that a modification and improvement of network management techniques is necessary. Nowadays, MV and LV distribution networks are not "passive" anymore: the presence of DG allows for a bi-directional flow of power, which makes them an "active" portion of the overall system. This direction of evolution is internationally identified with the term Smart Grid. It implies all the innovative structures and operations that are able:

- To maintain a high level of safety and reliability of the whole system.
- To cope with the many problems introduced by Distributed Generation.
- To manage and control the consumption units (Demand Response).
- To increase energy efficiency.
- To manage new technologies with reference to the electricity market.

For what concerns the ASM, the large penetration of renewables in the last years has caused an increment of the total energy exchanged and this trend is set to grow in the next years. Moreover, they have caused an increment of the costs in the ASM due to their high unpredictability. Nevertheless, this kind of resources have been treated in a privileged way. For instance, deviations between real and forecasted production have not been penalized, but simply remunerated. Therefore, no pressure was applied to renewables towards unbalance minimization. This situation has led to a higher difficulty in defining all the power reserves necessary to manage the unbalance of the grid [30]. For instance, in days with large generation by wind and PV and low load, it could happen that negative reserves are not sufficient and that only base-load plants are active, which must deliver at least a minimum power. In these cases, reduction of import becomes necessary. If this action this is not sufficient, non-programmable RES are curtailed. This does not represent a good solution since decarbonization is one of the main targets worldwide.

As previously introduced, the regulatory frameworks of the majority of ASMs in the world are tailor made on traditional, reliable and programmable generating units. It could be useful to open these markets to new players in order to reduce congestions and increase the security of the network. In particular, future regulation should allow participation to the ancillary services market of non-programmable RES connected to

the EHV-HV transmission network and DG connected to the MV-LV distribution network. Other innovative actors may be identified, such as Aggregators, Demand Response (DR) and Energy Storage Systems. In Italy, the Authority, with the resolution 300/2017/R/eel [123], has defined all the criteria to allow consumption units, non-relevant production units (including non-programmable RES and DG) and energy storage systems to take part to the ancillary services market.

The goal of this work is to evaluate the performance of a BESS in providing ancillary services. However, a brief overview on the main new actors could be useful to better understand the context of this particular application.

2.5.1 Aggregators

Aggregation consists in grouping distinct entities in a power system (consumers, producers, prosumers or any mix of these) to act as a single entity when proposing on the markets. The aggregator acts as an intermediary between Distributed Energy Resources (DERs) and the market manager. In Italy, according to the resolution 300/2017/R/eel [123], the aggregating body, acting as a single entity on the ASM, is called Balance Service Provider (BSP). The aggregation of production and consumption units within a geographical perimeter must cope with the grid model adopted by the algorithm for the selection of the offers on the ASM so that the movement of the units does not violate the network constraints. Different types of Aggregated Virtual Units (Unità Virtuali Abilitate - UVA) are defined:

- UVAP – Unità Virtuali Abilitate di Produzione: they are made only by non-relevant production units (either programmable or non-programmable), including energy storage systems.
- UVAC – Unità Virtuali Abilitate di Consumo: they include only consumption units (to date, all non-relevant).
- UVAM - Unità Virtuali Abilitate Miste: they can be made by non-relevant production units (both programmable and non-programmable), energy storage systems and consumption units.
- UVAN - Unità Virtuali Abilitate Nodali: they include relevant production units and/or non-relevant production units (either programmable or non-programmable) and, eventually, also consumption units under the same node of the national transmission grid.

In future years, UVAM and UVAN will overtake the division in UVAP and UVAC, remaining the only actors on the market.

2.5.2 Demand Response (DR)

The name Demand Response (DR) indicates the possibility for loads to play a significant role in the operation of the electric grid by reducing or shifting their power consumption to increase the reliability of the power system. In particular, DR becomes very important when the residual load is negative: the residual load is defined as the difference between the power demand and the generation of non-programmable RES, such as wind and solar PV. Methods of engaging customers in DR efforts include offering time-based rates such as time-of-use pricing, critical peak pricing, variable peak pricing, real time pricing and critical peak rebates. DR also includes direct load control programs which provide the ability for power companies to cycle air conditioners and water heaters on and off during periods of peak demand in exchange for a financial incentive and lower electricity bills [31].

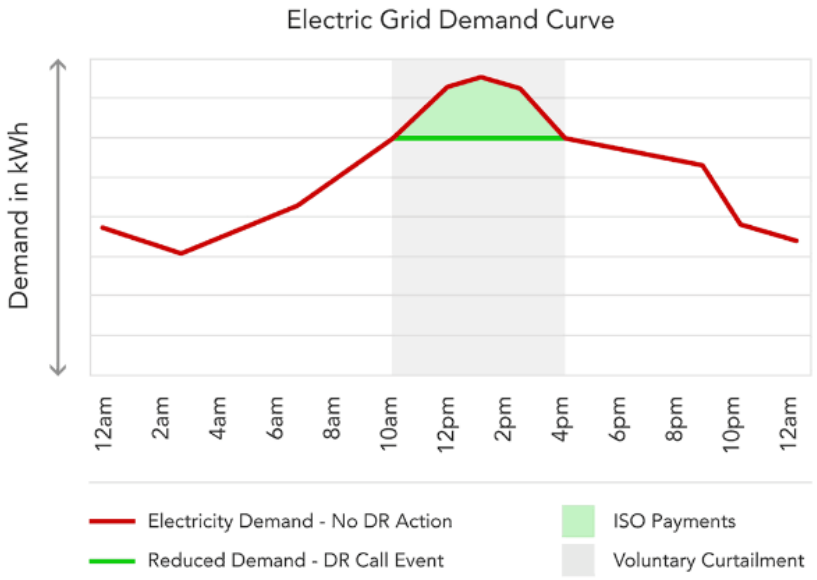

Figure 2.7 – Demand Response working principle [32].

Demand Response providers can be aggregated, forming a larger group and they are categorized according to their characteristics (response speed, frequency of intervention, period of intervention, programmability of recovery of demand curtailed…). DR is more frequently provided by consumption units with programmable and forecastable demand and/or with an autonomous power generation system, such an Uninterruptible Power Supply (UPS). Different policies

can be put in place to manage DR. For instance, in UK a demand response program involving industrial and large commercial units has been developed: these energy-intensive users can contract time of usage of interruptible loads, but, on the other side, the TSO can ask for load shedding in order to guarantee the network balance. Another example is the DR program tested in France on around 450 000 customers, which makes use of different prices for electricity according to weather (Tempo tarif). This program brought an average reduction of consumptions and, consequently, savings on the electricity bill. In Spain, the TSO can ask some industries to limit their demand during periods of time, varying from 45 min to 12 h, upon the condition that industrial consumers are informed in advance. Each year these industrial consumers receive a discount both in fixed and variable charges according to the number of requests to reduce their demand [33].

In Italy, following the resolution 300/2017/R/eel [123], Terna developed a pilot project, which started in June 2017, regarding the participation of loads to the ancillary services market [34]. The new actor on the scene is called UVAC (*see Paragraph 2.5.1*). The technical specifications for an UVAC are the following:

- At least 10 MW of power reduction within 15 minutes from Terna's request.
- Capability to maintain the power reduction for at least 4 consecutive hours.
- Consumption units must be in the same aggregation area defined by Terna.

In the ASM, UVAC are considered, for practical reasons, as generating units: a reduction of consumption of the UVAC is seen as an increment of injection.

2.5.3 Energy Storage Systems (ESS)

Energy Storage Systems (ESSs) are well suited for stationary applications, due to their ability in changing output immediately and very low operating cost when idle. Moreover, the application of energy storage systems in the ancillary services market is favored by the fact that some services are energy neutral, which means that the overall energy injections and absorptions are approximately equal over a period [35]. Unlikely traditional generating units, ESSs can provide some services only for a limited duration, due to their finite capacity. Another important quality of energy storage is the high dynamic response: their ramp rate largely overtakes the ones related to conventional units and they can follow irregular power profiles [36]. In general, no single ESS technology can meet the requirements for all possible

applications. Selection of ESS is based on the assessment of the characteristics of the different EES options against the requirements of the specific application.

Figure 2.8 shows the typical power and energy ratings of different energy storage technologies. The nominal discharge time at power rating is also shown within the range seconds-months.

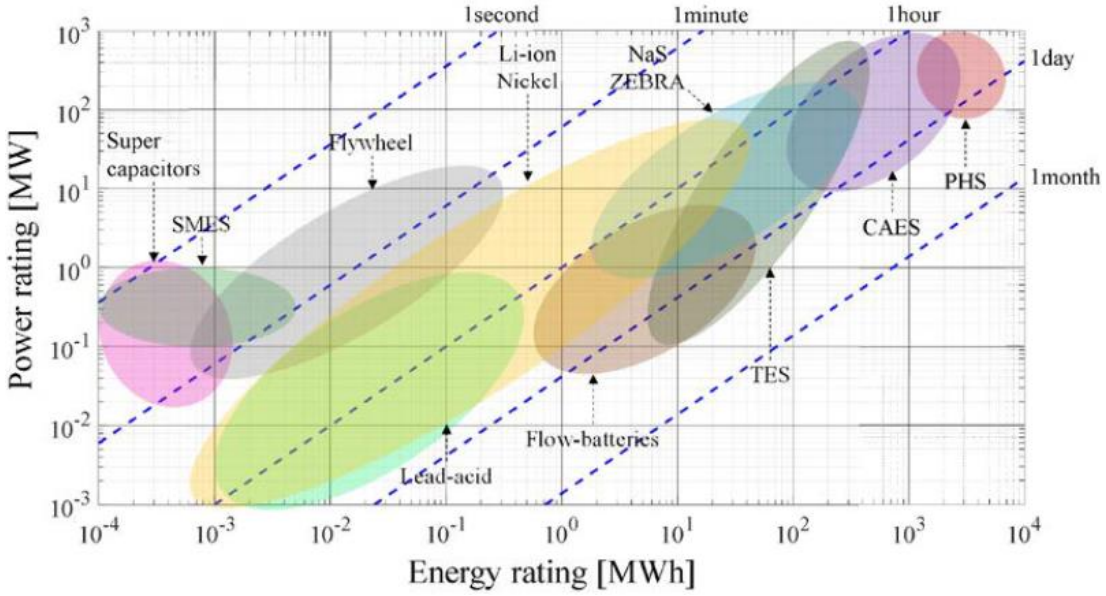

Figure 2.8 – Comparison of different ESS technologies in terms of rated power, storable energy and discharge time [5].

Note that Battery Energy Storage Systems (BESSs), and Lithium-ion technology in particular, occupy the wider area on the graph. The larger the area, the higher the suitability of the technology for a wider range of applications.

In the following Section, the deployment of BESSs for grid services provision is analysed, with particular attention on the ASM.

2.6 BESSs for ancillary services provision

In general, BESSs are suitable for many stationary applications in the electricity sector. Two macro-categories of stationary applications may be identified:

1. Off-grid applications: BESSs are deployed in conjunction with local generation, typically renewables, in order to provide electricity to remote areas of the world (rural electrification) and/or to be independent from the main grid. Generally,

these installations can range from tens of kWh (small stand-alone systems) up to hundreds of kWh (micro-grids).

2. Grid-tied applications: BESSs are deployed in order to provide both grid-support services on utility scale and for consumer use on the domestic scale.

Examples of stationary applications are voltage support, frequency regulation, spinning reserve, customer-side peak shaving, arbitrage, load levelling, renewable integration, off-grid installations and arbitrage/storage trade [5]. All these applications are collected in *Figure 2.9*.

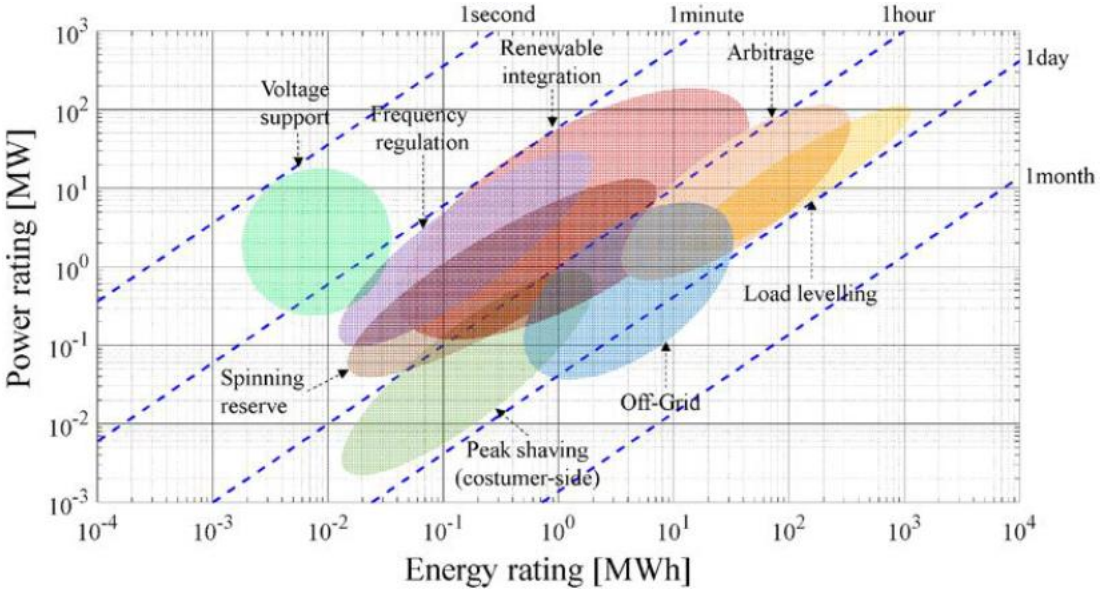

Figure 2.9 – Typical power and energy ratings required to energy storage technologies by different stationary applications [5].

By comparing the colored areas in *Figure 2.8* and *Figure 2.9*, it is clear that BESSs, and Li-ion BESSs in particular, are highly suitable to provide frequency regulation.

The objective of this work is to verify the ability of BESSs in providing primary and secondary frequency regulation from both technical and economical point of view. Nowadays, PCR and SCR are mainly provided by conventional generators, which are programmable and reliable. New regulatory frameworks are therefore necessary in order to allow BESSs to participate to the ASM. The main issues related to BESSs are:

- Minimum required size: the majority of ASM allow the participation of units with nominal power higher than a specific quantity (i.e. 10 MVA in Italy). Such large

dimensions can be obtained without any problem with a large stack of cells. The only issue is related to the high investment costs for such a large system.

- Negative reserve means power absorption: unlikely traditional generators, which can only inject power into the grid, BESSs can both inject or absorb power. They behave both as generators and as loads.
  For Battery Energy Storage Systems:

$$\begin{cases} P > 0 \; in \; case \; of \; Positive \; Reserve \; (injection) \\ P < 0 \; in \; case \; of \; Negative \; Reserve \; (absorption) \end{cases} \quad (2.3)$$

- Programmability: BESSs power response to frequency perturbations is clearly faster and more accurate during the transient phase compared to traditional power plants [36].
- Limited capacity: some services traded on the ASM, such as SCR and TCR, require providers to sustain the power output at least for a certain period. BESSs can provide these services for a lower time due to their limited capacity.

The most challenging requirement for BESS is service continuity. In fact, even if a zero-mean ancillary service signal is presumed, the battery will constantly decrease in the SoC level due to the internal efficiency that affects charge and discharge processes (as described in *Chapter 1*). If the battery reaches its capacity limits, service provision is interrupted and the provider incurs in penalties that reduce the overall profits. As already said, the device, which is adopted to preserve BESS from overpassing saturation limits, is called Battery Management System (BMS): a simple BMS evaluates the voltage and, if the maximum or minimum limit is reached, it limits the absolute value of the current, which can reach also zero (no energy flow). In this study, an indicator of technical performance to evaluate service continuity is introduced: Loss of Regulation (LoR). It is defined as the ratio between the energy not provided for the service $E_{np,service}$ due to exceeded BESSs limits and the overall regulating energy required in the evaluated period $E_{req,service}$:

$$LoR = \frac{E_{np,service}}{E_{req,service}} \cdot 100 \quad [\%] \quad (2.4)$$

Since regulation in place does not provide a clear framework regarding LoR valorization, in this work a simplifying assumption is made: a constant price is paid for the energy not provided p_{LoR} (€/MWh). This logic is applied to both PCR and SCR,

as detailed in the following chapters. The penalties associated to LoR are computed as follows:

$$Penalty_{LoR} = p_{LoR} \cdot E_{np,service} \quad [€] \tag{2.5}$$

The investigation of the technical and economic performances of BESSs in the provision of PCR and SCR is assuming higher relevance as a research topic. In this study, two cases are deeply analysed: single service provision (only Primary Control Reserve) and simultaneous multi-service provision (PCR and SCR).

2.6.1 BESS for single service provision: PCR

Primary Frequency Regulation is identified as one of the most promising and interesting regulation services for BESSs. Unlikely traditional generators, BESSs do not have a scheduled production and they can be fully dedicated to this service. Hence, the regulation droop, which in Italy is defined considering a regulating band of 1.5% of the nominal power for Relevant Production Units, could be rescaled based on the fraction of nominal power the BESSs is willing to use for PCR:

$$droop_{BESS} = \frac{1.5}{100} \cdot \frac{1}{\Delta\dot{P}_{PCR}} \cdot droop \quad [\%] \tag{2.6}$$

Where $\Delta\dot{P}_{PCR}$ is the regulating band of the BESS offered for PCR in per unit. For instance, the range 2-5% for droop, used nowadays for relevant production units in Italy, is translated in the range 0.03-0.075% for BESSs which adopt 100% of their nominal power as regulating band for PCR. This choice is useful for defining the control strategy of a BESS aiming to completely serve as AS provider.

The characteristics of this service and the remuneration schemes are different from one Country to another. For instance, this service can be mandatory/market based and poorly/highly remunerated, as previously introduced in *Paragraph 2.3.1*. Apart from the specific regulating mechanism in place, the PCR provision will be allowed as long as BESSs fulfil technical and commercial requirements set by the TSO. As already mentioned, one of the most important requirements for BESSs providing PCR is service continuity. In this case, LoR is calculated as follows:

$$LoR = \frac{E_{np,PCR}}{E_{req,PCR}} \cdot 100 \quad [\%] \tag{2.7}$$

Where:

$$E_{req,PCR} = \int_{t_{start}}^{t_{end}} \Delta\dot{P}_{PCR} \cdot P_{nom}\, dt \quad [MWh] \tag{2.8}$$

$$E_{np,PCR} = \int_{t_{start}}^{t_{end}} \Delta\dot{P}_{PCR} \cdot P_{nom}\, dt \Big|_{\substack{V<Vmin \\ V>Vmax}} \quad [MWh] \tag{2.9}$$

In this context, the implementation of SoC control strategies could be useful to enhance competitiveness of BESS and reduce LoR, as investigated in previous studies [37]. In this study, different SoC restoration techniques are adopted in case of single service provision: a description of such strategies is provided in *Chapter 4*. In *Chapter 5,* the results of single PCR provision in the framework of both Italian and Central Western Europe ASM are reported.

2.6.2 BESS for multi-service provision: PCR and SCR

In case of multi-service, SCR provision could have a positive effect on BESS, acting as a "passive" SoC management strategy. In this case, two types of SCR may be distinguished:

- Symmetric: the positive reserve equals the negative reserve offered on the ASM and they are equal to the minimum between the upward and the downward margin (e.g. Italian case).

$$\Delta P_{SCR,+} = \Delta P_{SCR,-} = \min(\Delta {P_{SCR,+}}^{0}; \Delta {P_{SCR,-}}^{0}) \tag{2.10}$$

- Asymmetric: positive and negative reserves are traded separately on the ASM. They can be different from each other: the upward band may be greater than the downward one and vice versa (e.g. German case). They are equal only if the SoC is equal to 50%.

$$\begin{cases} \Delta P_{SCR,+} = {\Delta P_{SCR,+}}^{0} \\ \Delta P_{SCR,-} = {\Delta P_{SCR,-}}^{0} \end{cases} \tag{2.11}$$

Where ${\Delta P_{SCR,+}}^{0}$ and ${\Delta P_{SCR,-}}^{0}$ are SCR bands before the application of symmetry constraints.

Recent studies [9]-[12]-[104] have demonstrated that multi-service provision can be valuable from both technical and economical point of view, limiting Loss of Regulation and increasing the overall profit. In particular, the asymmetric provision of SCR can be seen as an innovative solution in order to control the SoC of a Battery Energy Storage System. The working principle is the following one:

- When the SoC is close to the upper saturation limit, the BESS owner submits an offer on the ASM characterized by a very large band at a very low price for releasing power (negative reserve) and a very small band at a high price for absorbing power (positive reserve). The objective is to be accepted only for the negative reserve.

- When the SoC is close to the lower saturation limit, the BESS owner submits an offer on the ASM characterized by a very small band at a very high price for releasing power (negative reserve) and a very large band at a very low price for absorbing power (positive reserve). The objective is to be accepted only for the positive reserve.

In *Chapter 6,* PCR plus asymmetric SCR service provision is analysed mainly in the framework of the Italian ASM, taking into account the constraints related to the duration of market sessions (4-hours sessions) and considering the fact that offers must be placed on the market at least one hour and a half before the beginning of the market session [15]. Nevertheless, asymmetric SCR regulating bands are considered, as already happens in Germany, leading to a hybrid structure. The innovation brought by this work regards the application of a prediction tool to forecast the regulating energy required to the BESS by the end of the successive market session. The predictions are used by a controller to optimally define the regulating bands for Secondary Control Reserve to be traded on the ASM. In particular, different forecasting methods are compared and the best ones are included in the model for multi-service. Therefore, in the following Chapter, an overview of predictive analytics, of the main forecasting methods for time-series and their applications on BESSs is provided.

3. INTRODUCTION TO PREDICTIVE ANALYTICS

The aim of this Chapter is to provide a general overview of the working principle of predictive analytics in order to better understand how forecasting techniques can be used for improving both technical and economical performances of a Battery Energy Storage System in providing grid services. As stated in the previous Chapter, SoC prediction is a pivotal point in the implantation of an energy management strategy, in particular for bidding SCR bands one hour and a half before the beginning of the market session. In *Chapter 6*, the effectiveness of such forecasting techniques on the control strategy of a BESS providing multiple AS is analysed. A useful comparison with a standard statistical approach is presented.

Predictive analytics is a broad term describing a variety of advanced statistical and analytical techniques used to develop models that predict future events or behaviors [40]. Predictive analytics involves a large amount of data. Therefore, data management represents one of the main issues in this field. Nowadays, predictive analytics is adopted in many fields such as insurance, banking, marketing, financial services, energy, oil and gas, telecommunications, travel, healthcare, pharmaceuticals and many others. In this Chapter, the main focus is on time-series forecasting. A time series is a set of regular time-ordered observations of a quantitative characteristic of an individual or collective phenomenon taken at successive, in most cases equidistant, points of time [44].

3.1 The predictive analytics process

The predictive analytics process is characterized by different phases [41]:

1. Project definition: define the expected outcomes of the project and identify the datasets which are going to be used in the analysis.
2. Data collection: collect data from multiple sources and prepare them for the analysis.
3. Data analysis: it is the computational process of inspecting, cleaning, transforming and modelling data in order to extract underlying patterns, trends

and relationships in large datasets and transform them into an understandable structure for further use. The extraction of useful information from a dataset is known as Data Mining (or Knowledge Discovery in Databases – KDD). Data mining requires a pre-processing step: data cleaning and integration. This process allows to identify missing and/or incomplete data that can have an negative impact on the overall accuracy of the predictive model and to replace and/or correct them [40].

4. Statistical analysis: it enables to validate the findings, assumptions and hypothesis and to test them using standard statistical models.
5. Modelling: accurate predictive models about the future are provided and the best solution is chosen according to different metrics.
6. Deployment & Monitoring: the model is applied to new data and deployed into every day decision making processes. The performance of the model is monitored to ensure that it is providing the expected results: typically, the performance of a model reduces over time and it is necessary to update it or to build a new one.

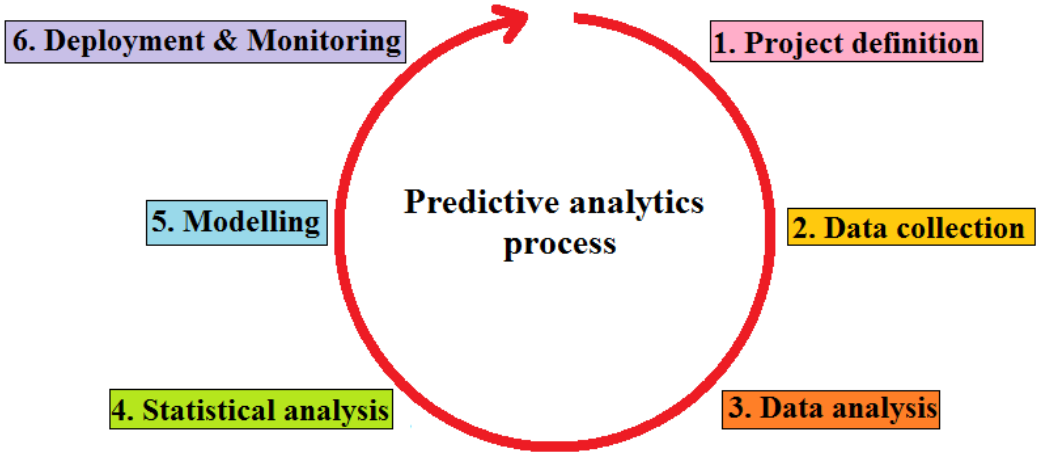

Figure 3.1 – The predictive analytics process.

3.2 Evaluating forecast accuracy

The accuracy of forecasts can be determined by considering how well a model performs on new data that were not used when fitting the model. Consequently, it is common practice to separate the available data into two portions:

1. Training set, used to estimate any parameter of a forecasting model.

2. Test set, used to evaluate its accuracy. Since test data are not used in building the model, they provide a reliable indication of how well the model is likely to forecast on new data.

Typically, the size of the test set is about 20% of the total sample, although this value depends on how long the total sample is and how far ahead you want to forecast. A model that well fits the training data will not necessarily forecast well. This phenomenon is known as over-fitting and it is as bad as failing to identify a systematic pattern in the data.

Figure 3.2 – The whole dataset is split into training set and test set [43].

The forecast error e_t is defined as the difference between an actual observed value and its forecast based on all the previous observations. The word "error" does not mean a mistake, but it refers to the unpredictable part of an observation. It can be written as:

$$e_t = y_t - \hat{y}_t \tag{3.1}$$

Where y_t is the actual observation at time t and $\hat{y}_t$ is the forecast at time t based on all the available data. Starting from the forecast error, forecast accuracy can be measured through different metrics. Two of the most commonly used metrics are:

- Mean Absolute Error (MAE)

$$MAE = \frac{1}{T} \cdot \sum_{t=1}^{T} |y_t - \hat{y}_t| \tag{3.2}$$

- Root Mean Square Error (RMSE)

$$RMSE = \sqrt{\frac{1}{T} \cdot \sum_{t=1}^{T} (y_t - \hat{y}_t)^2} \tag{3.3}$$

Where T is the number of predicted time steps (i.e. the number of predictions). MAE is conceptually simpler than RMSE: the use of squared distances makes RMSE more

difficult to interpret. Since in the RMSE errors are squared before they are averaged, the RMSE gives a relatively high weight to large errors. This means the RMSE should be more useful when large errors are particularly undesirable. The RMSE will always be larger or equal to the MAE: the greater difference between them, the greater the variance in the individual errors in the sample. If $RMSE = MAE$, then all the errors have the same magnitude.

A selection criterion for the choice of the prediction method could be to compare the RMSE with the standard deviation of the real observations, which represents the spread of actual data around the mean:

- If the RMSE is higher than the standard deviation, the prediction method is worse than predicting with the mean.
- If the RMSE is lower than the standard deviation, the prediction model is improving the prediction with the average value.

3.3 Overview of predictive models for time-series forecasting

Many types of predictive models for time-series forecasting may be found in literature. They can assume many shapes and sizes, depending on their complexity and the application for which they are designed. Some forecasting methods are extremely simple, but sometimes they can be surprisingly effective. Usually, they are used as benchmarks for other complex forecasting methods [42]. Examples are:

- Persistence (or Naïve approach): it is the simplest method, since it assumes that each forecast is equal to the value of the last observation.
- Seasonal Naïve method: it is useful for high seasonal data. Each forecast is equal to the last observed value from the same season of the year (e.g. the same month of the previous year).
- Drift method: it is a variation on the Naïve method that allows the forecasts to increase or decrease over time, where the amount of change over time (i.e. drift) is the average change seen in the historical data.

Among the main approaches found in literature for time-series forecasting there are ARMA/ARIMA models [46], Kalman filters [45] and Holt-Winters exponential smoothing [47]. Recently, advanced methods based on Artificial Intelligence (AI) have

attracted increasing attention in the field of time-series forecasting. They include Machine Learning (ML) algorithms such as Artificial Neural Networks (ANN) [50], Genetic Algorithms (GA) [49], Classification and Regression Trees (CART) [51], Support Vector Machines (SVM) [48]. In this study, two ML algorithms are adopted: Random Forest (RF) and NARX Neural Network. The following paragraphs give a brief description of the two working principle of the aforementioned forecasting techniques.

3.3.1 Random Forest (RF)

Before going into the detail of Random Forest (RF), it is necessary to introduce the concept of Decision Tree. Decision Tree is a type of supervised learning algorithm that can be used for both classification and regression problems (CART). Starting from an initial sample, data are continuously split into subsets based on the most significant feature/attribute in input variables. The general structure of a decision tree is represented in *Figure 3.3*.

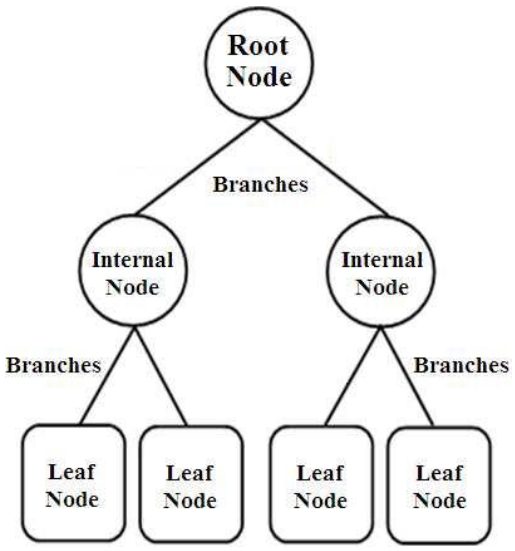

Figure 3.3 – General structure of a Decision Tree.

The main components of a decision tree are:

- Decision Node: where a decision is taken (i.e. where splitting occurs). The topmost decision node in a tree is the Root Node, which represents the entire dataset or sample. The others are called Internal Nodes.
- Leaf Node (or terminal node): it is the end node where splitting does not occur any more.

- Branch: it is the connection between two nodes.

As a problem usually has a large set of features, it results in large number of splits, which implies a huge tree. Such trees are complex and can lead to overfitting. Therefore, it is necessary to define a stopping criterion. One way of doing this is to set a minimum number of inputs for each leaf. Another possibility is to set the maximum depth of the model, which refers to the length of the longest path from the root to a leaf [52]. As already said, each split is performed considering the "best feature" in the node, which means the one that has the highest information gain. An example is shown in *Figure 3.4*.

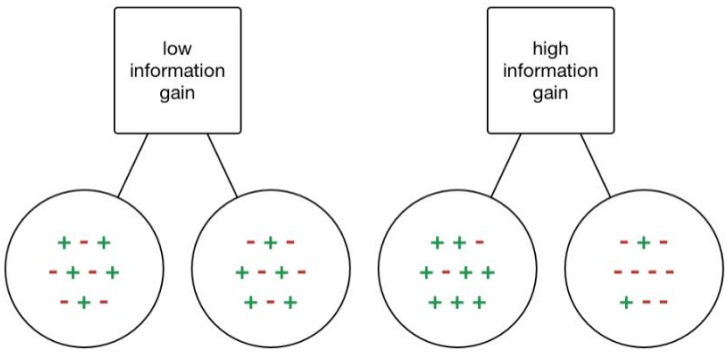

Figure 3.4 – Difference between a feature with low information gain and one with high information gain.

A Random Forest is an ensemble of simple Decision Trees. An ensemble is a Machine Learning concept in which the idea is to train multiple models using the same learning algorithm. In particular, RF is an extension of the Bagging technique. Bagging (or Bootstrap Aggregation) generates several subsets of data from the original training sample through random sampling with replacement: some observation may be repeated, while others may be never considered in each new training subset. Each subset of data is used to train a decision tree. As a result, an ensemble of many decision trees is created (as shown in *Figure 3.5*).

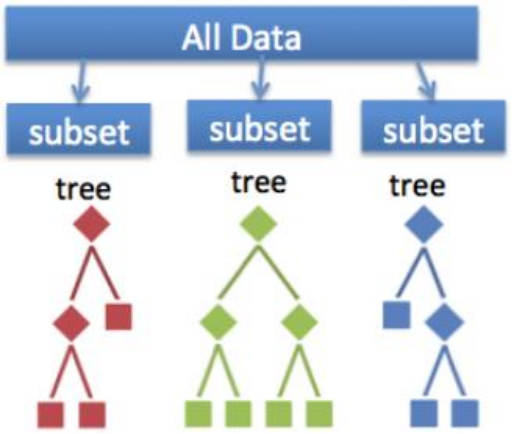

Figure 3.5 – Representation of an ensemble of decision trees [53].

The final prediction is obtained by averaging all the predictions of the decision trees. Random Forest is characterized by one extra step with respect to Bagging: in addition to taking the random subset of data, it also takes the random selection of features rather than using all features when splitting a node. This results in a wide diversity that generally prevents overfitting and results in a better model.

Another great quality of the RF algorithm is that it is very easy to measure the relative importance of each feature on the prediction. For instance, in regression problems, it is possible to compute how much each feature decreases the variance: the more a feature decreases the variance, the more important the feature is [54]. The variance decrease due to each feature can be averaged across the trees to determine the final importance of the variable. By looking at the feature importance, it is possible to decide which features to keep and which one to drop, since they do not contribute enough (or at all) to the prediction process. This is very important, because a general rule in machine learning is that the more are features, the more likely the predicting model will suffer from overfitting and vice versa.

3.3.2 Non-linear AutoRegressive eXogenous (NARX) Neural Network

An Artificial Neural Network (ANN) is a computing system inspired by the way biological nervous systems, such as the brain, process information [55]. ANNs are mathematical and computer science tools with a powerful capacity to learn, store and recall information. They can be seen as black-box modelling tools, which model complex non-linear relationships between inputs and outputs. The main elements of

an ANN are neurons, which are the processing units, and links (or synapses), which connect and transfer information from one neuron to another. The general architecture of an ANN is made by an input layer, one (or more) hidden layers and an output layer (as shown in *Figure 3.6*).

- Input layer: it collects information from the external environment, which are transferred to the hidden layer. Each input neuron represents an independent variable that has an influence over the output of the neural network. No computation is performed in any of the input nodes: they just pass on the information to the hidden nodes.
- Hidden layer: it performs computations and transfers information from the input layer to the output layer. It does not have any direct connection with the outside world (hence the name "hidden"). There can be multiple hidden layers in an ANN, based on the degree of complexity of the problem or the degree of accuracy required. Nevertheless, a high number of hidden layers does not always mean high accuracy [56]. Many researches have been made for evaluating the optimal number of hidden layers as well as the optimal number of hidden neurons in each layer, but a general rule has not been identified yet.
- Output layer: it is responsible for computations and transferring information coming from the network to the outside world. The number of neurons in the output layer represents the number of desired outputs.

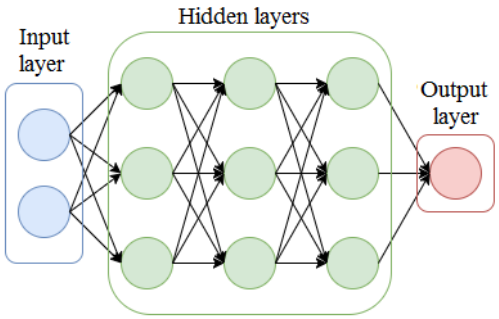

Figure 3.6 – Architecture of an Artificial Neural Network.

Many types of ANN models can be found in literature. One of the most promising algorithms for time-series prediction is the Non-linear AutoRegressive neural network with eXogenous inputs (NARX) [57]-[58]. The network uses a time-delayed (TDL) architecture with a feedback connection from the output layer to the input layer [59]: this memory ability of the NARX neural network allows the use of the past values of predicted or true time series and this may improve the overall performance.

There are two different architectures of NARX neural networks (see *Figure 3.7*):

- Open loop (or series-parallel) architecture: the future value of a time-series is predicted by using the present and past values of the inputs and the true past value of the time-series.
- Closed loop (or parallel) architecture: the prediction is made starting from the present and past values of the inputs and the past predicted values of the time-series.

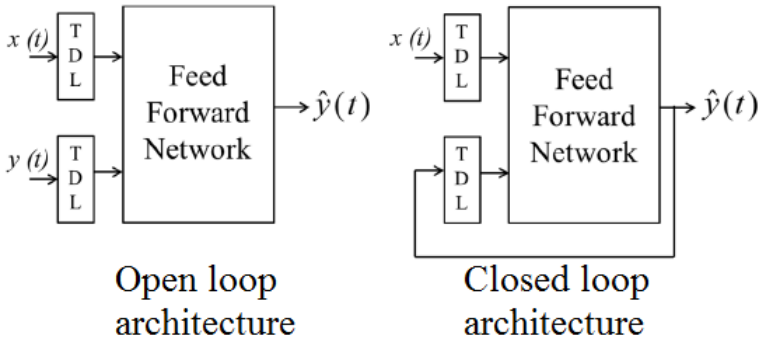

Figure 3.7 – Architectures of the NARX neural network [58].

Two equations describe respectively the open loop (3.4) and the closed loop (3.5) architectures:

$$\hat{y}(t+1) = F\begin{pmatrix} x(t+1), x(t), x(t-1), \dots, x(t-n_x), \\ y(t), y(t-1), \dots, y(t-n_y) \end{pmatrix} \tag{3.4}$$

$$\hat{y}(t+1) = F\begin{pmatrix} x(t+1), x(t), x(t-1), \dots, x(t-n_x), \\ \hat{y}(t), \hat{y}(t-1), \dots, \hat{y}(t-n_y) \end{pmatrix} \tag{3.5}$$

Where $F(\cdot)$ is the mapping function of the NARX neural network, $\hat{y}(t+1)$ is the output of the NARX at time t for time $t+1$ (prediction of y for the time $t+1$), $\{x(t+1), x(t), x(t-1), \dots, x(t-n_x)\}$ are the inputs of the NARX, $\{y(t), y(t-1), \dots, y(t-n_y)\}$ are the true past values of the time-series, $\{\hat{y}(t), \hat{y}(t-1), \dots, \hat{y}(t-n_y)\}$ are the past predicted values of the time-series, n_x is the number of input delays, n_y is the number of feedback delays. The previous equations are general expressions: input and feedback delays must be specified for each particular application or case study. Moreover, computational time is strongly affected by the number of input and feedback delays. Therefore, a correlation analysis could be performed on historical data in order to identify the main delays.

When true past values of the time-series are available, the open loop architecture is adopted for building the predicting model. Moreover, the open loop architecture has two main advantages: the use of true past values of the output improves the accuracy and it is typically faster than the closed loop architecture.

3.4 Forecasting techniques for BESS applications

One important factor associated with BESS is the investment cost: its negative impact on profitability can be reduced either by minimizing the capacity of the storage unit or by optimizing its operation. Many studies have been found in Literature, which stress how a good operational strategy can be remarkably improved by introducing forecasting techniques in control systems. However, results are hardly comparable. Some use perfect forecasts for investigation [90]-[91]-[92], others synthetic forecasts (modified measured time-series) [93]-[94] or forecasts by meteorological services [95]-[96]-[97].

The aims of these studies cover a wide range. E.g., in [98] the objective is to optimize the capacity of a NaS battery in order to shave power fluctuations of a wind farm as it interfaced with national grid; instead, in [99] the objective is to optimize power flows of a BESS-PV system in order to meet local loads and be profitable.

A typical technological solution is using a Model Predictive Controller (MPC), which is a family of digital controller algorithms that include an internal dynamic model of the process, a history of past control moves and an optimization cost function over the prediction horizon. In [100], Authors implement a MPC control system for the day-ahead aggregated presumption load forecast and the construction of an optimal dispatching strategy. Prosumers aggregations and utility-scale BESS coupled with interruptible renewable sources are typical fields in which forecasting technique are used, because simple algorithm can play a major role in performance improvements [101].

Moving closer to the topics of this study, MPC can be used also in frequency regulation applications [125]. In [102], historical values of frequency are used to feed a Grey Model algorithm, which is capable of predicting frequency multi-step ahead and use it in the optimization part of the controller. A Grey Model-based prediction of SoC level is used also in [112], in which Authors propose an intraday market session for PFR. Another example of improving strategy for PFR provision is [103]: in this case,

an improved SoC management strategy allows BESS to meet UK system requirements in order to be eligible for providing PFR.

Recent works tackled also the problem of simultaneous multi-service provision [9] [104], in which statistical methods are used to define SFR bands for the following market session in order not to saturate the battery. The goodness of results presented suggests that this strategy could be improved by increasing the accuracy of forecasting techniques.

Several work try to use Neural Networks for short-term predictions of electric loads [107]-[108]-[109]-[110]-[111]. For instance, [107] uses 8 predictors (such as month, day of the week, hour of the day, temperature, humidity …) to predict Saudi Arabia national grid profile, which is a profile characterized by an important seasonality feature. The chosen algorithm was a simple two-layered feed-forward neural network.

It is also possible to find examples of using Machine Learning algorithms for forecasting grid frequency [105]-[106]. In particular, [105] uses endogenous predictors (i.e. predictors coming from historical frequency data) and wind data to feed a multilayer feed-forward back propagation network, [106] continues the study and includes other exogenous predictor; in particular, a good improvement is achieved considering actual available power, load demand, power deficit and wind power. [106] shows how the optimization of the algorithm parameters (in this ase the number of neurons in the hidden layer) can have a crucial role in gaining accuracy (see *Figure 3.8*).

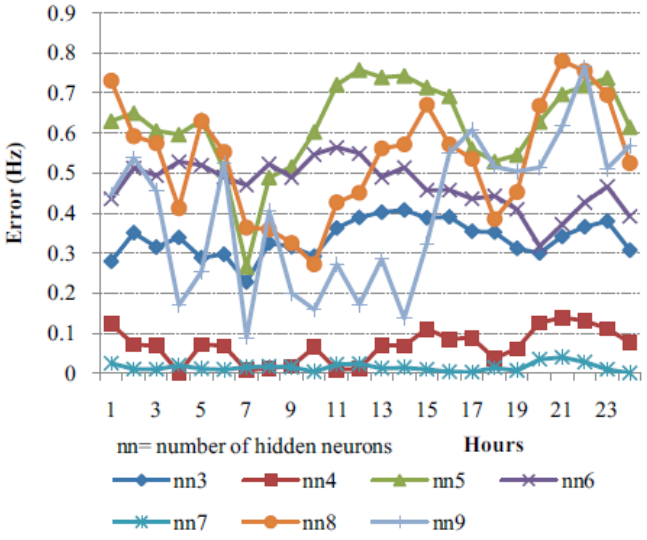

Figure 3.8 - Performance of ANN varying the number of hidden layers [106].

4. GOALS, METHODOLOGY AND MODELS ADOPTED

The objective of this research is to verify the ability of a Battery Energy Storage System in providing frequency regulation services to the electrical grid from both technical and economical point of view. In *Chapter 5* and *6*, two cases are deeply analysed: single service provision (only Primary Control Reserve), both with and without SoC restoration strategies, and multi-service provision (PCR and asymmetric SCR). In this Chapter, all the models adopted in the research are presented. At first, the definition of the BESS model considered in all the simulations is shown (cell, BMS, SoH, inverter, efficiency). Then, the model for PCR provision is detailed (PCR controller for all the SoC restoration strategies, PCR remuneration, LoR computation). Finally, the model for multi-service is described (SCR controller, LoR allocation and computation, SCR remuneration). All the models are implemented in a MATLAB®-Simulink™ environment.

The methodology adopted for the analysis of PCR provision (single service) is the following.

1. Base case analysis: PCR provision without SoC restoration strategies.
2. Implementation of four SoC management strategies to guarantee service continuity to the BESS: Dead Band strategy, Variable Droop strategy, SoC restoration with service interruption and SoC restoration without service interruption.
3. Comparison of the results of the different SoC control strategies both on a technical and on an economic perspective and identification of the best approach.
4. Sensitivity analysis on the main parameters of the best strategy for the optimization of technical and economical results.

For what concerns multi-service, PCR coupled with asymmetric SCR provision is analysed in the framework of the Italian ASM. In this case, SCR asymmetric bands' allocation is used as SoC restoration strategy. Therefore, the constraints related to the duration of market sessions (4-hours sessions) and the fact that offers must be placed on the market at least one hour and a half before the beginning of the market session [15] must be considered. In this context, a prediction tool that is able to forecast the

regulating energy required to the BESS by the end of the successive market session becomes necessary to optimally allocate bands for SCR. Consequently, the general methodology adopted for the study of multi-service provision is more complex than the one described for single PCR provision. The various steps are detailed in the following list.

1. Statistical analysis on the frequency and on the ACE in order to identify the main features of these two signals, which are used to define the main inputs of the predicting tools.
2. Prediction of the regulating energy associated to both PCR and SCR by using different forecasting methods: statistical method, Random Forest, NARX Neural Network, floating NARX, Hybrid Approach.
3. Evaluation of the best forecasting methods to be used in the simulation of multi-service provision.
4. Implementation of PCR plus asymmetric SCR using the results of the forecasting methods identified at point 3 (by keeping constant all the parameters, except for the predictions).
5. Comparison of the results of the different simulations on both technical and economical point of view and identification of the best approach.
6. Final sensitivity analysis on the EPR and comparison of the best result with the one coming from a "no-error" prediction (i.e. model fed with actual values).

Either for single service provision or for multi-services provision, the measurement of performances is based on the following quantities:

- LoR, average C-rate, system efficiency and BESS lifetime are considered to evaluate the technical performances.
- The Net Present Value (NPV) is considered as the main indicator of the economic viability of the investment. Moreover, two more indexes are considered: the Payback Time (PBT) and the Profitability Index (PI).

In the following paragraphs, the definition of the aforementioned economic indicators is given.

Net Present Value (NPV)

The NPV takes into account all the initial investment costs related to the BESS, the eventual replacement costs of the battery, all the yearly revenues deriving from the

service/services provision (including LoR penalties) and the Residual Value (RV) of the BESS at the end of the investment. The time horizon of the investment is fixed at a constant number of years N: in this study, 20 years are considered ($N = 20$).

The initial investment C_{inv} is sustained in year 0 and it is proportional to the installed capacity of BESS E_{nom}. Hence, it is necessary to know the specific battery cost c_{BESS} (€/MWh). This cost is continuously decreasing with time, as observed in *Figure 0.6 (b)* for Li-Ion batteries. It is defined as follows:

$$C_{inv} = c_{BESS} \cdot E_{nom} \quad [€] \tag{4.1}$$

Replacement costs C_{rep} are considered at the EoL of the battery. A replacement factor k_{rep}, between 0 and 1, is defined: it takes into account the fact the inverter and all the other elements of the BESS can last more than the battery. The following expression is used:

$$C_{rep} = k_{rep} \cdot C_{inv} \quad [€] \tag{4.2}$$

If at the end of the investment period the battery still has a residual life, the corresponding economic value is accounted in the Residual Value $RV(N)$ [€]:

$$\begin{cases} RV(N) = C_{rep} \cdot \left(1 - \dfrac{N - year_{last\ replacement}}{life_{BESS}}\right) & if\ life_{BESS} < calendar\ ageing \\ RV(N) = C_{rep} \cdot \left(1 - \dfrac{N - year_{last\ replacement}}{calendar\ ageing}\right) & if\ calendar\ ageing < life_{BESS} \end{cases} \tag{4.3}$$

Yearly revenues are considered starting from year 1 and they are simply calculated as 12 times the monthly revenues. The calculation of monthly revenues changes according to the type of service provision (single service or multi-service) and depending on the market model considered. Their full expressions are given in the following paragraphs. The two expressions for yearly revenues are:

$$Rev_{year,PCR} = 12 \cdot Rev_{month,PCR} \quad [€] \tag{4.4}$$

$$Rev_{year,PCR+SCR} = 12 \cdot Rev_{month,PCR+SCR} \quad [€] \tag{4.5}$$

Given all the previous variables, the NPV can be calculated:

$$NPV = -C_{inv} + \sum_{y=1}^{N} \frac{NCF(y)}{(1+r)^y} + \frac{RV(N)}{(1+r)^N} \quad [€] \tag{4.6}$$

Where r is the actualization rate (in this study $r = 6\%$, adopted for a medium-risk investment) and $NCF(y)$ is the Net Cash Flow in year y.

The two expressions adopted for the yearly NCF for the two cases analysed are:

$$NCF_{PCR}(y) = Rev_{year,PCR} - C_{rep} \quad [€] \tag{4.7}$$

$$NCF_{PCR+SCR}(y) = Rev_{year,PCR+SCR} - C_{rep} \quad [€] \tag{4.8}$$

Where C_{rep} is different from zero only in the years of replacement. The selection criteria for NPV is:

- If $NPV > 0$ the investment is convenient.
- If $NPV < 0$ the investment is not convenient.

Payback Time (PBT)

The PBT (or Payback Period) is defined as the time required to recover the cost of an investment. Investments with longer payback time are more risky than ones with shorter periods. This indicator is simple and easy to understand, but it has some drawbacks: it ignores the time value of money, it does not take into consideration the cash flows that occur after the PBT and it does not measure the profitability of the entire project since it only focuses on the time required to recover the initial investment cost.

Profitability Index (PI)

The PI is defined as the ratio between the net operating profits and the total investment costs (initial investment C_{inv} plus all the actualized replacement costs). It can be expressed in function of the NPV as follows:

$$PI = 1 + \frac{NPV}{C_{inv} + \sum_{y=y_{replacement}} \frac{C_{rep}(y)}{(1+r)^y}} \tag{4.9}$$

The selection criteria for the PI is:

- If $PI \geq 1$ the investment is attractive.
- If $PI < 1$ the investment is not attractive.

In this work, the PI is used only for comparing investments of different size (i.e. when a sensitivity analysis is made on the EPR).

4.1 The BESS model

In this Paragraph, the BESS model adopted in all the simulations is described. It includes different parts:

- The cell and the BMS models.
- The model for the computation of cycles.
- The SoH and lifetime model.
- The model of the inverter.
- The model for efficiency computation, both cell and system efficiencies.

These models are detailed in the following paragraphs.

4.1.1 The cell and the BMS models

An analysis of the main battery cell models, including their characteristics, their advantages and disadvantages, has been already provided in *Chapter 1*. In this study, an electrical model has been chosen for simulating the provision of grid services. Since the electrical battery model works with electrical variables, the utilization of this model gives a higher quantity of information with respect to the utilization of an empirical battery model: it is possible to monitor the variations of current, voltage and efficiency of the battery depending on the power set point imposed. In particular, a simple passive electrical model in the time-domain has been chosen for this work, as shown in *Figure 4.1*.

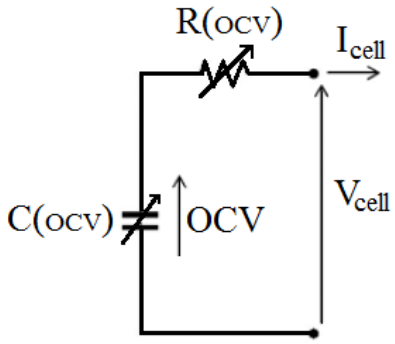

Figure 4.1 – Passive electrical model in the time domain adopted in the simulations.

In this model, C is the intercalation capacitance, which describes the accumulation and depletion of Li-ions within the electrode [5], and R is the internal resistance of the cell. These two electrical parameters have been identified experimentally through EIS and OCV tests performed on a particular Li-ion cell: the Boston Power Swing 5300

(*see APPENDIX A*). These tests have been performed in [5]. The results are reported in *Figure 4.2*.

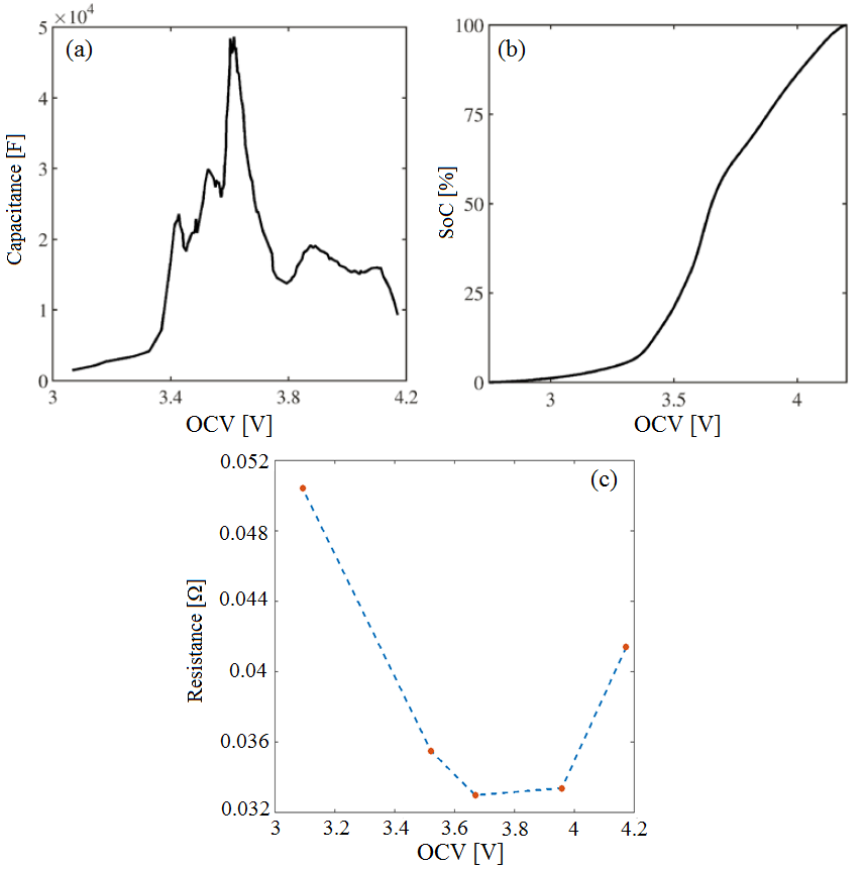

Figure 4.2 – Experimental curves for Boston Power Swing 5300: (a) Intercalation capacitance C(OCV); (b) SoC(OCV) characteristic; (c) Internal resistance R(OCV) [5];

The cell is characterized by a simple Battery Management System (BMS): it receives as inputs the current set point (corresponding to the power set point required for the service provision) and the voltage at the terminals of the cell and it limits the current output if the voltage reaches its lower or upper limits (*see APPENDIX*).

The Simulink™ model for the battery cell and the BMS is the following:

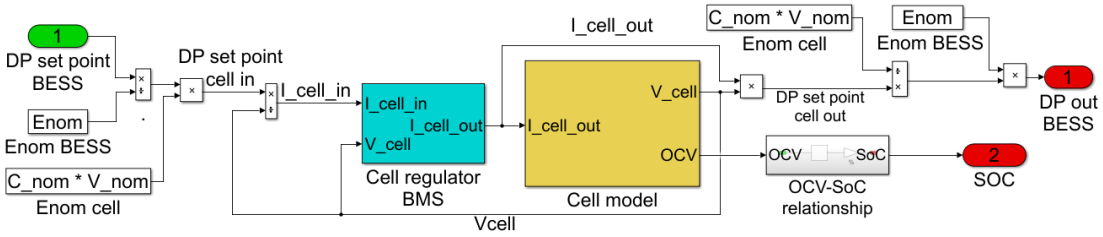

Figure 4.3 - Simulink™ model for the battery cell and the BMS.

In *Figure 4.3*, the cell model includes the passive electrical model previously described and the BMS model includes a PI block controller (proportional-integral) that receives the voltage signal as input and produces a variation of current ΔI. This ΔI is subtracted to the original current set point required to the cell, generating a new current signal. The general model of the cell and the BMS receives as input the power set point given by the single service/multi-service controller to the BESS (in green in *Figure 4.3*). This power set point is translated into a power set point for the individual cell and then into a current set point. In this model, a simplifying hypothesis is made: each cell is considered to work exactly in the same way, undergoing same SOC and voltage variations, having same efficiencies and same power outputs. This hypothesis is acceptable since the main goal of this work is not a design study for improving the cell. Two outputs are generated (in red in *Figure 4.3*):

1. The DC power output of the BESS, starting from the cell power output and scaling it up to the corresponding BESS power.
2. The SoC of the BESS, by considering the experimental SoC-OCV relationship shown in *Figure 4.2*.

4.1.2 Cycles computation

In this work, a full charge-discharge cycle is defined when the throughput Ah are equal to twice its nominal capacity of the cell (C_{nom}). In other words, the total number of cycles is equal to the average between the number of charging and discharging cycles. Therefore, the total number of cycles performed by a BESS is given by:

$$cycles_{tot} = \frac{cycles_{ch} + cycles_{disch}}{2} = \int_{t_{start}}^{t_{end}} \frac{|I_{cell}(t)| \cdot dt}{2 \cdot C_{nom}} \quad [\,] \qquad (4.10)$$

The model adopted in the simulation is the following one:

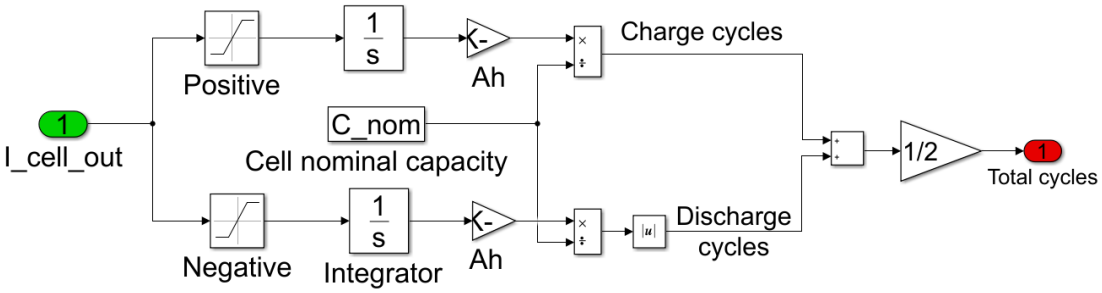

Figure 4.4 - Simulink™ model for cycles' computation.

4.1.3 SoH and lifetime model

As introduced in *Chapter 1*, degradation of batteries is characterized by two ageing mechanisms: cycle ageing and calendar ageing. In this study, the calendar ageing for the BESS is consider constant to 12 years [39]. On the other side, lifetime calculations linked to cycle ageing are performed after each simulation in order to give life expectancy for the whole system and to introduce replacement costs in economic simulation.

For what concerns cycle ageing, the nominal capacity does not remain constant for all the lifetime of the BESS, but it decreases with time depending on the operating conditions such as C-rates, SoC and temperature variations: this phenomenon is known as capacity fade. In this work, capacity decay is modelled through a simple empirical model, which takes into account the average C-rate over the whole period of simulation as the only stress factor. An experimental campaign on the Boston Swing5300 performed in [5] led to the following diagram:

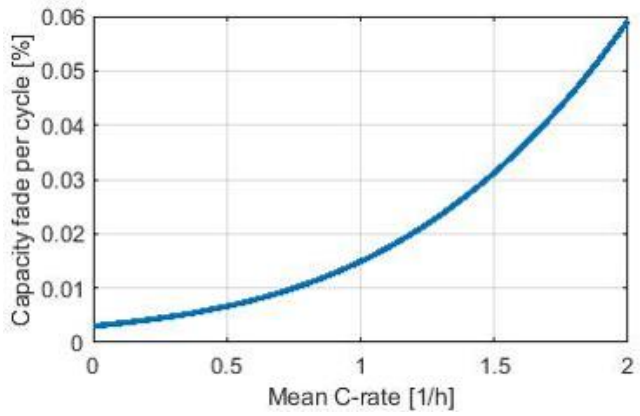

Figure 4.5 – Capacity fade per cycle as a function of the average C-rate for the Boston Swing5300 [5].

Lifetime calculations are performed as follows:

1. The average C-rate is calculated without taking into account the periods in which the C-rate is null.
2. Once the mean C-rate is calculated, the capacity fade per cycle (%/#cycle) is determined from *Figure 4.5*.

3. The maximum number of cycles $cycles_{max}$ is calculated taking into account that the End of Life (EoL) of a battery is defined as the moment in which the capacity becomes the 80% of the initial value:

$$cycles_{max} = \frac{100 - 80}{capacity\ fade\ per\ cycle} \quad [\#\ cycles] \tag{4.11}$$

4. Finally, the BESS lifetime in years is calculated dividing the maximum number of cycles associated to the EoL of the BESS $cycles_{max}$ by the equivalent number of cycles in one year $cycles_{tot,year}$:

$$life_{BESS} = \frac{cycles_{max}}{cycles_{tot,year}} \quad [years] \tag{4.12}$$

$$cycles_{tot,year} = \frac{cycles_{tot}}{n_{days}} \cdot 365 \quad [years] \tag{4.13}$$

Where $cycles_{tot}$ is the total number of cycles the BESS has cycled during the simulation period n_{days} (calculated as in *Paragraph 4.1.2*).

During the NPV calculation, the replacement cost of the BESS is considered at:

$$\begin{cases} y = life_{BESS} & if\ life_{BESS} < calendar\ ageing \\ y = calendar\ ageing & if\ calendar\ ageing < life_{BESS} \end{cases} \tag{4.14}$$

4.1.4 The inverter model

The inverter links the battery (DC side) to the grid (AC side). It receives as input the power provided or absorbed by the battery and gives as output the power provided or absorbed at the grid side. In this work, the inverter is simply modelled as a low-pass filter, whose expression is:

$$Gain \cdot \frac{1}{\tau \cdot s + 1} \tag{4.15}$$

The $Gain$ is a function of the efficiency of the inverter. It takes into account the fact that, during the charging process, the power flowing inside the battery is lower than the power absorbed at the grid side (i.e. after the inverter), while during the discharging process the power flowing outside from the battery is higher than the real

power injected into the grid. Therefore, the $Gain$ is equal to η_{INV} if the power is injected into the grid and $1/\eta_{INV}$ if the power is absorbed from the grid. The efficiency of the inverter is calculated with a lookup table representing the efficiency as a function of the power in per unit (see figure *Figure 4.6*). In this analysis, the nominal power of the inverter is considered equal to the nominal power of the BESS (P_{nom}). The time constant τ is equal to 40 ms.

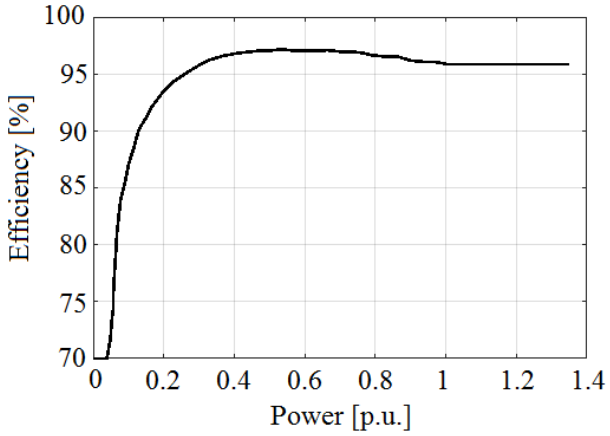

Figure 4.6 – Efficiency curve of the inverter as a function of the power in per unit.

The efficiency of the inverter is also considered both in the PCR controller and in the SCR controller for the correct computation of the power set points to be given to the BESS. In these cases, the dynamics are neglected.

4.1.5 Cell and system efficiency computation

In general, the energy efficiency is defined as the ratio between the absolute values of the energy cycled during the discharging phase E_{disch} and the energy cycled during the charging process E_{ch} when the final SoC variation is equal to zero:

$$\eta_E = \frac{|E_{disch}|}{|E_{ch}|} \quad with \quad \Delta SoC = 0 \tag{4.16}$$

Therefore, the energy efficiency of the cell $\eta_{E,cell}$ and the energy efficiency of the system $\eta_{E,sys}$ are computed as follows:

$$\eta_{E,cell} = \frac{|E_{disch,cell}|}{|E_{ch,cell}|} = \frac{\left|\int_{disch} V_{cell} \cdot I_{cell}\, dt\right|}{\left|\int_{ch} V_{cell} \cdot I_{cell}\, dt\right|} \quad with \quad \Delta SoC = 0 \tag{4.17}$$

$$\eta_{E,sys} = \frac{|E_{disch,sys}|}{|E_{ch,sys}|} = \frac{\left|\int_{disch} P_{out,sys}\, dt\right|}{\left|\int_{ch} P_{out,sys}\, dt\right|} \quad with \quad \Delta SoC = 0 \qquad (4.18)$$

Where V_{cell} is the cell voltage, I_{cell} is the current flowing in the cell and $P_{out,sys}$ is the real power exchanged by the BESS with the electrical grid. The efficiency of the system is always lower than the one of the cell because of the presence of the inverter and auxiliary services (cooling system, controller and other devices). In this study, the effect of auxiliaries on the BESS power output is not modelled.

4.2 Single service provision: PCR

In this Paragraph, the model adopted for the simulation of Primary Control Reserve provision is described. The overall Simulink™ model is represented in *Figure 4.7*.

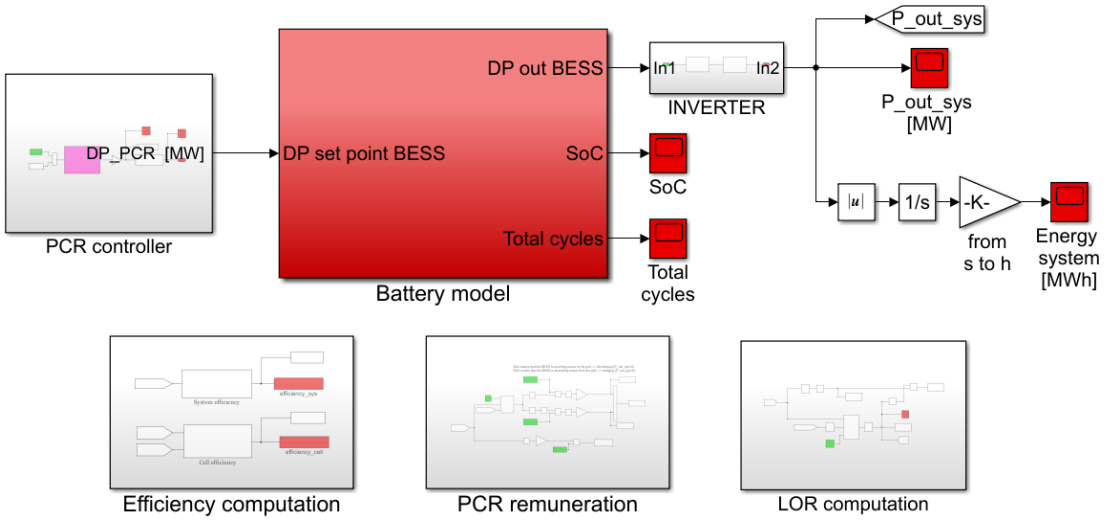

Figure 4.7 - Simulink™ model for the simulation of PCR provision.

The battery model (which includes the cell, the BMS and the total cycles' computation models), the efficiency computation block and the inverter model have been already described in *Paragraph 4.1*. The new elements introduced in this Paragraph are:

- The PCR controller, both with and without SoC restoration strategies.
- The model for the computation of LoR.
- The model for PCR remuneration.

4.2.1 Base case: no SoC restoration strategy

The standard PCR controller does not include any SoC restoration strategy. It is represented in *Figure 4.8*.

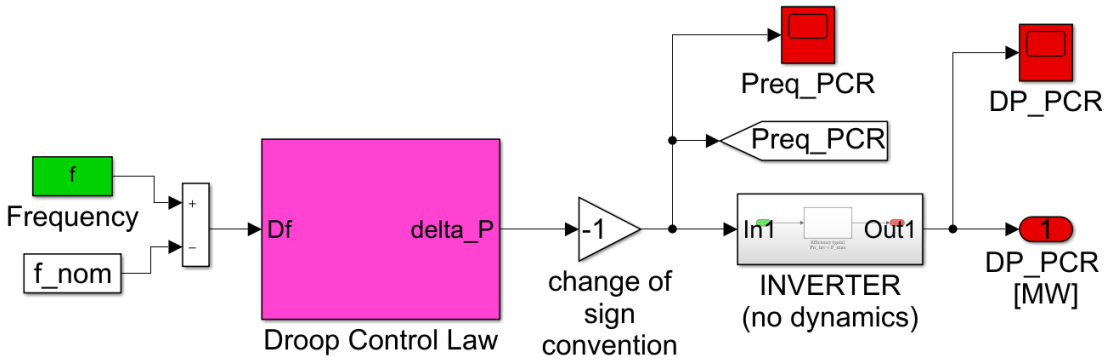

Figure 4.8 - Simulink™ model for the PCR controller without any SoC restoration strategy.

This model receives as input the frequency profile and, for each sample, it calculates the frequency displacement (Δf) from the nominal value (i.e. 50 Hz in this study). Then, according to the Droop Control Law explained in *Chapter 2*, the frequency variation is translated in a power set point at the grid side. Finally, the set point required on the AC side is converted into the corresponding power set point for the battery, by considering the efficiency of the inverter. In particular, the controller oversizes the power to be injected and undersizes the power to be absorbed by the battery. The gain equal to -1 in *Figure 4.8* represents the change of the sign convention between the droop control law and the BESS. In the droop control law, $P > 0$ means power injected into the grid and $P < 0$ means power absorbed. On the contrary, from the BESS point of view, $P > 0$ means power absorption and $P < 0$ means power injected by the BESS into the network.

4.2.2 Dead Band strategy

Given the droop control law explained in *Paragraph 2.3.1*, the power output of a provider of PCR is zero when the frequency is within the dead band (e.g. ±20 mHz in Italy). According to this strategy, it is possible exploit these "dead" periods to bring the SoC back to its reference value SoC_{ref}. In particular, when the frequency variation is inside the dead band (DB), the controller compares the level of the SoC with the reference value and defines a restoration power set point (as a fixed percentage of nominal power).

Figure 4.9 shows the working principle of the DB strategy:

- If SOC>SOC_{ref} the controller requires the BESS to release power (discharge).
- If SOC<SOC_{ref} the controller requires the BESS to absorb power from the grid (charge).

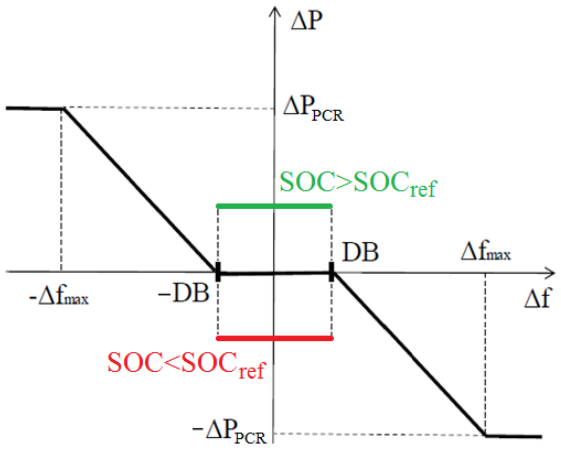

Figure 4.9 – Droop control curve in case of Dead Band strategy.

Figure 4.10 shows the Simulink™ model of the PCR controller with the DB strategy: the power profile required to the battery is the sum of the power profile defined by the standard droop control law and the one required by the DB restoration strategy.

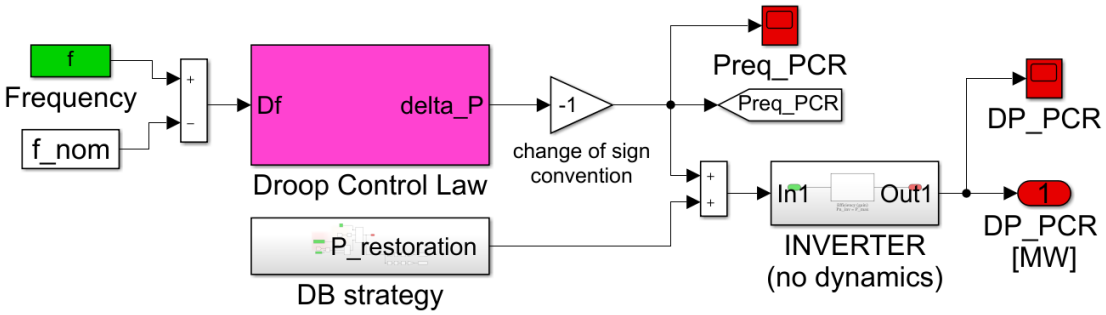

Figure 4.10 - Simulink™ model for the PCR controller with Dead Band strategy.

4.2.3 SoC restoration with service interruption

This control logic is activated when the BESS reaches its predefined saturation limits. Generally, two types of saturation limits may be considered: SoC thresholds (e.g. 10%-90%) and voltage thresholds. Usually, voltage thresholds are considered for a better preservation of the battery, since they could be reached even at SoC values far from 0% and 100%. In this study, voltage thresholds are taken into account: these limits

are defined starting from the datasheet of the Boston Swing 5300 (*see APPENDIX*). When this strategy is activated, the PCR provision is interrupted and the controller defines a high restoration power set point in order to bring the SOC back to its reference value, limit the duration of the interruption and avoid LoR. The restoration power is a percentage of the nominal power of the BESS (typically higher than 100%). Nevertheless, a high power means a severe C-rate and it has a negative impact on the lifetime of the BESS (as shown in *Chapter 1*). For this reason, an Activation Factor may be introduced: it avoids the instantaneous activation of the strategy due to short saturation events, as shown in *Figure 4.11*. In particular, SoC restoration starts with a certain delay only if one of the saturation limits is exceeded continuously for all the length of such a pre-defined delay. In this study, an Activation Factor equal to 50 s is chosen.

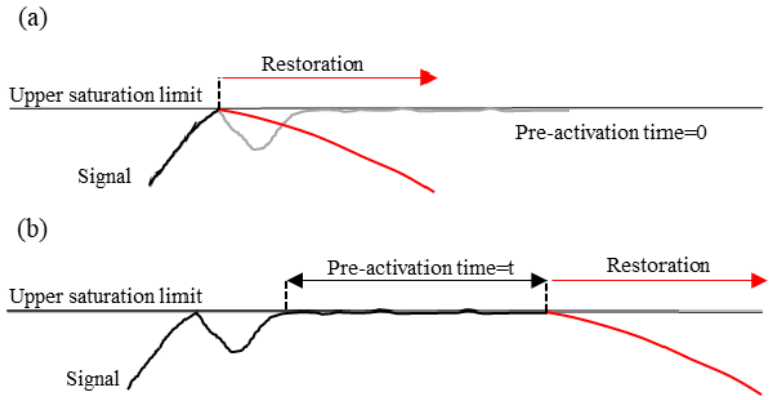

Figure 4.11 - SoC restoration strategy with service interruption: (a) instantaneous activation; (b) activation after the pre-activation time [37].

During the restoration process, the controller compares the SoC with the reference value and the procedure stops when SoC_{ref} is reached.

Figure 4.12 shows the Simulink™ model of the PCR controller with SoC restoration strategy with service interruption: service interruption is modelled through a switch.

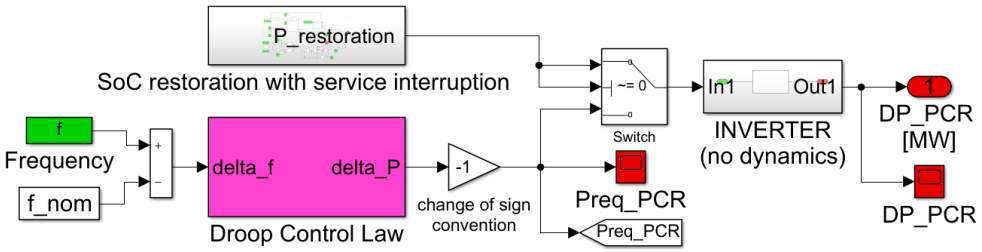

Figure 4.12 - Simulink™ model for the PCR controller with SoC restoration with service interruption.

4.2.4 SoC restoration without service interruption

Also in this control action, if one of the saturation limits is reached, the controller defines a constant power set point and the restoration process stops as soon as the SOC returns back to its reference value. Differently from the previous strategy, this power set point is added to the one defined by the Droop Control Law (as shown in *Figure 4.13*), thus avoiding service interruption and reducing penalties due to LoR. In this work, SoC thresholds are considered for the activation of this strategy rather than voltage thresholds. Another difference with respect to SoC restoration with service interruption regards the restoration power set point: it is much lower (below 100% of nominal power of the BESS) and, consequently, the Activation Factor is not considered.

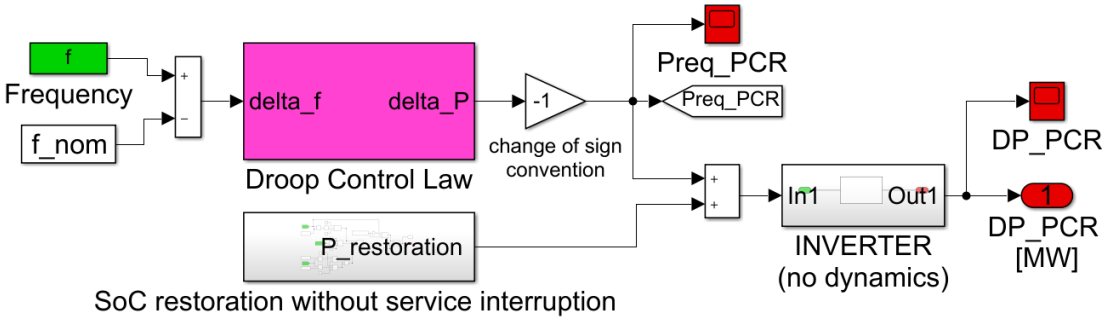

Figure 4.13 - Simulink™ model for the PCR controller with SoC restoration without service interruption.

4.2.5 Variable droop strategy

This strategy acts on the droop angle in order to regulate the SoC of the BESS. The value is not fixed to a constant, but it can range in a defined interval. In this case, the controller receives as inputs the frequency and the value of SoC of the BESS and defines the droop correction (Δdroop) to be applied to the "standard" fixed droop control curve. The working principle is the following:

- When the SoC is close to the upper saturation limit (100%), the BESS would like to absorb as little power as possible (maximum droop if Δf>0) and deliver as much power as possible (minimum droop if Δf<0), in order to avoid LoR.
- When SoC is close to the lower saturation limit (0%), the BESS would like to absorb as much power as possible (minimum droop when Δf>0) and deliver as little power as possible (maximum droop when Δf<0), in order to avoid LoR.

- When SoC equals 50%, the droop is at its reference value for both Δf>0 and Δf<0.

For intermediate SoC values the regulating droop varies linearly. In *Figure 4.14* an example of variable droop control law is given.

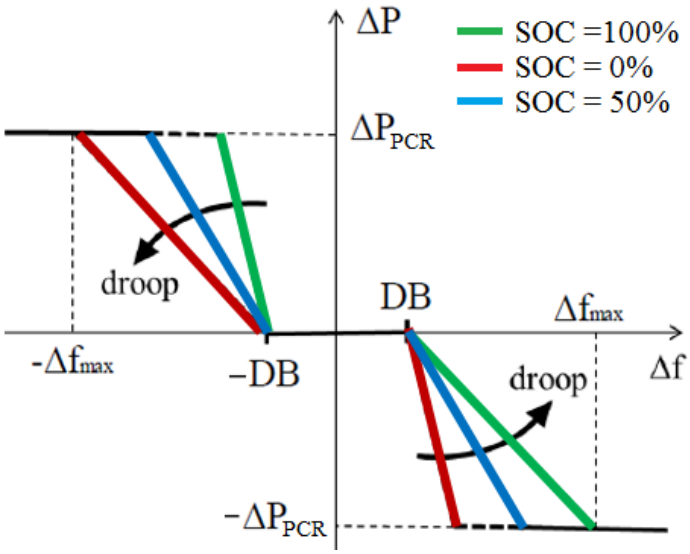

Figure 4.14 – Droop control curve for Variable Droop strategy.

This strategy reduces the tendency of the battery to reach the SoC saturation limits, but in case of long periods of under or over frequency its effectiveness will be compromised.

The model of the PCR controller with variable droop strategy is shown in *Figure 4.15*.

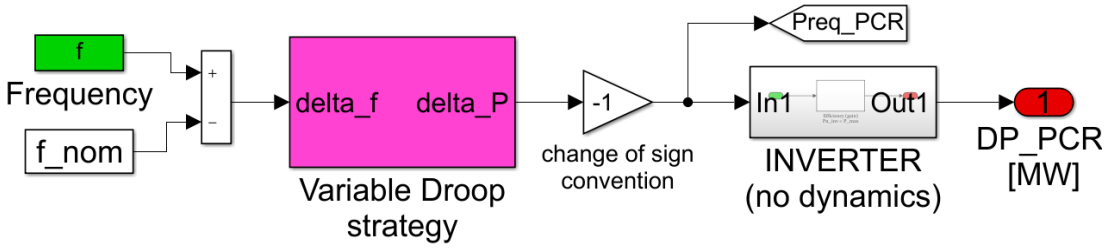

Figure 4.15 - Simulink™ model for the PCR controller with Variable Droop strategy.

4.2.6 Model for the computation of LoR

The LoR related to the single service provision is calculated always in the same way, either for the base case or for all the SoC restoration strategies. Given the expressions in *Paragraph 2.6.1*, a Simulink™ model for LoR computation has been realized (*Figure 4.16*).

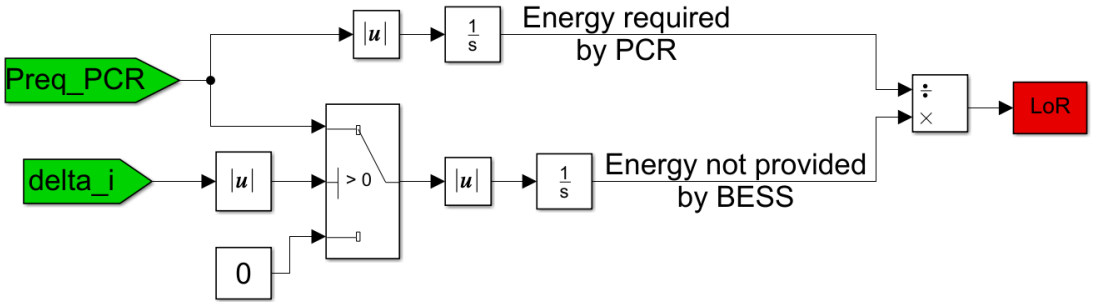

Figure 4.16 - Simulink™ model for the computation of LoR.

This model receives as inputs the power set point required by the PCR controller ($P_{req,PCR}$) and the current correction (ΔI) calculated by the BMS. When the BMS is on and is limiting the current set point of the cell ($\Delta I \neq 0$), the power required by the PCR controller is accounted as not provided by the BESS. By integrating this quantity over the simulation period and dividing it by the total energy required by the PCR controller, the LoR is calculated.

4.2.7 PCR remuneration model

In all the simulations, two types of PCR remuneration schemes are adopted: the Italian remuneration mechanism and the Central Western Europe (CWE) one.

In Italy, PCR remuneration depends on the zonal price and it is energy-based. In particular, the hourly prices (€/MWh) applied for PCR remuneration are defined in [25] as follows:

$$\begin{cases} p_{PCR,+}(h) = p_{DAM,z}(h) + \frac{1}{2} \cdot \left(K_{SCR,+} + K_{DAM,+}\right) \ for\ positive\ PCR \\ p_{PCR,-}(h) = p_{DAM,z}(h) - \frac{1}{2} \cdot \left(K_{DAM,-} + K_{SCR,-}\right) \ for\ negative\ PCR \end{cases} \quad (4.19)$$

Where $p_{DAM,z}(h)$ is the hourly zonal price registered on the DAM and $K_{SCR,+}$, $K_{DAM,+}$, $K_{SCR,-}$ and $K_{DAM,-}$ are four annual constants defined by Terna. In this study, the market zone considered is Northern Italy. The total revenues in the simulated period Rev_{PCR}^{ITA} are calculated as follows:

$$Rev_{PCR}^{ITA} = \sum_{h} \left(E_{inj,sys}(h) \cdot p_{PCR,+}(h) - E_{abs,sys}(h) \cdot p_{PCR,-}(h) \right) \quad [€] \quad (4.20)$$

Where $E_{inj,sys}(h)$ and $E_{abs,sys}(h)$ are respectively the total hourly energy injected and absorbed by the BESS.

In CWE (i.e. in Germany), PCR is traded through a weekly auction and its remuneration is based on capacity (power), based on a pay-as-bid mechanism [28]. In this study, a single weekly price in €/MW is considered and it is supposed to be constant for all the period of simulation (p_{GER}). Therefore, the total revenues in the simulated period Rev_{PCR}^{GER} are calculated as follows:

$$Rev_{PCR}^{GER} = \frac{\Delta P_{PCR} \cdot p_{GER}}{7} \cdot n_{days} \quad [€] \tag{4.21}$$

Where ΔP_{PCR} is the regulating band in MW offered for this service, p_{GER} is the weekly price and n_{days} is the duration of the simulation.

The LoR penalties are always calculated according to the equation (2.5).

In case of a SoC management strategy, also the revenues/costs for the energy traded for SoC restoration must be taken into account. In this study, a hypothesis is made: this energy is traded always considering the average remunerations for positive and negative PCR over the period of simulation (indicated with $p_{rest,+}$ for the energy injected and $p_{rest,-}$ for the energy absorbed). The following expression is used:

$$Rev_{rest} = E_{inj,rest} \cdot p_{rest,+} - E_{abs,rest} \cdot p_{rest,-} \quad [€] \tag{4.22}$$

Where $E_{inj,rest}$ and $E_{abs,rest}$ are respectively the total energy injected and absorbed for the SoC restoration strategy.

The general expressions of the monthly revenues for PCR provision that are adopted in NPV calculations (*see equation* (4.4)) are:

$$Rev_{month,PCR}^{ITA} = \left(Rev_{PCR}^{ITA} + Rev_{rest} - Penalty_{LoR}\right) \cdot \frac{30}{n_{days}} \quad [€] \tag{4.23}$$

$$Rev_{month,PCR}^{GER} = \left(Rev_{PCR}^{GER} + Rev_{rest} - Penalty_{LoR}\right) \cdot \frac{30}{n_{days}} \quad [€] \tag{4.24}$$

Where n_{days} is the duration of the simulation period.

4.3 Model for multi-service provision: PCR and asymmetric SCR

The overall Simulink™ model adopted for the simulation of multi-service provision is represented in *Figure 4.17*.

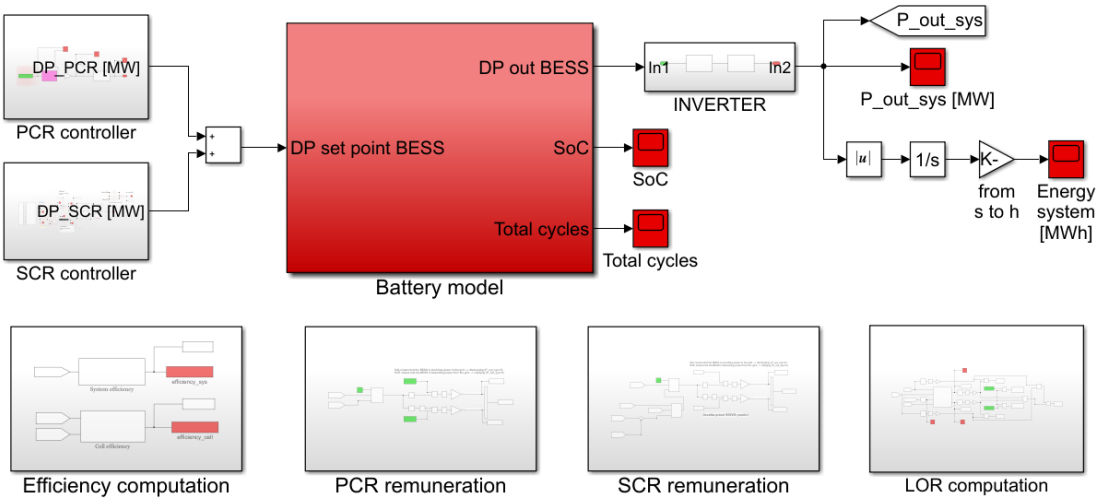

Figure 4.17 - Simulink™ model for the simulation of multi-service provision.

The battery model (which includes the cell, the BMS and the total cycles' computation models), the efficiency computation block and the inverter model have been already described in *Paragraph 4.1*. The PCR controller is the one with no SoC restoration strategy described in *Paragraph 4.2.1*. The innovations introduced in this Paragraph are:

- The SCR controller.
- A new model for LoR allocation and computation.
- A variation in the Italian PCR remuneration scheme.
- The model for SCR remuneration.

4.3.1 The SCR controller

The goal of the SCR controller is to define the upward and downward bands to be allocated for Secondary Control Reserve. In this study, symmetry constraints for these bands are not taken into account: the positive reserve $\Delta P_{SCR,+}$ and the negative reserve $\Delta P_{SCR,-}$ can be different, as already happens in Germany (*see Paragraph*

2.6.2). This asymmetric provision of SCR allows to better control the SoC of the Battery Energy Storage System:

- When the SoC is close to 100%, the BESS owner wants to allocate a large band for releasing power ($\Delta P_{SCR,+}$) and a small one to absorb power ($\Delta P_{SCR,-}$).
- When the SoC is close 0%, the BESS owner wants to allocate a large band for absorbing power ($\Delta P_{SCR,-}$) and a small one to release power ($\Delta P_{SCR,+}$).

In this work, these regulating bands are traded in the framework of the Italian ASM. In particular, two constraints are considered in the analysis: there are 6 market sessions of 4 hours each (i.e. the regulating bands offered on the market are constant for 4 hours) and offers must be placed on the market at least one and a half hours before the beginning of the market session [15]. For these reasons, the predictions of the total regulating energies associated to both PCR and SCR in the successive five and a half hours are necessary to identify the SoC of the BESS at the end of the following market session and to define $\Delta P_{SCR,+}$ and $\Delta P_{SCR,-}$ to place on the market.

A MATLAB® function has been implemented to calculate the regulating bands. The inputs are:

- The nominal energy of the BESS (E_{nom}).
- The actual value of the SoC of the BESS in the moment in which the prediction is made in per unit (SoC_{IN}).
- The upper and the lower limit for SoC in per unit (1 and 0).
- The regulating band associated to PCR in per unit of nominal power of the BESS ($\Delta \dot{P}_{PCR}$). In the simulation of multi-service provision, it is kept constant to 0.5.
- The regulating bands associated to SCR of the previous market session (i.e. the one in which the prediction is made) in per unit of nominal power of the BESS ($\Delta \dot{P}_{SCR,+}^{pre}$ and $\Delta \dot{P}_{SCR,-}^{pre}$).
- The prediction in MWh of the regulating energy associated to PCR in the successive one and a half hour (Y_{1P}) and in the successive market session (Y_{2P}). Sign convention is positive if absorbed.
- The standard deviations associated to the prediction errors of the regulating energy for PCR std_{1P} and std_{2P} in MWh.
- The prediction in MWh of the absorbed and injected regulating energy associated to SCR in the successive one and a half hour, respectively $Y_{1S,+}$ *and* $Y_{1S,-}$.

- The prediction in MWh of the absorbed and injected regulating energy associated to SCR in the successive market session, respectively $Y_{2S,+}$ and $Y_{2S,-}$.
- The standard deviations associated to the four prediction errors of the regulating energy for SCR $std_{1S,+}$, $std_{1S,-}$, $std_{2S,+}$ and $std_{2S,-}$ in MWh.
- The constant k_{CI} for Gaussian distributions, which multiplies the combined standard deviation (of the sum of prediction errors) and guarantees a certain confidence level of the predictions. In this study, this constant is equal to 1.96 (i.e. confidence level of 95%).

All the aforementioned predictions and the standard deviations refer to the battery side: they have been reported to the BESS side through the efficiency of the inverter. The function is able to find the regulating bands for SCR by solving a system of two equations. *Figure 4.18* is useful to understand the working principle of the function.

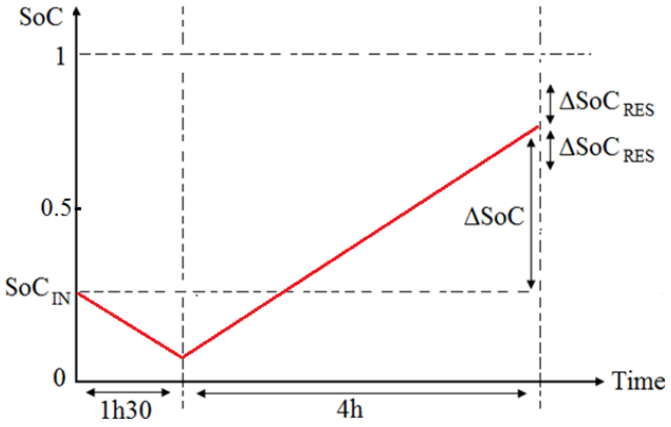

Figure 4.18 – Useful diagram for the derivation of the two equations.

The value of the SoC at the end of the successive market session is in the range:

$$(SoC_{IN} + \Delta SoC) \pm \Delta SoC_{RES} \tag{4.25}$$

Where ΔSoC is the predicted SoC variation at the end of the successive market session and ΔSoC_{RES} is the 95% confidence band around the final SoC value, whose expressions are:

$$\Delta SoC = \Delta SoC_{1P} + \Delta SoC_{1S} + \Delta SoC_{2P} + \Delta SoC_{2S} \tag{4.26}$$

$$\Delta SoC_{RES} = k_{CI} \cdot \sqrt{\sigma_{1P}^2 + \sigma_{1S}^2 + \sigma_{2P}^2 + \sigma_{2S}^2} \quad with \quad k_{IC} = 1.96 \tag{4.27}$$

Where ΔSoC_{1P}, ΔSoC_{1S}, ΔSoC_{2P}, ΔSoC_{2S}, σ_{1P}, σ_{1S}, σ_{2P} and σ_{2S} are functions of the variables introduced in the previous list. Their expressions are:

$$\Delta SoC_{1P} = \frac{Y_{1P}}{E_{nom}} \cdot \Delta\dot{P}_{PCR} \tag{4.28}$$

$$\Delta SoC_{2P} = \frac{Y_{2P}}{E_{nom}} \cdot \Delta\dot{P}_{PCR} \tag{4.29}$$

$$\Delta SoC_{1S} = \frac{1}{E_{nom}} \cdot \left(Y_{1S,+} \cdot \Delta\dot{P}^{pre}_{SCR,-} + Y_{1S,-} \cdot \Delta\dot{P}^{pre}_{SCR,+}\right) \tag{4.30}$$

$$\Delta SoC_{2S} = \frac{1}{E_{nom}} \cdot \left(Y_{2S,+} \cdot \Delta\dot{\boldsymbol{P}}_{\boldsymbol{SCR},-} + Y_{2S,-} \cdot \Delta\dot{\boldsymbol{P}}_{\boldsymbol{SCR},+}\right) \tag{4.31}$$

$$\sigma_{1P} = \frac{std_{1P}}{E_{nom}} \cdot \Delta\dot{P}_{PCR} \tag{4.32}$$

$$\sigma_{2P} = \frac{std_{2P}}{E_{nom}} \cdot \Delta\dot{P}_{PCR} \tag{4.33}$$

$$\sigma_{1S} = \frac{1}{E_{nom}} \cdot \left(std_{1S,+} \cdot \Delta\dot{P}^{pre}_{SCR,-} + std_{1S,-} \cdot \Delta\dot{P}^{pre}_{SCR,+}\right) \tag{4.34}$$

$$\sigma_{2S} = \frac{1}{E_{nom}} \cdot \left(std_{2S,+} \cdot \Delta\dot{\boldsymbol{P}}_{\boldsymbol{SCR},-} + std_{2S,-} \cdot \Delta\dot{\boldsymbol{P}}_{\boldsymbol{SCR},+}\right) \tag{4.35}$$

The goal of the function is to find two quantities (i.e. the two SCR regulating bands). Hence, two equations are needed to solve the problem. Starting from *Figure 4.18,* two worst-case conditions can be derived. The first worst-case condition is when the SoC at the end of the successive market session equals the upward SoC limit. Conversely, the second worst-case condition is when the final SoC value equals the downward limit. Therefore, the following system of equations is defined:

$$\begin{cases} SoC_{IN} + \Delta SoC + \Delta SoC_{res} = 1 \\ SoC_{IN} + \Delta SoC - \Delta SoC_{res} = 0 \end{cases} \tag{4.36}$$

Where ΔSoC and ΔSoC_{res} are functions of the two unknowns (i.e. the two SCR regulating bands $\Delta\dot{P}_{SCR,+}$ and $\Delta\dot{P}_{SCR,-}$). Since the values of ΔSoC and ΔSoC_{res} are

equal in both equations, the imposition of such system determines an expected value of SoC at the end of the successive market session equal to 50%, with a confidence interval around ranging between 0 and 100%, as shown in *Figure 4.19*.

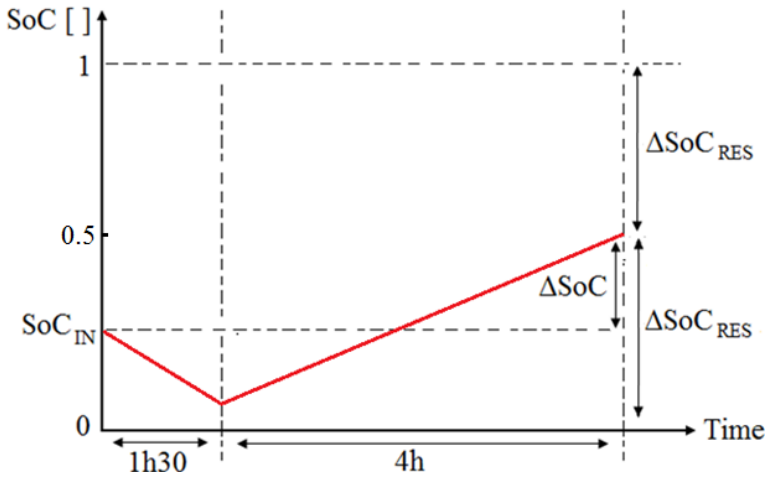

Figure 4.19 – Working principle of the SCR controller.

Each equation in (4.36) represents a hyperbola in the plane and the solutions of the system are given by their intersections. The function solves the system of equations and finds the two regulating bands for SCR $\Delta\dot{P}_{SCR,+}$ and $\Delta\dot{P}_{SCR,-}$. In this study, the maximum allowable band for both PCR and SCR provision is set to 1.3 per unit: since the regulating band for PCR is set constant to 0.5, this means the SCR bands calculated by the function can be at most 0.8. Nevertheless, this value is hardly ever reached in the simulations and the number of instants above 1 p.u. is monitored and checked to avoid to stress the system.

In this study, a simplifying hypothesis is made: the SCR bands are always accepted on the market at the average hourly zonal prices bid for the SCR for both positive and negative reserves (the market zone is Northern Italy) [115]. Therefore, $\Delta\dot{P}_{SCR,+}$ and $\Delta\dot{P}_{SCR,-}$, which are determined through the MATLAB® function previously described, are always accepted except for the case in which their hourly price is zero: it means that the secondary reserve is not required in that particular market zone for that hour. Finally, the actual power set points required to the BESS are determined by the ACE, which represents the percentage of SCR band required by the TSO to each service provider [118]:

$$\begin{cases} \Delta P_{SCR} = \Delta P_{SCR,+} = \Delta \dot{P}_{SCR,+} \cdot P_{nom} & if\ ACE = 100 \\ \Delta P_{SCR} = 0 & if\ ACE = 50 \\ \Delta P_{SCR} = \Delta P_{SCR,-} = -\Delta \dot{P}_{SCR,-} \cdot P_{nom} & if\ ACE = 0 \end{cases} \quad (4.37)$$

The regulating power ΔP_{SCR} varies linearly for intermediate values of ACE.

4.3.2 Model for LoR allocation and computation

In case of multi-service provision, the LoR must be allocated on each service for evaluating the security of provision and for penalties' computation. In particular, LoR occurs when the BMS limits the current set point of the cell ($\Delta I \neq 0$). In this situation, the actual power provided $P_{out,sys}$ is lower than the total power required P_{req} to the BESS.

$$|P_{out,sys}| < |P_{req}| \quad (4.38)$$

$$|P_{out,sys}| < |P_{req,PCR} + P_{req,SCR}| \quad (4.39)$$

In case of multi-service provision, services are ranked according to a priority index: in this study, PCR has the priority with respect to SCR.

Four different cases for LoR allocation are considered:

1. The signs of the powers required for the two services are different from each other: LoR is allocated only to the service which has the same sign of P_{req} and the power not provided for that service $P_{LoR,service}$ is equal to the total power required for the same service $P_{req,service}$.
2. The signs of the powers required for PCR and SCR are equal to each other and the absolute value of $P_{out,sys}$ is greater than the module of the power required for one service and lower than the module of the power requested for the other. In this case, LoR is allocated only to the latter and $P_{LoR,service}$ is equal to the power required for that service $P_{req,service}$.
3. The powers requested for the two services have the same sign and the absolute value of $P_{out,sys}$ is greater than the module of the power required to each service, but lower than their sum. In this case, the priority is considered: LoR is allocated

only to the service without priority (i.e. in our study SCR) and its value is equal to the total power required for that service ($P_{LoR,SCR} = P_{req,SCR}$).

4. The signs of the powers required for PCR and SCR are equal and the module of $P_{out,sys}$ is lower than the absolute value of the power required to each service: LoR is allocated to both services and their values are equal to the powers required ($P_{LoR,PCR} = P_{req,PCR}$ and $P_{LoR,SCR} = P_{req,SCR}$).

Figure 4.20 shows the Simulink™ model adopted for the allocation and for the computation of LoR.

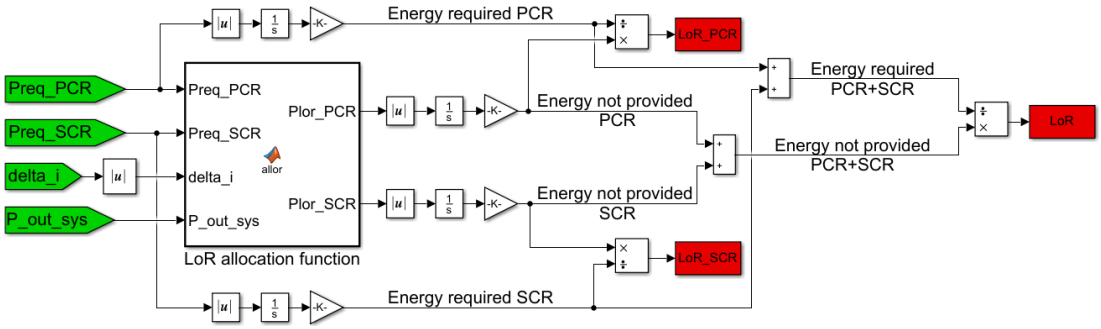

Figure 4.20 - Simulink™ model for LoR allocation and computation.

This model receives as inputs the power set point required by the PCR controller ($P_{req,PCR}$), the one required by the SCR controller ($P_{req,SCR}$), the current correction (ΔI) calculated by the BMS and the actual power provided by the BESS ($P_{out,sys}$). A MATLAB® function is used to allocate the LoR between the two services, considering the four cases previously described. Moreover, the total LoR index is calculated.

4.3.3 PCR and SCR remuneration models

For what concerns PCR remuneration, both the Italian and the German mechanisms described in *Paragraph 4.2.7* are considered.

$$Rev_{PCR}^{ITA} = \sum_{h} \left(E_{inj,PCR}(h) \cdot p_{PCR,+}(h) - E_{abs,PCR}(h) \cdot p_{PCR,-}(h) \right) \quad [€] \tag{4.40}$$

$$Rev_{PCR}^{GER} = \frac{\Delta P_{PCR} \cdot p_{GER}}{7} \cdot n_{days} \quad [€] \tag{4.41}$$

Where $E_{inj,PCR}(h)$ and $E_{abs,PCR}(h)$ are respectively the total hourly energy injected and absorbed by the BESS for PCR provision, $p_{PCR,+}(h)$ and $p_{PCR,-}(h)$ the hourly prices (€/MWh) applied for the Italian PCR remuneration, ΔP_{PCR} is the regulating

band in MW offered for PCR, p_{GER} is the weekly price for German remuneration and n_{days} is the duration of the simulation. The quantities to be remunerated in the Italian case $E_{inj,PCR}$ and $E_{abs,PCR}$ are identified starting from the power required to PCR $P_{req,PCR}$ when there is no Loss of Regulation for PCR:

$$\begin{cases} E_{inj,PCR} = -\int_{t_{start}}^{t_{end}} P_{req,PCR} \cdot dt \Big|_{P_{req,PCR} < 0} \\ E_{abs,PCR} = \int_{t_{start}}^{t_{end}} P_{req,PCR} \cdot dt \Big|_{P_{req,PCR} > 0} \end{cases} \quad when \;\; P_{LoR,PCR} = 0 \qquad (4.42)$$

The only SCR remuneration scheme adopted in this study is inspired to the Italian one. It is energy-based and, since it is assumed that SCR bands are always accepted on the market, average hourly zonal prices in €/MWh for positive and negative reserves are considered (respectively $p_{SCR,+}(h)$ and $p_{SCR,-}(h)$). In particular, the considered market zone is Northern Italy. The total revenues in the simulated period Rev_{SCR} are calculated as follows:

$$Rev_{SCR} = \sum_{h} \left(E_{inj,SCR}(h) \cdot p_{SCR,+}(h) - E_{abs,SCR}(h) \cdot p_{SCR,-}(h) \right) \quad [€] \qquad (4.43)$$

Where $E_{inj,SCR}(h)$ and $E_{abs,SCR}(h)$ are respectively the total hourly energies injected and absorbed by the BESS for SCR provision. These quantities are identified as follows:

- If $P_{LoR,SCR} = 0$ and $P_{LoR,PCR} \neq 0$, the two quantities are defined starting from the power required by SCR $P_{req,SCR}$.

$$\begin{cases} E_{inj,SCR} = -\int_{t_{start}}^{t_{end}} P_{req,SCR} \cdot dt \Big|_{P_{req,SCR} < 0} \\ E_{abs,SCR} = \int_{t_{start}}^{t_{end}} P_{req,SCR} \cdot dt \Big|_{P_{req,SCR} > 0} \end{cases} \qquad (4.44)$$

- If $P_{LoR,SCR} = 0$ and $P_{LoR,PCR} = 0$, the two quantities are defined starting from the difference between the total power provided by the BESS $P_{out,sys}$ and the one required by PCR $P_{req,PCR}$.

$$\begin{cases} E_{inj,SCR} = \int_{t_{start}}^{t_{end}} \left| P_{out,sys} - P_{req,PCR} \right| \cdot dt \Big|_{\substack{P_{out,sys} < 0 \\ P_{req,PCR} < 0}} \\ E_{abs,SCR} = \int_{t_{start}}^{t_{end}} \left| P_{out,sys} - P_{req,PCR} \right| \cdot dt \Big|_{\substack{P_{out,sys} > 0 \\ P_{req,PCR} > 0}} \end{cases} \quad (4.45)$$

LoR penalties for both PCR and SCR are calculated according to the equation (2.5).

Therefore, the final expressions of the monthly revenues for multi-service provision that are adopted in NPV calculations (*see equation* (5.4.)) are:

$$Rev^{ITA}_{month,PCR+SCR} = \left(Rev^{ITA}_{PCR} + Rev_{SCR} - Penalty_{LoR}\right) \cdot \frac{30}{n_{days}} \quad [€] \quad (4.46)$$

$$Rev^{GER}_{month,PCR+SCR} = \left(Rev^{GER}_{PCR} + Rev_{SCR} - Penalty_{LoR}\right) \cdot \frac{30}{n_{days}} \quad [€] \quad (4.47)$$

Where n_{days} is the duration of the simulation period and $Penalty_{LoR}$ are the total penalties for LoR:

$$Penalty_{LoR} = Penalty_{LoR,PCR} + Penalty_{LoR,SCR} \quad [€] \quad (4.48)$$

5. SIMULATIONS & RESULTS: SINGLE SERVICE PROVISION (PCR)

This Chapter is dedicated to the presentation of the simulations and the results of Primary Control Reserve provision obtained with the models presented in *Chapter 4*. At first, the setup of the simulations is described in *Section 5.1*. Then, the base case is presented in *Section 5.2*. In *Section 5.3*, the different SoC restoration strategies are compared. Finally, in *Section 5.4* a sensitivity analysis is made on the main parameters of the best strategy identified in the previous Section, with particular attention on the optimization of the EPR.

5.1 Setup of simulations

In this Section, all the technical and economical parameters adopted in the simulations of PCR are detailed. This part is preceded by the presentation of the frequency profile used as input of the simulation.

5.1.1 Frequency profile

In this study, all the simulations of PCR are performed considering real frequency data measured in the IoT-Storage Lab in Politecnico di Milano (on the low voltage network). These data have been collected in the period 15 Februray-19 March 2017 with a 1 Hz sampling frequency without interruptions. The complete frequency profile is reported in *Figure 5.1*.

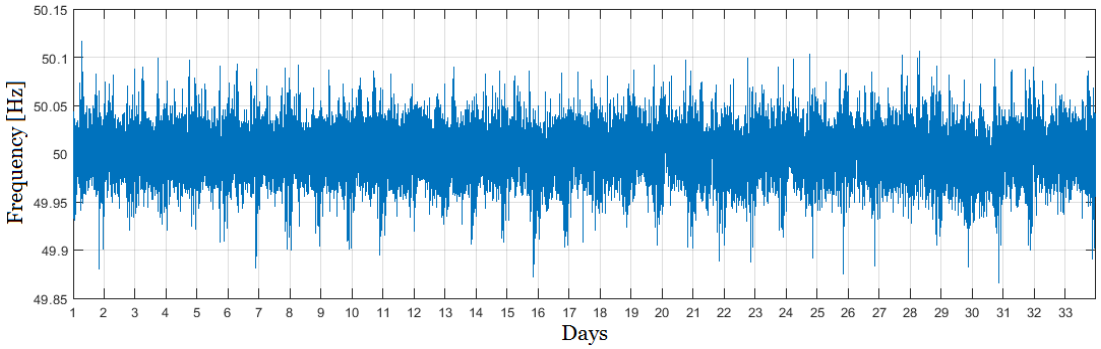

Figure 5.1 - Frequency profile measured in the IoT-Storage Lab in Politecnico di Milano in the period 15 Februry-19 March 2017.

In order to validate such a frequency signal, a comparison with another frequency profile measured in the same synchronous area over the same period has been made (i.e. Continental Europe, *see Section 2.3*). In particular, frequency data provided by one of the German TSOs, 50Hertz Transmission GmbH, have been used [114]: they have been collected on the high voltage network. *Figure 5.2 - (a)* shows the comparison between the two aforementioned profiles.

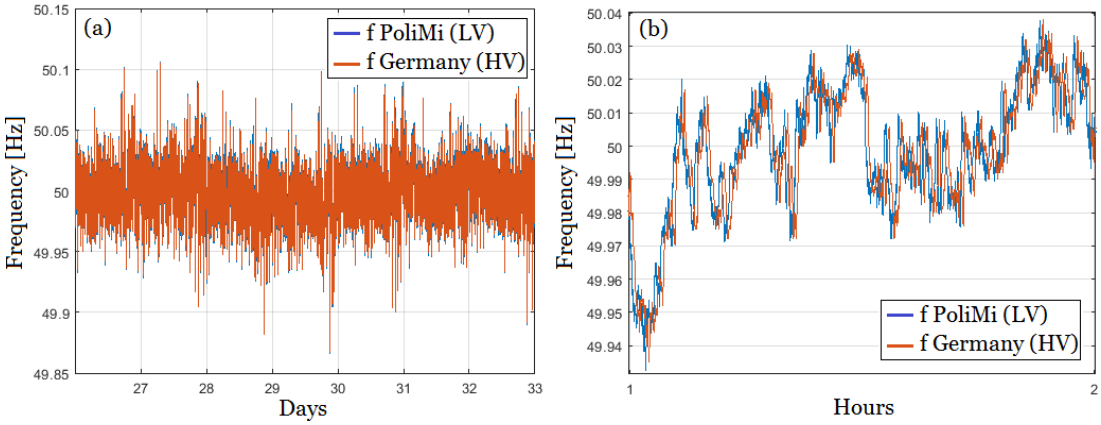

Figure 5.2 - (a) Comparison over one week: 13-19 March 2017; (b) Zoom of (a) over one hour: 1-2 a.m. on 14 March 2017.

By analysing *Figure 5.2 - (b)*, it is clear that the two frequency profiles are consistent: they are almost perfectly overlapped. Two are the negligible differences between the two signals. First, the frequency trend measured in the IoT-Storage Lab shows slightly larger fluctuations with respect to the frequency profile collected by the German TSO: this is due to the different voltage levels at which data are collected. Moreover, the two signals are not fully aligned, but this is due to the fact that the two sampling clocks are not perfectly synchronized. Therefore, the frequency signal is validated and its use in all the simulations of PCR is justified. The time horizon chosen for such simulations is 30 days (from 15 February to 16 March 2017). The results obtained on the simulated month are then extended to the whole lifetime of the system in order to make economical evaluations.

5.1.2 Technical setup

As previously introduced in *Chapter 4*, the battery technology adopted in this study is Li-ion: the reference cell is the Boston Power Swing 5300, whose features are specified in the *APPENDIX*. For what concerns the whole BESS, the SoC at the beginning of each simulation is always 50%, the maximum and the minimum allowable SoC values

are respectively 0% and 100%, the nominal power is 1 MW and the nominal energy is 1 MWh (i.e. the EPR is 1) and the calendar ageing is 12 years. Regarding the PCR controller, a reference droop of 5%, a dead band of 20 mHz, a PCR regulating band of 100% the nominal power (i.e. equal to the nominal power) and a reference SoC of 55% for all restoration strategies are considered. The droop is opportunely rescaled for BESSs according to the equation (2.6) in *Paragraph 2.6.1*: the aforementioned 5% corresponds to 0.075%. All these technical parameters are summarized in *Table 5.1*.

Table 5.1 – Technical parameters adopted in the simulations of PCR provision.

Technical parameters	Symbol	Value
Nominal power	P_{nom}	1 MW
Nominal energy	E_{nom}	1 MWh
Initial SoC	SoC_{start}	50 %
Minimum SoC	SoC_{min}	0 %
Maximum SoC	SoC_{max}	100 %
Calendar ageing	-	12 years
Droop	-	0.075 % (equivalent to 5 %)
Dead band	DB	20 mHz
PCR regulating band	$\Delta\dot{P}_{PCR}$	100 %
Reference SoC	SoC_{ref}	55 %

The technical setup shown in *Table 5.1* is kept constant during the comparison of all the SoC management strategies. Afterwards, once the best strategy is identified, a sensitivity analysis is made on its main parameters, including reference SoC and EPR.

5.1.3 Economic setup

In the economic analysis, the time horizon of the investment is set to 20 years and the actualization rate (or internal rate of return) is set to 6%. The investment cost is sustained in year 0: a specific BESS cost of 400 k€/MWh and a replacement factor of 0.5 are considered (*see Chapter 4 for complete expressions*). For what concerns PCR remuneration, two mechanisms are considered:

- Italian remuneration scheme, whose expressions for the valorization of positive and negative PCR are given in *Paragraph 4.2.7*. The hourly zonal prices registered

on the DAM during the simulation period are downloaded from the GME website [115] and the four annual constants given by Terna refer to 2017 [116].

- German (Central Western Europe) remuneration scheme, based on weekly auctions. In this case, a single weekly price is used for all the duration of the simulation: it is set to 2500 €/MW per week, which is the average yearly value for PCR remuneration in 2017 [117].

The economic valorization of the energy not provided (LoR) is set to 150 €/MWh in all the simulations. In the following paragraphs, some considerations on the impact of LoR valorization on the overall revenues are made. Finally, the prices for the energy traded for SoC restoration are defined as the average remunerations for positive and negative PCR over the period of simulation: 95 €/MWh gained for the energy injected and 30 €/MWh paid for the energy absorbed. *Table 5.2* summarizes the economic setup.

Table 5.2 - Economic parameters adopted in the simulations of PCR provision.

Economic parameters	Symbol	Value
Investment horizon	N	20 years
Actualization rate	r	6%
Specific BESS cost	c_{BESS}	400 €/MWh
Replacement factor	k_{rep}	0.5
German remuneration	p_{GER}	2500 €/MW per week
LoR valorization	p_{LoR}	150 €/MWh
Price of restoration energy injected	$p_{rest,+}$	95 €/MWh
Price of restoration energy absorbed	$p_{rest,-}$	30 €/MWh

5.2 Base case: PCR provision without any SoC restoration strategy

The reference case is characterized by the absence of any SoC management strategy. It is based on the standard fixed-droop control law explained in *Paragraph 2.3.1*. The main technical results of the simulation and the NPV are reported in *Table 5.3* and *Figure 5.3* shows the power provided by the BESS, the SoC and the power not provided because of LoR.

Table 5.3 – Simulation results for the reference case: no SoC restoration strategy.

Total energy ($E_{out,sys}$) [MWh/month]	64.8
Restoration energy absorbed ($E_{abs,rest}$) [MWh/month]	-
Restoration energy injected ($E_{inj,rest}$) [MWh/month]	-
Cycles ($cycles_{tot}$) [#/month]	32.0
Average C-rate [1/h]	0.252
Cell efficiency ($\eta_{E,cell}$)	94.8%
System efficiency ($\eta_{E,sys}$)	84.8%
LoR	17.5%
BESS lifetime ($life_{BESS}$) [years]	11.6
NPV_{ITA} [k€]	- 497.3
NPV_{GER} [k€]	726.0

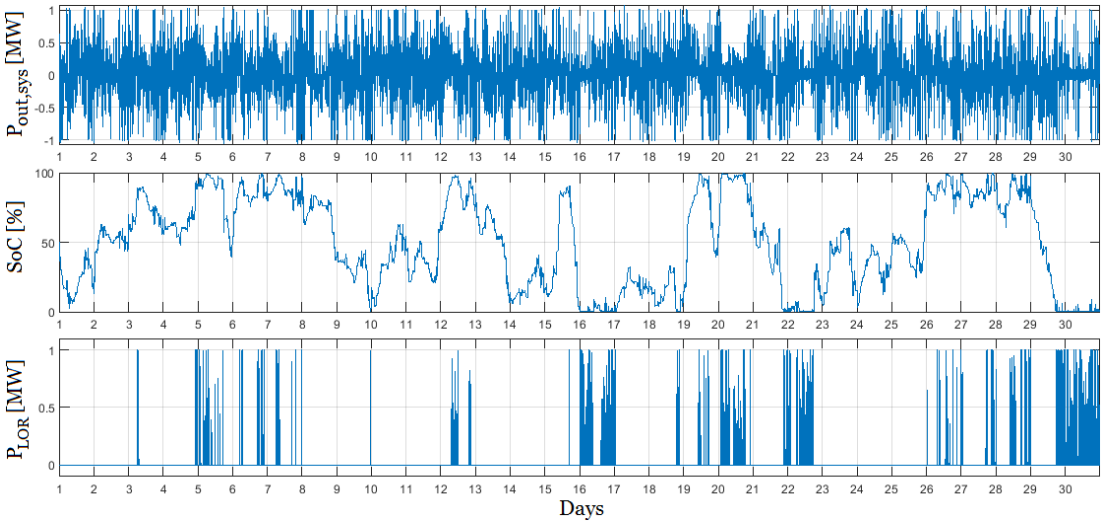

Figure 5.3 – Power output of the BESS, SoC and power not provided during the period of simulation.

In the reference case, a LoR of 17.5% is obtained. As previously explained in *Paragraph 4.1.1*, when the battery reaches its lower or upper voltage limits the BMS turns on and reduces the current. Therefore, the computation of the energy not provided begins even if the battery does not reach its SoC saturation limits, as shown in *Figure 5.3*. The cell efficiency is higher than the system efficiency: this is due to the presence of the inverter, which causes a reduction of performances. In presence of auxiliary services (which are not modelled in this study), the overall efficiency would be further decreased. The average C-rate and the number of cycles in the simulation period determine a BESS lifetime of 11.6 years (*see Paragraph 4.1.3*), which is similar

to the calendar ageing (12 years). For what concerns the NPV, PCR provision with the Italian remuneration scheme is absolutely not convenient (i.e. NPV_{ITA} is lower than zero). On the contrary, the German remuneration scheme generates a positive NPV after 20 years. For this reason, in the following analysis only the NPV calculated with the Central Western Europe remuneration mechanism is considered.

5.3 SoC restoration strategies

In this Section, the results for each SoC restoration strategy are presented. The best configuration of each method is used in the final comparison among the strategies, presented in *Paragraph 5.3.5*.

5.3.1 Variable droop strategy

This SoC control strategy does not generate a restoration power set point, but it acts directly on the Droop Control Curve, as shown in *Figure 4.14*. In this case, a sensitivity analysis is made on the droop range around the reference value: 5±2%, 5±2.5% and 5±3% are considered. These values are opportunely rescaled for the BESS according to the equation (2.6) in *Paragraph 2.6.1*. The main results are listed in *Table 5.4*.

Table 5.4 - Comparison of the results of the variable droop strategy considering different droop ranges.

Droop range	5±2%	5±2.5%	5±3%
Total energy ($E_{out,sys}$) [MWh/month]	68.5	69.1	69.8
Restoration energy absorbed ($E_{abs,rest}$) [MWh/month]	-	-	-
Restoration energy injected ($E_{inj,rest}$) [MWh/month]	-	-	-
Cycles ($cycles_{tot}$) [#/month]	33.8	34.2	34.5
Average C-rate [1/h]	0.272	0.276	0.279
Cell efficiency ($\eta_{E,cell}$)	94.8%	94.8%	94.8%
System efficiency ($\eta_{E,sys}$)	85.2%	85.2%	85.2%
LoR	7.5%	6.0%	4.9%
BESS lifetime ($life_{BESS}$) [years]	10.7	10.5	10.3
NPV_{GER} [k€]	865.6	885.6	903.4

All the results are very similar among them. By increasing the droop range, a slight increase of the total energy cycled by the BESS, the number of cycles and the average C-rate can be observed. Consequently, a slight reduction of the BESS lifetime occurs.

Nevertheless, the main difference among the three cases affects the LoR, which passes from 7.5% to 4.9%. This reduction of the energy not provided causes a reduction of the penalties associated to LoR and a consequent increase of the NPV. Therefore, for the final comparison with the other strategies, the droop range 5±3% is considered (i.e. corresponding to 0.075±0.045%).

5.3.2 Dead band strategy

In this case, a sensitivity analysis is made on the percentage of nominal power of the BESS used as restoration power set point. In particular, three values are considered: 5%, 10% and 15% of nominal power. The main results are listed in *Table 5.5*.

Table 5.5 – Comparison of the results of the DB strategy considering different restoration power set points.

Restoration power (percentage of nominal power)	5%	10%	15%
Total energy ($E_{out,sys}$) [MWh/month]	94.5	119.9	144.5
Restoration energy absorbed ($E_{abs,rest}$) [MWh/month]	15.2	28.0	41.0
Restoration energy injected ($E_{inj,rest}$) [MWh/month]	8.6	19.6	30.5
Cycles ($cycles_{tot}$) [#/month]	45.7	59.2	71.1
Average C-rate [1/h]	0.127	0.164	0.197
Cell efficiency ($\eta_{E,cell}$)	96.0%	96.7%	96.8%
System efficiency ($\eta_{E,sys}$)	76.8%	80.5%	83.8%
LoR	8.4%	4.4%	2.09%
BESS lifetime ($life_{BESS}$) [years]	9.9	7.2	5.7
NPV_{GER} [k€]	883.5	953.1	890.1

By increasing the restoration power set point, the overall system exchanges more energy in order to keep the SoC profile close to the reference value (55%). Consequently, the energy not provided (LoR) decreases. Moreover, the efficiency increases: this is mainly due to the lower LoR (the BESS works farther from its voltage limits). Regarding the BESS lifetime, the higher the power involved in SoC control, the higher the total number of cycles and the average C-rate: this results in a lower lifetime of the BESS. The values of the NPV in case of restoration power set point equal to 5% and 15% the nominal power are similar: the former is characterized by a 10 years lifetime, but it has a higher LoR; the latter shows a better LoR, but a lower lifetime. Therefore, from now on, the case with a restoration power equal to 10% the nominal

power of the BESS is taken as optimal case for the DB strategy because it shows the highest NPV and it represents a good tradeoff between lifetime and LoR.

5.3.3 SoC restoration with service interruption

Also in this case, a sensitivity analysis is made on the SoC restoration power set point. As previously explained in *Paragraph 4.2.3*, a high restoration power set point is adopted in order to limit the PCR service interruption. In particular, four values are investigated: 100%, 150%, 200% and 250% of nominal power. The main results are shown in *Table 5.6*.

Table 5.6 - Comparison of the results of the SoC restoration strategy with service interruption considering different restoration power set points.

Restoration power (percentage of nominal power)	100%	150%	200%	250%
Total energy ($E_{out,sys}$) [MWh/month]	85.8	85.5	85.9	86.4
Restoration energy absorbed ($E_{abs,rest}$) [MWh/month]	10.2	9.9	10.1	10.3
Restoration energy injected ($E_{inj,rest}$) [MWh/month]	5.0	4.2	4.0	3.8
Cycles ($cycles_{tot}$) [#/month]	42.6	42.2	42.4	42.7
Average C-rate [1/h]	0.340	0.341	0.341	0.347
Cell efficiency ($\eta_{E,cell}$)	94.0%	93.3%	92.6%	91.9%
System efficiency ($\eta_{E,sys}$)	85.0%	84.3%	83.7%	83.1%
LoR	4.8%	3.9%	3.2%	2.7%
BESS lifetime ($life_{BESS}$) [years]	7.6	7.7	7.6	7.5
NPV_{GER} [k€]	842.2	850.1	854.5	852.7

All the results in the four cases are very similar. As in the DB strategy, the amount of energy absorbed for SoC management is higher than the one injected. LoR is strongly reduced with respect to the reference case (i.e. 17.5%). The high value of C-rate (around 0.34) is justified by the high restoration power set points adopted in the strategy, but this reduces the overall efficiency. The higher number of cycles with respect to the base case is due to the higher quantity of energy cycled by the BESS. Even the lifetime of the BESS is similar in the four cases. For what concerns the economics, the NPVs for 150%, 200% and 250% power set points are similar among them and greater than the NPV for 100%. For the comparison with all the other SoC control strategies, the intermediate case with 200% power set point is considered.

5.3.4 SoC restoration without service interruption

As explained in *Paragraph 4.2.4*, in this strategy two new parameters are introduced: the SoC thresholds for the activation of the restoration strategy (SoC_{down} and SoC_{up}). Differently from the previous strategy, voltage thresholds are not considered anymore and the power set point is much lower because PCR provision is not interrupted. *Table 5.7* shows the results of this strategy with 10% and 90% as SoC thresholds and restoration power equal to 50% the nominal power of the BESS.

Table 5.7 – Results of SoC restoration strategy without service interruption considering 10% and 90% as SoC thresholds and 50% as restoration power.

Restoration power (percentage of nominal power)	50%
SoC activation thresholds	10%-90%
Total energy ($E_{out,sys}$) [MWh/month]	84.0
Restoration energy absorbed ($E_{abs,rest}$) [MWh/month]	10.6
Restoration energy injected ($E_{inj,rest}$) [MWh/month]	5.5
Cycles ($cycles_{tot}$) [#/month]	41.2
Average C-rate [1/h]	0.315
Cell efficiency ($\eta_{E,cell}$)	94.8%
System efficiency ($\eta_{E,sys}$)	86.0%
LoR	0.6%
BESS lifetime ($life_{BESS}$) [years]	8.2
NPV_{GER} [k€]	935.6

As in the DB strategy and in SoC restoration with service interruption, the energy absorbed for SoC control is about twice the energy injected: the main reason of this is that the internal efficiency tends to discharge the battery over time. For what concerns cycles, average C-rate, efficiency and BESS lifetime, the values are similar to the ones obtained in the previous strategy (*see Table 5.6*). The most interesting result in *Table 5.7* is the strong reduction of LoR: it is almost zero because the activation of the strategy at 10% and 90% of SoC prevents the BESS from not providing energy for Primary Frequency Regulation. This means that the impact of LoR penalties on the overall revenues is very low. For this reason, the NPV after 20 years is rather high.

5.3.5 Final comparison among SoC restoration strategies

In this Paragraph, a comparison among the different SoC control strategies is provided. *Table 5.8* collects all the results and *Figure 5.4* shows the behavior of the SoC of the battery for each strategy.

Table 5.8 – Comparison among the different SoC restoration strategies.

STRATEGIES	BASE CASE	VARIABLE DROOP	DB	SoC REST. WITH	SoC REST. WITHOUT
Tot. energy [MWh/month]	64.8	69.8	119.9	85.9	84.0
Rest. en. abs. [MWh/month]	-	-	28.0	10.1	10.6
Rest. en. inj. [MWh/month]	-	-	19.6	4.0	5.5
Cycles [#/month]	32.0	34.5	59.2	42.4	41.2
Average C-rate [1/h]	0.252	0.279	0.164	0.341	0.315
Cell eff.	94.8%	94.8%	96.7%	92.6%	94.8%
System eff.	84.8%	85.2%	80.5%	83.7%	86.0%
LoR	17.5%	4.9%	4.4%	3.2%	0.6%
BESS lifetime [years]	15.1	10.3	7.2	7.6	8.2
NPV_{GER} [k€]	726.0	903.4	953.1	854.5	935.6

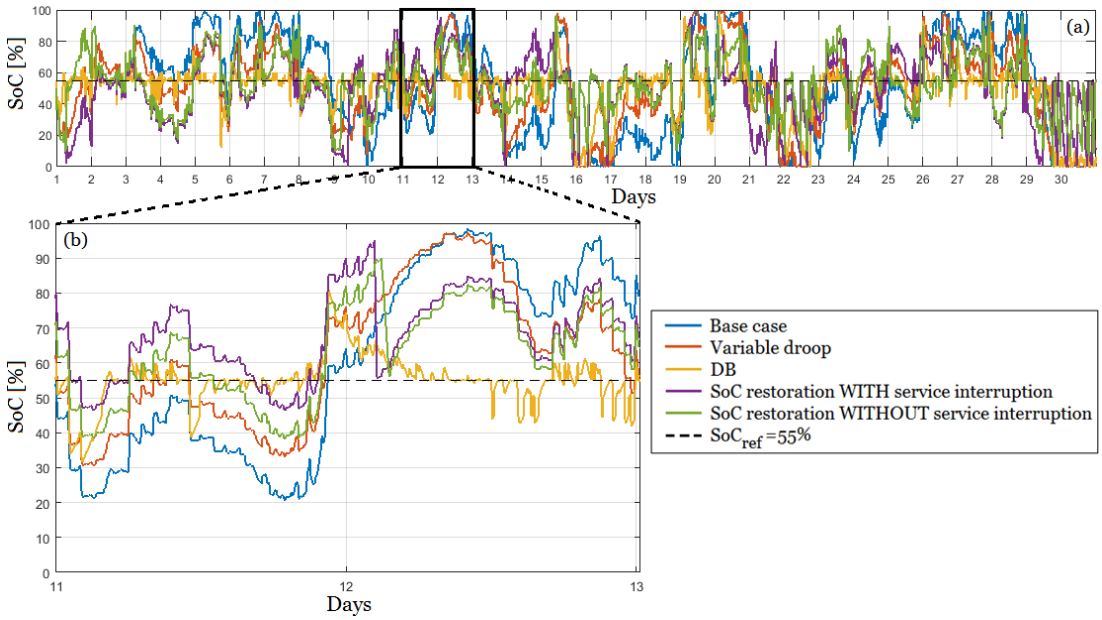

Figure 5.4 – (a) SoC profiles of the different control strategies during the 30 days of simulation; (b) zoom between day 11-13.

By analysing *Figure 5.4 – (a)*, it is clear that the DB strategy keeps the SoC close to the reference value. In the variable droop strategy, the slope of the SoC decreases with respect to the reference case when approaching 100%, as expected. For what concerns the SoC restoration with service interruption, it is activated when the upper voltage limits is hit: for this reason, the restoration starts before the SoC reaches 100% and stops when the SoC_{ref} is reached. Finally, the SoC restoration without service interruption begins when SoC equals 90% and lasts until the reference value is touched.

The implementation of any SoC restoration strategy causes an increment of the total energy cycled by the BESS with respect to the reference case, as shown in *Table 5.8*. In particular, the DB strategy exchanges the greatest amount of energy, hence it shows the highest number of cycles: this occurs because this strategy is often activated (i.e. every time the frequency is inside the dead band). Since the C-rate depends on the power cycled by the BESS, the lowest average C-rate is obtained with the DB strategy, which is characterized by a low power set point. On the contrary, the highest average C-rate belongs to SoC restoration with service interruption, whose power set point is very high. The C-rate in the variable droop strategy is similar to the base case. The lifetime of the BESS decreases in all the strategies with respect to the base case since more energy is cycled by the system. Regarding the LoR, all the strategies perform better than the reference case. The lowest value is shown by SoC restoration without service interruption (i.e. LoR is almost null). From the economic perspective, all the strategies improve the NPV with respect to the reference case. The highest NPV belongs to the dead band strategy, followed by SoC restoration without service interruption. *Figure 5.5* reports the LoR and the NPV of the different strategies.

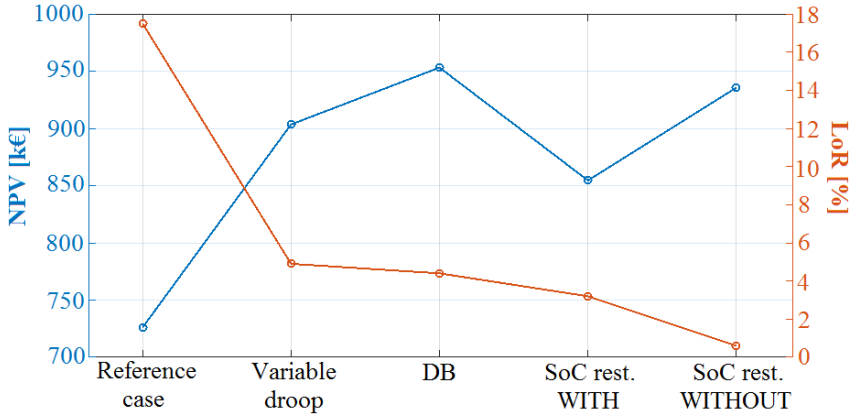

Figure 5.5 – LoR and NPV of the different SoC control strategies.

By analysing *Figure 5.5*, SoC restoration without service interruption shows a high NPV over 20 years and a LoR close to zero: the overall economics of this strategy do not suffer a possible increase of LoR valorization (p_{LoR}). Conversely, the NPV of all the other strategies decreases a lot if the price for the energy not provided increases: this is because they are characterized by a higher LoR (see *Figure 5.6*).

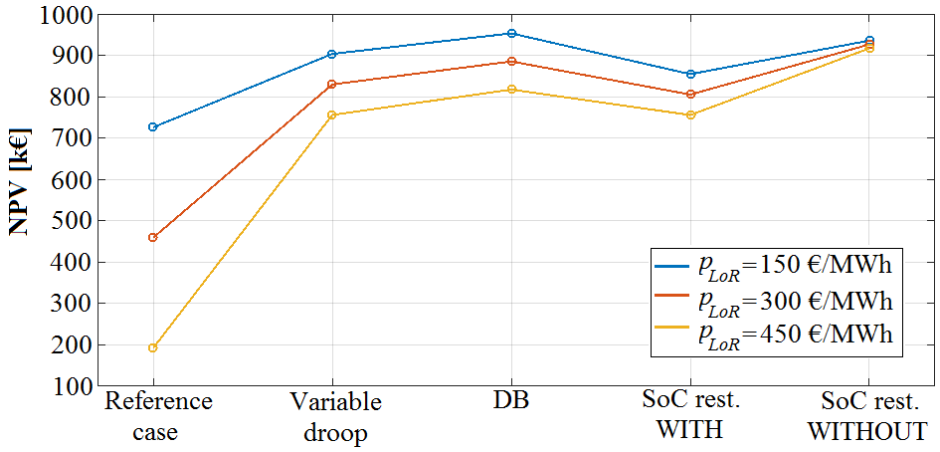

Figure 5.6 – Impact of LoR valorization p_{LoR} on the NPV of the different strategies.

For this reason, SoC restoration without service interruption is identified as the best strategy and an optimization of its main parameters is performed in the following Section.

5.4 Sensitivity analysis on the main parameters of the best strategy

In this Section, a sensitivity analysis on the main parameters of the SoC restoration strategy without service interruption is done. At first, SoC thresholds and restoration power set point are investigated in *Paragraph 5.4.1*. Then, the reference SoC is optimized in *Paragraph 5.4.2*. Finally, a sensitivity analysis on the EPR is performed in *Paragraph 5.4.3*.

5.4.1 SoC activation thresholds and restoration power set point

In this case, 9 configurations are investigated, obtained by the combination of three couples of SoC thresholds (5-95%, 10-90% and 15-85%) and three values for restoration power set points (25%, 50% and 75% of the nominal power). Only LoR, BESS lifetime and NPV are reported in *Table 5.9*.

Table 5.9 – Sensitivity analysis on SoC thresholds and restoration power set points.

SoC thresholds	Restoration power	LoR	BESS lifetime [years]	NPV_{GER} [k€]
5-95%	25%	3.0%	8.8	915.9
5-95%	50%	2.3%	8.1	911.2
5-95%	75%	1.5%	7.9	907.7
10-90%	25%	1.1%	8.6	943.4
10-90%	50%	0.6%	8.2	935.6
10-90%	75%	0.4%	7.9	927.0
15-85%	25%	0.5%	8.4	954.7
15-85%	50%	0.0%	8.1	954.8
15-85%	75%	0.0%	7.8	934.7

Generally, LoR and BESS lifetime decrease when increasing the restoration power set point. SoC thresholds equal to 5% and 95% show the worst performances, either from the technical point of view (highest LoR) or by the economic perspective (lowest NPV). The optimal configuration must be found among the remaining six. In particular, 15-85% SoC thresholds with 50% of nominal power as restoration power set point is identified as the optimal setup. Its NPV is the highest among all the configurations (954.8 k€). LoR is zeroed and this is a huge advantage with respect to all the other setups because a possible increase of LoR valorization (p_{LoR}) would not affect at all the overall revenues.

5.4.2 Reference SoC

Starting from the optimal configuration found in the previous Paragraph, a sensitivity analysis is performed on the reference SoC (SoC_{ref}) at which the restoration strategy stops. In particular, four values are considered: 50%, 55%, 60% and 65%. LoR, BESS lifetime and NPV are collected in *Table 5.10*.

Table 5.10 – Sensitivity analysis on the reference SoC, considering 15-85% SoC thresholds and 50% of restoration power set point.

Reference SoC	LoR	BESS lifetime [years]	NPV_{GER} [k€]
50%	0.0%	7.9	939.7
55%	0.0%	8.1	954.8
60%	0.0%	8.0	954.7
65%	0.0%	8.1	952.8

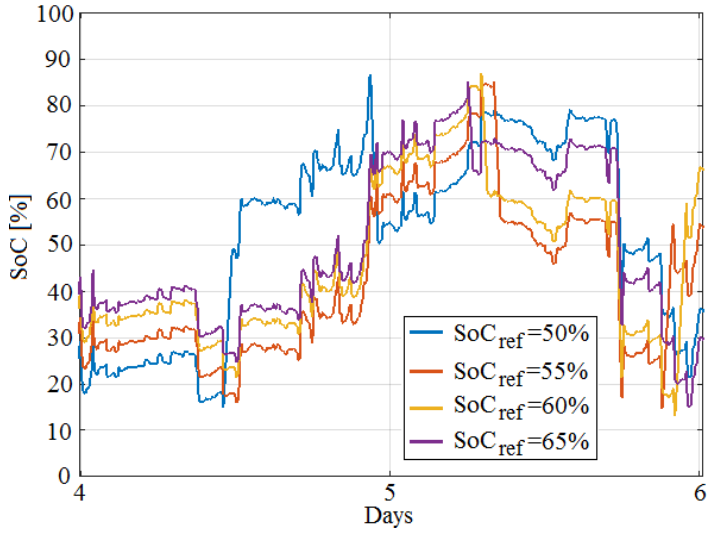

Figure 5.7 – SoC profiles in day 4-6 for different reference SoC values.

Figure 5.7 shows that when the SoC reaches 85% (i.e. the upper threshold), the SoC restoration strategy without PCR service interruption is activated with a restoration power set point equal to 50% of the nominal power and it stops when the reference SoC is reached. Similar results are obtained for all the cases analysed, as shown in *Table 5.10*. The lifetime of the BESS is more or less constant around 8 years. Loss of Regulation is always null: this means that no penalties are paid for the energy not provided for the Primary Frequency Regulation service. For what concerns the NPV, the lowest value is obtained for a reference SoC equal to 50%, while the other three configurations are characterized by similar values. Therefore, in order not to have an excessive unbalancing between the reference State of Charge and the SoC thresholds (15-85%), SoC_{ref} equal to 55% is chosen as the optimal value.

5.4.3 EPR optimization

In this Paragraph, a sensitivity analysis on the EPR is performed starting from the optimal configuration of the SoC restoration strategy without service interruption:

- SoC thresholds: 15-85%.
- Restoration power set point: 50% of the nominal power.
- Reference SoC: 55%.

In this analysis, the nominal power of the BESS is assumed constant to 1 MW (*see Table 5.1*). Therefore, varying the EPR means varying the nominal energy of the BESS. The considered values of EPR are: 0.5, 0.75, 1, 1.25, 1.5 and 1.75.

Table 5.11 – Sensitivity analysis on the EPR of the optimal configuration of the strategy.

EPR	0.5	0.75	1	1.25	1.5	1.75
Tot. energy [MWh/month]	89.7	86.5	85.0	85.7	83.5	83.6
Rest. en. abs. [MWh/month]	18.1	13.8	11.9	11.0	9.5	9.2
Rest. en. inj. [MWh/month]	10.1	7.9	6.9	6.3	5.2	5.7
Cycles [#/month]	88.9	57.0	41.7	33.5	27.3	23.4
Average C-rate [1/h]	0.650	0.427	0.316	0.254	0.210	0.179
Cell eff.	89.7%	93.1%	94.9%	95.9%	96.5%	97.1%
System eff.	81.6%	84.5%	86.1%	87.0%	87.6%	88.0%
LoR	2.8%	0.3%	0.0%	0.0%	0.0%	0.0%
BESS lifetime [years]	2.2	4.9	8.1	11.1	14.6	17.8
Profitability Index *PI*	2.22	2.58	2.61	2.44	2.05	1.77

The results in *Table 5.11* show that by increasing the EPR, the energy required by the BESS for SoC restoration, the number of cycles and the average C-rate decrease. In particular, when the EPR is equal to 0.5 and 0.75, the average C-rate is very high: the battery is particularly stressed and this causes a low efficiency and a very low lifetime. Moreover, since the BESS is smaller for those values of EPR, a non-zero LoR is observed. In all the other cases ($EPR \geq 1$), LoR is null and no penalties must be paid for the energy not provided. From the economic point of view, the NPV is not considered anymore, but the Profitability Index is evaluated: this index is useful for comparing investments of different sizes, such as it happens in this case (*see formula (4.9) in Chapter 4*).

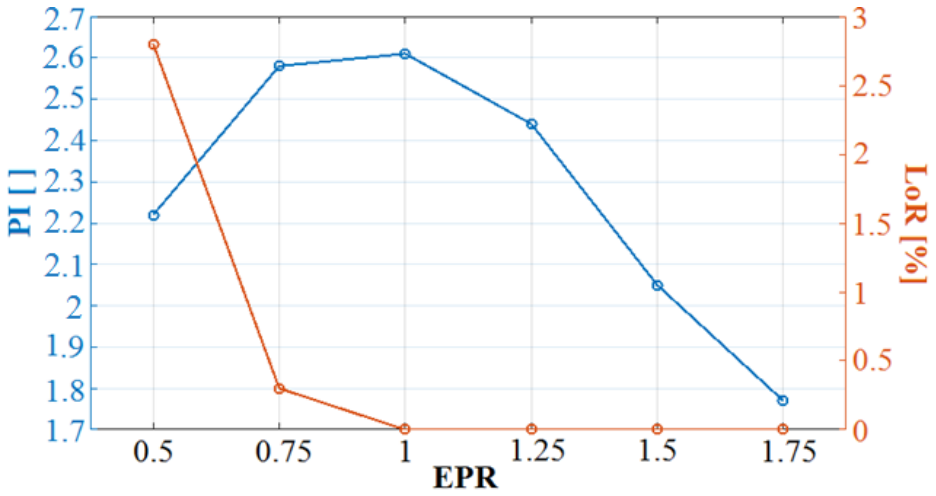

Figure 5.8 – PI and LoR for the different values of EPR.

All the configurations are characterized by a PI greater than one, which means that the investment is attractive. The lowest PI is registered for EPR equal to 1.75: this is because the initial investment costs are very high due to the big dimensions of the BESS (i.e. high nominal energy). Moreover, EPR equal to 0.5 and 1.5 are not the best solutions because: in the former, the lifetime of the BESS is too short and replacement costs decrease the overall PI; in the latter, the initial investment is too high. By analysing *Figure 5.8*, a maximum for the PI may be identified for EPR values between 0.75 and 1.25. In particular, an EPR equal to 1 is identified as the best value because it is characterized by the highest PI and a LoR equal to zero.

As final remark, the computational effort for each simulation performed in this Chapter (32 scenarios, each one covering a 30 days period) has been 1.15-1.30 h using an Intel® Core™ i7 4790–16GB RAM.

6. SIMULATIONS & RESULTS: MULTI-SERVICE PROVISION (PCR AND ASYMMETRIC SCR)

In this Chapter, the results of the simulations of multi-service provision are presented. As stated in *Chapter 4*, the asymmetric SCR band allocation works as a SoC restoration strategy. In order to do so, predictions on battery energy fluxes based on frequency and on the Area Control Error (ACE) are necessary. *Section 6.1* presents a preliminary statistical study on the European grid frequency and on ACE, a signal sent by the Italian TSO (i.e. Terna), which determines the share of secondary band that must be used by market players. This analysis is useful in order to assess the general characteristics of these to signals, which are used to build the predictors for the forecasting methods described in following parts of the Chapter. *Section 6.2* describes how the forecasting methods mentioned in *Chapter 4* (statistical, Random Forest, NARX neural network, floating NARX, Hybrid Approach) are implemented in terms of choice of predictors, training and test sets, optimization process and performance comparison. Moreover, a detailed explanation on which energy fluxes are forecasted and how they are computed is provided. The goal of this methodology is to obtain the quantities required by the SCR controller described in *Paragraph 4.3.1*. In principle, other methodologies and forecasting techniques can be used as long as quantities are coherent. *Section 6.3* describes the technical and economic setup of the simulations. *Section 6.4* presents the results of multi-service provision using the predictions of the best forecasting approaches identified in the previous Section (by keeping constant all the other parameters). Afterwards, the best approach is further investigated through a sensitivity analysis on the EPR. Finally, a comparison with the results of an ideal case of "no-error" prediction is provided (i.e. by feeding the model with the actual values).

6.1 Statistical study on grid frequency and Area Control Error

For each signal, the analysis consists of two parts. At first, a general overview on mean and standard deviations considering different years, different months and different

types of day (working, pre-holiday and holiday) is given. The scope of this part is to evaluate the seasonality of the signals. Secondly, data are collected in quarter-hour averages and typical daily profiles are investigated, looking for daily patterns.

6.1.1 European grid frequency

Three years of frequency data (2015, 2016 and 2017) have been downloaded from the website of one of the German TSOs, 50Hertz Transmission GmbH [114], and they refer to the Continental Europe synchronous area (see *Section 2.3*). They sampling frequency is 1 Hz. Initially, an analysis on the mean and standard deviation for each month is provided and results are collected in and shown in *Figure 6.1*. The mean values are discounted of the nominal 50 Hz.

Table 6.1 - Monthly mean and standard deviation of European grid frequency.

Frequency	Mean [mHz]			Standard deviation [mHz]		
Month	2015	2016	2017	2015	2016	2017
Jan	-0.05	0.65	0.36	20.36	20.88	22.01
Feb	-0.05	-0.04	0.22	21.55	20.93	21.65
Mar	0.69	0.49	0.10	21.91	20.61	22.58
Apr	-1.09	-0.57	-0.81	20.32	20.76	21.52
May	NaN	0.39	0.10	NaN	19.91	20.25
Jun	-1.18	-1.13	0.41	18.16	19.02	19.42
Jul	-0.16	-0.29	0.00	18.41	17.60	19.57
Aug	-1.09	0.20	-0.11	17.05	18.55	19.55
Sep	0.44	-0.24	-0.50	19.85	19.53	21.46
Oct	-0.44	-0.16	0.76	21.42	21.29	23.34
Nov	-0.41	-0.47	-1.01	20.13	20.31	22.92
Dec	0.19	-0.19	0.55	18.58	20.20	21.97

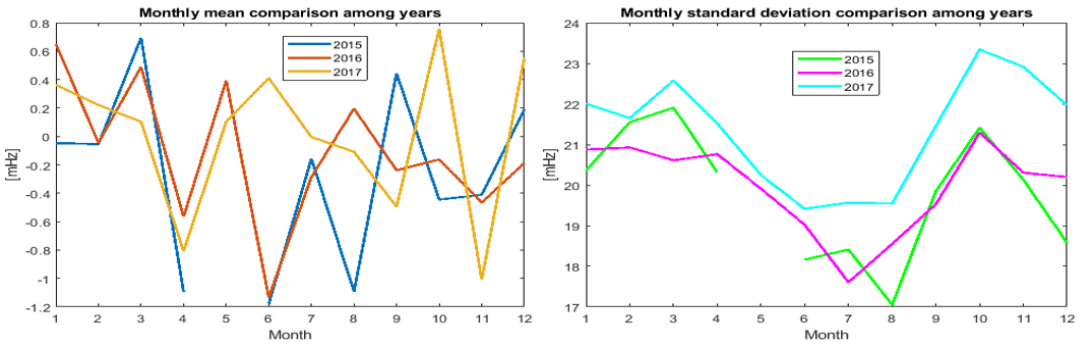

Figure 6.1 – Monthly mean and standard deviation of European grid frequency.

Figure 6.1 shows that the mean stays inside a small range around the nominal value without particular patterns. Conversely, the standard deviation shows a clear

seasonality: in cold months, frequency is more variable with respect to hot months in every year considered. Moreover, volatility is higher in 2017: this could be due to the increase share of renewable sources inside the grid. This aspect highlights how solving this problem can have pivotal importance in future energy scenarios.

After the monthly comparison, another feature could be useful to highlight: the impact of the type of day. Three types of days are considered: working days, pre-holidays and holidays. Working days are characterized by higher energy fluxes due to the high electric load. Holidays' cluster includes Sundays, 1st January, 6th January, Easter and 24th-25th-26th-31st December. Specific Italian holidays are not taken into account since national holidays are not in common with other Countries in the Continental Europe area. Pre-holidays are Saturdays and the days preceding each single holiday. Results are collected in *Table 6.2*.

Table 6.2 - Mean and standard deviation of European grid frequency by type of day.

Frequency	Mean [mHz]			Standard deviation [mHz]		
Type of day	2015	2016	2017	2015	2016	2017
Working day	-0.44	-0.44	-0.15	10.43	10.38	11.23
Pre-holiday	-0.34	-0.30	0.05	9.02	8.63	9.52
Holiday	1.22	1.47	0.55	9.39	9.15	10.06

Working days are usually in under-frequency and experience a higher volatility with respect to pre-holidays and holidays, due to the aforementioned higher energy fluxes, which stress the system.

In order to investigate the presence of daily patterns, a quarter-hour frequency profile is used, as shown in *Figure 6.2*. In this way, a lower amount of data is involved, easing the overall analysis (i.e. for each day, 96 data rather than 86400 samples).

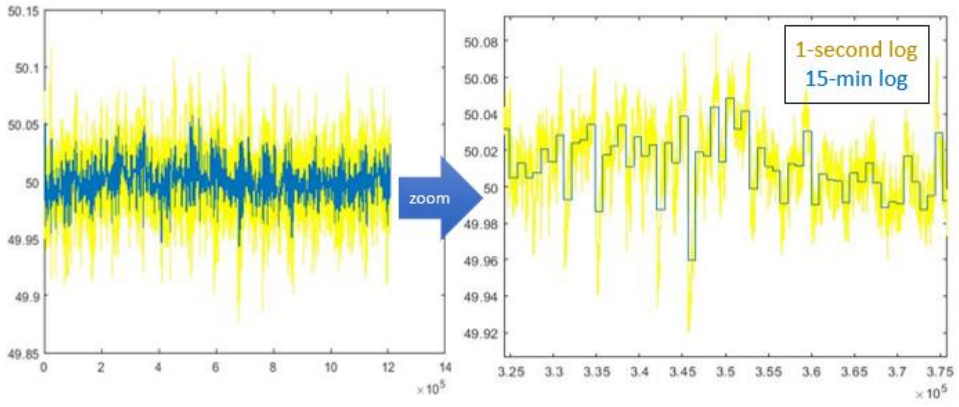

Figure 6.2 - Averaged quarter-hour frequency.

Figure 6.3 shows the mean daily frequency profile, the 96 quarter-hour daily boxplots and quarter-hour standard deviation of two months in 2017 (January and July). The boxplots include information about the median, quartiles and outliers. Standard deviation bar representation is not in scale, but the height of the bars reflects the real values.

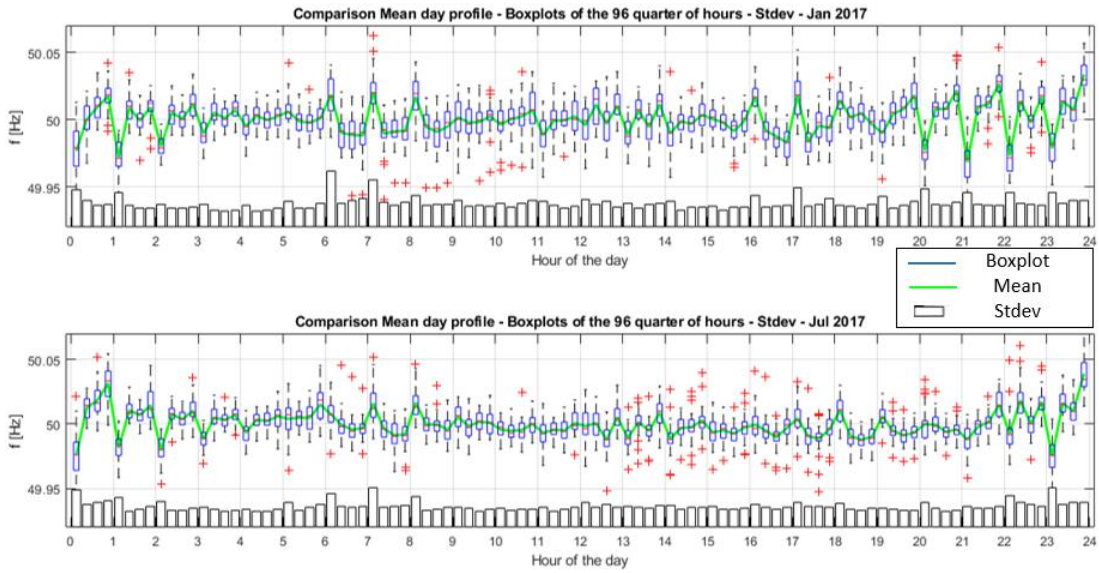

Figure 6.3 – Boxplots, mean daily profile and standard deviations in January 2017 and June 2017 for frequency.

The two frequency profiles look similar and some daily patterns are evident (especially in the periods 0-3 and 20-24). Hour-changing pattern is due to the scheduled production, which is hourly-based, as is described in [113]. This behavior looks very similar despite the two months are very different. *Figure 6.4* shows the three yearly mean day frequency profiles and the seasonal mean days in 2017.

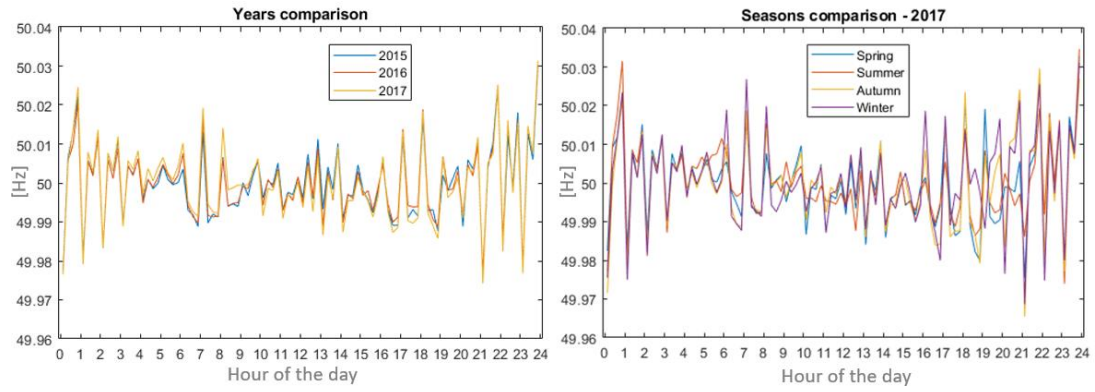

Figure 6.4 – Frequency: yearly mean day profiles and seasonal mean days in 2017.

The yearly mean day profile is characterized by a clear pattern and it is very similar across years. Moreover, seasonal mean days in 2017 do not present large differences. Meteorological seasons are considered (e.g. Spring: 1st March – 30th May). The main differences among seasons are evident in the morning and in the evening hours, which experience the most relevant changes across the year (e.g. at 7 am in summer photovoltaic plants are already on and lights are switched off). Late evening and night hours almost overlap in both graphs.

Summing up the outcomes:

- Even though grid frequency may be considered stochastic, daily patterns are present and they are mainly determined by the market structure.
- The first quarter of hour of an hour is usually unbalanced with respect to the other three.
- These patterns are clearer at late evening and night, which are characterized by a low load with respect to the other parts of the day.
- Seasonality appears relevant only in middle hours of the day.
- Cold months and holidays are less volatile with respect to hot months and working days.

6.1.2 Area Control Error (ACE)

The ACE is a regulating signal sent every minute by the Italian TSO, Terna. It is available since June 2015 and downloadable from [118]. In this study, the ACE refers to Continental Italy and the period 1 June 2015–31 December 2018 is considered. See *Paragraph 2.3.2* for more information about its meaning. In this analysis, the same framework adopted for frequency is followed. Firstly, mean and standard deviation of ACE for each month in the three years is provided in *Figure 6.5*.

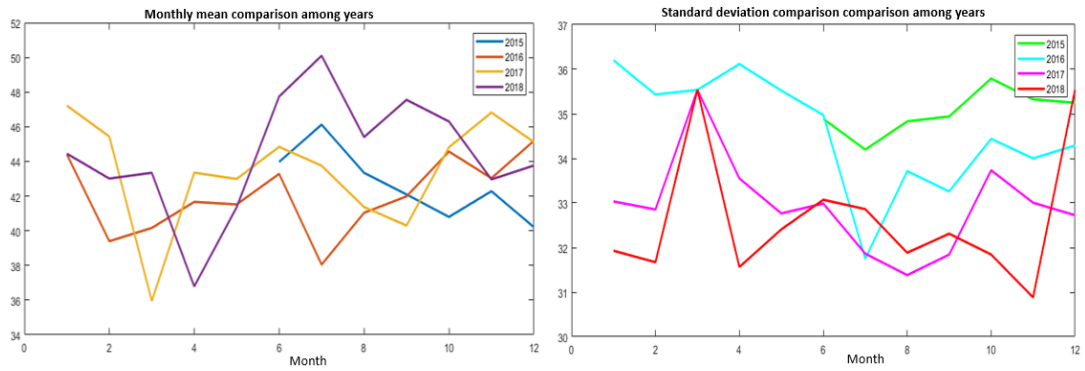

Figure 6.5 - Monthly mean and standard deviation of ACE.

The mean is always lower than 50: it means that secondary market players are typically asked to provide negative SCR (i.e. reduce their power output rather than increasing it). One of the reasons of this is that Authority puts in place cautionary measures in order to prevent dishonest behaviors of traditional plants aimed at manipulating local energy balance in order to be called to provide positive secondary reserve, which is highly remunerated with respect to the negative one. Differently from frequency, mean and standard deviation of ACE do not seem to have particular seasonal patterns. The influence of the type of day is captured in *Figure 6.6*.

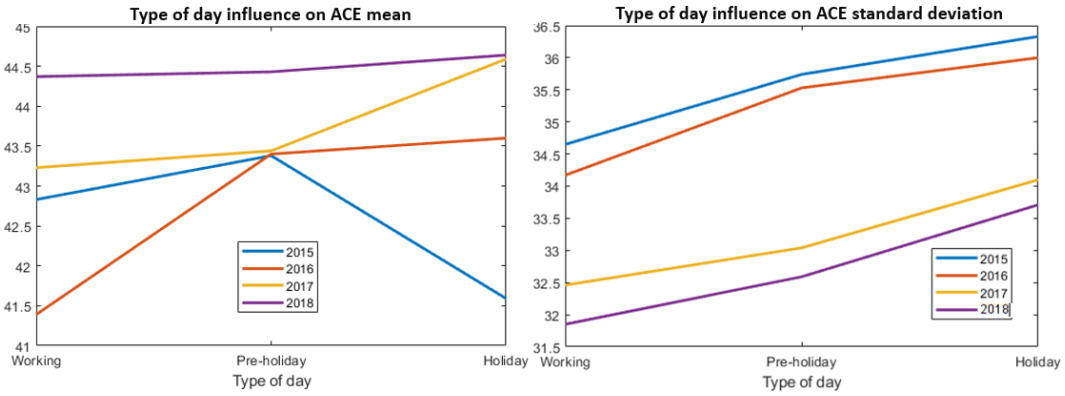

Figure 6.6 – Influence of the type of day on ACE.

By looking at the standard deviations, it is possible to see that first two years (2015-2016) and last two years (2017-2018) are coupled. Among the causes of this decrease of volatility there could be the Authority intervention aimed at stopping fraudulent behavior of market players [126]-[127]-[128].

Mean daily profiles show more relevant differences if different months are compared, but it is still possible to find some patterns in some hours of the day (see *Figure 6.7*).

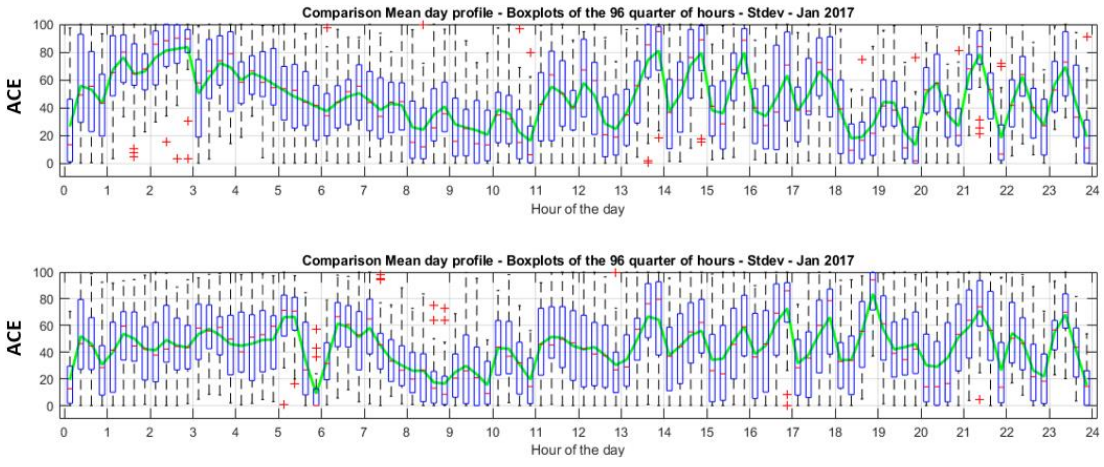

Figure 6.7 - Boxplots and mean day profiles in January 2017 and June 2017 for ACE.

The yearly mean day profile is rather clear, but seasonality has a more relevant effect with respect to frequency. The period of maximum predictability is early afternoon (see *Figure 6.8*).

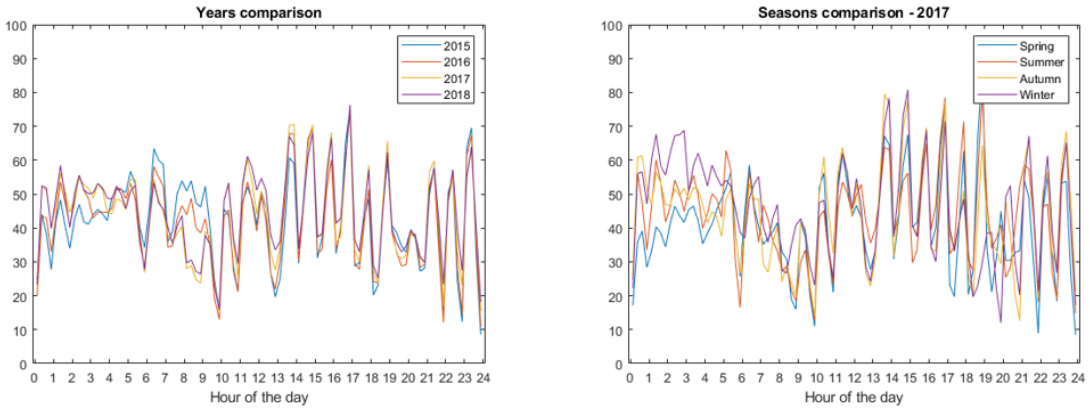

Figure 6.8 – ACE: yearly mean day profiles and seasonal mean days in 2017.

ACE shares many characteristics with frequency (daily patterns depending on the market structure, daily profiles very similar among years and seasons), but also presents some differences (differences among months are larger for ACE with respect to frequency, the mean of the ACE is always lower than 50). In this study, when dealing with predictors' construction, they are treated in the same way, as presented in following sections.

6.2 Forecasting methods implementation

In this Section, the methodology through which forecasts are implemented in this work is presented. As mentioned in *Chapter 4*, five methods have been analysed: Statistical, Random Forest, NARX Neural Network, floating NARX and Hybrid Approach. Before going into the detail of the methods, an introduction on data preparation, a description of the quantity to be forecasted and how they are computed is necessary. The analysis is performed in MATLAB® environment.

6.2.1 Data preparation

The MATLAB® function for calculating the SCR regulating bands (*see Paragraph 4.3.1*) requires six quantities in MWh to be forecasted:

- T_{1P}, the regulating energy required by PCR in the next one and a half hour.
- T_{2P}, the regulating energy required by PCR in next market session.

- $T_{1S,+}$ and $T_{1S,-}$, positive and negative regulating energy required by SCR in next one and a half hour.
- $T_{2S,+}$ and $T_{2S,-}$, positive and negative regulating energy required by SCR in next market session.

These six T_{jk} (where "j" can be 1 or 2 and "k" can be "P", "$S,+$"or "$S,-$") represent the actual values, Y_{jk} represent the respective predictions. For instance, the bid for the market session 4:30-8:30 must be performed by 3:00. Hence the prediction must be done by that time. In this case, the period of T_{1k} quantities will be 3:00-4.30 and the period of T_{2k} will be 4:30-8:30. This means that Y_{1k} forecast must cover a period of 1.30 hours, while Y_{2k} forecast must cover 5.30 h.

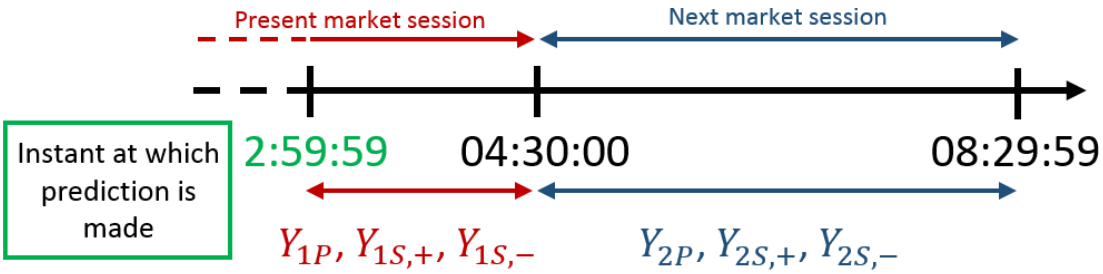

Figure 6.9 - Timeline for forecast horizon.

Six training sets are needed, which are the historical time-series of the aforementioned quantities. Since they represent the energetic content of regulating signals, they are computed starting from frequency and ACE. The proposed methodology does not aim to predict frequency and ACE and use them to compute Y_{jk}, but the goal is to forecast directly their energetic content in fixed periods of time and use these predictions to build the desired outcomes. The first thing to decide is the timescale, which is the minimum interval of time considered. In this study, the reference is 15 minutes. Whichever value is chosen, the energy content of signals in this timescale ($E_P^{15min}, E_{S,+}^{15min}, E_{S,-}^{15min}$) is computed with the procedure detailed in the following list. If T_{tr} is the training period (i.e. the period for which data are available) and N_{tr} is the number of quarter hours in T_{tr}:

- Divide the regulating signal profile in N_{tr} continuous separate logs.
- For every log, starting from the regulating signal, compute power set point with the Signal-to-Power relationship.

- Integrate the power set point in the whole quarter of hour in order to obtain N energy set points.

The regulating signals are frequency for E_P^{15min} and ACE for $E_{S,+}^{15min}$ and $E_{S,-}^{15min}$. The Signal-to-Power relationship is the Droop Control Law for PCR (using equation (2.1) with $droop_{BESS}$ defined in (2.6)) and equation (2.2) for SCR. The sign convention for power and energy is positive if absorbed. Therefore, either the sign of frequency or ACE must be inverted. In the context of prediction, the following assumptions are made: (i) nominal power of BESS is 1 MW; (ii) regulating band of 100% the nominal power in both cases; (iii) droop is 5%. Hence, ΔP_{PCR} in (2.1) and ΔP_{SCR} in (2.2) are equal to 1 MW, $\Delta \dot{P}_{PCR}$ in (2.6) is equal to 1 so that $droop_{BESS}$ is 0.075%. An example of this procedure is shown in *Figure 6.10* for E_P^{15min}.

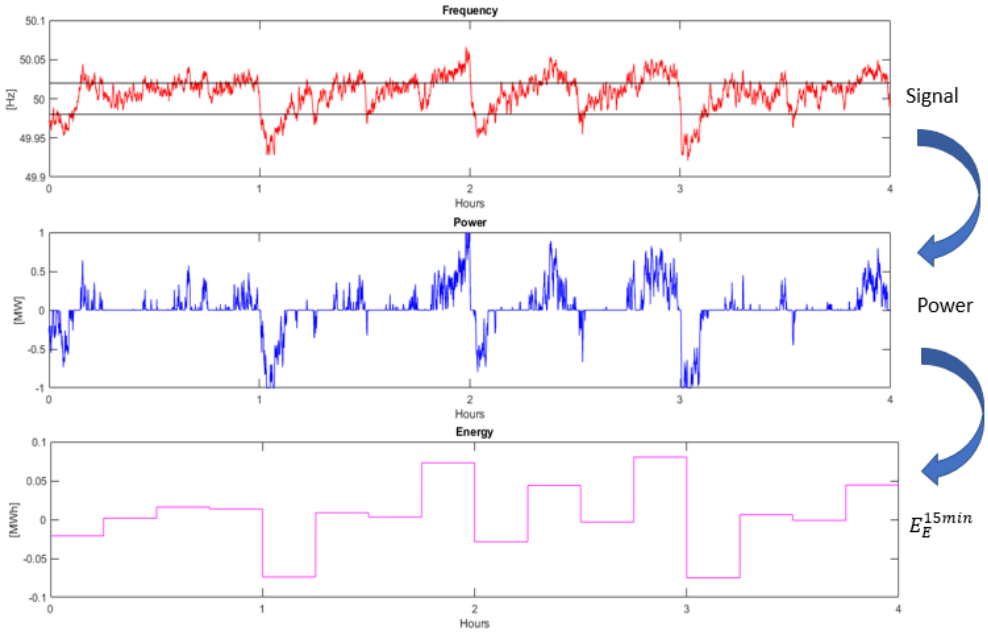

Figure 6.10 - Process to compute energy content of frequency in quarter-hour base.

So far, three sets composed by N_{tr} values are available. These are the "bricks" to build the six T_{jk} required and the predictors. In particular, calling $E_k^{15min}(i_{tr})$ (with $i_{tr} = 1{:}\,N_{tr}$) the energies associated to each 15-minute period:

$$T_{1k}(i_{tr}) = \sum_{i_{tr}+1}^{i_{tr}+6} E_k^{15min}(i_{tr}) \tag{6.1}$$

$$T_{2k}(i_{tr}) = \sum_{i_{tr}+7}^{i_{tr}+22} E_k^{15min}(i_{tr}) \tag{6.2}$$

In the quarter of hour i_{tr}, $T_{1k}(i_{tr})$ covers the following hour and a half and $T_{2k}(i_{tr})$ the subsequent market session, as in *Figure 6.9*. All these quantities are evaluated at the grid side. In order to bring them on the battery side, the inverter efficiency must be considered and this is embedded in the SCR band-allocating function.

6.2.2 Predictors

Forecasting algorithms require predictors. The training set, for every period i_{tr}, consists of m predictors $P_{jk,m}(i_{tr})$ plus the actual value T_{jk}. These quantities are used to train the model. The test set refers to period T_{test} divided in N_{test} quarter-hours i_{test} ($i_{test} = 1{:}\,N_{test}$). In this case, only the m predictors are fed to the model, which returns the prediction $Y_{jk}(i_{test})$. For this reason, all predictors must be computed with respect to values that are known in the moment of prediction.

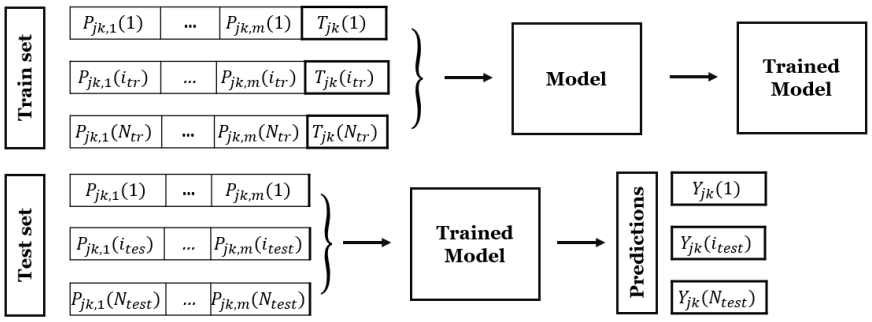

Figure 6.11 - Forecasting process.

Two families of predictors are used in this work:

- Label-type, which include the characteristics of the period in which the prediction is made. In this work, three label-type predictors are considered: (i) q, a number between 1 and 96 that represents the quarter-hour of the day; (ii) type of day (working day, pre-holiday and holiday); (iii) month.
- Endogenous-type, which include quantities computed starting from frequency, ACE and E_k^{15min} in periods that precede the prediction time. Examples are average values over the previous hours, difference between values or average values of previous hours. In principle, this family can be indefinitely broad. Therefore, only the main representative timeframes are considered (30 min, 1 h, 2 h, 4 h).

For the training set, endogenous-type predictors can be computed ex-ante starting from historical values. For the test set, they are calculated every time prediction is

made. Hence, in real-life applications the system must be able to collect frequency and ACE signals in order to feed the model. In this study, the training set is defined depending on availability of frequency and ACE data (*see Table 6.3*), while the test set is established based on the simulation period (13/03/2017-31/12/2017).

Table 6.3 – Training set and test set.

	Frequency	ACE
Training set	01/01/2015-12/03-2017	01/06/2015-12/03-2017
Test set	13/03/2017-31/12/2017	13/03/2017-31/12/2017

Another choice must be done: (i) feed the predicting model with the actual quarter-hour values E_k^{15min} and cumulate the quarter-hour predictions in order to obtain the six desired quantities Y_{jk} (ex-post elaboration); (ii) feed the predicting model with the actual quarter-hour values cumulated over the desired period and directly take the output given by the model (ex-ante elaboration). In this study, an ex-ante elaboration is adopted.

6.2.3 Statistical method

The statistical method is very simple: predictions are made considering the mean over the training period and standard deviations of the signals in the training period. No optimization procedure is necessary and the inputs for the multi-service model are:

$$Y_{jk} = \frac{1}{N_{train}} \sum_{i=1}^{N_{train}} T_{jk}(i) \tag{6.3}$$

$$std_{jk} = \sqrt{\sum_{i=1}^{N_{train}} \frac{(T_{jk}(i) - Y_{jk})^2}{N_{train}}} \tag{6.4}$$

Where N_{train} is the number of quarter hours in the training period.

Table 6.4 - Results of the statistical method.

Y_{1P}	Y_{2P}	$Y_{1S,+}$	$Y_{1S,-}$	$Y_{2S,+}$	$Y_{2S,-}$	
-0.002	0.003	0.569	-0.323	1.551	-0.924	[MWh]
std_{1P}	std_{2P}	$std_{1S,+}$	$std_{1S,-}$	$std_{2S,+}$	$std_{2S,-}$	
0.088	0.189	0.377	0.306	0.731	0.591	[MWh]

These values reflect some aspects previously mentioned. For instance, the regulating charging energy is higher with respect to regulating discharging energy related to the ACE (in both cases): this reflects the fact that the average of ACE is lower than 50 (see *Paragraph 6.1.2*). Y_{1P} and Y_{2P} are little because they take into account the net sum of positive and negative regulating energies.

6.2.4 Random Forest (RF)

The Random Forest is a Machine Learning algorithm, which can be adopted for time-series prediction. Its working principle is explained in *Paragraph 3.3.1*. For this method and for all the others considered in this study, predictors' choice and optimization of architecture's parameters is performed.

Minimum leaf size is chosen as stopping criterion when splitting a node (*see Paragraph 3.3.1*). Hence, the main RF architecture parameters are: (i) the number of decision trees in the forest; (ii) the minimum leaf size. A preliminary analysis shows that a number of trees higher than 100 does not lead to an appreciable improvement in performances and causes an increase in computational time. Moreover, the optimal value for minimum leaf size is found between 5 and 10. Therefore, 100 trees with minimum leaf size equal to 5 is the setup adopted in the following optimization process.

A peculiarity of Random Forest is the possibility to estimate the importance of predictors through a performance indicator that computes how many times those features are present in the decision nodes of the trees (i.e. Curvature test). The more a feature is used for splitting a node, the more relevant it is. An example is provided in *Figure 6.12*, in which the two most relevant predictors are highlighted.

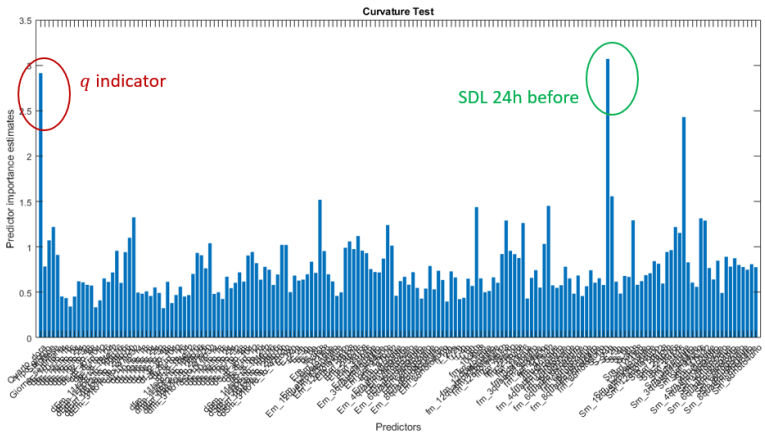

Figure 6.12 - Example of predictors' importance indicators.

In principle, the RF forecasting model can be fed with many predictors and less important ones can be gradually removed in order to keep only the most relevant ones. This process is summarized in *Figure 6.13*.

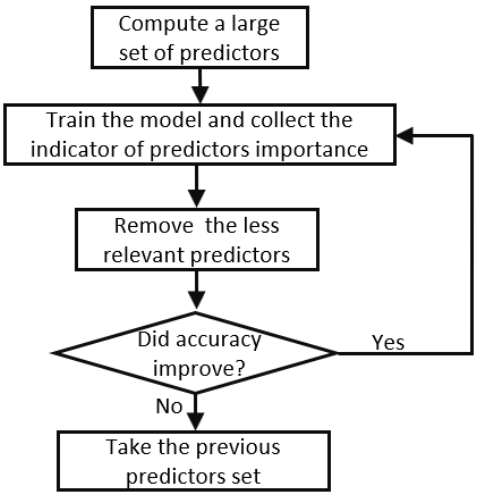

Figure 6.13 - Optimization of the number of predictors for Random Forest.

In this study, the initial set of predictors contains about 250 elements and about 40 are removed at each iteration. The optimal number of predictors is usually found between 90 and 180. Training set and test set periods are the same adopted for the Statistical method (*see Table 6.3*). Computational time for the train of the network depends on the number of predictors, number of leaves, number of trees and on the training period. Using 140 predictors, 100 trees, 5 leaf size and 2 years as training period this time is about 2 h. Once the algorithm is trained, the prediction is performed in few seconds.

6.2.5 NARX Neural Network

The memory ability of a NARX Neural Network makes it suitable for time-series prediction: not only past values of predictors, but also true or predicted past values of the time-series are used (as shown in *Paragraph 3.3.2*). In this study, the open loop architecture is adopted for building the predicting model because the true past values of the output time-series are available and it is faster than the closed loop architecture. Therefore, the quantity to be predicted in time step t depends on the predictors and on the true past values of the time-series in time steps $\{t - d_1, t - d_2, \dots, t - d_n\}$: in this case, input delays n_x and feedback delays n_y are the same ($n = n_x = n_y$). These delays are specified in the setup.

For what concerns this algorithm, the only parameter to be optimized is the net structure, that is the number of hidden layers and the number of hidden neurons per layer. For instance, a {10 10 5} configuration presents 3 hidden layers having respectively 10, 10 and 5 hidden neurons. The higher the complexity of the neural network, the greater the computational time. Not necessarily a complex network leads to more accurate results. Also in this case, a preliminary analysis is performed to assess the most performing configuration: {5}, {10}, {15} and {10 10} are identified.

The next step is the optimization of predictors and delays. The tool adopted for this assessment is *cross-correlation*: given two signals S_1 and S_2, it provides a degree of similarity of these signals as function of the delay applied to S_2. In case of discrete signals, it involves computation of covariances. A high input-output correlation means that the input has a significant effect on the output when a non-linear regression model, as NARX, is used. Hence, cross-correlation is applied in this study for evaluating which are the predictors that are best correlated to the signals to forecast and their respective delays, providing "one-shot" an information on both representative predictors and delays. Before using this tool, signals need to be normalized, otherwise differences in the order of magnitudes may affect the outcome, providing meaningless results.

Since the prediction in a given time step depends on the past values of predictors according to the delays, a shorter set should be chosen in order contain computational time (i.e. number of inputs is number of predictors times the number of delays). The process to identify the main predictors and delays is the following:

- Compute a large set of endogenous predictors starting from frequency, ACE and E_k^{15min}.
- Normalize predictors and signals to predict.
- Perform cross-correlation between predictors and the signal to predict in the training set (S_1 is E_k^{15min} if ex-post elaboration, Y_{jk} if ex-ante elaboration; S_2 is the predictor).
- For every predictor, list the most important delays considering the cross-correlation index.
- Collect all the predictors together with the ordered relevant delays and cross-correlation indexes in a table.
- Pick the most relevant predictors and delays to build the forecasting model.

It is possible to pick different sets of predictors and delays from the general table and compare their performances (e.g. a large set versus a more compact one). As for the Random Forest, a larger number of predictors does not necessarily imply a higher accuracy. A simulation campaign for evaluating the performances of the different sets of relevant predictors and delays with the aforementioned configurations {5}, {10}, {15} and {10 10} is performed.

The outcomes of this analysis are six NARX neural networks, one for each quantity to be predicted. The networks are trained considering all the available training set and they are used for predicting the quantities in the test period (*see Table 6.3 and Figure 6.14*).

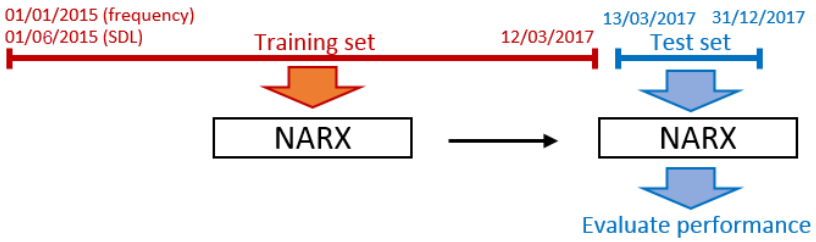

Figure 6.14 – Training and test set for NARX prediction.

In this way, peculiar patterns that refer to few days before the prediction may not be captured, since they are diluted in a large training set or belong to the test set. Hence, it may be interesting to evaluate the performance of the optimal nets found in this analysis by adopting a floating NARX over the test period and varying the depth of the training set. Also in this case computational time depends on number of predictors, number of delays, training period and complexity of the net architecture (i.e. number of hidden layers and neurons per layer). For a common setup adopted in this study (that is 20-30 predictors, 10-15 delays, 2 years of data and {10 10} configuration), this time is about 1 h, much less than Random Forest.

6.2.6 Floating NARX

Considering the optimal setup for the NARX neural network (in terms of predictors, delays and net configuration), a further step can be to adopt a floating NARX over the test period and evaluate the influence of the depth of the training period. In this case, more than six networks are created. In this study, for each quantity to be forecasted, one NARX neural network is built for predicting each day of the test period (13/03/2017-31/12/2017) considering n previous days as training period (i.e. 294 NARX for each quantity to be forecasted), as shown in *Figure 6.15*.

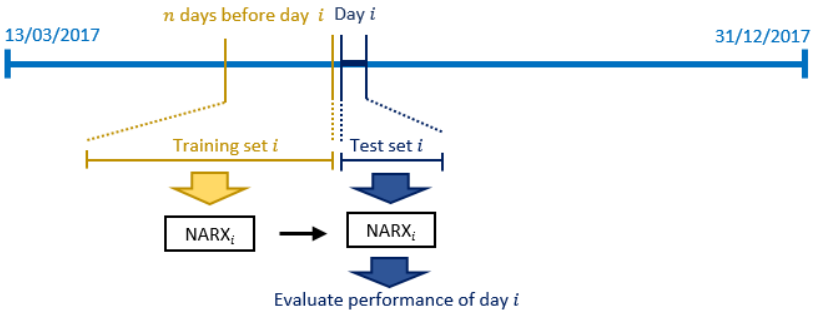

Figure 6.15 - Training and test sets for each day of the floating NARX prediction.

In particular, five configurations are investigated as depth of the training set: 5, 7, 10, 15 and 30 days. In any case, 7 days is found as optimal number of days for the training set. The final output of the floating NARX is an array including all the predictions in the period 13/03/2017-31/12/2017 for each quantity to be forecasted. Performance indicators are calculated starting from such arrays. Computational effort depends on the same parameters of NARX, but in this case the training period is few days: a single net (i.e. one day of prediction) is optimized in less than one minute.

6.2.7 Hybrid Approach

The Hybrid Approach uses all the previous forecasting methods to build a new one. The idea behind this method is to predict a particular period using the method that best performs in that time frame. Assuming to have M different prediction methods, the procedure is the following:

1. Predict the desired quantities in the period 12/03/2016-31/12/2016 (same period of the previous year) and calculate the prediction errors.
2. Separate the prediction errors by type of day t (working day, pre-holiday, holiday).
3. For each type of day t, calculate the standard deviation of the prediction errors per quarter of hour q. Three daily profiles of standard deviation are obtained.
4. A value of standard deviation is assigned to each quarter of hour in the test period (12/03/2017-31/12/2017) by extracting it from one of the three profiles calculated in the previous point depending on the type of day.

Once all the standard deviations profiles in the test period are obtained for all the M prediction methods, it is possible to implement the hybrid prediction. Two approaches are investigated to predict each time step in the test period i_{test}:

- Best Hybrid Prediction, in which the forecast is the prediction given by the method with the lowest standard deviation.
- Weighted Hybrid Prediction, in which the forecast is the weighted average of the predictions given by all the methods.

$$Y_{jk}^{hybrid}(i_{test}) = \frac{P_1(q,t) \cdot Y_{jk}^1(i_{test}) + \cdots + P_M(q,t) \cdot Y_{jk}^M(i_{test})}{P_1(q,t) + \cdots + P_M(q,t)} \tag{6.5}$$

  Weights are computed starting from a decreasing function of the standard deviation: the lower the standard deviation, the higher the weight associated to method *m* and vice versa. Different weight functions can be used: the exponential is adopted in this study.

In this analysis, only NARX and floating NARX neural networks are used in the Hybrid Approach because they are characterized by training errors that are comparable with test errors, so that weights are consistent. Conversely, test errors in RF are about twice the training errors and they cannot be used. *Figure 6.16* shows how the hybrid prediction is built in the two cases described before: (a) Best Hybrid Prediction and (b) Weighted Hybrid Prediction.

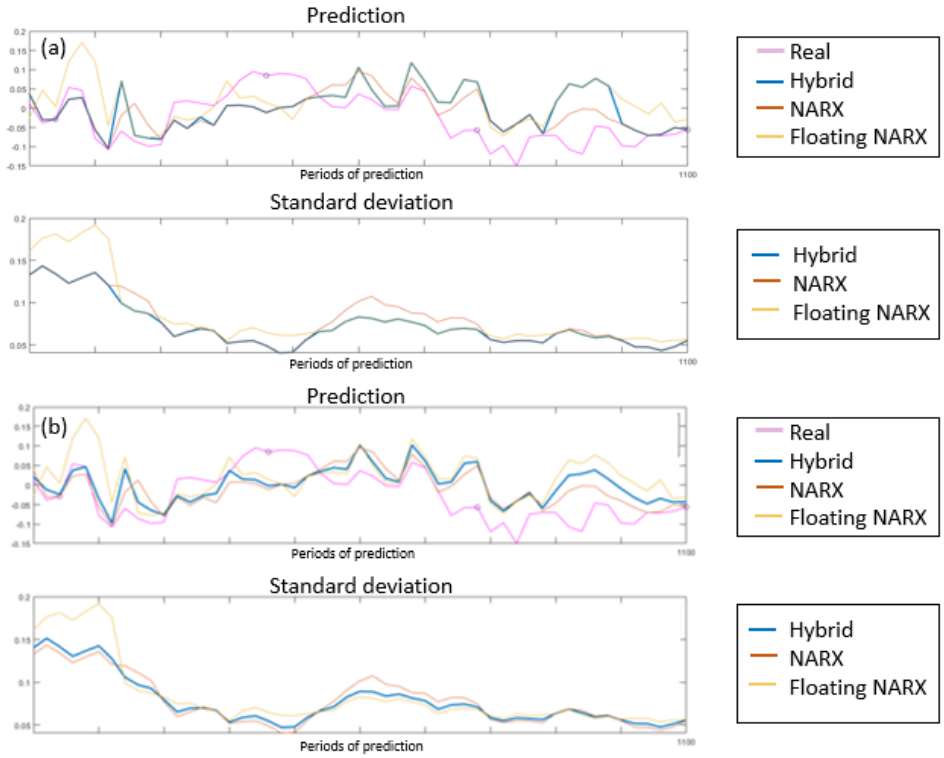

Figure 6.16 - Creation of Hybrid Approach: (a) Best Prediction; (b) Weighted Prediction.

In (a), the hybrid profile is superimposed to the best case between NARX and floating NARX. In (b), the hybrid profile is inside the band between NARX and floating NARX profiles. The Weighted Hybrid Prediction with exponential weight function performs better than the Best Hybrid Prediction for every Y_{jk} and its results are presented in the final comparison in the following Paragraph.

6.2.8 Performance comparison

Root Mean Squared Error (RMSE) is chosen as Key Performance Index (KPI) for forecasting method accuracy:

$$RMSE_{jk}^{m} = \sqrt{\sum_{i_{test}=1}^{N_{test}} \frac{(T_{jk}^{m}(i_{test}) - Y_{jk}^{m}(i_{test}))^2}{N_{test}}} \tag{6.6}$$

$RMSE_{jk}$ is the standard deviation of prediction errors of Y_{jk} (assuming a zero-mean Gaussian error distribution): the smaller this quantity, the more accurate the forecasting method, the better the SCR band management, since less uncertainty has to be managed. The reference is the statistical method, whose $RMSE$ is the actual standard deviation of results. The expected output for advanced forecasting methods should improve the statistical method (i.e. errors should be less dispersed).

Before showing the comparison among the methods, a last remark has to be done. Prediction errors belonging to the NARX neural network are not completely stochastic, but show a recognizable pattern. Therefore, a new strategy can be tested, which consists in correcting the predictions in each quarter of hour $Y_{jk}(i_{test})$ with the typical errors in the training set considering the type of day $\bar{e}_{jk}^{train}(q,t)$:

$$Y_{jk}^{with\ errors}(i_{test}) = Y_{jk}(i_{test}) + \bar{e}_{jk}^{train}(q,t) \tag{6.7}$$

This can be consistently done if error distributions in training and test sets are very similar: this occurs for the NARX (as shown is *Figure 6.17*), but not for RF, in which training errors are about a half of test errors. Also the floating NARX includes the typical errors of the training set, which change every day, and even in this case accuracy increases.

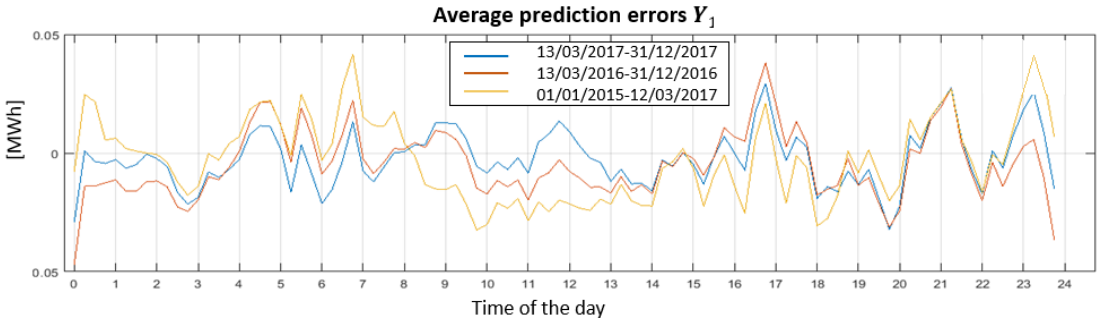

Figure 6.17 - Average daily errors for the prediction of Y_{1P} using NARX, comparing different datasets.

The final comparison among all the forecasting methods is reported in *Table 6.5*. The optimal setups for each single methods are different with respect to forecasted quantity (e.g. NARX predictors, delays and configuration for Y_{1P} are different from the ones for Y_{2P}) . The Reference is given by the standard deviation of the actual values T_{jk} in the test set. In particular, the RMSEs reported in *Table 6.5* are computed taking into account not all the N_{test} quarter of hour in the test period, but only the specific ones in which prediction is used to compute bands (i.e. every four hours). If the RMSE is lower than the standard deviation, it means that the forecasting method is better than forecasting with the mean. Optimization is carried out considering four quantities instead of six: Y_{1S} and Y_{2S} are the total regulating energies associated to ACE. Then, the optimal setup for Y_{1S} is used to obtain $Y_{1S,+}$ and $Y_{1S,-}$ to be used in the SCR band allocation function and the same is done for Y_{2S}.

Table 6.5 – Comparison among RMSEs of the different forecasting methods.

RMSE [MWh]	Standard Deviation	Random Forest	NARX	Floating NARX	Hybrid Approach	Improvement
Y_{1P}	0.1059	0.0962	0.0943	0.1076	**0.0900**	**15.10%**
Y_{2P}	0.2083	0.1912	0.1884	0.2385	**0.1773**	**14.93%**
Y_{1S}	0.6304	0.6003	0.5887	0.5947	**0.5451**	**13.53%**
Y_{2S}	1.1856	1.1425	1.1508	1.1536	**1.0807**	**8.85%**

All methods, except the Floating NARX, enhance the accuracy of prediction. The Hybrid Approach allows to improve NARX even with Floating NARX, whose performances are worse than the statistical prediction. This is a remarkable outcome, since it demonstrates that putting together multiple forecasting tools, even if not very accurate, could lead to a better instrument. Random Forest and NARX performances are very similar.

In this study, three datasets composed by 12 quantities (6 predictions and 6 standard deviations) are used in the multi-service provision model to feed the SCR band allocation function (*see Paragraph 4.3.1*):

1. Statistical dataset: it is very simple to implement; mean values and standard deviations are collected from the training set and are kept constant in the whole simulation period.
2. NARX neural network dataset: it is the best single forecasting tool.
3. Hybrid Approach dataset: it is the overall optimal forecasting method.

The results of multi-service provision by using the three aforementioned datasets are presented in following Section.

As final remark, *Table 6.6* collects average computational times and number of training needed for the optimization procedure of each one of the 6 quantities to forecast. Floating NARX setup has been optimized starting from the optimal case of simple NARX, hence its optimization required less effort.

Table 6.6 – Computational effort for forecasting methods optimization.

Prediction Method	Training Period	Computational effort	Number of trainings performed
RF	2 years	2 h	30
NARX	2 years	1 h	120
Floating NARX	7 days	Seconds	25

6.3 Multi-service: setup of simulations

In this Section, all the technical and economical parameters adopted in the simulations of multi-service provision are detailed.

The simulation period is 13/03/2017-31/12/2017, as stated in *Paragraph 6.2.2* (294 days). The frequency profile adopted in the simulation has been downloaded from the website of one of the German TSOs, 50Hertz Transmission GmbH [114]. ACE has been downloaded from Terna website [118].

Technical and economical setups regard both SCR and PCR. The technical setup adopted for PCR is the same shown in *Table 5.1* for single PCR provision, except for the PCR regulating band $\Delta\dot{P}_{PCR}$, which is fixed and equal to 50% the nominal power of the BESS (hence $droop_{BESS}$ is the double of the former case, *see equation* (2.6)).

Conversely, the SCR regulating bands, defined by the band allocation function in the SCR controller, change every 4 hours and the upper limit for both of them is 80% the nominal power of the BESS. The confidence level for multi-service controller is set to 95%, hence k_{CI} is 1,96. The EPR for initial comparison is set equal to 1 (i.e. nominal energy equal to 1 MWh). The technical setup of the simulations is summarized in *Table 6.7*.

Table 6.7 - Technical parameters for multi-service provision.

Technical parameters	Symbol	Value
Nominal power	P_{nom}	1 MW
Nominal energy	E_{nom}	1 MWh
Initial SoC	SoC_{start}	50%
SoC limits	SoC_{min}/SoC_{max}	0%/100%
Calendar ageing	-	12 years
Droop	-	0.15% (equivalent to 5%)
Dead band	DB	20 mHz
PCR regulating band	$\Delta\dot{P}_{PCR}$	50%
SCR regulating bands	$\Delta P_{SCR,+}$, $\Delta P_{SCR,-}$	Variable – max 80%
Normal score	k_{CI}	1.96 (referred to CI = 95%)

The economic parameters for PCR provision are the ones listed in *Table 5.2*, except for the prices of the energy traded for SoC restoration that are not present anymore. In this case, only the results obtained with the PCR remuneration mechanism adopted in the Central Western Europe area (i.e. German model), which is power-based and traded through a weekly auction, are shown. In particular, a single weekly price is used: it is set to 2500 €/MW per week, which is the average yearly value for PCR remuneration [117]. The results obtained with the Italian PCR retribution scheme are not shown because PCR provision is poorly remunerated, since it is mandatory, as demonstrated in *Paragraph 5.2*. Instead, SCR retribution is mainly inspired on the Italian framework (pay-as-bid and energy based): there are 6 market sessions per day of 4 hours each. The only difference is represented by the possibility to have asymmetric SCR bands, as already happens in Germany: in this case, SCR band allocation can be used as a SoC restoration technique (*see Paragraph 4.3.1*). In this study, an assumption is made: the SCR bands defined by the controller are always accepted on the market at the average hourly price bid for both positive and negative secondary reserves [115]. A price allocation strategy is a possible direction for further researches. The economic valorization of the energy not provided (LoR) is set to 150

€/MWh in all the simulations. These remarks lead to a hybrid market structure that nowadays is not present in any market, but it is built starting from two different European paradigms.

Table 6.8 - Economic parameters adopted in the simulations of multi-service provision.

Economic parameters	Symbol	Value
Investment horizon	N	20 years
Actualization rate	r	6%
Specific BESS cost	c_{BESS}	400 €/MWh
Replacement factor	k_{rep}	0.5
German PCR remuneration	p_{GER}	2500 €/MW per week
SCR remuneration	$p_{SCR,+}$, $p_{SCR,-}$	Variable (average hourly prices)
LoR valorization	p_{LoR}	150 €/MWh

6.4 Multi-service: results of simulations

In this Section, the numerical results of the simulations of multi-service provision are presented. In *Paragraph 6.4.1*, the results obtained using different forecasting methods (Statistical, NARX, Hybrid) in the SCR band allocation function are shown. Then, a sensitivity analysis on EPR is done in order to further optimize the strategy and evaluate the impact of this quantity on the outcomes (*Paragraph 6.4.2*). In *Paragraph 6.4.3*, the results of the ideal No-error Prediction are shown and compared with the ones obtained in the optimal configuration. In the No-error Prediction case, the prediction is the real value of regulating energy required in next periods and the standard deviations are null. Time spent on computation for 294-day period has been 12 h using the same computational tool adopted for single service simulations (Intel® Core™ i7 4790–16GB RAM).

6.4.1 Forecasting methods comparison

The results of multi-service provision obtained using different forecasting methods in the SCR band allocation function are shown in *Table 6.9*. The reference case is single PCR provision considering 100% PCR regulating band. All the results are rescaled on a monthly basis.

Table 6.9 - Results for multi-service: reference case and forecasting methods' comparison.

	Reference	Statistical	NARX	Hybrid
Total energy ($E_{out,sys}$) [MWh/month]	59.4	89.8	95.9	95.2
PCR energy required ($E_{req,PCR}$) [MWh/month]	70.1	35.0	35.0	35.0
SCR energy required ($E_{req,SCR}$) [MWh/month]	-	66.8	73.4	72.1
Cycles ($cycles_{tot}$) [#/month]	30.1	43.7	46.7	46.3
Average C-rate [1/h]	0.241	0.124	0.133	0.132
Cell efficiency ($\eta_{E,cell}$) [%]	94.2	97.6	97.4	97.5
System efficiency ($\eta_{E,sys}$) [%]	83.7	80.7	81.4	81.3
LoR [%]	20.9	3.3	2.8	2.2
LoR_{PCR} [%]	20.9	4.4	3.5	2.8
LoR_{SCR} [%]	-	2.8	2.5	1.9
BESS lifetime ($life_{BESS}$) [years]	12.8	10.6	9.8	9.9
NPV [k€]	719.3	517.0	551.0	558.9
PBT [years]	4.5	5.4	5.1	5.1

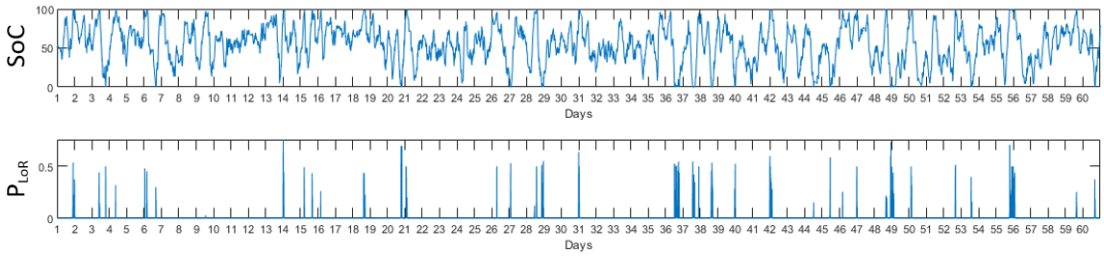

Figure 6.18 - Zoom on the first 60 days of simulation of multi-service provision with the Hybrid Approach: SoC and P_{LoR}.

By analysing *Table 6.9*, $E_{out,sys}$ is always different from the sum of $E_{req,PCR}$ and $E_{req,SCR}$: this occurs due to the presence of the efficiency of the battery, LoR and the fact that power set points of PCR and SCR do not always have the same sign. The results of the reference case are very similar to the ones belonging to the base case in *Chapter 5 (see Table 5.3)*, as expected: all the setup parameters are the same, except for the simulation period. The outcomes of multi-service provision are similar for all the forecasting methods. This happens for two reasons: (i) the best improvement in prediction KPI is equal to 15% (as shown in *Table 6.5*); hence, the multi-service controller allocates similar SCR bands for all the methods; (ii) PCR still plays a major role in energy fluxes and remuneration. Nevertheless, multi-service provision is able to achieve some interesting outcomes. Firstly, the overall amount of energy fluxed by the battery in a month increases by about 30% with respect to the base case: BESS

operation is more effective in terms of services provided. Moreover, LoR decreases to acceptable levels (around 2-3%) with respect to single service provision. In all the cases, the C-rate is lower than single service provision even if the overall energy cycled by the BESS increases: this means that battery works more often, lowering the amount of time in which it is idle. The cell efficiency is very high and the gap with the system efficiency is due to presence of the inverter efficiency, which is very low for small C-rate values. In general, the best results among the three forecasting methods are obtained for the Hybrid Approach: the increase in the accuracy of prediction (*see Table 6.5*) brings to a better SCR band management system in terms of LoR and NPV.

For what concerns revenues, more details are provided. In the Hybrid Approach, monthly net revenues are 7938 €: 5536 € come from PCR provision (equal for all the multi-service cases since the PCR band is the same), 2760 € come from SCR provision and 358 € are the LoR penalties. In single PCR provision, monthly net revenues are doubled with respect to the multi-service case because 100% of PCR band is allocated (11072 €), but LoR penalties are much higher (2201 €). Nevertheless, even if LoR penalties are very high, the NPV in the reference case is greater than the one in the Hybrid Approach due to the higher net profits. Due to the high LoR value (20.9%), the single PCR provision would suffer a possible increase of LoR valorization that would decrease the overall NPV. Regarding BESS lifetime, it is higher in the base case because it is characterized by a lower number of cycles per month: the impact of cycles on lifetime is larger than the one given by the C-rate.

Figure 6.19 shows the working principle of the SCR controller with asymmetric band allocation for the Hybrid Approach:

- When the SoC is close to 100%, the controller defines a large discharge band ($\Delta P_{SCR,+}$) and a low charge band ($\Delta P_{SCR,-}$).
- When the SoC is close to 0%, the controller defines a low discharge band ($\Delta P_{SCR,+}$) and a large charge band ($\Delta P_{SCR,-}$).
- When the SoC is close to 50%, similar bands are defined.

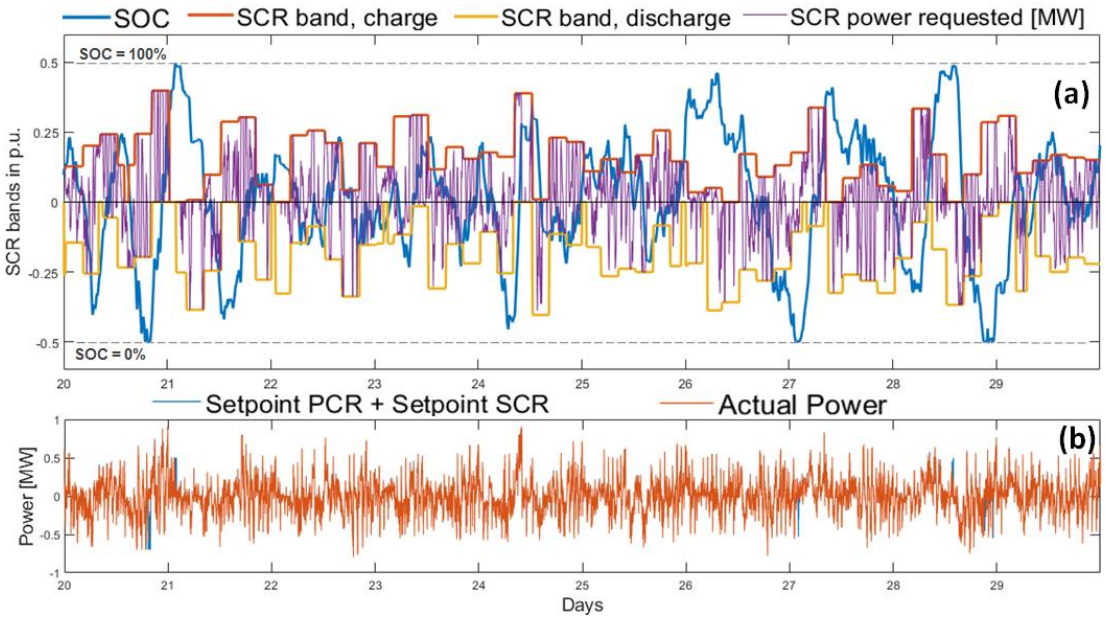

Figure 6.19 – Zoom on 10 days of simulation of multi-service provision with the Hybrid Approach: (a) SCR band management; (b) total required and actual power.

By looking at *Figure 6.19 - (a)*, the behavior is coherent with the expected one. For instance, in day 26 the SoC is close to the upper limit and the SCR controller allocates a large discharge band (in yellow) and a small charge band (in red), thus avoiding saturation. Moreover, the real SCR power (in violet) is enclosed in the area defined by the two SCR band profiles: this is because the real power depends on the value of the ACE, which represents the percentage of SCR band required by the TSO (*see equation (4.37) in Paragraph 4.3.1*). In *Figure 6.19 - (b),* the total power profile required by the two services (in blue) and the actual power profile delivered by the BESS (in red) at the grid side are represented. They are always superimposed, except when SoC saturation limits are reached and LoR occurs.

6.4.2 Sensitivity analysis on EPR

In this Paragraph, a sensitivity analysis on the EPR is performed starting from the optimal configuration found in the previous Paragraph: multi-service provision with the Hybrid prediction approach. In this analysis, the nominal power of the BESS is assumed constant to 1 MW. Therefore, varying the EPR means varying the nominal energy of the BESS. The values of EPR that have been investigated are: 0.5, 0.75, 1, 1.25, 1.5, 1.75 and 2. In this case, a further economic index is considered to compare investments of different sizes: the Profitability Index (*see Chapter 4*). The results are shown in *Table 6.10*.

Table 6.10 - Results of multi-service (Hybrid Approach): sensitivity analysis on the EPR.

EPR	0.5	0.75	1	1.25	1.5	1.75	2
$E_{out,sys}$ [MWh/month]	55.4	76.7	95.2	113.3	131.3	148.9	166.1
$E_{req,PCR}$[MWh/month]	35.0	35.0	35.0	35.0	35.0	35.0	35.0
$E_{req,SCR}$ [MWh/month]	26.7	51.3	72.1	92.1	111.6	130.6	149.0
$cycles_{tot}$ [#/month]	53.8	49.7	46.3	44.2	42.7	41.6	40.7
Average C-rate [1/h]	0.176	0.143	0.132	0.125	0.120	0.117	0.114
$\eta_{E,cell}$ [%]	95.7	97.0	97.5	97.7	97.9	98.0	98.0
$\eta_{E,sys}$ [%]	75.0	78.4	81.3	83.5	85.1	86.3	87.2
LoR [%]	5.0	2.8	2.2	1.9	1.7	1.6	1.5
LoR_{PCR} [%]	7.2	3.9	2.8	2.3	1.9	1.6	1.5
LoR_{SCR} [%]	2.2	2.1	1.9	1.8	1.7	1.6	1.5
$life_{BESS}$ [years]	7.9	9.1	9.9	10.5	10.9	11.3	11.6
NPV [k€]	509.1	550.5	558.9	566.1	563.2	568.4	561.2
PBT [years]	3.3	4.2	5.1	5.9	6.5	7.1	7.7
PI	2.69	2.27	1.97	1.90	1.74	1.65	1.56

The energy required by the PCR is equal in all cases, being nominal power and PCR regulating band constant. Differences in energy fluxes are determined by the energy required by SCR, which increases together with EPR: this happens because the BESS has a higher capacity and larger SCR bands are defined by the SCR controller. BESS lifetime increases from 7.9 to 11.6 years when the EPR increases: both the number of equivalent cycles per month and the average C-rate decrease, leading to a lower stress for the battery. The efficiencies show an interesting behavior: the gap system-cell efficiency, which is due to the efficiency of the inverter, decreases with the increase of EPR. The reason of this lies in the fact that the nominal power of inverter is set equal to nominal power of the BESS and its efficiency is a function of power in per unit (*see Figure 4.6*). Conversely, C-rates refer to the nominal capacity, which is proportional to the nominal energy of the BESS. Therefore, similar C-rates at different EPR imply different powers. In particular, the higher the EPR, the higher the power, the higher the inverter efficiency, the lower the aforementioned gap. The impact of this issue is an efficiency gap that passes from 20% (at low EPR values) to 10% (at high EPR values). For what concerns LoR, it decreases when the EPR increases (from 5% to 1.5%): the asymmetric SCR band allocation has a positive effect on SoC restoration (the higher the energy required by SCR, the lower the LoR). This behavior is shown *Figure 6.20* and in *Figure 6.21-(a)*.

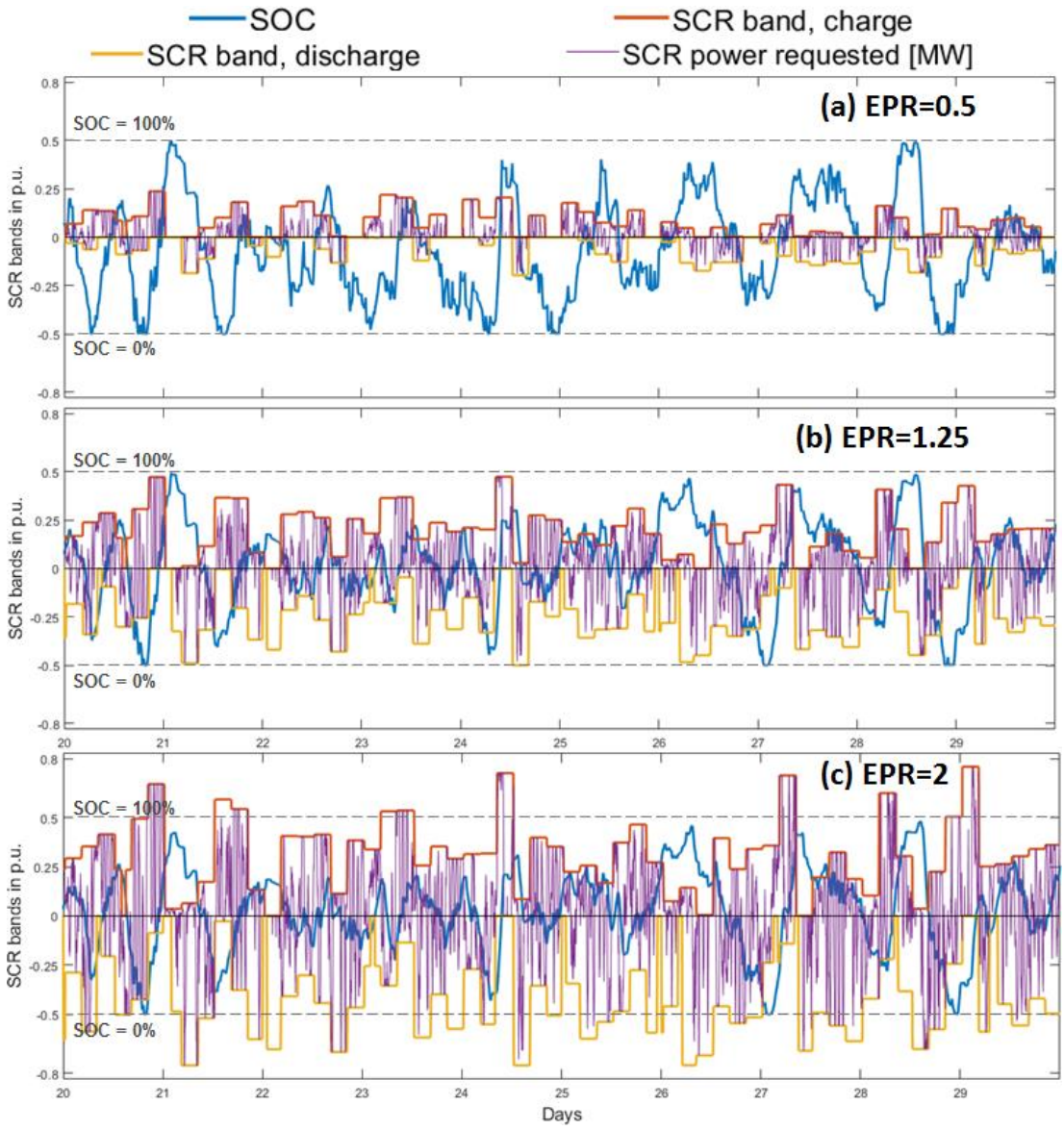

Figure 6.20 - SCR band management considering EPR equal to: (a) 0.5; (b) 1.25; (c) 2.

By analysing *Figure 6.20,* SCR bands almost reach their upper limit (i.e. 0.8 p.u.) when EPR is equal to 2, while at lower EPR values the SCR regulating bands are much smaller. This means that SCR has less potential to restore the SoC at low EPR.

For what concerns the economical parameters, NPV and PI as function of the EPR are reported in *Figure 6.21-(b)*. The NPV are quite similar despite the big difference in the initial investment costs (200 k€ at EPR 0.5 vs. 800 k€ at EPR 2): this increase in investment costs is paid back by the energy-based SCR remuneration, which rewards the higher fluxes. The PI instead captures the effect of the different sizes of the investment and shows large differences (it varies between 2.69 at EPR 0.5 and 1.56 at EPR 2). Therefore, the optimal value of EPR is in the range 1-1.25, which are

characterized by low LoR, high NPV and intermediate PI. For these reasons, in the following Paragraph, EPR equal to 1 is considered for a comparison with the results obtained in case of no-error prediction.

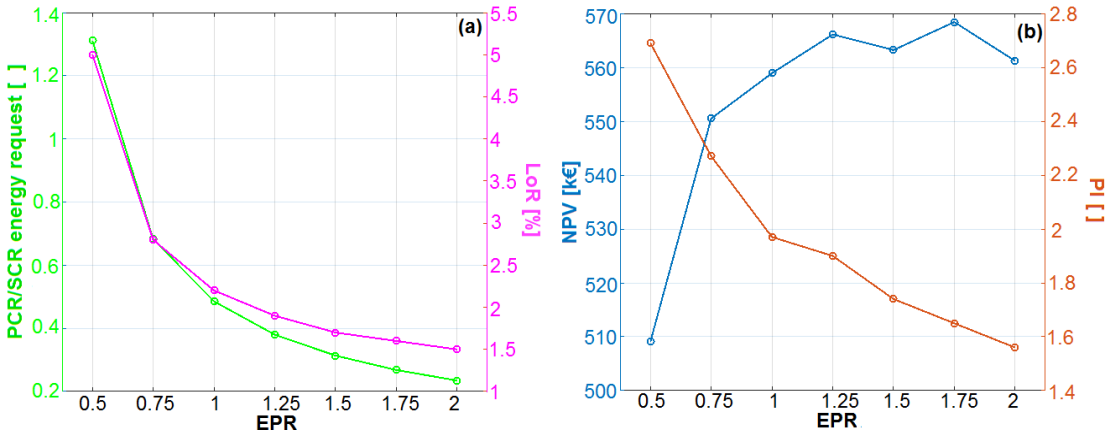

Figure 6.21 – (a): PCR/SCR energy request and LoR; (b): NPV and PI.

6.4.3 No-error Prediction

In this Paragraph, the results of multi-service provision considering the Hybrid forecasting approach and EPR=1 are compared with the ones obtained adopting a "no-error" prediction. No-error Prediction means that the MATLAB® function in the SCR controller is fed with the six actual values of regulating energy and no standard deviations (i.e. Y_{1P}, Y_{2P}, $Y_{1S,+}$, $Y_{1S,-}$, $Y_{2S,+}$ and $Y_{2S,-}$ are no more predictions, but actual values and $std_{1P} = std_{2P} = std_{1S,+} = std_{1S,-} = std_{2S,+} = std_{2S,-} = 0$). The aim of this Paragraph is to provide an ideal case that could possibly motivate further researches in the matter of frequency, ACE and regulating energy prediction. The results are shown in *Table 6.11* and *Figure 6.22* reports the different SCR band management.

Since standard deviations are null (i.e. no confidence interval is applied to them), SCR regulating bands are very large and they often reach the saturation limit (i.e. 0.8 p.u.). Therefore, energy fluxes remarkably increase in case of No-error Prediction: the total energy is about the double with respect to the one in case of Hybrid prediction. For what concerns LoR, it is not null because the SCR controller does not take into account the complete SoC profile, but only the final value at the end of the successive market session. Hence, during the market session, it is possible to have SoC saturation due to particular combinations of frequency-ACE patterns. Therefore, LoR is very similar to the one obtained in case of Hybrid prediction (around 2%).

Table 6.11 – Comparison of the results of multi-service provision between Hybrid and No-error Prediction.

	Hybrid	No-error Prediction
Total energy ($E_{out,sys}$) [MWh/month]	95.2	166.0
PCR energy required ($E_{req,PCR}$) [MWh/month]	35.0	35.0
SCR energy required ($E_{req,SCR}$) [MWh/month]	72.1	150.3
Cycles ($cycles_{tot}$) [#/month]	46.3	80.8
Average C-rate [1/h]	0.132	0.225
Cell efficiency ($\eta_{E,cell}$) [%]	97.5	96.1
System efficiency ($\eta_{E,sys}$) [%]	81.3	85.5
LoR [%]	2.2	2.6
LoR_{PCR} [%]	2.8	2.1
LoR_{SCR} [%]	1.9	2.7
BESS lifetime ($life_{BESS}$) [years]	9.9	4.9
NPV [k€]	558.9	717.4
PBT [years]	5.1	3.6

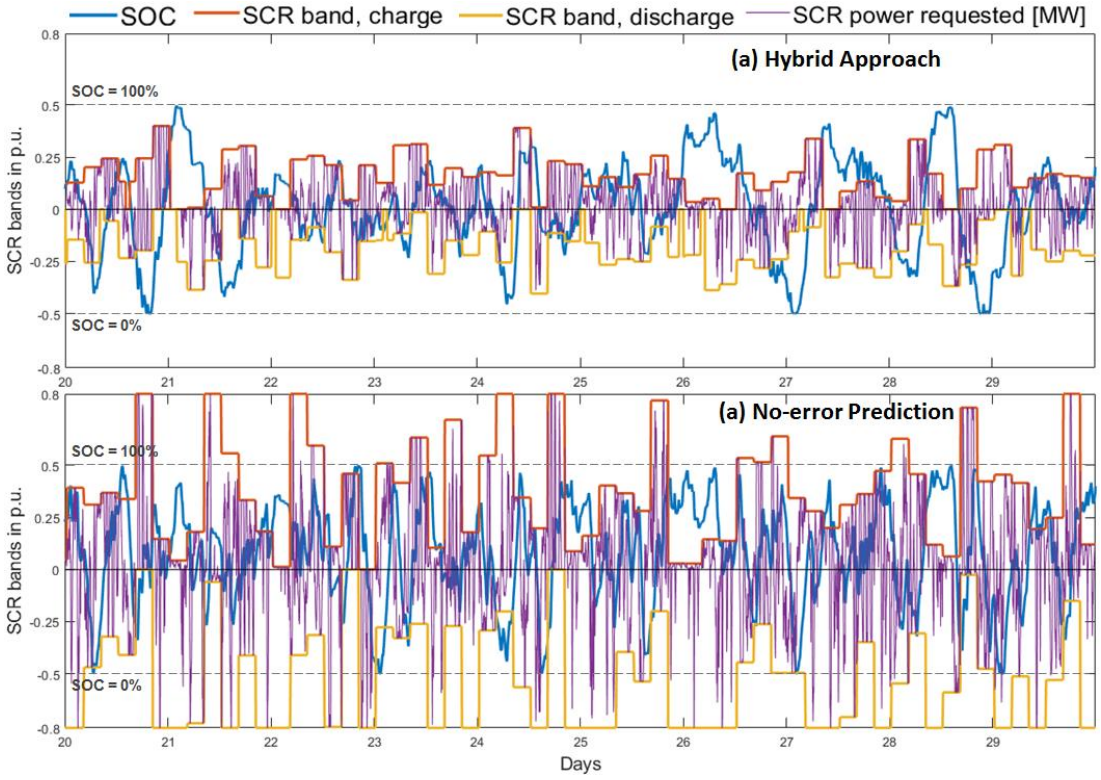

Figure 6.22 - SCR band management at EPR 1 considering: (a) Hybrid Approach; (b) No-error Prediction.

This outcome shows that the working principle of the SCR controller is actually able to exploit the improved accuracy of predictions without negative impacts on LoR, making the investment more profitable. Regarding the economic results, the No-error Prediction generates a higher NPV and a lower PBT since more energy is cycled by the BESS and a higher remuneration of SCR is obtained. Nevertheless, multi-service provision considering the Hybrid prediction method is able to reach good results in economic terms: the NPV is about the 75% of the one obtained with the No-error Prediction. Results open fruitful possibilities in the improvement of prediction accuracy, investigating different forecasting techniques and different type of predictors with respect to the ones used in this work.

CONCLUSION

In this work, the ability of a Battery Energy Storage System (BESS) in providing frequency services to the electrical network has been investigated in the framework of the Ancillary Services Market (ASM). In particular, two services have been analysed: Primary Control Reserve (PCR) and Secondary Control Reserve (SCR). For what concerns PCR retribution, two ASM paradigms have been considered: the Italian and the Central Western Europe mechanism (i.e. German). Conversely, SCR retribution has been evaluated considering the general Italian ASM framework, with the only exception of being able to have asymmetric SCR bands, as already happens in Germany.

The analysis has been performed in two directions. At first, single service provision of PCR has been analysed. Different State of Charge (SoC) management techniques have been investigated and a sensitivity analysis has been performed on the main parameters of the best strategy.

Afterwards, multi-service provision of PCR and asymmetric SCR has been treated. In this case, a novel energy management system has been implemented: asymmetric SCR regulating bands are allocated taking into account the results of advanced forecasting techniques. The outcomes of the simulations of multi-service provision adopting different predicting tools have been compared and a sensitivity analysis has been performed on the Energy-to-Power Ratio (EPR) for the best forecasting approach.

This study involves many broad and complex fields and requires a comprehensive analysis. For this reason, before showing all the results of the simulations, a literature review of the main topics has been provided in the first chapters:

1. Battery Energy Storage Systems: electrochemical phenomena inside the cell, Lithium-ion battery technologies and battery models have been presented.
2. Ancillary Services Market: frequency regulation services, Italian and German ASM paradigms for PCR and SCR, future scenarios and BESS exploitation in the ASM have been described.

3. Predictive analytics: the forecasting process, evaluation metrics, the main predictive models for time-series and the application of forecasting techniques with BESS have been discussed.

A large part of this work (*Chapter 4*) has been dedicated to the presentation of the methodology and the models adopted, useful to understand the results of the simulations presented in the last two chapters. All the simulations and the models have been implemented in a MATLAB®-Simulink™ environment.

The main outcomes for single PCR provision are summarized in the following list:

- PCR provision adopting the Italian remuneration scheme is absolutely not convenient (i.e. the NPV is lower than zero). This is because, nowadays, in Italy PCR provision is poorly remunerated since it has been designed as a mandatory service for Relevant Production Units (i.e. the remuneration logic in place today is devoted to reimburse traditional power plants for the market costs due to the provision of the service). On the contrary, the German PCR remuneration scheme (i.e. power-based, weekly auction) is profitable and generates a positive NPV after 20 years.
- The implementation of any SoC restoration strategy causes an increment of the total energy cycled by the BESS and an enhancement of both technical and economic performances: LoR is strongly reduced with respect to standard PCR provision (i.e. fixed Droop Control Law) and the NPV increases in all the cases. SoC restoration without service interruption is identified as the optimal strategy because it shows a high NPV and a LoR close to zero (it does not suffer a possible increase of LoR valorization). The optimization of the main parameters of this strategy allows to obtain better results.

In the following lines, the main outcomes of multi-service provision are reported:

- A statistical analysis of frequency and Area Control Error is useful to identify the main patterns of these signals to be used in the definition of the predictors for the forecasting models.
- In all the cases analysed, the asymmetric SCR band allocation works as a “passive” SoC restoration strategy: it keeps the SoC far from its saturation limits and LoR is strongly reduced with respect to the single standard PCR provision (from 21% to 2-3%).

- The utilization of advanced forecasting techniques in the SCR band allocation function allows to improve the performances with respect to the standard statistical case. In particular, the best results are obtained with the predictions given by the Hybrid neural network (i.e. lowest LoR and highest NPV).
- The sensitivity analysis on EPR in case of multi-service provision with the Hybrid prediction approach shows that an increase of EPR causes an increase of the total energy cycled by the BESS due to the larger bands defined by the SCR controller. Moreover, a large EPR brings to a low LoR. The NPV does not change much when increasing the EPR, while the PI decreases.
- The ideal case of No-error Prediction shows that the working principle of the SCR controller is able to exploit more accurate forecasts, since the lower uncertainty determines higher energy fluxes that are not paid in terms of LoR.

Regarding the BESS model considered in this study, two are the main limitations: (i) the behavior of a single cell is considered as representative of the entire battery pack (i.e. the power set point of the BESS are rescaled to the cell level); (ii) auxiliaries' electric consumption is not modelled. For what concerns multi-service provision model, the main simplification regards the fact that SCR bands are always accepted on the market.

Possible directions for future researches on this topic could be:

1. To include the effect of auxiliaries and other BESS components in the model.
2. To develop a price allocation strategy for the SCR market.
3. To improve the accuracy of predictions by adopting different forecasting techniques.
4. To couple a BESS providing grid services with other applications, such as domestic or PV plant, to improve the operation and/or increase the economic return of such application.

APPENDIX A

Data sheet of the Li-ion cell adopted in the study: Boston Swing 5300

Type	Lithium ion (Rechargeable) Lithium - LiNMC
Model	Swing5300
Configuration	1S 1P
Nominal Voltage	3.65V
Capacity*	Nominal: 5.3Ah Typical: 5.3Ah Minimum: 5.3Ah *:Standard discharge 0.2C to 2.75 V
Nominal Eenrgy	19.3Wh
Energy Density	490Wh/l
Energy Gravimetric	207Wh/kg
Service Life	>1000 cycles : (100% DOD) >2000 cycles : 90% DOD) >3000 cycles : 80% DOD)
Internal Resistance	15.5mOhm
Charge Mode	Standard charging method: - Constant current (CC) 3.7A (0.7C) to 4.2V - Constant voltage (CV) 4.2V to 50 mA
Charge Voltage	4.2
Max. Charge Current	10.6A
Discharge Cutoff Voltage	2.75V
Max. Discharge Current	Continuous: 13A Pulsed: 10A Allowable 10s pulse capability (0% to 50%DOD): 1000W/Kg
Weight	Approx. 93.5g
Dimensions	Heigth = 64.80mm Length = 37.30mm Width = 19.00mm
Container/Housing	Aluminium
Temperature Range	Charge: -20 ~ 60 °C Discharge: -40 ~ 70 °C Storage: -40 ~ 60 °C

APPENDIX B

In the context of this research, the foundations for a future collaboration between Politecnico di Milano and the Joint Research Centre - JRC in Ispra (VA) have been laid. In particular, the BESS in the JRC Smart Grid Interoperability Laboratory – SGILab (Li-ion, 500kWh/250kW [129]) could represent a matter of interest for the purposes of this study.

Fig. A – BESS at the SGILab of JRC in Ispra (VA) [130].

Two technical meetings have been held during the work:

Day	Main topics
01/08/2018	Preliminary meeting in which the aim of the thesis has been introduced. The Smart Grid Lab has been visited, with particular focus on the BESS.
18/12/2018	The results of the analysis of single service provision and the future steps of the study have been presented. A second visit to the Smart Grid Lab has been performed.

A third meeting is planned on 12th April 2019 in which the final results of the research are going to be shown and proposals for further researches in this field are going to be made.

In case of a future collaboration with the JRC, a fruitful research path could be the experimental validation of a numerical model of the BESS present in the SGILab, which includes also the effects of real auxiliaries. Such a BESS model could be integrated in the overall model proposed in this work in order to provide more generalizable results.

LIST OF FIGURES

LIST OF TABLES

LIST OF ACRONYMS

AC	Alternate Current
ACE	Area Control Error
AI	Artificial Intelligence
ANN	Artificial Neural Network
ARIMA	Autoregressive Integrated Moving Average
ARMA	Autoregressive Moving Average
AS	Ancillary Services
ASM	Ancillary Services Market
BESS	Battery Energy Storage System
BMS	Battery Management System
BoL	Beginning of Life
BSP	Balance Service Provider
CAES	Compressed Air Energy Storage
CART	Classification And Regression Trees
CES	Chemical Energy Storage
CQ	Clearing Quantity
CrES	Cryogenic Energy Storage
CWE	Central Western Europe
DAM	Day-Ahead Market
DB	Dead Band
DC	Direct Current
DER	Distributed Energy Resources
DG	Distributed Generation
DoD	Depth of Discharge
DP	Double Polarization
DR	Demand Response
EES	Electrical Energy Storage
EFR	Enhanced Frequency Response
EHV	Extra-High Voltage
EIS	Electrochemical Impedance Spectroscopy
EMES	Electro-Magnetic Energy Storage
ENTSO-E	European Union of Transmission System Operators for Electricity
EoL	End of Life
EPR	Energy to Power Ratio
ESS	Energy Storage System
EV	Electric Vehicle
FACTS	Flexible Alternating Current Transmission System
FB	Flow Battery
FES	Flywheel Energy Storage
GA	Genetic Algorithm

GME	Gestore dei Mercati Energetici
HTES	High Temperature Energy Storage
HV	High Voltage
IDM	Intra-Day Market
KDD	Knowledge Discovery in Databases
KPI	Key Performance Indicator
LCO	Cobalt-Oxide Li-ion battery
LFP	Iron-Phosphate Li-ion battery
Li-ion	Lithium-ion battery
LMO	Manganese-Oxide Li-ion battery
LoR	Loss of Regulation
LTO	Titanium-oxide Li-ion battery
LV	Low Voltage
MAE	Mean Absolute Error
MB	Mercato di Bilanciamento
MCP	Marginal Clearing Price
MES	Mechanical Energy Storage
ML	Machine Learning
MSD	Mercato dei Servizi di Dispacciamento
MV	Medium Voltage
NARX	Non-linear Autoregressive Exogenous
NCA	Nichel-Cobalt-Alluminium-Oxide Li-ion battery
NCF	Net Cash Flow
NMC	Nickel-Manganese-Cobalt-oxides Li-ion battery
NPS	New Policies Scenario
NPV	Net Present Value
OCV	Open Circuit Voltage
PBT	Payback Time
PCR	Primary Control Reserve
PFR	Primary Frequency Regulation
PHS	Pumped Hydro Storage
PI	Profitability Index
PV	Photovoltaic
PX	Power Exchange
RES	Renewable Energy Sources
RF	Random Forest
RG	Regional Group
RMSE	Root Mean Square Error
RPU	Relevant Production Unit
RV	Residual Value
SCES	Supercapacitor Energy Storage
SCR	Secondary Control Reserve
SDGs	Sustainable Development Goals
SEI	Solid Electrolyte Interface

SEM	Scanning Electron Microscope
SFR	Secondary Frequency Regulation
SMES	Superconducting Magnetic Energy Storage
SoC	State of Charge
SoE	State of Energy
SoH	State of Health
SVM	Support Vector Machine
TCR	Tertiary Control Reserve
TES	Thermal Energy Storage
TFR	Tertiary Frequency Regulation
TSO	Transmission System Operator
UPS	Uninterruptible Power Supply
UVA	Unità Virtuali Abilitate
UVAC	Unità Virtuali Abilitate di Consumo
UVAM	Unità Virtuali Abilitate Miste
UVAN	Unità Virtuali Abilitate Nodali
UVAP	Unità Virtuali Abilitate di Produzione
UVRP	Unità per la Verifica della Regolazione Primaria

References

[1] IEA, “World Energy Outlook 2018”.

[2] IRENA, “Renewable Capacity Statistics 2018”.

[3] X. Luo, J. Wang, M. Dooner and J. Clarke, “Overview of current development in electrical energy storage technologies and the application potential in power system operation”, Appl. Energy, vol. 137, pg. 511–536, 2015.

[4] O. Krishan, S. Suhag, “An updated review of energy storage systems: Classification and applications in distributed generation power systems incorporating renewable energy resources”, International Journal of Energy Research 2018, pg. 1-40, Nov 2018.

[5] C. Brivio, “Battery energy storage systems: Modelling, Applications and Design criteria”, 2017.

[6] Bloomberg New Energy Finance (BNEF), “New Energy Outlook 2017”, 2017.

[7] Sandia, “Doe Global Energy Storage Database”, 2016.

[8] J.H. Eto et al., “Use of Frequency Response Metrics to Assess the Planning and Operating Requirements for Reliable Integration of Variable Renewable Generation”, Dec 2010.

[9] G. Rancilio, “Battery Energy Storage Systems for Ancillary Services Provision”, 2018.

[10] Terna, “Progetti pilota di accumulo” [Online]. Available: https://www.terna.it/it-it/sistemaelettrico/progettipilotadiaccumulo.aspx.

[11] E. Namor, F. Sossan, R. Cherkaoui, M. Paolone, “Control of Battery Storage Systems for the Simultaneous Provision of Multiple Services”, IEEE Transactions on Smart Grid, 2018.

[12] M. Benini, S. Canevese, D. Cirio, A. Gatti, “Battery Energy Storage Systems for the Provision of Primary and Secondary Frequency Regulation in Italy”, 2016 IEEE 16th International Conference on Environment and Electrical Engineering (EEEIC), Jun 2016.

[13] K. Counsell, L. Evans, “Day-Ahead Electricity Markets: Is There a Place for a Day-Ahead Market in the NZEM?”, New Zealand Institute for the study of Competition and Regulation Inc., 2003.

[14] NPTEL, Electrical engineering, Restructured Power Systems, “Market Architecture” [Online]. Available: https://nptel.ac.in/courses/108101005/17.

[15] GME, Gestore dei Mercati Energetici, “Mercato elettrico a pronti (MPE)” [Online]. Available: http://www.mercatoelettrico.org/it/Mercati/MercatoElettrico/MPE.aspx.

[16] C. Bovo, “The Italian Electricity Market”, Slides of the course *Electricity Market*, Politecnico di Milano, 2016.

[17] A. Gonzalez-Aparicio, A. Zucker, “Impact of Wind Power Uncertainty Forecasting on the Market Integration of Wind Energy in Spain”, Applied Energy, n. 159, pg. 334-349, 2015.

[18] H. Holttinen, J. Kiviluoma, N. Cutululis, A. Gubina, A. Keane, F. Van Hulle, “Ancillary services: technical specifications, system needs and costs”, DTU, Dec 2012.

[19] European Commission, “Commission Regulation (EU) 2016/631 of 14 April 2016 establishing a network code on requirements for grid connection of generators”, Official Journal of the European Union, 2016.

[20] ENTSO-E, European Network of Transmission System Operators for Electricity, “Regional groups” [Online]. Available: https://docstore.entsoe.eu/about-entso-e/system-operations/regional-groups/Pages/default.aspx.

[21] ENTSO-E, European Network of Transmission System Operators for Electricity, “[Press Release] Continuing frequency deviation in the Continental Europe Power System originating in Serbia/Kosovo: Political solution urgently needed in addition to technical”, Mar 2018. [Online]. Available: https://www.entsoe.eu/news/2018/03/06/press-release-continuing-frequency-deviation-in-the-continental-european-power-system-originating-in-serbia-kosovo-political-solution-urgently-needed-in-addition-to-technical/.

[22] European Parliament, Parliamentary questions, “Subject: Kosovo cutting supply to European electricity grid”, Jun 2018. [Online]. Available: http://www.europarl.europa.eu/doceo/document/E-8-2018-003028_EN.html.

[23] National Grid ESO, “Enhanced frequency response (EFR)”, [Online]. Available: https://www.nationalgrideso.com/balancing-services/frequency-response-services/enhanced-frequency-response-efr?technical-requirements.

[24] Terna, “Allegato A.15 - Partecipazione alla regolazione di frequenza e frequenza/potenza”, Codice di Rete, 2008.

[25] Terna, “Avvio del meccanismo di remunerazione della regolazione primaria di frequenza”, Mar 2014.

[26] ENTSO-E, European Network of Transmission System Operators for Electricity, “Survey on Ancillary Services Procurement, Balancing Market Design 2017”, May 2018.

[27] VDN, “Transmission Code 2007: Netz- und Systemregeln der deutschen Übertragungsnetzbetreiber”, Aug 2007.

[28] REGEILLESTUNG.NET, “Common tendering for primary control reserve” [Online]. Available: https://www.regelleistung.net/ext/static/prl.

[29] S. Just, “The German market for system reserve capacity and balancing energy”, EWL Working Paper, No. 06/15, University of Duisburg-Essen, Chair for Management Science and Energy Economics, Aug 2015.

[30] M. Delfanti, V. Olivieri, “Possibili modalità innovative di approvvigionamento delle risorse per il servizio di dispacciamento da fonti rinnovabili non programmabili e generazione distribuita”, Studio condotto per l’Autorità per l’energia elettrica e il gas, Giu 2013.

[31] U.S. Department of Energy, “Demand response” [Online]. Available: https://www.energy.gov/oe/activities/technology-development/grid-modernization-and-smart-grid/demand-response.

[32] Good Energy, "Demand response" [Online]. Available: http://www.goodenergy.com/Energy-Efficiency/demand-response.

[33] J. Torriti, M. G. Hassan, M. Leach, "Demand response experience in Europe: Policies, programmes and implementation", Energy, 2009.

[34] Terna, "Progetto pilota su partecipazione della domanda al MSD ai sensi della delibera 300/2017/R/eel Incontro con gli Operatori", May 2017.

[35] T. Lee, "Energy Storage in PJM – Exploring frequency regulation market transformation", Kleinman Center for Energy Policy, Jul 2017.

[36] F. Bignucolo, R. Caldon, M. Coppo, F. Pasut, M. Pettinà, "Integration of Lithium-Ion Battery Storage Systems in Hydroelectric Plants for Supplying Primary Control Reserve", Energies 2017, Vol. 10 (1), 2017.

[37] P. Iurilli, "Modelling and Analysis of Battery Energy Storage Systems for Primary Control Reserve Provision", 2017.

[38] Boston Power, "Swing5300 Data-Sheet," 2018.

[39] P. Gyan, "Calendar Ageing modeling of Lithium-ion batteries", Jun 2015. [Online]. Available: http://www.mat4bat.eu/wp-content/uploads/2014/03/Calendar-ageing-modeling-of-Lithium-Ion-batteries_Gyan_Renault.pdf.

[40] C. Nyce, "Predictive Analytics White Paper", American Institute for Chartered Property Casualty Underwriters/Insurance Institute of America, 2007.

[41] PAT Research, "What is predictive analytics?" [Online]. Available: https://www.predictiveanalyticstoday.com/what-is-predictive-analytics/.

[42] Otexts, "3.1. Some simple forecasting methods" [Online]. Available: https://otexts.com/fpp2/simple-methods.html.

[43] Otexts, "3.4. Evaluating forecast accuracy" [Online]. Available: https://otexts.com/fpp2/accuracy.html.

[44] OECD, "Glossary of statistical terms – Time series" [Online]. Available: https://stats.oecd.org/glossary/detail.asp?ID=2708.

[45] G. W. Morrison, D. H. Pike, "Kalman filtering applied to statistical forecasting", Management Science, Vol. 23, n. 7, Mar 1977.

[46] R. Adhikari, R. K. Agrawal, "An Introductory Study on Time Series Modeling and Forecasting", 2013.

[47] P. S. Kalekar, "Time series Forecasting using Holt-Winters Exponential Smoothing", Kanwal Rekhi School of Information Technology, 2004.

[48] K. Kim, "Financial time series forecasting using support vector machines", Neurocomputing, Vol. 55, Issues 1-2, pg. 307-319, 2003.

[49] Y. K. Al-Douri, H. Al-Chalabi, J. Lundberg, "Time Series Forecasting using Genetic Algorithm", The Twelfth International Conference on Advanced Engineering Computing and Applications in Sciences, 2018.

[50] A. Tealab, “Time series forecasting using artificial neural networks methodologies: A systematic review”, Future Computing and Informatics Journal, Vol. 3, Issue 2, pg. 334-340, Dec 2018.

[51] Nesreen K. Ahmed, Amir F. Atiya , Neamat El Gayar & Hisham El-Shishiny, “An Empirical Comparison of Machine Learning Models for Time Series Forecasting”, Econometric Reviews, Vol. 29, Issues 5-6, pg. 594-621, 2010.

[52] Towards Data Science, “Decision Trees in Machine Learning” [Online]. Available: https://towardsdatascience.com/decision-trees-in-machine-learning-641b9c4e8052.

[53] Towards Data Science, “Seeing the random forest from the decision trees: An explanation of Random Forest” [Online]. Available: https://towardsdatascience.com/seeing-the-random-forest-from-the-decision-trees-an-intuitive-explanation-of-random-forest-beaa2d6a0d80.

[54] Towards Data Science, “Feature Selection Using Random forest” [Online]. Available: https://towardsdatascience.com/feature-selection-using-random-forest-26d7b747597f.

[55] C. Stergiou, D. Siganos, “Neural Networks” [Online]. Available: https://www.doc.ic.ac.uk/~nd/surprise_96/journal/vol4/cs11/report.html.

[56] S. Saxena, “Artificial Neuron Networks (Basics) - Introduction to Neural Networks” [Online]. Available: https://becominghuman.ai/artificial-neuron-networks-basics-introduction-to-neural-networks-3082f1dcca8c.

[57] L. G. B. Ruiz, M. P. Cuéllar, M. D. Calvo-Flores, M.D.C.P. Jiménez, “An Application of Non-Linear Autoregressive Neural Networks to Predict Energy Consumption in Public Buildings”, Energies 2016, 9(9), 684, 2016.

[58] Z. Boussaada, O. Curea, A. Remaci, H. Camblong, N. M. Bellaaj, “A Nonlinear Autoregressive Exogenous (NARX) Neural Network Model for the Prediction of the Daily Direct Solar Radiation”, Energies 2018, 11, 620, Mar 2018.

[59] K. Hatalis, P. Pradhan, S. Kishore, R. S. Blum, A. J. Lamadrid, “Multi-step Forecasting of Wave Power Using a Nonlinear Recurrent Neural Network”, 2014 IEEE PES General Meeting | Conference & Exposition, 2014.

[60] A. Casalegno, “Slides of Course in Electrochemical Energy Conversion and Storage”, Politecnico di Milano, 2017.

[61] C. W. Hamann, A. Hanìmnett, W. Vielstich, “Electrochemistry”, 2nd Edition, Chapter 3 Wiley-Vch, 2007 (textbook).

[62] X. Luo, J. Wang, M. Dooner, and J. Clarke, “Overview of current development in electrical energy storage technologies and the application potential in power system operation,” Appl. Energy, vol. 137, pp. 511–536, 2015.

[63] B. Dunn, H. Kamath, J. Tarascon, “Electrical Energy Storage for the Grid: A Battery of Choices”, Science, vol. 334, pg. 928-935, Nov 2011.

[64] G. J. May, A. Davidson, B. Monahov, “Lead batteries for utility energy storage: A review”, Journal of Energy Storage, vol. 15, pg. 145-157, Feb 2018.

[65] V. G. Lacerda, A. B. Mageste, I. J. B. Santos, L. H. M. da Silva, M. do C. H. da Silva, "Separation of Cd and Ni from Ni–Cd batteries by an environmentally safe methodology employing aqueous two-phase systems," J. Power Sources, vol. 193, no. 2, pp. 908–913, Sep 2009.

[66] B. Scrosati, J. Garche, "Lithium batteries: Status, prospects and future", J. Power Sources, vol. 195, pg. 2419-2430, 2010.

[67] F. Díaz-González, A. Sumper, O. Gomis-Bellmunt, R. Villafáfila-Robles, "A review of energy storage technologies for wind power applications," Renewable and Sustainable Energy Reviews, vol. 16, pp. 2154-2171, 2012.

[68] E. O. Ogunniyi, H. Pienaar, "Overview of Battery Energy Storage System Advancement for Renewable (Photovoltaic) Energy Applications", Domestic use of Energy – International Conference towards energy solutions for the developing world", Apr 2017.

[69] A. Barré, B. Deguilhem, S. Grolleau, M. Gérard, F. Suard, D. Riu, "A review on lithium-ion battery ageing mechanisms and estimations for automotive applications", Journal of Power Sources 241 (2013).

[70] J. Wang et al., "Degradation of lithium ion batteries employing graphite negatives and nickelecobaltemanganese oxide þ spinel manganese oxide positives: Part 1, aging mechanisms and life estimation", Journal of Power Sources 269 (2014).

[71] D. Zane, A. Antonini, M. Pasquale, "Morphological study of SEI film on graphite electrodes", Journal of Power Sources 97-98, pg. 146-150, 2001.

[72] Y. Zhang, C. Wang, X. Tang, "Cycling degradation of an automotive LiFePO4 lithium-ion battery", Journal of Power Sources 196. Pg. 1513–1520, 2011.

[73] S. Lee, S. Seo, Y. Jin, H. Shim, D. Kim, "A graphite foil electrode covered with electrochemically exfoliatedgraphene nanosheets", Electrochemistry communications 12, pg. 1419-1422, 2010.

[74] J. Vetter, P. Nov´ak, M.R. Wagner, C. Veit, K.-C. M¨oller, J.O. Besenhard, M. Winter, M. Wohlfahrt-Mehrens, C. Vogler, A. Hammouche, "Ageing mechanisms in lithium-ion batteries", Journal of Power Sources 147 (2005) 269–281.

[75] M. Park, X. Zhang, M. Chung, G. B. Less, A. M. Sastry, "A review of conduction phenomena in Li-ion batteries", Journal of Power Sources 195, pg. 7904–7929, 2010.

[76] I. Bloom et al., "An accelerated calendar and cycle life study of Li-ion cells", Journal of Power Sources 101 (2), 2001.

[77] R.P. Ramasamy, R.E. White, B.N. Popov, "Calendar life performance of pouch lithium-ion cells", Journal of Power Sources 141 (2), 2005.

[78] W. Bögel, J.P. Büchel, H. Katz, "Real life EV battery cycling on the test bench", Journal of Power Sources 72, (1), 1998.

[79] B. Stiaszny, J. C. Ziegler, E. E. Krauß, M. Zhang, J. P. Schmidt, E. Ivers-Tiffée, "Electrochemical characterization and post-mortem analysis of aged LiMn2O4 - NMC/graphite lithium ion batteries part II: Calendar aging", Journal of Power Science 258, pg. 61-75, 2014.

[80] M. R. Jongerden, B. R. Haverkort, “Which battery model to use?”, IET Softw., vol. 3, no. 6, p. 445, 2009.

[81] M. Thele, O. Bohlen, D. Uwe Sauer, E. Karden, “Development of a voltage-behavior model for NiMH batteries using an impedance-based modeling concept”, Journal of Power Sources, n. 175, pp. 635-643, 2007.

[82] J. Lee et al., “Modeling and real time estimation of lumped equivalent circuit model of a lithium ion battery”, Power Electronics and Motion Control Conference, 2006.

[83] A. Shafiei, A. Momeni, S. S. Williamson, “Battery Modeling Approaches and Management Techniques for Plug-in Hybr” 2010. [Online]. Available: http://ieeexplore.ieee.org/stamp/stamp.jsp?arnumber=6043191.

[84] G. Piłatowicz, A. Marongiu, J. Drillkens, P. Sinhuber, D. U. Sauer, “A critical overview of definitions and determination techniques of the internal resistance using lithium-ion, lead-acid, nickel metal-hydride batteries and electrochemical double-layer capacitors as examples,” J. Power Sources, vol. 296, pp. 365–376, Nov 2015.

[85] S. Barcellona, “A novel lithium ion battery model: A step towards the electrochemical storage systems unification” 2017 6th International Conference on Clean Electrical Power (ICCEP), pg. 416–421, 2017.

[86] E. Samadani et al., “Empirical modeling of lithium-ion batteries based on electrochemical impedance spectroscopy tests”, Electrochim. Acta, vol. 160, pp. 169–177, 2015.

[87] H. He, R. Xiong, J. Fan, “Evaluation of Lithium-Ion Battery Equivalent Circuit Models for State of Charge Estimation by an Experimental Approach”, Energies 2011, 4, 582-598, 2011.

[88] Solartron analytical, “Electrochemical Impedance Spectroscopy for battery Research and Development”, 1996.

[89] N. Devillers, M.-C. Péra, S. Jemei, F. Gustin, D. Bienaimé, “Complementary characterization methods for Lithium-ion Polymer secondary battery modeling”, Electr. Power Energy Syst., vol. 67, pp. 168–178, 2014.

[90] J. Weniger, T. Tjaden, V. Quaschning, “Sizing and Grid Integration of Residential PV Battery Systems”, 8th International Renewable Energy Storage Conference and Exhibition, IRES 2013, Berlin, 2013.

[91] J. Li, M.A. Danzer, “Optimal charge control strategies for stationary photovoltaic battery systems”, Journal of Power Sources. 258, pg. 365–373, 2014.

[92] A. Sabo, B. Wille-Haussmann, C. Wittwer, Betriebsstrategien für PV-Batteriesysteme im Stromnetz, in: VDE Kongress 2012, Stuttgart, 2012.

[93] C. Williams, J. Binder, M. Danzer, F. Sehnke, M. Felder, “Battery Charge Control Schemes for Increased Grid Compatibility of Decentralized PV Systems”, 28th European Photovoltaic Solar Energy Conference and Exhibition, Paris, 2013.

[94] A. Zeh, R. Witzmann, “Operational Strategies for Battery Storage Systems in Low-voltage Distribution Grids to Limit the Feed-in Power of Roof-mounted Solar Power Systems”, Energy Procedia. 46, pg. 114–123, 2014.

[95] J. Weniger, J. Bergner, T. Tjaden, V. Quaschning, "Bedeutung von prognosebasierten Betriebsstrategien für die Netzintegration von PV-Speichersystemen", 29. Symposium Photovoltaische Solarenergie, Bad Staffelstein, 2014.

[96] Y. Riesen, P. Ding, S. Monnier, N. Wyrsch, C. Ballif, "Peak Shaving Capability of Household Grid-Connected PV-System with Local Storage: A Case Study", 28th European Photovoltaic Solar Energy Conference and Exhibition, Paris, 2013.

[97] J. Weniger, J. Bergner, V. Quaschning, "Integration of PV power and load forecasts into the operation of residential PV battery systems", 4th Solar Integration Workshop, Berlin, 2014.

[98] K. Ogimi, A. Yoza, A. Yona, T. Senjyu, T. Funabashi, "A study on optimum capacity of battery energy storage system for wind farm operation with wind power forecast data", 2012 IEEE 15th International Conference on Harmonics and Quality of Power [Online]. Available: https://ieeexplore.ieee.org/abstract/document/6381230.

[99] Y. Riffonneau, S. Bacha, F. Barruel, S. Ploix, "Optimal Power Flow Management for Grid Connected PV Systems With Batteries", IEEE Transactions on Sustainable Energy, Vol. 2, no. 3, pg. 309-320, Jul 2011.

[100] F. Sossan, E. Namor, R. Cherkaoui, M. Paolone , "Achieving the Dispatchability of Distribution Feeders through Prosumers Data Driven Forecasting and Model Predictive Control of Electrochemical Storage" , IEEE Transactions on Sustainable Energy, Vol. 7, no. 4, pg. 1762-1777, Oct 2016.

[101] J. Bergner, J. Weniger, T. Tjaden, V. Quaschning, "Feed-in power limitation od grid-connected PV battery systems with autonomous forecast-based operation", 29th European Photovoltaic Solar Energy Conference and Exhibition.

[102] M. Khalid, A. V. Savkin, "Model Predictive Control Based Efficient Operation of Battery Energy Storage System for Primary Frequency Control", 2011 11th Int. Conf. Control, Automotion, Robotics and visions, Singapore, 7-10 Dec 2010.

[103] B. Gundogdu, D.T. Gladwin, M.P. Foster, D.A. Stone, "A Forecasting Battery State of Charge Management Strategy for Frequency Response in the UK System", 2018 IEEE International Conference on Industrial Technology (ICIT), Lyon, France.

[104] E. Namor, F. Sossan, R. Cherkaoui, M. Paolone, "Control of Battery Storage Systems for the Simultaneous Provision of Multiple Services", IEEE Transactions on Smart Grid, Feb 2018.

[105] H. Chen, C.A. Canizares, A. Singh. "ANN-Based Short-Term Load Forecasting in Electricity Markets", Proceedings of the IEEE Power Engineering Society Transmission and Distribution Conference, 2: pg. 411–415, 2001.

[106] S. R. Deshmukh, D. J. Doke, Y. P. Nerkar, "A statistical frequency estimation for generation scheduling under availability based tariff," 23rd National Convention of Electrical Engineers, Pune, India, 2007.

[107] A. J. Al-Shareef, E. A. Mohamed, E. Al-Judaibi, "One hour ahead load forecasting using artificial neural network for the western area of Saudi Arabia," International Journal of Electrical Systems Science and Engineering, vol. 1, pg. 35-40, 2008.

[108] H. Steinherz Hippert, C. Eduardo Pedreira, R. Castro Souza. "Neural Networks for Short-Term Load Forecasting: A Review and Evaluation", IEEE Transactions on Power Systems, Vol. 16, No. 1, February 2001.

[109] O. A. Alsayegh. “Short-Term Load Forecasting Using Seasonal Artificial Neural Networks”, International Journal of Power and Energy Systems, Vol. 23, No. 3, 2003.

[110] T. Senjyu, H. Takara, K. Uezato, T. Funabashi, “One Hour-Ahead Load Forecasting Using Neural Network”, IEEE Transactions on power systems, Vol. 17, no. 1, Feb 2002.

[111] A. G. Baklrtzis, V. Petrldis, S. J. Klartzis, M. C. Alexiadls, A. H. Malssis, “A Neural Network Short Term Load Forecasting Model for the Greek Power System”, IEEE Transactions on power systems, Vol. 11, no. 2, May 1996.

[112] B. Xu, A. Oudalov, J. Poland, A. Ulbig, G. Andersson, “BESS Control Strategies for Participating in Grid Frequency Regulation”, IFAC Proceedings Volumes, Vol. 47, Issue 3, pg. 4024-4029, 2014.

[113] A. Oudalov, D. Chartouni, C. Ohler, “Optimizing a Battery Energy Storage System for Primary Frequency Control”, IEEE Transactions on Power systems, Vol. 22, no. 3, 2007.

[114] 50Hertz Transmisssion GmbH, “Transparency” [Online]. Available: https://www.50hertz.com/en/Transparency.

[115] GME, “Esiti dei mercati e statistiche” [Online]. Available: http://www.mercatoelettrico.org/it/Esiti/MGP/EsitiMGP.aspx.

[116] Terna, “Costanti annue per la determinazione dei prezzi applicati ai fini della valorizzazione economica del servizio di regolazione primaria di frequenza”, 2017.

[117] REGEILLESTUNG.NET, “Search for tender” [Online]. Available: https://www.regelleistung.net/ext/tender/.

[118] Terna-SunSet Area Pubblica, “Livelli Regolazione Secondaria” [Online]. Available: https://myterna.terna.it/SunSet/Public/Pubblicazioni.

[119] United Nations Climate Change, “The Kyoto Protocol - Status of Ratification” [Online]. Available: https://unfccc.int/process/the-kyoto-protocol/status-of-ratification.

[120] Sustainable Development Goals, “Transforming our world: the 2030 Agenda for Sustainable Development” [Online]. Available: https://sustainabledevelopment.un.org/post2015/transformingourworld.

[121] RTE, “January 10th : RTE calls on interruptible industrialists” [Online]. Available: .https://clients.rte-france.com/lang/an/visiteurs/services/actualites.

[122] RTE, “Network frequency” [Online]. Available: http://clients.rte-france.com/lang/an/visiteurs/vie/vie_frequence.jsp.

[123] ARERA, “Delibera Maggio 2017 300/2017/R/eel" [Online]. Available: https://www.arera.it/it/docs/17/300-17.htm.

[124] Terna, “Progetto Pilota UPI” [Online]. Available: http://www.terna.it/SistemaElettrico/MercatoElettrico/ProgettiPilotaexdel3002017REEL/ProgettoPilotaUPI.aspx.

[125] C. Brivio, S. Mandelli, M. Merlo, “Battery energy storage system for primary control reserve and energy arbitrage”, Sustainable Energy, Grids and Networks, Vol. 6, pg. 152-165, Jun 2016.

[126] Qualenergia.it, “Allarme costi sul mercato del dispacciamento elettrico. Chi ci sta guadagnando?” [Online]. Available: https://www.qualenergia.it/articoli/20160620-allarme-costi-su-mercato-dispacciamento-elettrico-chi-ci-sta-guadagnando/.

[127] Qualenergia.it, “Mercato elettrico e speculazione sul MSD, interviene l’Autorità” [Online]. Available: https://www.qualenergia.it/articoli/20160627-mercato-elettrico-e-speculazione-su-msd-interviene-aeegsi/.

[128] ARERA, “Mercato dell’energia elettrica. Revisione della disciplina degli sbilanciamenti effettivi – Interventi prioritari” [Online]. Available: https://arera.it/it/schedetecniche/16/316-16st.htm.

[129] E. Kotsakis, A. Lucas, N. Andreadou, G. Fulli, M. Masera, “Recent research conducted at the SGILab towards an efficient and interoperable smart grid”, 2018 AEIT International Annual Conference, Oct 2018.

[130] LEAF COMMUNITY, “Le forme dell’energia” [Online]. Available: http://www.leafcommunity.com/le-forme-dellenergia/.